Universidad de Huelva

Departamento de Química “Profesor José Carlos Vílchez Martín”

Biotechnological potential of a highly acidic-habitat microalga

Memoria para optar al grado de doctora
presentada por:

María Robles Garrido

Fecha de lectura: 23 de febrero de 2026

Bajo la dirección de los doctores:

Carlos Vílchez Lobato

Inés Garbayo Nores

Huelva, 2026

Universidad de Huelva

Departamento de Química
"Profesor José Carlos Vílchez Martín"

Programa de Doctorado
Ciencia y Tecnología Industrial y Ambiental

Tesis Doctoral

BIOTECHNOLOGICAL POTENTIAL OF A HIGHLY ACIDIC-HABITAT MICROALGA

POTENCIAL BIOTECNOLÓGICO DE UNA MICROALGA DE AMBIENTE ALTAMENTE ÁCIDO

Memoria para optar al grado de doctora presentada por:
María Robles Garrido

Bajo la dirección de los doctores:
Carlos Vílchez Lobato
Inés Garbayo Nores

Huelva, 2026

VICERRECTORADO DE DOCTORADO, POLÍTICA LINGÜÍSTICA Y BIBLIOTECA

Escuela de Doctorado

Universidad de Huelva

DECLARACIÓN DE HONESTIDAD ACADÉMICA DE TESIS DOCTORAL

Apellidos y Nombre: Robles Garrido María

DNI o Pasaporte: 49111336B

El/la estudiante de doctorado abajo firmante declara que la presente Tesis Doctoral es un trabajo original y que todo el material utilizado está citado siguiendo un estilo de citas y referencias reconocido y recogido en el apartado de bibliografía.

El/la estudiante de doctorado es consciente de la normativa de evaluación de la Universidad de Huelva en lo concerniente al plagio y de las consecuencias académicas que presentar un trabajo plagiado puede acarrear.

Fecha y Firma del estudiante

ROBLES GARRIDO MARIA - 49111336B

Firmado digitalmente por ROBLES GARRIDO MARIA - 49111336B
Fecha: 2025.11.25 09:42:16 +01'00'

Contents

Summary for the TESEO Ministry database

Coccomyxa onubensis (*C. onubensis*) was isolated from the Tinto River, an acidic environment with high metal content, mainly Fe and Cu. In **chapter 2**, we evaluated its response to stressors of its natural habitat: salt, Fe, high irradiance and nitrogen limitation. Under Fe or high light, *C. onubensis* reduced antenna size, improving the photosynthetic use of light and biomass productivity. Although N limitation or salt stress affected photosynthetic performance, efficiency values remained close to those of viable algal cultures. These results enabled the design of processes for biomass and valuable molecules production. Thus, in **chapter 3**, growth optimization, which is required for eventual larger scale cultivation, was performed. Next, *C. onubensis* growth in air-fluidized bag system was proven stable and photosynthetically viable and with no growth of opportunistic species, which becomes advantageous for massive production. Antioxidant compounds showed distinct trends: lutein and phenolics increased early in the first cycle, while reduced light availability appeared to decrease chlorophyll antenna size.

Chapter 4 evaluated the growth of *C. onubensis* under different nitrogen limitation levels. N limitation decreased growth and photosynthetic performance but enhanced carbohydrate and lipid accumulation by 2.07-fold and 1.13-fold, respectively, at 0.01 mM NO_3^-. Fatty acid content increased with decreasing N, peaking at 1.54-fold above the control at 0.01 mM NO_3^-. N limitation significantly increased saturated fatty acids (SAFAs) and monounsaturated fatty acid (MUFAs), especially C18:1 which increased by 88-fold. In contrast, 5 mM nitrate favored C18:3 accumulation and lowered SAFAs and MUFAs. Thus, manipulation of N can direct biomass composition toward biofuel or food production.

In **chapter 5** we analyzed the effect of different levels of Fe on the microalga viability and its antioxidant response. Moderate Fe levels induced oxidative stress in the microalga increasing superoxide dismutase and flavonoid content. Antioxidant capacity correlated with Fe concentration, and target molecules such as carotenes, xanthophylls and polyphenols increased. These compounds have recognized anti-inflammatory activity, leading to **chapter 6**, where we evaluated microalgal extracts in THP-1 cells. Extracts from cultures grown at 0.25 mM Fe showed the highest levels of these molecules and produced a 50% reduction in TNFα secretion in differentiated macrophages. This highlights the potential of microalgae from acidic environments as sources of natural anti-inflammatory agents.

Chapter 7 explored two additional extremophilic microalgae: *Chroococcidiopsis* sp. (cyanobacterium from endolithic, hyper-arid environment, Atacama) and *Elliptochloris* sp. (microalga from hyper-acidic habitat, Tinto River). *Chroococcidiopsis* sp. grows as aggregated to survive the harsh conditions of Atacama Desert. However, aggregates can reduce light and nutrient availability of the inner cells. Low-frequency ultrasound pulses proved efficient in disaggregating *Chroococcidiopsis* sp., improving growth of the cyanobacterium. *Elliptochloris* sp. was grown on crude technical glycerin or glucose bubbled with either only air or air containing 2.5% CO_2. Mixotrophy with CO_2 enabled higher biomass productivity and increased SAFAs content. Nevertheless, mixotrophy with only air resulted in an increase of both saturated and unsaturated fatty acids, but biomass productivities were lower. Together with low-pH protection against contamination, *Elliptochloris* sp. appears suitable for large-scale production within circular-economy frameworks. Overall, this thesis demonstrates that extremophilic photosynthetic microorganisms, traditionally considered less productive than non-extremophiles, hold substantial biotechnological potential.

Keywords: Microalgae, extremophiles, oxidative stress, photosynthesis, antioxidants

Resumen para las bases de datos del ministerio TESEO

Coccomyxa onubensis (C. *onubensis*) fue aislada en río Tinto, un entorno ácido con alta concentración de metales, en especial Fe y Cu. En el **capítulo 2**, evaluamos su respuesta a estresores de su hábitat natural: sal, Fe, luz y limitación de nitrógeno. Bajo Fe o luz, *C. onubensis* redujo el tamaño de antena, mejorando el uso fotosintético de la luz y la productividad de biomasa. Aunque la limitación de N o el estrés salino afectaron el rendimiento fotosintético, los valores de eficiencia se mantuvieron cercanos a los de cultivos viables. Estos resultados permitieron diseñar procesos para la producción de biomasa y moléculas de interés. Así, en el **capítulo 3**, se realizó una optimización del crecimiento necesaria para un eventual cultivo a mayor escala. Posteriormente, el crecimiento de la microalga se demostró estable y fotosintéticamente viable en un sistema de bolsas fluidizadas, sin crecimiento de especies oportunistas, lo cual resulta ventajoso para la producción masiva. Los compuestos antioxidantes mostraron tendencias diferenciadas: la luteína y los compuestos fenólicos aumentaron al inicio del primer ciclo, mientras que la disminución de la disponibilidad de luz pareció reducir el tamaño de la antena de clorofila.

El **capítulo 4** evaluó el crecimiento de *C. onubensis* bajo distintos niveles de limitación de nitrógeno. La limitación de N redujo el crecimiento y el rendimiento fotosintético, pero aumentó la acumulación de carbohidratos y lípidos, 2.07 y 1.13 veces respectivamente, a 0.01 mM NO_3^-. El contenido de ácidos grasos aumentó a medida que disminuyó el N, alcanzando un máximo 1.54 veces superior al control a 0.01 mM NO_3^-. La limitación de N incrementó significativamente los ácidos grasos saturados (SAFAs) y monoinsaturados (MUFAs), especialmente C18:1, que aumentó 88 veces. En contraste, 5 mM de nitrato favoreció la acumulación de C18:3 y redujo SAFAs y MUFAs. Así, la manipulación de N puede dirigir la composición de la biomasa hacia la producción de biocombustibles o alimentos.

En el **capítulo 5** analizamos el efecto de distintos niveles de Fe sobre la viabilidad de la microalga y su respuesta antioxidante. Niveles moderados de Fe indujeron estrés oxidativo, aumentando los niveles de superóxido dismutasa y flavonoides. La capacidad antioxidante correlacionó con la concentración de Fe, y aumentó la producción de carotenos, xantofilas y polifenoles. Estos compuestos poseen actividad antiinflamatoria reconocida, por lo que en el **capítulo 6** evaluamos su actividad en células THP-1. Cultivos crecidos con 0.25 mM Fe mostraron los niveles más altos de estas moléculas y redujeron un 50% la secreción de TNFα en macrófagos diferenciados. Esto resalta el potencial de microalgas de ambientes ácidos como fuentes de agentes antiinflamatorios naturales.

El **capítulo 7** exploró dos microalgas extremófilas adicionales: *Chroococcidiopsis* sp. (cianobacteria de ambiente hiperárido de Atacama) y *Elliptochloris* sp. (microalga del del río Tinto). *Chroococcidiopsis* sp. crece en forma de agregados para sobrevivir a las duras condiciones del desierto. Sin embargo, estos agregados pueden reducir la disponibilidad de luz y nutrientes de las células internas. Pulsos de ultrasonido de baja frecuencia resultaron eficientes en desagregar *Chroococcidiopsis* sp., mejorando el crecimiento de la cianobacteria. *Elliptochloris* sp. se cultivó en glicerina técnica cruda o glucosa, burbujeadas con aire o aire con 2.5% CO_2. Mixotrofía con CO_2 permitió mayor crecimiento e incrementó el contenido de SAFAs. No obstante, mixotrofía solo con aire aumentó tanto los ácidos grasos saturados como insaturados, pero con menor crecimiento. Junto con la protección frente a la contaminación por el bajo pH, *Elliptochloris* sp. parece adecuada para producción a gran escala dentro de modelos de economía circular. En conjunto, esta tesis demuestra que los microorganismos fotosintéticos extremófilos, tradicionalmente considerados menos productivos, poseen un notable potencial biotecnológico.

Palabras clave: Microalgas, extremófilos, estrés oxidativo, fotosíntesis, antioxidantes

Extended summary

Microalgae in nature are usually subjected to abiotic stress, which may be due to changes in the salinity of the environment, temperature variation, ultraviolet radiation, lack of nutrients or the presence of metal cations, among other factors. Under these extreme conditions, microalgae produce certain metabolites to maintain homeostasis by resolving and minimizing the impact of stress. Some metabolites produced to counteract the stress impact have commercial value, including chlorophylls, terpenoids, phenolic compounds, polyunsaturated fatty acids (PUFAs) and even polysaccharides, among others, with antioxidant, antimicrobial and anti-inflammatory bioactivity. Therefore, incubation conditions for microalgae cultures leading to the accumulation of these molecules would be highly useful to design efficient biotechnological processes to obtain extracts with potential bioactivity. Although extensive research is being conducted in this field, selecting microalgal species that exhibit robust and productive growth while being suitable to produce specific target compounds remains challenging, as biological contamination by other microalgal species can rapidly lead to culture collapse.

Extremophilic microorganisms play a key role in that field as they are able to live under extreme conditions, such as acidic conditions, extreme aridity, high salinities, high or very low temperatures, by means of the expression of adaptation mechanisms. Thus, these microorganisms have a greater adaptation capacity to cope with harsh oxidative conditions of their habitats. This adaptability is partly based on the expression of secondary metabolic pathways leading to the biosynthesis of unique, valuable molecules with applications in human and animal health. These molecules include highly antioxidant phenolic compounds, peptides, indole derivates and terpenes, among other valuable biomolecules groups.

This is the case of the microalga species studied in this thesis, *Coccomyxa onubensis* (*C. onubensis*). The microalga strain used in this study was isolated from Tinto River. The so-called "red river" flows along 100 km from the Iberian Pyrite Belt down to the Atlantic Ocean and is one of the most extensive examples of extreme acidic environments, exhibiting low pH values in the range of 1.7 to 3.1 and presence of cations in solution, of which Fe (II) and (III) and Cu (II) have a relevant quantitative presence. The Fe (III) concentration in the Tinto River waters are as high as 30 $g \cdot L^{-1}$. The lower solubility of CO_2 and O_2 in acidic waters limits the growth of photosynthetic species to the superficial layer of the acidic waters where carbon and oxygen availability are greater. Consequently, the photosynthetic apparatus of the acidotolerant microalga must be able to adapt to the high PAR and UV irradiance levels of the region. *C. onubensis* has also been described as a halotolerant species, being able to grow in media with salt concentrations of about 500 mM. Moreover, *C. onubensis* proliferates in the abovementioned habitat with a nitrogen concentration as low as 0.05 mM nitrate, which is also an eventual sign of the possible adaptability of the microalga in N-deficient media. The described natural adaptability makes *C. onubensis* a suitable candidate for this thesis dissertation.

In **chapter 2**, we evaluated the response of *C. onubensis* to different stressors based on the natural habitat of the microalga. The results obtained revealed a noticeable adaptability of the microalga to the imposed abiotic stress factors, salt, Fe (III), high irradiance and nitrogen limitation. *C. onubensis* responds to Fe (III) or high irradiance stress by reducing the antenna size to maximize the photosynthetic use of light, resulting in higher biomass productivity relative to control cells. Additionally, although the cultivation of *C. onubensis* under nitrogen limitation or salt stress significantly affects the photosynthetic chain of the microalga, the photosynthetic efficiency values obtained remained close to those typically observed in viable

algal cultures. Furthermore, moderate biomass productivity values were also obtained. These adaptation capabilities can be further applied to the biomass production of microalgae under abiotic stress caused by environmental pollution, providing insights into various areas relevant to society, such as animal and human nutrition, health, agriculture, and water treatment.

Studying the photosynthetic performance of the microalga allows applying this information to the design of production processes aimed at obtaining biomass and biotechnologically valuable molecules. Additionally, for large scale cultivation, optimization of key growth influencing factors is crucial to ensure light and nutrient availability and, therefore, the viability of the microalgal culture. Nevertheless, the massive production of acidophilic microalgae (not exploited yet) has been reported to be hypothetically constrained by limited productivity, primarily due to the extreme pH conditions of the medium. Thus, in **chapter 3** we optimize growth-influencing factors in a factorial 3^3 aiming at designing efficient conditions to growth *C. onubensis* under repeated-batch production, in air-fluidized open bags. The mathematical model predicted that the optimal condition for maximum biomass productivity was no addition of Fe (III) to *C. onubensis* cultures and growing the microalga under moderate levels of temperature and light irradiance (28.9 °C and 486 μmol photon·m^{-2}·s^{-1}). Accordingly, following this growth optimization, the results suggest that *C. onubensis* can be cultivated in an easy-to-operate air-fluidized bag system, achieving a maximum productivity of 0.17 g·L^{-1}·d^{-1}.

The results of productivity obtained in this chapter with *C. onubensis* suggest that microalgae from highly acidic environments could be produced as efficiently as other non-extremophilic photosynthetic microorganisms. Light irradiance was maintained constant. Therefore, light availability within the photic zone of *C. onubensis* cultures was primarily influenced by the dynamics of the repeated-batch cultivation cycles and the progressive increase in cell density though each cycle. Accordingly, several trends in the variation of antioxidants compounds were observed. On the one hand, at the beginning of the first cycle, the adaptation phase to the imposed conditions, light possibly causes oxidative stress in *C. onubensis* resulting in an increase in the content of lutein and phenolic compounds as a defense mechanism. On the other hand, when light availability decreases or the microalga gets acclimated to the imposed conditions, a decrease in chlorophyll antenna size seems to occur, representing a physiological acclimation of the microalga to the reduced light availability in high-cell density cultures as a strategy to maximize light absorption. The growth of *C. onubensis* in 30 L air-fluidized, open bags has proven stable and photosynthetically viable and with no growth of opportunistic species, which becomes advantageous for massive production.

The referred adaptability of the microalga to nitrogen limitation in its natural habitat motivated us to analyze some of their physiological and metabolic responses, which are described in **chapter 4**. In microalgal cultures, nitrogen deprivation leads to a markedly reduced synthesis of nitrogen-rich biomolecules such as proteins and chlorophylls. This typically results in lower photosynthetic efficiency and, consequently, growth inhibition or cessation. However, under such stress conditions, metabolic energy may be redirected toward the synthesis of nitrogen-free, carbon-rich biomolecules such as carbohydrates and lipids. This study aimed to investigate lipid biosynthesis and accumulation in *C. onubensis* under varying degrees of nitrogen limitation, achieved by adjusting nitrogen availability to 0.01, 0.3, 1, 5, and 26 mM (nitrogen-replete condition). The results confirmed the essential role of inorganic nitrogen in the growth and viability of *C. onubensis*, as nitrogen limitation led to decreased growth and photosynthetic performance. Nonetheless, nitrogen limitation significantly enhanced the accumulation of carbohydrates and lipids, with increases of 2.07-fold and 1.13-fold, respectively, at 0.01 mM NO_3^-. Fatty acid content progressively increased as nitrogen

availability decreased, reaching its highest level—1.54-fold higher than the control—in cultures grown with the lowest nitrogen concentration (0.01 mM NO_3^-). A partial lipidomic analysis revealed that nitrogen limitation significantly increased the total content of saturated fatty acids (SAFAs), specifically C18:0 and C16:0, by 2.87- and 2.08-fold, respectively. Remarkably, the monounsaturated fatty acid (MUFA) C18:1 increased by 88-fold. Conversely, the polyunsaturated fatty acid (PUFA) C18:3 decreased by approximately 1.84-fold under nitrogen limitation. In contrast, cultures grown with 5 mM nitrate accumulated higher levels of C18:3 and lower levels of SAFAs and MUFAs. These findings suggest that manipulating nitrogen concentration in *C. onubensis* cultures can serve as an effective strategy to obtain fatty acid-enriched biomass tailored either for biofuel production or as a food supplement, depending on the desired degree of fatty acid unsaturation. Additionally, the results may indicate a potential ecological role for *C. onubensis* as a source of electron donors supporting bacterial growth in its natural habitat, such as acidic pit lakes, an aspect further discussed in this study.

Based on the photosynthetic response of *C. onubensis* to increasing Fe (III) levels found in chapter 2, in **chapter 5** we analyze the effect of different levels of Fe (III) on the microalga viability and its antioxidant response. The results suggest that the addition of moderate Fe (III) levels to *C. onubensis* cultures results in improved growth and photosynthetic viability. Increases in the intracellular levels of the enzyme superoxide dismutase (SOD) and flavonoids, used as antioxidant response biomarkers, point at Fe (III)-mediated oxidative stress induction to occur. The apparent decrease in the content of other phenolic molecules and polyunsaturated fatty acids might be understood as a sign of antioxidant molecules involvement in reactive oxygen species (ROS) scavenging. In conclusion, the noticeable antioxidant capacity displayed by *C. onubensis* allows the use of moderate Fe (III) levels to trigger accumulation of valuable antioxidant molecules without affecting microalgal growth. Among these molecules, terpenoids, such as astaxanthin and lutein, (poly)phenolic compounds (e.g. caffeic and gallic acids), polyunsaturated fatty acids, and sterols have been described to display anti-inflammatory effects. Therefore, in **chapter 6** we analyze the anti-inflammatory activity of microalgal extracts in THP1 cells as a function of Fe (III) concentration and microalgal growth stage. Additionally, we compare the anti-inflammatory capacity of the extracts with the antioxidant activity and the target antioxidant compounds produced by the microalga with the aim to determine the antioxidant compounds that have a greater impact in the anti-inflammatory response of the extracts.

The results suggested a direct relationship between the antioxidant capacity of the microalgal extracts and Fe (III) concentration in the culture medium. Consequently, the production of some of the target antioxidant molecules, including carotenes, xanthophylls and (poly)phenols, increased. The levels of these molecules increased the most in cell extracts obtained from microalgal cultures at 0.25 mM of Fe (III), which was correlated with a 50 % increase in the inhibition of the production of pro-inflammatory interleukin TNFα in THP-1 differentiated human macrophages. Nevertheless, Fe (III) concentration had no significant effect on the inhibition of the production of other pro-inflammatory interleukins (IL-6 and IL-1β), whereas *C. onubensis* extracts obtained from cultures exposed to varying levels of both light irradiance and Fe (III) influenced the production of these cytokines. Accordingly, it can be hypothesized that the synergistic interaction between Fe (III) concentration and light irradiance in *C. onubensis* cultures may enhance the anti-inflammatory activity of *C. onubensis* extracts, which are enriched in valuable antioxidant molecules. Overall, this study highlighted the utility of a microalgal species from a highly acidic environment as a novel, natural source of anti-inflammatory agents, based on its ability to cope with the oxidative conditions of its habitat.

In addition to *Coccomyxa*, in **chapter 7** we have explored specific characteristics of the cultivation of two other extremophilic microalgae, *Chroococcidiopsis* sp. (cyanobacterium from endolithic, hyper-arid environment, Atacama) and *Elliptochloris* sp. (microalga from hyper-acidic habitat, Tinto River). The aim was to obtain initial key information of their production, as a first step toward the analysis of their biotechnological potential. In this thesis chapter we used a *Chroococcidiopsis* sp. strain isolated from the endolithic habitat of the Atacama Desert, the driest desert in the world due to the extremely scarce rainfall, low level of relative humidity and extremely high incident solar radiation. To survive these conditions and reduce the cell exposure to the incident UV radiation, *Chroococcidiopsis* sp. grows in the form of aggregates, diminishing the associated photo-oxidative damage. However, this adaptation strategy can reduce the availability of both light and nutrients to the growing cells. This study showed that the low-frequency ultrasound (LFU) pulses were efficient in disaggregating *Chroococcidiopsis* sp. aggregates, improving light and nutrient availability to the cells. The length of the ultrasound pulses can be optimized to achieve complete disaggregation of the aggregates without affecting cell viability. The disaggregation of aggregates can lead to more homogeneous cultures and lower the energy required for mechanical agitation. Additionally, our results indicated an improved growth of the cyanobacterium in disaggregated cultures.

Depending on species, other strategies could be considered for efficient biomass production. This has been tested with another (non-aggregating) highly acidic-habitat microalga, *Elliptochloris* sp., isolated by our team, Microalgae Biotechnology Unit (BITAL) at University of Huelva. Photoautotrophic algal cultivation is challenging due to the shadowing effect produced by an increase in the number of cells; under such circumstances, mixotrophic growth might be an efficient alternative. We grew cultures of the autochthonous acidotolerant microalga *Elliptochloris* sp. on crude technical glycerin or glucose bubbled with either only air or air containing 2.5 % (v/v) CO_2. We found that CO_2 strongly influenced the production of *Elliptochloris* sp., as higher growth occurred in mixotrophy with CO_2-enriched air compared to that with only air. Mixotrophy with CO_2-enriched air enabled to reach higher biomass productivity and facilitated an increase in the relative abundance of saturated fatty acids. Nevertheless, mixotrophy with only air resulted in an increase of both saturated and unsaturated fatty acids, but biomass productivities were lower. These results, along with the limited biological contamination facilitated by low pH, suggest that this microalga might be attractive for large-scale production within the circular economy model.

Overall, the results presented in this thesis dissertation demonstrate the significant potential for enhancing the growth of extremophilic photosynthetic microorganisms, which have traditionally been regarded as less efficient for biomass production compared to non-extremophilic species. Intensive research into their physiology, biochemistry, genomics, proteomics, and process engineering is expected to reveal their considerable biotechnological potential.

Abbreviations

Oxidative stress and anti-inflammatory response

ROS	Reactive oxygen species	CAT	Catalase
RNS	Reactive nitrogen species	TNFα	Tumor necrosis factor-α
$O_2^{\bullet-}$	Superoxide radical	NF-κB	Nuclear factor kappa B
•OH	Hydroxyl radical	IκB	Inhibitors of NF-κB
SOD	Superoxide dismutase	ILs	Interleukins

Fatty acids and biosynthesis-related molecules

FAs	Fatty acids	DHAP	Dihydroxyacetone phosphate
FAMEs	Fatty acid methyl esters	GAP	Glyceraldehyde phosphate
TAG	Triacylglyceride	SFAs	Saturated fatty acids
LPA	Lysophosphatidic acid	UFAs	Unsaturated fatty acids
PA	Phosphatidic acid	PUFAs	Polyunsaturated fatty acids
DAG	Diacylglycerol	MUFAs	Monounsaturated fatty acids
ER	Endoplasmic reticulum	EPA (C20:5)	Eicosapentaenoic acid
DES	Desaturases	DHA (C22:6)	Docosahexaenoic acid
ELO	Elongases	ALA (C18:3)	Linolenic acid
OCS	Organic carbon sources	DDA (C22:2)	Docosadienoic acid
G3P	Glycerol-3-phosphate	C16:0	Palmitic acid
G6P	Glucose-6-phosphate	C18:0	Stearic acid
F6P	Fructose-6-phosphate	C17:1	Heptadecenoic acid
ADP	Adenosine diphosphate	C18:1	Oleic acid
ATP	Adenosine triphosphate	C18:2	Linoleic acid
$NADP^+$	Nicotinamide adenine dinucleotide phosphate oxidated		
NADPH	Nicotinamide adenine dinucleotide phosphate reduced		

Growth measurement and cell structures

dw	Dry weight		
OD	Optical density	Mlg	Mucilage
Th	Thylakoids	TEM	Transmission electron microscopy
CW	Cell wall	VSA	Vesicular activity
Ch	Chloroplasts	EPS	Exopolysaccharide

Photosynthesis chain and JIP parameters

PSII/PSI	Photosystem II and I	qP	Photochemical quenching
RCs	Reaction centers	NPQ	Non-photochemical quenching
Cyt b	Cytochrome b6f	PQ	Plastoquinone
PC	Plastocyanin	PQH_2:	Plastoquinol
Q_A	Quinone A	FVM:	Like-flavonoid molecules
Q_B	Quinone B	Fd	Ferredoxin
ΔpH	pH gradient	FNR	Ferredoxin-$NADP^+$ reductase
ETC	Electron transport chain	PAR	Photosynthetically active radiation
FeS	Iron/sulfur cluster belonging to redox proteins		
Chl	Chlorophyll		
ChlF	Chlorophyll fluorescence		
F_0	Fluorescence intensity at 50μs, minimal fluorescence level		
F_M	Maximal fluorescence intensity		
F_V	Variable fluorescence		

V_J	Relative variable fluorescence at 2 ms (J step)
M_0	Normalized value of the initial slope, net rate of closure of the RCs
F_V/F_M	Maximum quantum yield of PSII
F_V/F_0	Maximum primary yield of photochemistry of PSII
N	Turn-over number Q_A
Area	Area between fluorescence curve and F_M
S_M	Normalized area
ABS/RC	Absorption flux per RC
TR_0/RC	Trapped energy flux per RC
ET_0/RC	Electron transport flux per RC
DI_0/RC	Dissipated energy per RC
φ_{Po}	Maximum quantum yield of primary photochemistry
φ_{Eo}	Probability that an absorbed photon will move an electron into the ETC
ψ_o	Probability that a trapped exciton moves further than Q_A^-
φ_{Do}	Maximum quantum yield of non-photochemical de-excitation
PI_{ABS}	Performance index

Statistics

ANOVA	Analysis of variance
RSM	Response surface methodology
PCA	Principal component analysis
PCs	Principal components

CHAPTER

1

General introduction and thesis outline

Table of contents

1. Introduction

1.1. The worldwide needs for novel sources of energy, food, chemicals, and pharmaceuticals.

The current energy model based on oil and other fossil fuels is nearing its end. Such an energy model strongly affects the environment due to the emission of CO_2 into the atmosphere, which significantly contributes to climate change (González-López et al., 2009). Thus, sustainable energy sources that have a lesser impact on the environment need to be identified. In addition, with the growing world population and the anticipated food shortage, there is a need for alternative, suitable natural sources for production of essential nutrients such as proteins and lipids (Henchion et al., 2017). Traditional natural resources for food production are insufficient to meet the needs of humanity. In such a context, microalgae are on the way to becoming an essential part of our lives, as they are a fast-growing green source of sustainable and highly valued market products, including bioactive compounds, as schematically represented in Figure 1.1. Additionally, microalgae do not need arable land to grow and have a higher growth rate than terrestrial plants (Abdul Latif et al., 2019). Microalgae are also efficient organisms for the mass production of biomass, which could alternatively be used as raw material to generate biofuels (Schenk et al., 2008). Furthermore, microalgae and their components currently find application in numerous areas of relevance to society such as animal and human nutrition, health, agriculture and water treatment, among others (Forján et al., 2015).

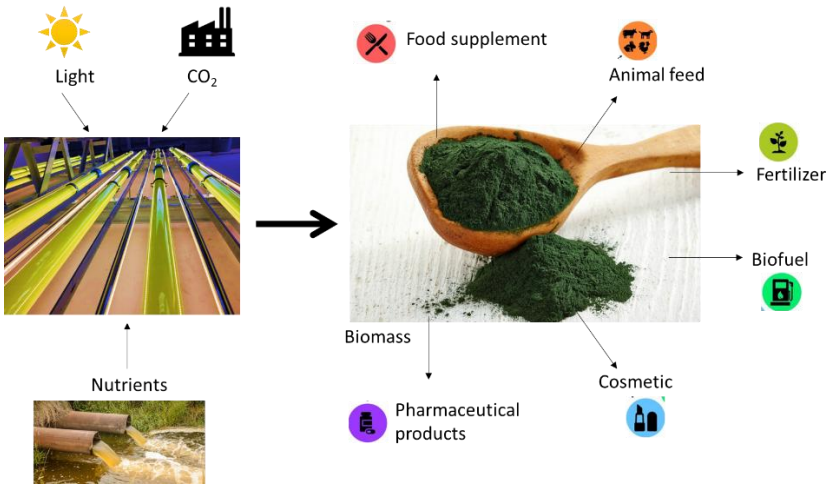

Figure 1.1. Schematic representation of circular economy, i.e., inclusion of natural or waste resources in the microalgal production cycle to produce biomass which finds applications in different areas of interest.

However, this goal is threatened by anthropogenic climate change which has the potential to dramatically reduce photosynthetic biomass yields in affected regions (Lobell et al., 2008). Abiotic stress negatively influences plant growth and development and ultimately causes reduction in agricultural production worldwide (Rodziewicz et al., 2014). Various abiotic factors, such as salinity, nutrient deprivation, drought, heavy metals, high light, and extreme temperature, result in a range of adverse effects in plants

and lead to the overproduction of reactive oxygen species (ROS), which are highly reactive, resulting in oxidative stress (Faseela et al., 2020). ROS are unavoidably produced in the cell, and thus they may have an important function as signaling molecules (Lamers et al., 2008). Nevertheless, an imbalance of ROS causes strong oxidative damage as they react with proteins, lipids, and nucleic acids to produce their oxidation (Das and Roychoudhury, 2014). Microalgae cope with oxidative stress by accumulating antioxidant compunds, many of them valuable to human health.

1.2. Oxidative stress generation in microalgae

Light is essential to photosynthetic microorganisms. However, when light intensity overpasses photosynthetic rate, the supply of electrons at PSII exceeds its capacity to accept electrons, i.e. an excess reduction rate of the primary acceptor of electrons Q_A, causing imbalances between Q_A/Q_A^- (Mandal et al., 2022). At this point, the photosynthetic chain becomes blocked; thus, to reduce the excess of electrons, molecular oxygen (O_2) accepts a single electron but inevitably generating ROS (Foyer and Hanke, 2022; Mandal et al., 2022). Superoxide radical ($O_2\bullet^-$), besides singlet oxygen, is usually the first ROS to be formed, as represented in Figure 1.2. When $O_2\bullet^-$ is reduced by a second electron, hydrogen peroxide (H_2O_2) is produced, these species undergo transformation into the more reactive and toxic form, hydroxyl radical (•OH) (Halliwell, 2006). This oxygen species causes oxidative damage in cell membranes as •OH groups attack the double bonds of phospholipids giving rise to epoxy groups, which promotes stronger membrane lipids hydrocarbon chains interaction, thus resulting in membrane fluidity loss. Moreover, •OH can also attack DNA nitrogen bases, giving rise to mutations that seriously impair cell life (Das and Roychoudhury, 2014).

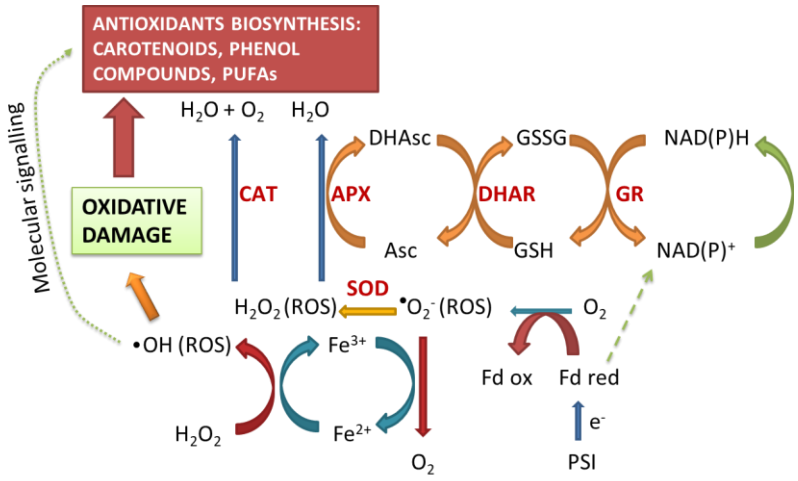

Figure 1.2. Reactive oxygen species (ROS) formation and antioxidant enzymatic system in microalgae. GSSG: Oxidized Glutathione; GSH: Reduced Glutathione; NADP(+,H): nicotinamide adenine dinucleotide phosphate (oxidized, reduced); Asc: reduced ascorbate; DHAsc: dehydroascorbate; CAT: catalase; SOD: superoxide dismutase; APX: ascorbate peroxidase; DHAR: dehydroascorbate reductase; GR: glutathione reductase; Fd red: reduced ferredoxin, with electrons from PSI; Fd ox: oxidized ferredoxin.

In turn, Fe is necessary for microalgae as it plays a key role in cellular biochemistry due to its redox properties (Gao et al., 2022). However, Fe becomes highly toxic at relatively

high concentrations due to its oxidative action through the Fenton reaction, which leads to the production of ROS. This reaction is represented in Figure 1.2 and consists of an oxidation process catalyzed by transition metals, usually iron, in which highly ROS, such as the HO•, are generated from H_2O_2 (Gulcin and Alwasel, 2023).

Similarly, when microalgae are N-deprived, the synthesis of N-rich biomolecules (proteins, chlorophylls) is decreased, leading to growth limitation (Markou et al., 2017). Additionally, chloroplast division is inhibited, which provokes a decrease in the number of thylakoid membranes per chloroplast unit while the synthesis of D1 protein also decreases, resulting in the synthesis of fewer functional RCs (Kolber et al., 1988). Salinity stress in plants leads also to growth inhibition, leaf chlorosis, malfunction of the chloroplasts, and photoinhibition (Dąbrowski et al., 2016). Additionally, salinity stress mainly inhibits the repair of photodamaged PSII and suppresses the de novo synthesis of D1 proteins (Allakhverdiev et al., 2002). Damages in, or inactivation of PSII-RCs affect the electron transport chain (ETC) which, in turn, could end in a generation of ROS (Mandal et al., 2022).

1.3. Microalgae as a source of antioxidant compounds.

As indicated above, microalgae in nature are usually subjected to abiotic stress, which may be due to changes in the salinity of the environment, temperature variation, ultraviolet radiation, lack of nutrients or the presence of metal cations, among other factors. Under these extreme conditions, microalgae produce certain metabolites to maintain homeostasis by resolving and minimizing the impact of stress. Some metabolites produced to counteract the stress impact have commercial value (Paliwal et al., 2017), including chlorophylls, terpenoids, phenolic compounds, polyunsaturated fatty acids (PUFAs) and even polysaccharides (Figure 1.3), among others, with antioxidant, antimicrobial and anti-inflammatory bioactivity. PUFAs, particularly long chain omega-3 fatty acids, are highly susceptible to oxidation, as their double bonds are targeted by ROS, producing lipoperoxides. Carotenoids are antioxidant molecules, and microalgae increase their intracellular concentration to neutralize excess free radicals derived from oxidative stress (Ferrat et al., 2003). Polyphenols quench free radicals, and this chemical capacity has evidenced their efficiency in cellular protection against oxidative stress. Flavonoids display a range of cell functions including acting as redox transfer moieties and UV radiation dissipation.

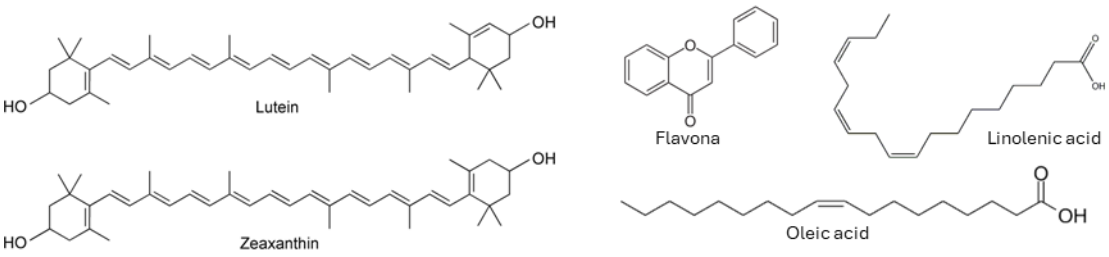

Figure 1.3. Structure of target antioxidant molecules containing double bonds and chemical groups able to quench free radicals.

The above-mentioned biomolecules are represented in Figure 1.3 and share common applications based on their proven antioxidant capacity: a number of microalgal PUFAs, carotenoids and phenolic compounds have been reported to display biological activities valuable to human health, including anticancer, antioxidant and anti-inflammatory capacities (Goiris et al., 2014; Montero-Lobato et al., 2018). Therefore, incubation conditions for microalgae cultures leading to the accumulation of these molecules would be highly useful to design efficient biotechnological processes to obtain extracts with potential bioactivity. Although extensive research is being conducted in this field, selecting microalgal species that exhibit robust and productive growth while being suitable to produce specific target compounds remains challenging, as biological contamination by other microalgal species can rapidly lead to culture collapse.

1.4. Potential of extremophilic microalgae.

Considering the climate change scenario and, therefore, the increasing environmental changes which increase abiotic stress levels, the study of extremophilic microorganisms gains interest. That is, most microorganisms live in moderate temperature environments, from 15 to approximately 37 °C, pH around 7, salinity between 0.9 and 3 % and atmospheric pressure. However, extremophilic microorganisms are able to live under extreme conditions, such as acidic conditions, extreme aridity, high salinities, high or very low temperatures, by means of the expression of adaptation mechanisms (Canganella and Wiegel, 2011). Thus, these microorganisms have a greater adaptation capacity to cope with harsh oxidative conditions of their habitats. This adaptability is partly based on the expression of secondary metabolic pathways leading to the biosynthesis of unique, valuable molecules with applications in human and animal health. These molecules include highly antioxidant phenolic compounds, peptides, indole derivates and terpenes, among other valuable biomolecules groups (Robles et al., 2023). The study of extremophilic microorganisms allows us to understand the limits of life on earth, thus providing answers to fundamental questions about the origin, distribution, and evolution of life (Varshney et al., 2015).

This is the case of the microalga species studied in this thesis, *Coccomyxa onubensis* (*C. onubensis*). The microalga was isolated from Tinto River (Figure 1.4). The so-called "red river" flows along 100 km from the Iberian Pyrite Belt down to the Atlantic Ocean and is one of the most extensive examples of extreme acidic environments, exhibiting low pH values in the range of 1.7 to 3.1 and presence of cations in solution, of which Fe (II) and (III) and Cu (II) have a relevant quantitative presence (Amils et al., 2014; Fernández-Remolar et al., 2003). In spite of these extreme conditions, this river has been reported to contain a high level of biodiversity, including many eukaryotic organisms (algae, fungi, and protists) as the main contributors to the biomass production in the river (Garbayo et al., 2008; López-Archilla et al., 2001). It has been shown that the extremely acidic conditions of the Tinto River basin are not just the product of 5,000 years of mining activity in the area but the consequence of an active underground bioreactor that obtains its energy from the oxidation of sulfur minerals of the Iberian Pyrite Belt (Amils et al., 2014). The bio-oxidation of pyrite produces a sulfate-enriched

acidic solution (pH roughly between 1 and 3) that prevents ferric iron precipitation (Fernández-Remolar et al., 2003), contrary to what occurs in neutral conditions. Several photosynthetic microalgae species adapted to the low pH and the oxidative stress produced by the dissolved metal ions in the river, in addition to strong metal tolerance has been found in the river (Garbayo et al., 2012). This is the case of *C. onubensis* (Fuentes et al., 2016), microalga of study in this thesis, and *Elliptochloris* sp. (chapter 7 of this thesis).

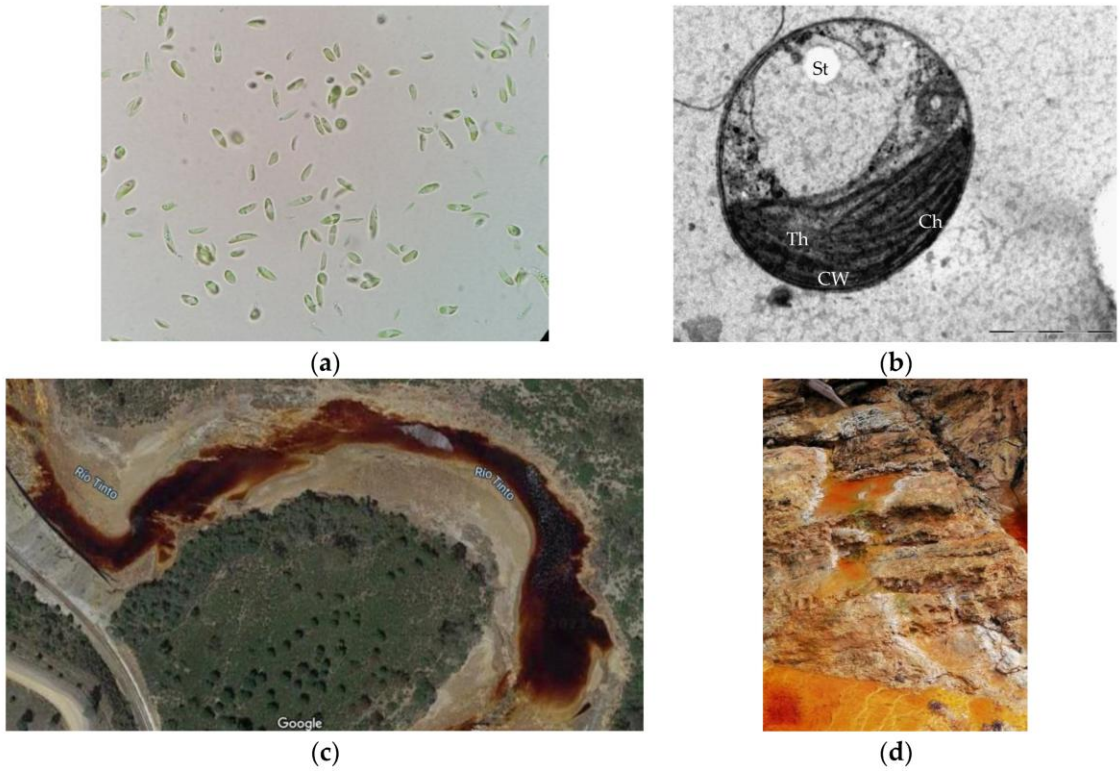

Figure 1.4. *C. onubensis*: light, 100x amplification (**a**) and transmission electron microscopy (**b**), scale bar 1 µm (x 30,000). Abbreviations: Ch, Chloroplasts; Th, Thylakoids; St, Starch grains; CW, Cell wall. Tinto River: Satellite image of google maps (**c**) and sampling location (**d**).

This ability of microalgae to adapt to the acidic environment might be due to the impermeability of the plasma membrane to protons, among other reasons. This allows the cells maintaining a neutral cytoplasmic pH, also supported by a highly active ATP-synthase activity that pumps protons out of the cell. This leads to the maintenance of high proton concentrations in the extracellular medium, considerably increasing the osmotic pressure that also confers moderate halotolerance to acidotolerant microalgae (Gimmler et al., 1988; Gross, 2000), as it is also the case of *C. onubensis* (Fuentes et al., 2016). Maintaining a neutral intracellular pH in an acidic environment requires energy, which reduces the energy available for growth (Messerli et al., 2005). Low energy levels, along with the low availability of dissolved inorganic carbon in acidic water, may limit biomass productivity in large production processes. However, in an acidic environment, microalgae have developed strategies to compensate for this low inorganic carbon availability by evolving mechanisms to improve carbon uptake (Vaquero et al., 2013). This allows these extremophilic microorganisms, such as *C. onubensis*, to show

moderate levels of productivity in acidic liquid cultures. The membrane adaptability to the acidic environment might also partly explain the capability of *C. onubensis* to grow in high concentrations of Fe (III) (as high as 30 $g \cdot L^{-1}$) in its natural habitat (Fernández-Remolar et al., 2004).

The described natural adaptability makes *C. onubensis* a suitable candidate for this thesis. For the reasons explained above, including the cited scientific evidence, it is thought that the microalga must be adapted to cope with different salt and Fe (III) levels, high irradiance levels, and nitrogen limitations, among others. The ability of *C. onubensis* to survive in such an extreme environment is largely due to its capacity to activate secondary metabolic pathways leading to the biosynthesis of unique and valuable antioxidant molecules. Among these bioactive compounds, carotenoids (primarily lutein), polyphenols and PUFAs, such as linolenic and linoleic acids, are main representatives which have applications in both human and animal health (Navarro et al., 2016). Furthermore, the cultivation of *C. onubensis* at acidic pH offers a significant advantage for open-system production, as it naturally limits the growth of opportunistic contaminants (Fuentes et al., 2016).

In addition to *Coccomyxa*, in this Thesis we have explored specific characteristics of the cultivation of two other extremophilic microalgae, *Chroococcidiopsis* sp. (cyanobacterium from endolithic, hyper-arid environment, Atacama) and *Elliptochloris* sp. (microalga from hyper-acidic habitat, Tinto River). The study of these species was aimed at obtaining initial key information of their production, as a first step toward the analysis of their biotechnological potential.

2. Aims and thesis outline

This Thesis aims to explore the biotechnology potential of a highly acidic-habitat microalga isolated from the acidic water of Tinto River by inducing oxidative stress levels in the microalga to induce its antioxidant response. As reported above, this environment is known for its harsh conditions for life, including high levels of metals in solution, mainly Fe (II), Fe (III), and Cu (II), and a pH range of about 1.7–3.1. Moreover, *C. onubensis* proliferates in the abovementioned habitat with a nitrogen concentration as low as 0.05 mM nitrate, which is also an eventual sign of the possible adaptability of the microalga to N-deficient media. In acidic waters, CO_2 is not solved in the form of bicarbonate, and its bioavailability depends on each microalga´s capacity to incorporate CO_2. O_2 in acidic waters limits the growth of photosynthetic species to the superficial layer of the acidic waters where carbon and oxygen availability are greater. Consequently, the photosynthetic apparatus of the acidotolerant microalga must be able to adapt to the high PAR and UV irradiance levels of the region. *C. onubensis* has also been described as a halotolerant species, being able to grow in media with salt concentrations of about 500 mM. The described natural adaptability makes *C. onubensis* a suitable candidate for this thesis outline.

For the reasons explained above, **chapter 2** explores the adaptative photosynthetic response of the microalga when exposed to certain abiotic stress factors and levels. Based on the above-mentioned conditions of the natural environment of the microalga, different levels of Fe (III), nitrogen limitation, high irradiance and salt stress was selected as abiotic stress conditions in this chapter. Some studies have shown that rapid chlorophyll fluorescence (ChlF) can be used as an effective tool to estimate the effect of various stress factors on plants. Accordingly, this chapter evaluates the growth, viability and photosynthetic performance by using ChlF technology of the highly acidic-habitat microalga *C. onubensis*, after exposure to the above-mentioned abiotic stress factors.

In turn, in **chapter 3** we evaluate the possibility of maintaining the microalga in a long-term cultivation based on repeated-batch cultivation in an air-fluidized bag system. At the same time, biomass samples were analyzed in order to determine the optimal growth stage to maximize the recovery of valuable compounds. Prior to the long-term cultivation, the growth of the microalga and the accumulation of valuable molecules was studied based on the variation of temperature, Fe (III) and light levels in a factorial 3^3 experiment, in order to optimize these growth-influencing factors for efficient biomass production.

The referred adaptability of the microalga to nitrogen limitation in its natural habitat motivated us to analyze some of their physiological and metabolic responses, which are described in **chapter 4**. We analyzed growth viability under different degrees of nitrogen limitation and the variation in the biosynthesis and accumulation of different valuable compounds. Considering that culture conditions leading to nitrogen limitation results in a limited synthesis of N-rich molecules (proteins and chlorophylls), we make special emphasis in chapter 4 to the variation of fatty acids content and the analysis of the fatty acid profile of the microalga under nitrogen limitation.

Based on the photosynthetic response of *C. onubensis* to increasing Fe (III) levels found in chapter 2, in **chapter 5** we analyze the effect of different levels of Fe (III) on the microalga viability and its antioxidant response. In this sense, the photochemical activity of *C. onubensis* stressed cells under Fe (III) addition was less negatively affected than that of common microalgae under similar conditions. That is also coherent with previous reports referring to the strong enzymatic antioxidant response of *C. onubensis* when subjected to oxidative stress. We hypothesize that modulated stress triggered by Fe (II) and/or Fe (III) in acidophilic or acid-tolerant microalgal cultures, adapted to cope with oxidative conditions, might address increased productivity of antioxidant molecules (flavonoids, other phenolic compounds, PUFAs and/or carotenoids). Thus, this study analyzes the microalgal growth and antioxidant response of *C. onubensis* to Fe-mediated stress, attempting to find a suitable balance between stress and growth: triggering accumulation of antioxidant molecules while preventing culture productivity from decaying.

The results obtained in chapter 5 suggest that modulation of Fe (III) allows producing an antioxidant-rich biomass in *C. onubensis* cells. Among these molecules, terpenoids, such as astaxanthin and lutein, (poly)phenolic compounds (e.g. caffeic and gallic acids), polyunsaturated fatty acids, and sterols have been described to display anti-inflammatory effects. Therefore, in **chapter 6** we analyze the anti-inflammatory activity of microalgal extracts in THP1 cells as a function of Fe (III) concentration and microalgal growth stage. Additionally, we compare the anti-inflammatory capacity of the extracts with the antioxidant activity and the target antioxidant compounds produced by the microalga with the aim to determine the antioxidant compounds that have a greater impact in the anti-inflammatory response of the extracts.

Finally, in **chapter 7** we explore the potential of other extremophiles for their efficient production and accumulation of valuable compounds. The study of these species was aimed at obtaining initial key information of their production, as a first step toward the analysis of their biotechnological potential. This is the case of *Elliptochloris* sp. isolated also from the acidic waters of Tinto River, whose ability to grow mixotrophically was studied. Photoautotrophic algal cultivation is challenging due to the shadowing effect produced by an increase in the number of cells. Under such circumstances, the use of an extra organic carbon source supports activities in the cell related to metabolic energy production, while promotes fatty acid biosynthesis in the chloroplast. Thus, in this chapter the growth and photosynthetic viability of the microalga was studied together with variation in fatty acid compounds. On the other hand, the extremotolerant cyanobacterium *Chroococcidiopsis* sp. isolated from the hyper-arid Atacama Desert (north Chile) has been described to growth in an aggregate form to protect itself from the extreme radiations of the area. Despite the benefits of the aggregates to dissipate part of the radiation, this growth pattern limits the light availability of the inner cells resulting, therefore, in a growth limitation. In this sense, in this chapter we analyze the effect of ultrasound treatment as a tool to disaggregate cells and increase the productivity of the cyanobacterium.

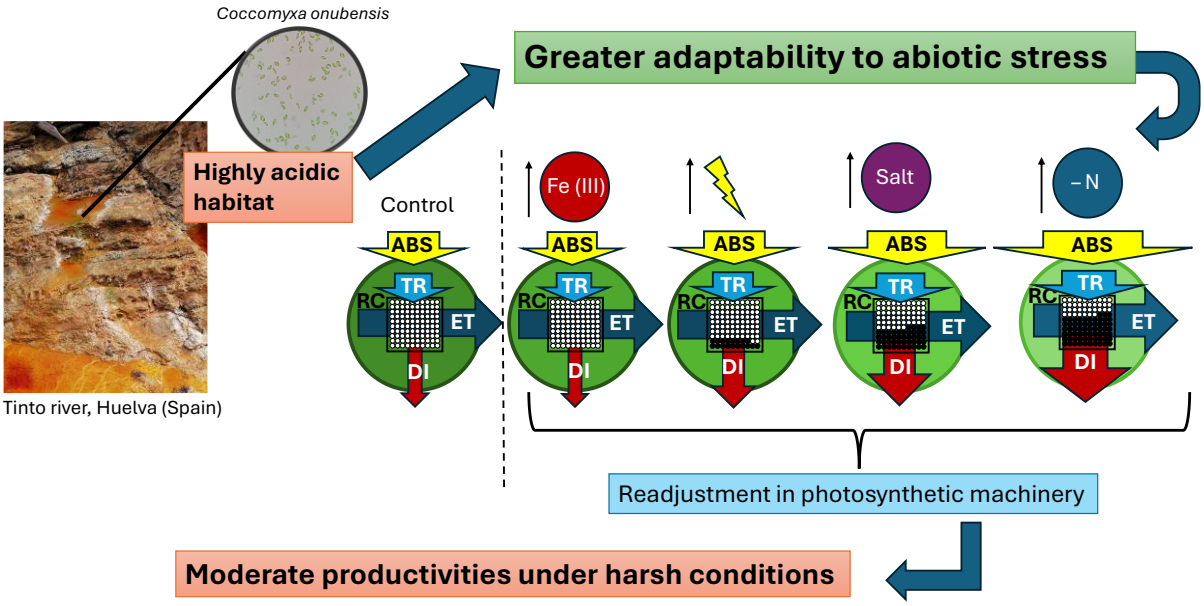
Coccomyxa onubensis
Tinto river, Huelva (Spain)
Highly acidic habitat
Greater adaptability to abiotic stress
Control
Fe (III)
Salt
– N
ABS
TR
RC
ET
DI
Readjustment in photosynthetic machinery
Moderate productivities under harsh conditions

CHAPTER

2

Photosynthesis of a highly acidic-habitat microalga under abiotic stress

Table of contents

Abstract: The current energy model strongly affects the environment because of the emission of CO_2 into the atmosphere, which significantly contributes to climate change. Under such conditions, microalgae can serve as an alternative, suitable natural source to produce essential nutrients, and their biomass can alternatively be used as raw material to generate biofuels. However, climate change generates abiotic stress that substantially reduces the yields of organisms in affected regions. Extreme microorganisms have naturally adapted to cope with extreme physicochemical conditions. In this study, we evaluated the response of *Coccomyxa onubensis* (*C. onubensis*), a microalga isolated from a highly acidic-habitat when exposed to different stressors. Based on the natural habitat, the results obtained revealed a noticeable adaptability of the microalga to the imposed abiotic stress factors, salt, Fe (III), high irradiance and nitrogen limitation. *C. onubensis* responds to Fe (III) or high irradiance stress by reducing the antenna size to maximize the photosynthetic use of light, resulting in higher biomass productivity relative to control cells. Additionally, although the cultivation of *C. onubensis* under nitrogen limitation or salt stress significantly affects the photosynthetic chain of the microalga, the photosynthetic efficiency values obtained remained close to those typically observed in viable algal cultures. Furthermore, moderate biomass productivity values were also obtained. These adaptation capabilities can be further applied to the biomass production of microalgae under abiotic stress caused by climate change, providing insights into various areas relevant to society, such as animal and human nutrition, health, agriculture, and water treatment.

Keywords: Photosynthesis performance, highly acidic-habitat microalga, abiotic stress factor, NPQ protocol, biomass productivity, climate change.

1. Introduction

Environmental pollution has increased since the beginning of the industrial revolution in the 19th century and it has become a transnational issue that affects ecosystems, air, water, and soil, and is directly related to human health and well-being (Tarafdar et al., 2023). Extreme environmental contamination has primarily been caused by carbon dioxide emission (from burning of fossil fuel, industrialization, human activities, among others) (Singh and Dhar, 2019). The accumulation of CO_2 in the atmosphere traps the IR radiation emitted from the surface of the Earth following absorption of sunlight and heats our planet, driving an alarming trend of continual increase in global surface and ocean temperatures, termed global warming (Zandalinas et al., 2021). Global warming in turn drives a drastic change in our environment that is accompanied by an increase in the frequency and intensity of droughts and heat waves, as well as of other abiotic stress conditions such as flooding, salinity, and freezing stresses.

In this sense, abiotic stress factors are major environmental problems that negatively influence plant growth and development and ultimately decrease agricultural production worldwide (Rodziewicz et al., 2014). Various abiotic factors, such as salinity, nutrient deprivation, drought, heavy metals, high irradiance, and extreme temperature, result in various adverse effects in plants and lead to the overproduction of reactive oxygen species (ROS), which are highly reactive, resulting in oxidative stress (Faseela et al., 2020). ROS are unavoidably produced in cells; thus, they have important functions as signaling molecules (Lamers et al., 2008). However, an imbalance of ROS causes strong oxidative damage, as they react with proteins, lipids, and nucleic acids, resulting in their oxidation (Das and Roychoudhury, 2014).

Reactive oxygen species (ROS) originate from electron transport processes, with the photosynthetic electron transport chain (ETC) acting as a major source of electrons for ROS reduction processes (Foyer and Hanke, 2022). For example, light is essential for microorganisms that perform photosynthesis. However, when the light intensity exceeds the photosynthetic rate, the supply of electrons to the PSII quencher pool exceeds its capacity to accept electrons, i.e., the primary acceptor of electron Quinone A (Q_A) undergoes excess reduction, thus causing imbalances in the Q_A/Q_A^- ratio (Mandal et al., 2022). At this point, the photosynthetic ETC gets blocked; molecular oxygen (O_2) can accept a single electron, which contributes to a decrease in the excess electrons in the photosynthetic electron flow, thus leading to ROS production (Foyer and Hanke, 2022; Mandal et al., 2022). Along with singlet oxygen, superoxide radical ($O_2\bullet^-$) is usually the first ROS to be formed. When $O_2\bullet^-$ is reduced by a second electron, hydrogen peroxide (H_2O_2) is produced, and these species transform into the most reactive and toxic form, hydroxyl radical (•OH) (Halliwell, 2006). This oxygen species causes oxidative damage to the cell membrane, as •OH groups attack the double bonds of phospholipids, giving rise to epoxy groups, which promote stronger membrane lipid hydrocarbon chain interactions, thus addressing the loss of membrane fluidity. Moreover, •OH can attack the nitrogen bases in DNA, resulting in mutations that greatly reduce cell survival (Das and Roychoudhury, 2014).

Iron (Fe) is necessary for microalgae, as it plays a key role in cellular biochemistry due to its redox properties (Gao et al., 2022). However, Fe becomes highly toxic at high concentrations because of its oxidative action through the Fenton reaction, which leads to the production of ROS. This reaction consists of an oxidation process catalyzed by transition metals, usually iron, in which high levels of ROS, such as the hydroxyl radical (HO•), are generated from H_2O_2 (Gulcin and Alwasel, 2023).

Similarly, when microalgae are deprived of N, the synthesis of N-rich biomolecules (proteins, chlorophylls) becomes inhibited, which leads to growth limitations (Markou et al., 2017). Additionally, chloroplast division is inhibited, which leads to a decrease in the number of thylakoid membranes per chloroplast, while the synthesis of D1 protein also decreases, resulting in the synthesis of fewer functional RCs (Kolber et al., 1988). Salinity stress in plants also leads to growth inhibition, leaf chlorosis, chloroplast malfunction, and photoinhibition (Dąbrowski et al., 2016). Salinity stress mainly inhibits the repair of photodamaged PSII and suppresses the *de novo* synthesis of the D1 protein (Allakhverdiev et al., 2002). Damage to or inactivation of PSII RCs affects the ETC, which, in turn, can lead to ROS production (Mandal et al., 2022).

Studying extremotolerant microorganisms allows us to understand the limits of the conditions in which life is possible, thus providing answers to fundamental questions about the origin, distribution, and evolution of life (Varshney et al., 2015). Additionally, these microorganisms have a greater ability to adapt to different oxidative conditions because of the harsh conditions of their habitats. This adaptability is partly based on the expression of secondary metabolic pathways leading to the biosynthesis of unique, valuable molecules with applications in human and animal health. These molecules include highly antioxidant phenolic compounds, peptides, indole derivates, and terpenes, among other valuable biomolecule groups (Robles et al., 2023).

Coccomyxa onubensis (*C. onubensis*) is a highly acidic-habitat microalga isolated from the acidic waters of the Tinto River (Huelva). This environment is known for its harsh conditions for organisms, including high levels of metals in solution, mainly Fe (II), Fe (III), and Cu (II), and a pH range of about 1.7–3.1 (Amils et al., 2014). The Fe (III) concentration in the Tinto River waters are as high as 30 $g \cdot L^{-1}$ (Fernández-Remolar et al., 2004). The lower solubility of CO_2 and O_2 in acidic waters limits the growth of photosynthetic species to the superficial layer of the acidic waters where carbon and oxygen availability are greater. Consequently, the photosynthetic apparatus of the acidotolerant microalga must be able to adapt to the high PAR and UV irradiance levels of the region (Gómez et al., 2007). *C. onubensis* has also been described as a halotolerant species, being able to grow in media with salt concentrations of about 500 mM (Fuentes et al., 2016). Moreover, *C. onubensis* proliferates in the abovementioned habitat with a nitrogen concentration as low as 0.05 mM nitrate (Bottaro et al., 2025), which is also an eventual sign of the possible adaptability of the microalga in N-deficient media. The described natural adaptability makes *C. onubensis* a suitable candidate for this study.

For the reasons explained above, including the cited scientific evidence, it is thought that the microalga must be adapted to cope with different salt and Fe (III) levels, high irradiance levels, and nitrogen limitations. Some studies have shown that rapid

chlorophyll fluorescence (ChlF) can be used as an effective tool to estimate the effect of various stress factors on plants (Kalaji et al., 2016). A key advantage is that ChlF technology is noninvasive, which allows valuable information about the photosynthetic process to be obtained without destroying or even damaging the tested samples (Falcioni et al., 2023). Studies on the photosynthetic performance of microalgae that are found in extreme environmental conditions (e.g., pH < 3) are scarce. The only related reference found in indexed journals (JCR) describes the photosynthetic activity performance of low-pH and heavy metal-tolerant phototrophic biofilms (Souza-Egipsy et al., 2011). Accordingly, the present study could be the first attempt to evaluate the viability and photosynthetic performance of the highly acidic-habitat microalga *C. onubensis*, after exposure to the abovementioned abiotic stress factors.

2. Materials and methods

2.1. Microalgal strain and culture conditions

The organism used for this work was the microalga *Coccomyxa onubensis* ACCV1 (SAG 2510), an acidotolerant and halotolerant microalga isolated from the acidic waters of the Tinto River (Huelva) in the sampling area at latitude 37.5851153° and longitude −6.550754°, by Microalgae Biotechnology Unit (BITAL), of the Department of Chemistry "Professor Jose Carlos Vílchez Martín," from the Faculty of Experimental Sciences and CIQSO of the University of Huelva, Spain (Fuentes et al., 2016).

C. onubensis was grown in an optimized liquid culture medium, K9. The constituents of K9 (per liter) were as follows: 3.95 g K_2SO_4, 0.1 g KCl, 0.5 g K_2HPO_4, 0.41 g $MgCl_2$, 2.29 g KNO_3, 0.01 g $CaCl_2$, and 5 mL of Hutner traces, which were prepared as previously described (Garbayo et al., 2012), containing a Fe (II) concentration of 17.98 µM. Fe is more bioavailable at low pH than at neutral or basic pH, Fe (III) was used in this study because it is more soluble than Fe (II) (Johnson et al., 2012). *C. onubensis* cultures were prepared at an initial concentration of, approximately, 0.2 $g \cdot L^{-1}$, from a mother culture in the middle of the linear growth phase, the pH was adjusted to 2.5. As summarize in Table 2.1, the cultures were subjected to different abiotic stress factors: Fe (III) stress, added at 2 mM in the form of $FeCl_3 \cdot 6H_2O$ (VWR, Belgium); salt stress, added at 300 mM in the form of NaCl; nitrogen limitation stress, added at 10 µM in the form of KNO_3 and high irradiance stress at 900 µmol (photon)$\cdot m^{-2} \cdot s^{-1}$. The level at which the abiotic stress factors were selected was based on previous studies (Robles et al., 2023) and unpublished data. The cultures were established in a culture room at 25 °C ± 2. Light was supplied by white light fluorescent tubes, reaching the cultures at a constant irradiance of 150 µmol (photon)$\cdot m^{-2} \cdot s^{-1}$ (900 µmol (photon)$\cdot m^{-2} \cdot s^{-1}$ for the culture exposed to high irradiance) for 24 h, and the cultures were bubbled with air enriched with 2.5% (v/v) CO_2.

Table 2.1. Abiotic stress culture conditions selected for *C. onubensis*.

Culture condition	Control	Fe (III)	Irradiance	- N	Salt stress
Irradiance (µmol photon$\cdot m^{-2} \cdot s^{-1}$)	150	150	**900**	150	150
Fe (mM)	0.01798	**2**	0.01798	0.01798	0.01798
NaCl (mM)	-	-	-	-	**300**
NO_3^- (mM)	26	26	26	**0.01**	26

Abbreviature: —N (nitrogen limitation culture).

2.2. Growth and biomass productivity determination

Growth was followed by measuring optical density (OD) of the cultures at 750 nm in a Cary 60 UV–Vis spectrophotometer (Agilent Technologies, USA) equipped with temperature control system adjusted to 25 °C. The OD_{750} data expressed in absorption

unit (UA) provided information of culture turbidity, which is proportional to the amount of biomass present in the culture (Shuler and Kargi, 2005).

Productivity, the increase in biomass in a culture over time, was calculated through the following equation:

$$Productivity\ (g \cdot L^{-1} \cdot d^{-1}) = \frac{C_t - C_0}{t_t - t_0}$$

where C_t and C_0 represent the cell density for times t and zero. Cell density was determined by measuring the dry weight (dw) of the biomass contained in 2 mL of culture medium.

2.3. Photosynthetic performance determination

Photosynthetic performance of the microalga after exposing to different abiotic stress parameters were measured with the portable PAM fluorimeter AquaPen-C AP-C 100 (Photon Systems Instruments, Czech Republic) using the FluorPen 1.1.2.6 software to access the data. Culture samples were diluted so that all Chl fluorescence measurements were performed on samples with the same cell concentration, OD_{750} = 0.2 (OD_{750}, optical density at 750 nm). OJIP test and NPQ protocol were performed in 15 min dark-adapted cells. The typical polyphasic OJIP curve provides information on the kinetics and heterogeneity involved in the reduction of the plastoquinone (PQ) and Q_A which is the primary electron acceptor. In addition, by analyzing the Chl fluorescence transients of the OJIP test, different JIP parameters could be calculated which are described in Table 2.2 and discussed throughout the text. On the other hand, NPQ protocol is the most typically used measuring approach to quantify photochemical and non-photochemical quenching.

The Chl fluorescence transients of the OJIP test were obtained using an actinic light and based on the procedure described below. Routinely, the F_0 (fluorescence rise of the O phase) was recorded at time of 50 ls, the F_J (fluorescence rise of the J phase) at time 2 ms, F_I (fluorescence rise of the I phase) at 60 ms, and F_M was the maximum of fluorescence recorded in test (typically at 250–400 ms). The Chl fluorescence analysis in the present study was based on the Q_A model and energy fluxes described by (Strasser et al., 2000). Briefly, as it is illustrated in Figure 2.1, photons are absorbed by the antennae pigments (ABS) resulting in their excitation (Chl*). Part of this excitation energy is dissipated, mainly as heat and less as fluorescence emission F, and another part is channeled as trapping flux (TR) to the reaction center RC and converted to redox energy by reducing the electron acceptor Q_A to Q_A^-, which is then reoxidized to Q_A thus creating an electron transport (ET) that leads ultimately to CO_2 fixation. OJIP curves were normalized to intracellular chlorophyl concentration.

Table 2.2. Terms and formulae of the JIP parameters used in this study calculated by analyzing the Chl fluorescence transients of the OJIP test.

Parameters	Formulae	Terms
F_0	$F_{50\mu s}$	Fluorescence intensity at 50μs, minimal fluorescence level
F_M	-	Maximal fluorescence intensity
F_V	$F_M - F_0$	Variable fluorescence
V_J	$(F_{2ms} - F_0)/ (F_M - F_0)$	Relative variable fluorescence at 2 ms (J step),
$M_0 \equiv dV/dt$	$4\cdot(F_{300} - F_0)/ (F_M - F_0)$	Normalized value of the initial slope, net rate of closure of the RCs
F_V/F_M	-	Maximum quantum yield of PSII
F_V/F_0	-	Maximum primary yield of photochemistry of PSII
N	$S_M\cdot M_0\cdot(1/V_J)$	Turn-over number Q_A
Area	$\int_0^{t_{Fmax}} (F_M - F_t)dt$	Area between fluorescence curve and F_M
S_M	Area / F_V	Normalized Area
ABS/RC	$M_0\cdot(1/ V_J)\cdot(1/ \varphi_{Po})$	Absorption flux per RC
TR_0/RC	$M_0\cdot(1/ V_J)$	Trapped energy flux per RC
ET_0/RC	$M_0\cdot(1/ V_J)\cdot \psi_o$	Electron transport flux per RC
DI_0/RC	(ABS/RC) – (TR_0/RC)	Dissipated energy per RC
$\varphi_{Po} \equiv TR_0/ABS$	$(1 - F_0)/F_M$	Maximum quantum yield of primary photochemistry
$\varphi_{Eo} \equiv ET_0/ ABS$	$(1 - F_0/F_M)\cdot \psi_o$	Probability that an absorbed photon will move an electron into the ETC
$\psi_o \equiv ET_0/ TR_0$	$1 - V_J$	Probability that a trapped exciton moves further than Q_A^-
φ_{Do}	$1 - \varphi_{Po}\cdot F_0/F_M$	Maximum quantum yield of non-photochemical de-excitation
PI_{ABS}	$(1/(ABS/RC)\cdot(\varphi_{Po}/(1-\varphi_{Po}))\cdot(\psi_o/(1- \psi_o)$	Performance index

The NPQ protocol starts by giving a measuring light to acquire minimal level of fluorescence F_0. A short saturating flash of light is then applied to reduce the plastoquinone pool and measure maximum fluorescence in the dark-adapted state, F_M. After a short dark relaxation, the sample is exposed to actinic irradiance for tens to hundreds of seconds to elicit a transient of the Kautsky effect. Moreover, a sequence of saturating flashes is applied on top of the actinic light to probe the nonphotochemical quenching NPQ and effective quantum yield of photosynthesis Qy in light adapted state. After exposure to continuous illumination, the relaxation of non-photochemical quenching is determined by means of saturating pulses applied in dark.

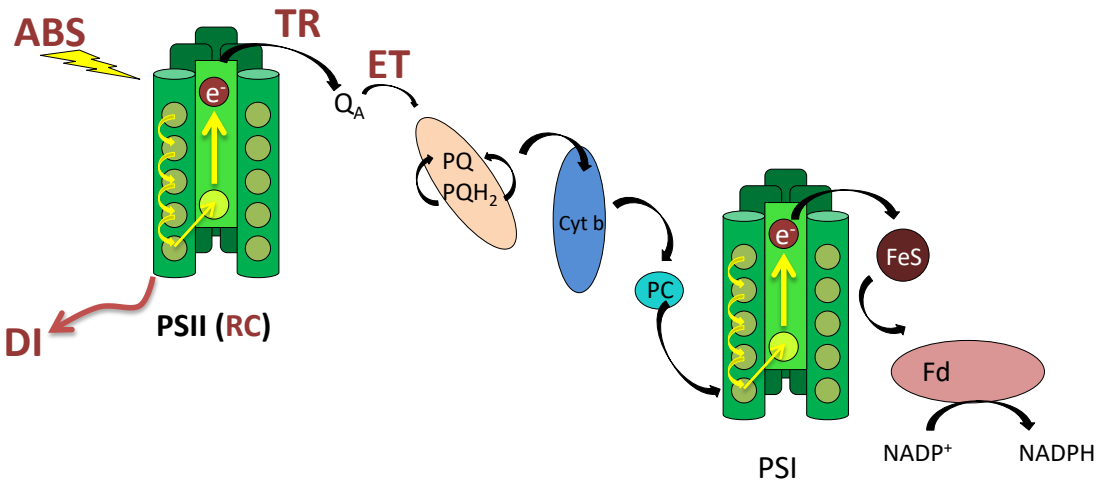

Figure 2.1. Schematic representation of the Q_A model and energy fluxes described by (Strasser et al., 2000) for Chl fluorescence analysis. Abbreviatures: photosystem II; PSI: photosystem I; Q_A: quinone A; PQ: plastoquinone; PQH_2: plastoquinol; FeS: iron/sulfur cluster belonging to redox proteins; Cyt b: cytochrome b6f; PC: plastocyanin; Fd: ferredoxin.

2.4. Chlorophyll determination

Chlorophyll (Chl) content was determined as described by Robles et al. (2023). Culture samples, containing 1 or 2 mL, were centrifuged at 3 *g* for 5 min model Minispin (Eppendorf, Germany), methanol was added to the pellet and the mixture was placed in an ultrasound bath model bath Ultrasons H-D 3000866 (Selecta, Spain) with a power of 330W at 60 °C for 5 min to weaken the microalgal cell wall. After another centrifugation step, the supernatant was collected and analyzed by UV/Visible spectrophotometry. Modified Arnon's equations were used to calculate chlorophyll and carotenoid concentrations in the extracts.

2.5. Statistics

Unless otherwise stated, all data are presented as the mean of three replicates and the standard deviations are shown in the corresponding figures and tables. The data from the different treatments were evaluated by constructing univariate statistical models and performing the analysis of variance (ANOVA) (confidence of 95 % was considered for determining statistical significance). Tukey's test was also applied to identify significant differences between all the treatments studied, without reference to a specific control. All analyses were performed using the Minitab 22 software. Additionally, Principal Component Analysis (PCA) was carried out to get a closer insight into the relation between the measured JIP parameters using infostat/L.

3. Results

As reported in the Introduction section, *Coccomyxa onubensis* (*C. onubensis*) is a microalga found in a highly acidic habitat. It was isolated from the acidic waters of the Tinto River (Huelva). Based on the harsh conditions of this natural habitat, the microalga must adapt to cope with different levels of abiotic stress. Information on the photosynthetic performance of organisms living in highly extreme conditions (e.g., pH < 3) is scarce. Thus, we evaluated the cell viability and photosynthetic performance of *C. onubensis* exposed to high levels (compared to standard culture media) of salt and Fe (III), increasing irradiance levels, and nitrogen limitation.

First, we determined whether the abiotic stress levels selected were within the sublethal range for the microalga. The effects of different abiotic stress factors on the growth of *C. onubensis* were evaluated by analyzing the time-dependent evolution of optical density (OD) at 750 nm and overall biomass productivity (Figure 2.2).

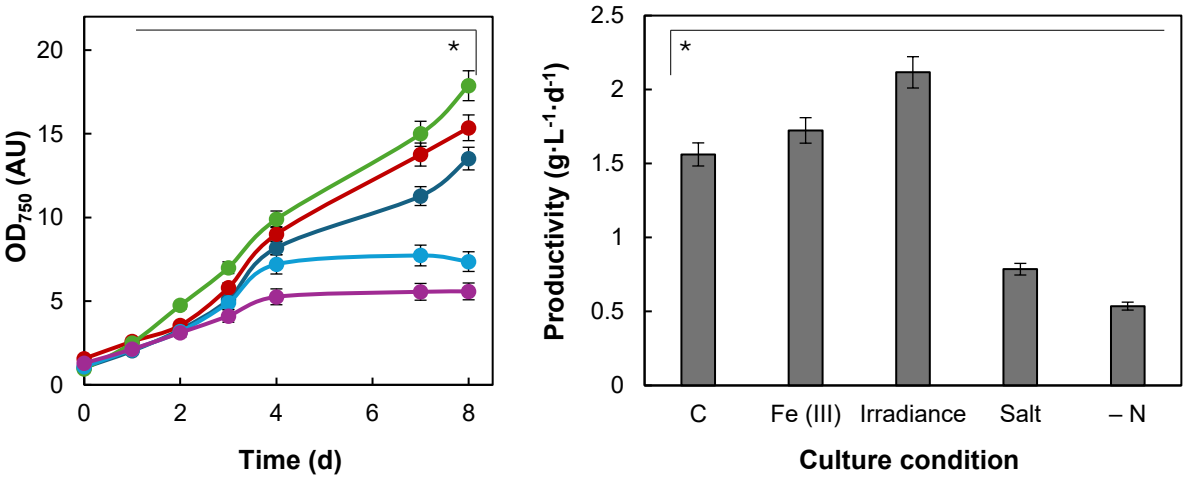

Figure 2.2. Effects of different abiotic stress factors on the growth of the microalga *C. onubensis*. (**a**) Optical density at 750 nm (OD_{750}) and (**b**) biomass productivity. Legend: Control culture (C, dark blue line); Fe (III) stress (Fe (III), red line); high irradiance stress (irradiance, green line); salt stress (salt, light blue line); nitrogen limitation stress (—N, purple line). (*) Represents the significant differences of all treatments relative to the control cultures with 95 % confidence.

Figure 2.2 shows the time-dependent evolution of the growth of *C. onubensis*, measured as optical density (OD) at 750 nm, as a function of the abiotic stress factor to which the microalga was exposed. Similar growth curves were obtained for the cultures grown under high irradiance or Fe (III) stress (Figure 2.2a), except for the last days of cultivation, in which the cultures grown under high irradiance stress presented slightly higher OD values. Both growth curves were steeper than those obtained for the control culture, resulting in higher biomass productivity (Figure 2.2b). In contrast, for the cultures grown under salt or nitrogen limitation stress, a slow-down of growth was obtained, therefore resulting in significantly lower biomass productivity than that recorded for the control culture. These results supported the expected growth reduction under nitrogen limitation/starvation and in the presence of high levels of salt.

Abiotic stress affects the growth of the microalga *C. onubensis*, which might have an impact in the photosynthetic performance. Figure 2.3 shows the effects of abiotic stress factors on the photosynthetic efficiency of PSII ($\mathbf{F_V/F_M}$), which was obtained via Chl fluorescence measurements of dark-adapted culture samples. Considering the variation in growth on day 4 of cultivation, the measurements of the photosynthetic performance of the microalga included in this study belong to this growth stage (four-day, mid-linear growth phase).

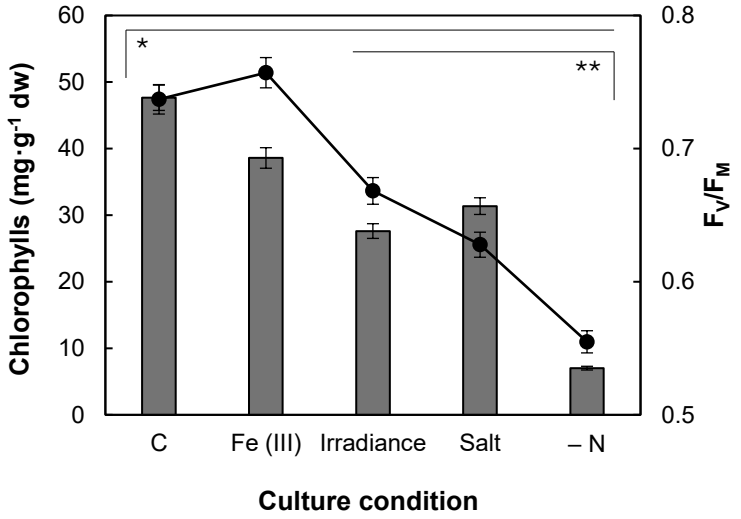

Figure 2.3. Effects of different abiotic stress factors on the photosynthetic efficiency (F_V/F_M, dots) and intracellular chlorophyll concentration (bars) of the microalga *C. onubensis*. The data corresponds to day 4 of cultivation. Symbols: C (control culture), - N (nitrogen limitation stress). (*) Represents the significant differences of all the treatments relative to the control cultures with 95 % confidence for the intracellular chlorophyll concentration (*) and F_V/F_M (**).

Figure 2.3 shows the variations in the photosynthetic efficiency of PSII ($\mathbf{F_V/F_M}$) and the intracellular chlorophyll concentration of *C. onubensis* cultures as a function of the abiotic stress factors to which the microalga was exposed. Cultures grown under Fe (III) stress presented $\mathbf{F_V/F_M}$ values that were slightly greater than those recorded for the control culture, whereas the intracellular chlorophyll concentration was 19 % lower, suggesting an apparent reduction in the size of the antenna to maximize the photosynthetic use of light. On the other hand, when *C. onubensis* was grown under high irradiance, salt, or nitrogen limitation stress, both the $\mathbf{F_V/F_M}$ values and the intracellular chlorophyll concentration were significantly lower than those recorded for the control culture. The cultures grown under nitrogen limitation stress presented the lowest values of $\mathbf{F_V/F_M}$ and cell chlorophyll concentration. Interestingly, inverse tendencies were recorded for *C. onubensis* cultures grown under high irradiance or salt stress, i.e., under high irradiance stress, lower intracellular chlorophyll contents, and higher $\mathbf{F_V/F_M}$ values were recorded than under salt stress for *C. onubensis* cultures.

Along with the parameter $\mathbf{F_V/F_M}$, Chl fluorescence signals can be used to obtain valuable information on the PSII performance status, as is the case for the polyphasic (multiphase) rise of Chl fluorescence transients and OJIP curves (Figure 2.4). Additionally, by analyzing the Chl fluorescence transients of the OJIP test, different JIP

parameters were calculated (Figure 2.5). Several studies have shown that rapid ChlF can be used as an effective tool to monitor the photosynthetic physiological status of plants under abiotic stress (Kalaji et al., 2016). Thus, the next figures show an in-depth analysis of the photosynthetic performance of *C. onubensis* under different abiotic stress conditions.

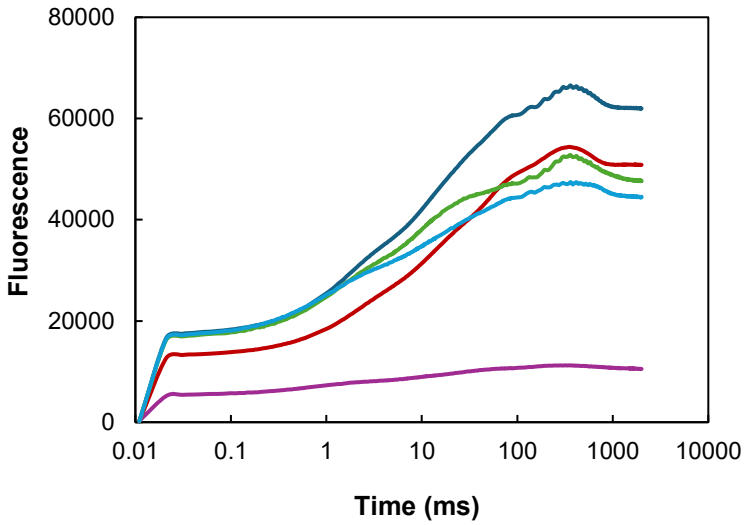

Figure 2.4. Log time scale of Chl fluorescence transients (OJIP test) of *C. onubensis* as a function of abiotic stress factors on day 4 of cultivation. Control culture (dark blue line); Fe (III) stress (red line); high irradiance stress (green line); salt stress (light blue line); nitrogen limitation stress (purple line).

Figure 2.4 shows the log time scale of Chl fluorescence transients (OJIP test) of *C. onubensis* as a function of the abiotic stress factors to which the microalga was exposed. Chl a fluorescence (OJIP) transients showed a typical polyphasic rise in *C. onubensis* cultures. The figure shows that different abiotic stress factors affected the Chl fluorescence intensity emitted by the microalga, as shown by a decrease in the fluorescence level relative to that of the control culture. Cultures grown under high irradiance or salt stress presented similar OJ steps than those recorded for the control culture, whereas a decrease in the J-step was obtained, thus suggesting a lower efficiency in the reduction of Quinone B (Q_B), and therefore, reoxidation of Quinone A (Q_A). On the other hand, cultures grown under Fe (III) or nitrogen limitation stress presented lower O-step values than control culture. The lowest Chl fluorescence transients were obtained when *C. onubensis* was cultivated under nitrogen limitation stress, resulting in an almost straight line. When the OJIP shape is a straight line, electron transport after Q_A is inhibited, and the OEC cannot provide electrons to PSII and reduce PQ (Markou et al., 2016).

Figure 2.5 shows a comparison of values from selected technical fluorescence parameters, the so-called JIP parameters. The values shown in Figure 2.5 were calculated by analyzing the Chl fluorescence transients of the OJIP test as a function of the abiotic stressors to which *C. onubensis* was exposed. The values obtained from stressed cultures were normalized relative to those obtained from the control culture. The regular shape of the spider plot indicates data from the control culture. JIP parameters differ among abiotic stress factors and consequently allow the selection of

those parameters that are specifically and intensively affected under different abiotic stress. The most significant differences in the spider plot obtained for *C. onubensis* were found in cultures grown under salt or nitrogen limitation stress relative to those of the control culture, indicating that photosynthetic performance was more affected by these abiotic stress factors (Table S2.1 of Supplementary Material).

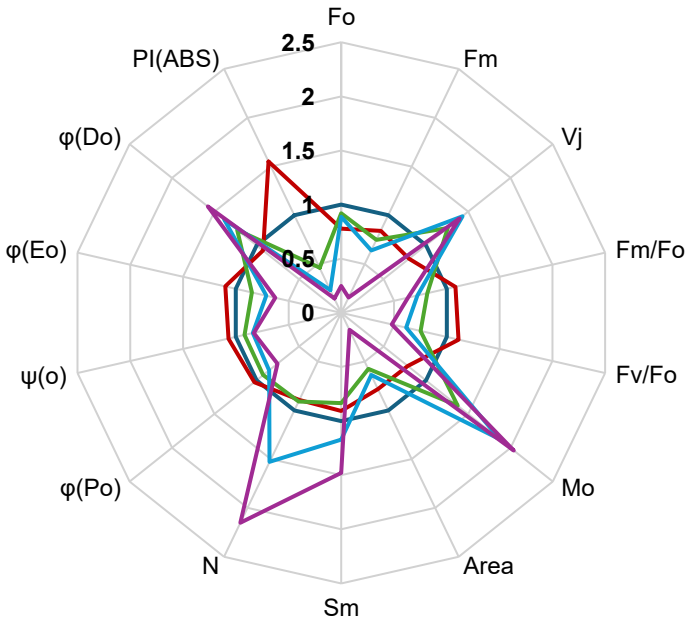

Figure 2.5. Spider plot of selected technical fluorescence parameters normalized to the control culture of *C. onubensis* cultures as a function of abiotic stress factors on day 4 of cultivation. Control culture (dark blue line); Fe (III) stress (red line); high irradiance stress (green line); salt stress (light blue line); nitrogen limitation stress (purple line).

A multiparametric analysis was performed to gain deeper insights into the relationships among the measured JIP parameters. Principal component analysis (PCA) is an exploratory technique that concentrates the information of measured variables in new complex variables that are not correlated with each other (Blackhall et al., 2020). These new variables, called principal components (PCs), are linear combinations of the original variables and explain the maximum variation in the parameters. The PCA results are shown in Figure 2.6, along with the correlation matrix between the different parameters that are presented in Table 2.3. Figure 2.6 explains 97.4 % of the variability of the presented parameters; the first principal component (PC1) accounted for about 87.9 % of the total changes in *C. onubensis* and was explained mainly by $\mathbf{TR_0/RC}$, **ABS/RC**, $\mathbf{DI_0/RC}$, $\boldsymbol{\phi_{Po}}$, $\boldsymbol{\phi_{Do}}$, and $\mathbf{F_V}$, among others, whereas the second component (PC2) accounted for 9.5 % of the changes and was sensitive to $\mathbf{V_J}$, $\mathbf{F_0}$, $\mathbf{ET_0/RC}$, and $\mathbf{PI_{ABS}}$. The figure also shows the JIP parameters that were positively correlated, to a large extent, with the abiotic stress factor tested. Nevertheless, the description and variation of JIP parameters as a function of the specific stress conditions, together with their correlation, are described along with the text.

Figure 2.5 shows how minimal fluorescence ($\mathbf{F_0}$) and maximal fluorescence ($\mathbf{F_M}$), as obtained in Figure 2.4, decreased irrespective of the abiotic stress factor tested. The decrease was greater for the cultures grown under nitrogen limitation stress by (75 and

85 %, respectively) than for the control culture. Several JIP parameters can be calculated through F_M and F_0: variable fluorescence ($\mathbf{F_V = F_M - F_0}$), the maximum primary yield of PSII photochemistry ($\mathbf{F_V/F_0}$) and the maximum quantum yield of PSII ($\mathbf{F_V/F_M}$, Figure 2.3). $\mathbf{F_V/F_0}$ expresses the ratio between the rate constants of photochemical and non-photochemical deactivation of excited Chl molecules; this parameter indicates proper functioning of PSII (Strasser et al., 2000). $\mathbf{F_V/F_0}$ is the most sensitive component of the photosynthetic ETC (Kumar et al., 2020). $\mathbf{F_V/F_0}$ decreased by 25, 49 and 53 % after exposing *C. onubensis* to either high irradiance stress, salt or nitrogen limitation stress, respectively, whereas a slight increase of 11 % was obtained after the microalga was exposed to Fe (III) stress. Similarly, the maximum quantum yield of non-photochemical de-excitation ($\boldsymbol{\phi_{Do}}$) increased by 23, 38 and 57 %, respectively, after the cultures were exposed to high irradiance, salt, or nitrogen limitation stress, whereas a slight decrease of 8 % was obtained after exposure to Fe (III) stress.

The decrease in $\mathbf{F_V/F_0}$ indicates that the ratio between the rate constants of photochemical and non-photochemical deactivation of excited Chl molecules decreases. As shown in Figure 2.6, $\mathbf{F_V/F_0}$ was negatively correlated with $\boldsymbol{\phi_{Do}}$, which was also confirmed by the correlation matrix (Table 2.3), suggesting an increase in the dissipation of absorbed energy as heat or fluorescence in cultures grown on salt, with N limitation or high irradiance stress.

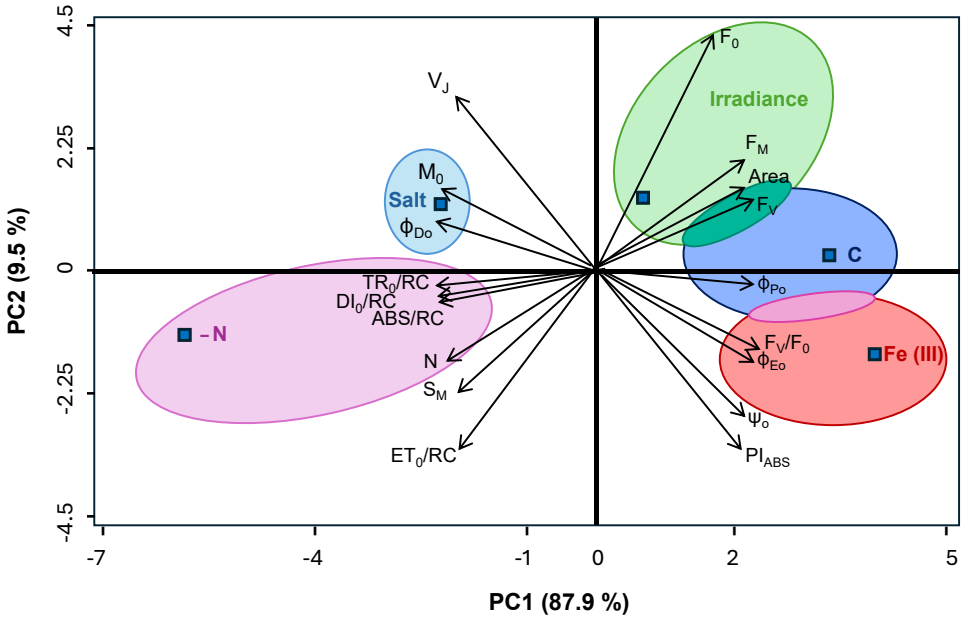

Figure 2.6. Principal component analysis (PCA) was performed after exposing *C. onubensis* cells to different abiotic stress factors on day 4 of cultivation. The blue squares represent the different abiotic stress factors tested on the microalga; the arrows represent the Chl a fluorescence parameters in two dimensions (PC1 and PC2); the ovals represent JIP parameters that positively correlate with the abiotic stress factors; the horizontal and vertical thick lines correspond to the 0 scale.

The cultivation of *C. onubensis* under certain abiotic stress factors seems to activate NPQ mechanisms in the microalga. To study the redox state of the microalga, JIP parameters related to primary photochemistry were analyzed. The relative variable fluorescence at 2 ms (J step), $\mathbf{V_J}$, is a measure of the fraction of the primary quinone

electron acceptor of PSII in its reduced state (Q_A^-/Q_A). An increase of 25, 43 and 40 % in $\mathbf{V_J}$ was recorded after exposing the microalga to high irradiance, salt, or nitrogen limitation stress, respectively. Similarly, the turnover number **N** increased by 53 and 115 % after exposing *C. onubensis* cells to salt or nitrogen limitation stress, respectively; **N** represents the number of times the Q_A becomes reduced until F_M is reached (Strasser et al., 2000). Thus, the results obtained suggested an over-reduction in the primary quinone acceptor when *C. onubensis* was grown under nitrogen deficiency or salt stress.

On the other hand, when Fe (III) was added to *C. onubensis* cells, $\mathbf{V_J}$ decreased by 20 %, suggesting that a lower fraction of the primary quinone electron acceptor of PSII was in its reduced state (Q_A^-/Q_A). Along with the 10 % decrease in **N**, the latter possibly resulted in a lower pressure in the electron transport chain (ETC) of the microalga and a greater efficiency in the photosynthetic use of absorbed light. Similarly, although an increase of 25 % was recorded in cultures grown under high irradiance stress, a decrease of 10 % in **N** was recorded. Thus, the lower pressure in the reduction of Q_A seems to evidence a possible photoacclimation mechanism to reduce the photon flux to be transported through the ETC.

In the context of $\mathbf{V_J}$, a decrease in **area** was obtained irrespective of the abiotic stress factor tested in *C. onubensis* cells. The maximum area corresponds to that obtained from the moment of PSII excitation by actinic light to the moment when the F_t value equals F_M (t_{Fmax}), i.e., the area between the photochemical induction curve and F_M. Thus, this parameter represents the size of the plastoquinone pool in the reducing site of PSII (Strasser et al., 2000). The **area** decreased by 43, 22, 37, and 83 % after *C. onubensis* was exposed to high irradiance stress, Fe (III), nitrogen limitation, or salt stress, respectively. The decrease in the **area** indicates the inhibition of the electron transport rate from the reaction center to the quinone pool, producing an excess of excitation energy, which is generally dissipated as heat (Faseela et al., 2020). However, this statement did not match the results obtained in our study, as the variations obtained in area did not correlate with the variations obtained in $\mathbf{V_J}$ levels after exposing *C. onubensis* cells to different abiotic stress factors or with the obtained $\boldsymbol{\phi_{D_0}}$ data (PCA: Figure 2.6, and correlation matrix: Table 2.3).

Thus, to compare different culture conditions, the **area** must be normalized by F_V ($\mathbf{S_M}$ = area/F_V). The parameter $\mathbf{S_M}$ is a measure of the energy needed to close all reaction centers (Strasser et al., 2000). An increase in $\mathbf{S_M}$ of 17 and 43 % was obtained in cultures grown under nitrogen limitation or salt stress, respectively, indicating that fluorescence levels were below F_M for a longer duration. According to the PCA results, $\mathbf{F_M}$ was positively correlated with **Area** and $\mathbf{F_V}$ but negatively correlated with $\mathbf{S_M}$ and **N** (Figure 2.6), which was also shown by the correlation matrix (Table 2.3). However, the normalized value of the initial slope ($\mathbf{M_0}$), the net rate of closure of the RCs, increased by 37, 83 and 107 % after *C. onubensis* cells were exposed to high irradiance, salt, or nitrogen limitation stress, respectively. Interestingly, lower $\mathbf{S_M}$ and **N** values were recorded in *C. onubensis* cells after exposing the microalga to high irradiance or Fe (III) stress, suggesting lower pressure in the ETC of the microalga.

Table 2.3. Grid correlation matrix showing the correlation between the Chl a fluorescence parameters.

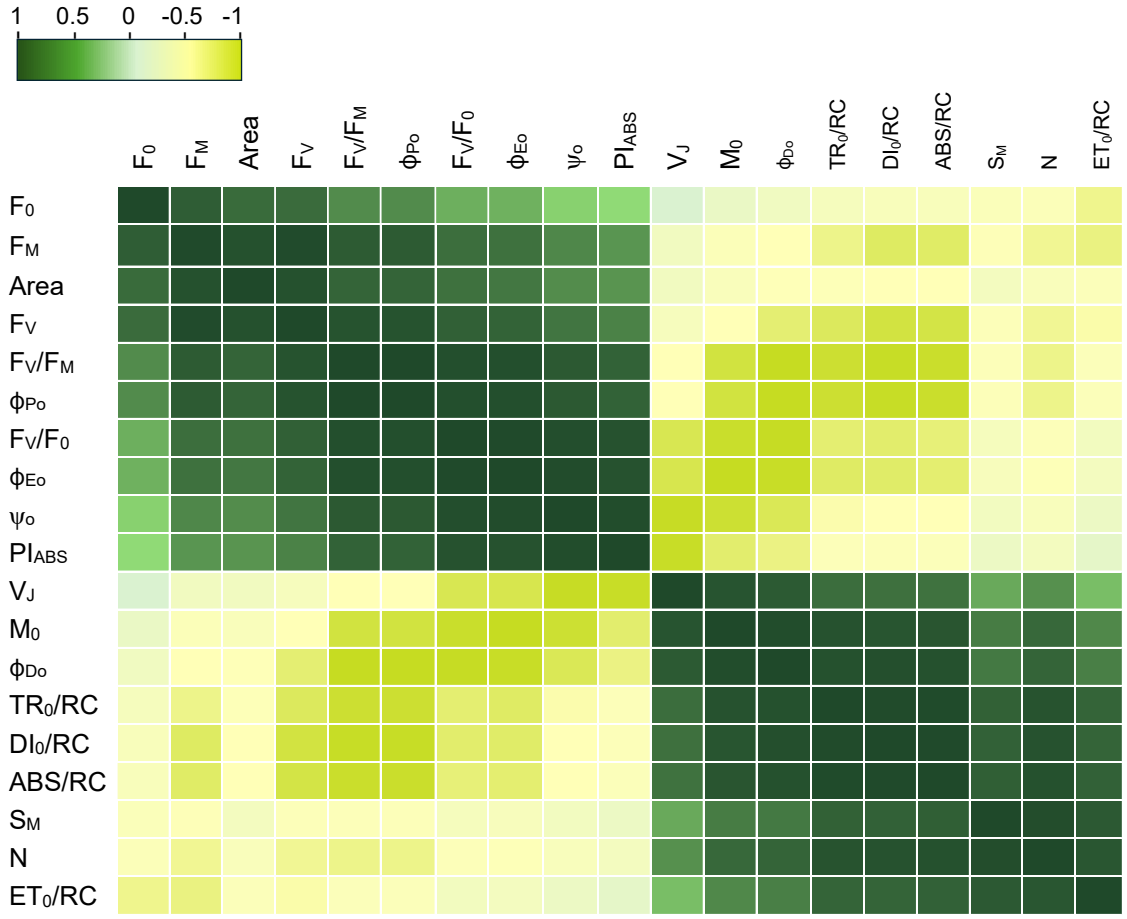

Trapping led to an increase in the net closure rate of the RCs (M_0), whereas electron transport led to a decrease in that rate. The variations in the specific energy fluxes (**ABS/RC**, **TR_0/RC**, **ET_0/RC**, and **DI_0/RC**) are analyzed in Table 2.4 and schematically represented in Figure 2.7.

As shown in Table 2.4, the trapped energy flux per RC (**TR_0/RC**) increased by 9, 30 and 45 % after exposing *C. onubensis* cells to high irradiance, salt, or nitrogen limitation stress, respectively, whereas it decreased by 2 % in Fe (III)-added cultures. On the other hand, the electron transport flux per RC (**ET_0/RC**) increased by 5, 9 and 21 % after exposing *C. onubensis* cells to Fe (III), salt, or nitrogen limitation stress, respectively, whereas interestingly, the same value as that in control culture cells was obtained under high irradiance stress. As $\mathbf{M_0 = TR_0 - ET_0}$, the greater increase in TR relative to ET in cultures grown under high irradiance, salt, or nitrogen limitation stress explained the greater values of **M_0** obtained, i.e., the ETC was more quickly reduced under these abiotic stress conditions. The direct consequence was a decrease in the **ET_0/TR_0** ratio by 8, 16, and 17 % after *C. onubensis* was exposed to these abiotic stress factors, respectively. **ET_0/TR_0** represents the probability that a trapped exciton moves further than Q_A^- (**ψ_0**); thus, the growth of *C. onubensis* under these abiotic stress conditions was associated with a lower efficiency of electronic transport beyond Q_A^-, especially under nitrogen limitation and salt stress. An opposite pattern was obtained in

the Fe (III)-added cultures, resulting in an increase in ψ_0 by 7 %, and therefore, an increase in the electronic transport chain.

Table 2.4. Heatmap of specific energy fluxes calculated through the Chl fluorescence transients of the OJIP test after exposing *C. onubensis* cells to different abiotic stress factors on day 4 of cultivation. Each parameter value was normalized to that of the control culture.

	ABS/RC	TR_0/RC	ET_0/RC	DI_0/RC
Control				
Fe (III)				
Irradiance				
Salt				
– N				

Consequently, the probability that an absorbed photon will move an electron into the ETC ($\mathbf{ET_0/ABS} = \phi_{Eo}$) decreases by 15, 29 and 38 % after exposing *C. onubensis* to these abiotic stress factors. A reduction in ϕ_{Eo} indicated that the capability of photosynthetic electron transport from the PSII donor side to the PSI end acceptors was negatively affected by the abovementioned abiotic stress factors, thus decreasing the photosynthetic capacity of the microalga (Kumar et al., 2022). The opposite pattern was obtained in Fe (III)-added cultures, resulting in an increase in ϕ_{Eo} by 10 %, and therefore, a positive effect on the ETC.

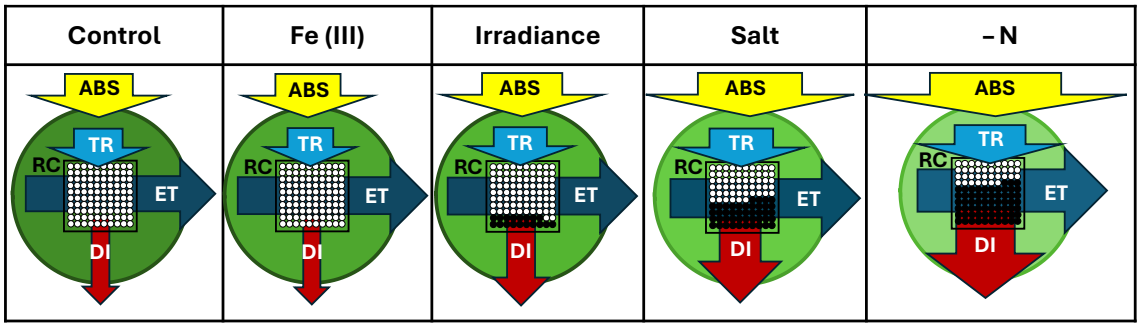

Figure 2.7. Microalgal cell model of specific energy flux variation (per RC) after exposing *C. onubensis* cells to different abiotic stress factors on day 4 of cultivation. Diagram adapted from (Faseela et al., 2020) Symbols: RC (reaction center), ABS (absorption flux per RC), TR (trapped energy flux per RC), ET (electron transport flux per RC), DI (dissipated energy per RC), RC white circles (active RCs), RC black circles (inactive RCs), and microalgal green color degradation (chlorophyll content variation).

The absorption flux (**ABS/RC**) increased by 18, 53 and 93 % after exposing *C. onubensis* cells to high irradiance, salt, or nitrogen limitation stress, respectively, whereas it decreased by 5 % in Fe (III)-added cultures. The **ABS/RC** can be used as a good indicator of the apparent antenna size. However, an increase in **ABS/RC** can also reflect the inactivation of a fraction of RCs (Markou et al., 2017). Similarly, $\mathbf{DI_0/RC}$ increased by 45, 113 and 204 % after exposing *C. onubensis* cells to high irradiance, salt

or nitrogen limitation stress and decreased by 12 % in Fe (III)-added cultures. The direct consequence is a decrease in the maximum quantum yield of the primary photochemistry by 8, 15, and 25 %, $\mathbf{TR_0/ABS} = \mathbf{\phi_{Po}}$. The decrease in $\mathbf{\phi_{Po}}$ ($\mathbf{F_V/F_M}$) indicated that PSII RCs were damaged or photochemically inactive under these abiotic stress conditions (Kumar et al., 2022). Thus, the results revealed the inactivation of a fraction of RCs when the microalga was subjected to salt or nitrogen limitation stress.

Consistent with the obtained results, a significant decrease of 54, 77 and 84 % occurs in $\mathbf{PI_{ABS}}$ on an absorption basis in *C. onubensis* cells after exposure to high irradiance, salt, or nitrogen limitation stress, respectively. $\mathbf{PI_{ABS}}$ is one of the most valuable and comprehensive parameters related to plant vitality and one of the most suitable parameters for investigating the photosynthetic efficiency and effects of abiotic stress on PSII in plants (Faseela et al., 2020). PI is the product of three independent characteristics: (i) the concentration of active reaction centers per Chl unit, (ii) a parameter related to primary photochemistry, and (iii) a parameter related to electron transport (Strasser et al., 2000). Thus, the results revealed that the growth of cultures subjected to salt or nitrogen limitation stress resulted in a decrease in microalgal viability, possibly due to a decrease in the number of active RCs. On the other hand, an increase in the $\mathbf{PI_{ABS}}$ of 55 % was obtained after exposing *C. onubensis* cells to Fe (III) stress, which increased cell viability.

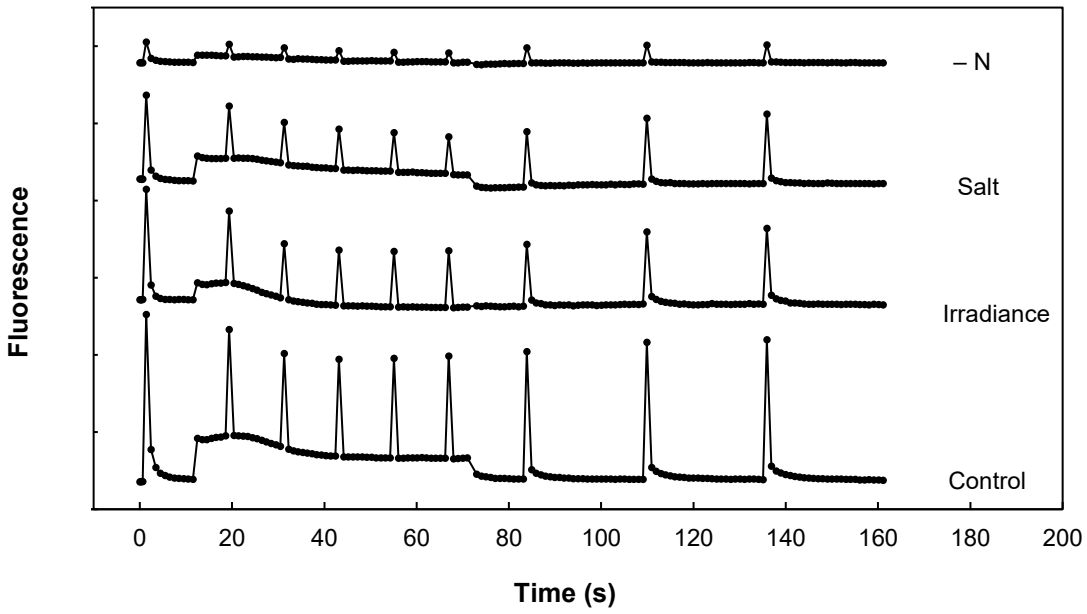

Figure 2.8. NPQ protocol analysis of *C. onubensis* cells cultivated under different abiotic stress factors at day 4 of cultivation. Symbols: – N (nitrogen limitation stress).

The NPQ system of the microalga may have been activated after *C. onubensis* cells were exposed to high irradiance, salt, or nitrogen limitation stress. To confirm these findings, variations in NPQ were determined as a function of each abiotic stress factor (Figures 2.8 and 2.9). Figure 2.8 shows a decrease in Chl fluorescence yields irrespective of the abiotic stress factor to which the microalga was exposed. The decrease was greater in the cultures grown under nitrogen limitation stress, indicating greater activation of the NPQ system, possibly due to an increase in the activity of thermal processes to

dissipate excess energy. These curves indicated that the levels at which the abiotic stress factors were tested affected the NPQ system of the microalga. Figure 2.9 shows the variation in two parameters calculated through the NPQ protocol: photochemical (q_P) and non-photochemical (NPQ) quenching.

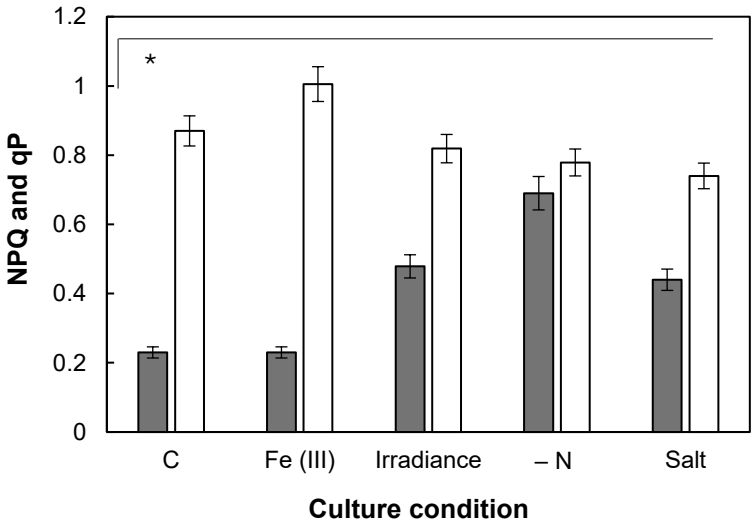

Figure 2.9. Photochemical (empty bar, q_P) and non-photochemical (grey bar, NPQ) quenching of *C. onubensis* cells cultivated under different abiotic stress factors at day 4 of cultivation. Symbols: C (control culture), – N (nitrogen limitation stress). (*) Represents the significant differences of all the treatments relative to the control cultures with 95 % confidence.

Figure 2.9 shows the variations in the q_P and NPQ of *C. onubensis* cells as a function of the abiotic stress factor to which the microalga was subjected. NPQ increased irrespective of the abiotic stress factor tested, indicating the activation of the NPQ system in the microalga as a possible protection mechanism against abiotic stress conditions. As shown in Figure 2.8, the increase in NPQ was greater in cultures grown under nitrogen limitation stress. Regarding q_P, a slight decrease of about 5 to 15 % was recorded irrespective of the abiotic stress factor tested in the microalgal cultures. The decrease in q_P indicated that the abiotic stress conditions tested decreased the number of open PSII centers, as well as the inability of PSII to transfer the generated electrons beyond Q_A in the ETC, hence decreasing photochemistry (Markou et al., 2016).

These results provided insights into the photosynthetic performance of highly acidic-habitat microalga in response to the harsh conditions of their habitat. The next section focuses on comparing the effects of the different factors tested and interpreting their variations.

4. Discussion

In this study, we evaluated the photosynthetic response of a highly acidic-habitat microalga to different abiotic stress conditions: high irradiance, Fe (III), nitrogen limitation, and salt stress. As described in the Introduction section, based on the harsh conditions of its natural habitat, the microalga is expected to be adapted to cope with the abovementioned abiotic stress factors. Recent studies have shown that rapid ChlF can be used as an effective tool to monitor the photosynthetic physiological state of plants under abiotic stress (Kalaji et al., 2016). We evaluated the viability and photosynthetic performance of the microalga when exposed to the abovementioned abiotic stress conditions. The findings of this study provided key scientific information to understand the photosynthetic response of highly acidic-habitat microalgae to environmental stressors, and consequently, the ability of microalgae to develop under harsh conditions, which can trigger the production of valuable compounds. First, the growth of the microalga was evaluated (Figure 2.2) under the abiotic stress conditions selected to ensure that cultivation conditions were within the sublethal range for the microalga. The results revealed that the levels at which the abiotic stress factors were selected affected the growth of *C. onubensis*, where high irradiance or Fe (III) stress increased biomass productivity, and the opposite effect was exerted by nitrogen limitation or salt stress. This could be a consequence of the effect produced by the stressors on the photosynthetic performance of the microalga.

$\mathbf{F_V/F_M}$ values, i.e. PSII photosynthetic efficiency (Figure 2.3) were within the typical range for healthy cultures, about 0.6–0.7, which generally indicates that the culture is not under stress and is viable (Maxwell and Johnson, 2000; Zijffers et al., 2010), except for the cultures grown under nitrogen limitation stress, which presented $\mathbf{F_V/F_M}$ values slightly lower than the above-cited range. Thus, the data obtained could be interpreted in favor of the hypothesis that the photosynthetic machinery of the acidotolerant microalga *C. onubensis* must be adapted to cope with different abiotic stress factors. However, although the $\mathbf{F_V/F_M}$ values were within the range of those of healthy and viable cultures, the values decreased after the microalga was exposed to the abovementioned abiotic stress factors, except in Fe (III)-added cultures. Variations in the photosynthetic performance of *C. onubensis* under different abiotic stress conditions were analyzed in detail in this study.

4.1. Effects of nitrogen limitation or salt stress on the photosynthetic performance

These results suggested that nitrogen limitation or salt stress, at the tested levels, negatively affected the photosynthetic performance of the microalga. This was indicated by the decline in the J-step obtained in the OJIP curves compared to those of the control cells (Figure 2.4), indicating a possible overreduction in Q_A, and therefore, a decrease in the capacity for the reoxidation of Q_A^- (Markou et al., 2016). This was also confirmed by the significantly higher values obtained in $\mathbf{V_J}$ and $\mathbf{M_0}$. The increase in $\mathbf{V_J}$ reflected, in turn, the accumulation of Q_A^-, whereas the increase in $\mathbf{M_0}$ indicated that the net rate of reaction center closure was mainly in the oxidized state (Matorin et al., 2013). This finding agreed with the higher levels of **N** obtained, indicating again an increase in the

number of times Q_A was reduced in the time span from 0 to t_{Fmax}, which was also represented by PSI cyclic electron transport as photoprotection (Singh et al., 2022). Similarly, the lower $\mathbf{S_M}$ values obtained suggested that the maximum fluorescence level could be reached sooner, as fewer electrons were needed to reduce the number of PS II electron acceptors (Aparicio et al., 2022). The direct consequence of that is the decrease in $\boldsymbol{\psi_0}$, the probability that a trapped exciton moves further than Q_A^-. These changes indicated that *C. onubensis* cultures grown in the presence of these abiotic stress factors result in lower efficiency in electronic transport beyond Q_A^-.

In this sense, although the irradiance levels were the same as those in the control culture cells, after *C. onubensis* was exposed to salt or nitrogen limitation stress, an overreduction in Q_A seems to occur. The abovementioned findings allowed us to hypothesize the generation of eventual damage to the photosynthetic chain. Consequently, the dissipated energy increased (DI_0/RC) and a possible inhibition in the ETC was suggested to occur. The decrease in $\boldsymbol{\phi_{E0}}$, the probability that an absorbed photon will move an electron into the ETC, confirmed that hypothesis. This indicated a reduction in the capability of photosynthetic electron transport to transport electrons from the PSII donor side to the PSI end acceptors, and therefore, a decrease in the photosynthetic capacity of the microalga (Kumar et al., 2022). This decrease occurred in a greater proportion in the cultures grown under nitrogen limitation stress, which agreed with the almost straight-line OJIP shape obtained. The straight line obtained showed that nitrogen limitation inhibits electron transport after Q_A and that the OEC cannot provide electrons to PSII and reduce PQ (Markou et al., 2016).

Inhibiting the ETC directly leads to the activation of the NPQ system of the microalga (Figures 2.8 and 2.9). Damage to PSII RCs or inactivation of RCs are the primary reasons for the inhibition of the ETC. The decrease in q_P indicated that the abiotic stress conditions tested decreased the number of available open PSII centers and the inability of PSII to transfer electrons beyond Q_A, hence negatively affecting photochemistry (Markou et al., 2016). This was also suggested by the significant decrease in the $\mathbf{F_V/F_0}$ values along with the increase in $\boldsymbol{\phi_{D0}}$ and $\mathbf{DI_0/RC}$, indicating an increase in the dissipation of absorbed energy as heat or fluorescence (Strasser et al., 2000). This finding was consistent with the decrease in $\boldsymbol{\phi_{P0}}$ ($\mathbf{F_V/F_M}$), indicating that PSII RCs were damaged or photochemically inactive in the presence of these abiotic stress factors (Kumar et al., 2022). Thus, the results revealed that RCs might be inactivated when the microalga is subjected to salt or nitrogen limitation stress. The increase in NPQ might be understood as a protection mechanism against the excessive generation of electrons, which protects microalgal photosystems from photoinhibition and even damage (Markou et al., 2017).

The results obtained were consistent with the higher values of $\mathbf{PI_{ABS}}$ obtained, indicating that nitrogen limitation and salt stress affect cell vitality, and therefore, lead to oxidative stress in the microalga. As reported in the Introduction section, the synthesis of protein D1 is affected under nitrogen limitation, resulting in the synthesis of fewer functional RCs (Kolber et al., 1988). Similarly, salinity stress mainly inhibits the repair of photodamaged PSII and suppresses the *de novo* synthesis of D1 proteins

(Allakhverdiev et al., 2002). This finding is consistent with our results, which revealed that nitrogen limitation or salt stress damages or inactivates PSII RCs. Considering that irradiance levels remained the same both under those stress conditions and in the control culture, the capacity of the microalga to photosynthetically use these provided photons is lower under those stressors, causing an overreduction in the primary quinone acceptor (Q_A), as suggested by our results. Some studies (Foyer and Hanke, 2022; Mandal et al., 2022) have shown that electron overflow in the ETC can result in the inhibition of photosynthesis due to imbalanced $NAD(P)^+$/NAD(P)H ratios, thus allowing the chemical opportunism of ROS to increase their oxidative activity on photosynthetic electron carriers while increasing the overall oxidative pressure on chloroplast biochemistry and structures. Consequently, the ETC was inhibited, and therefore, the OEC could not provide electrons to PSII, thus increasing the activation of the NPQ system of the microalga as a photoprotective mechanism.

These results were similar to those obtained by Markou et al. (2017) in *Chlorella vulgaris* under nitrogen limitation (until a minimum $NaNO_3$ concentration of 88.2 μM), which suggested that the performance of PSII decreased due to a decrease in the number of RCs in proportion to N availability with greater energy dissipation activity, which is a probable outcome of the decrease in the need of the cells for reductants due to lower metabolic activity under N limitation. Similarly, Faseela et al. (2020) analyzed the effects of salt stress (100 mM NaCl) on rice seedlings and suggested that the OEC complex was affected; thus, electron transport from the PSII donor side to the PSII reaction center was inhibited. Ji et al. 2018 studied the photosynthetic performance of *Scenedesmus obliquus* at a maximal salt concentration of 20 mM NaCl and found that the PSII reaction centers were damaged, the primary reaction of photosynthesis was inhibited, and photosynthetic ETC was hindered. Nevertheless, it is worth noting that the extremophilic nature of *C. onubensis* may account for the differences observed in photosynthetic performance under stress, compared to non-extremophilic species. Although the stress conditions tested were more severe than those applied to the non-extremophilic microalgae referenced above, the *C. onubensis* $\mathbf{F_V/F_M}$ values remained close to those typically observed in viable algal cultures. Moreover, microalgal growth was not completely inhibited. These findings suggest that *C. onubensis* possesses a higher capacity for adaptation to various oxidative stress conditions.

The referred overall decrease in the photochemical transduction of absorbed light in stressed cultures, including a rapid increase in the net rate of reaction center closure at PSII, is consistent with cell protection actions against the expected increase in stress-mediated ROS production in chloroplasts. The rapid increase in ROS in the chloroplasts of microalgal cells subjected to stress was reported by Foyer and Hanke, (2022); the stress conditions studied are found in acidic mine drainages. Our results agreed with the hypothesized ability of the highly acidic environment of microalgal species to decrease the expression and/or activity of reduced-electron carriers, which are electron sources for ROS, in the photochemical light transduction process. This conservative action can preserve the viability of acidophilic species by reducing oxidative damage while maintaining cell activity and spending minimum energy, close to that required for cell

maintenance. Overall, extremely slow growth in natural habitats (very low N availability), increased non-photochemical quenching for excess energy dissipation, and increased closure rates of reaction centers explained the main arrangements in terms of photosynthetic performance found in this study.

4.2. Effects of high irradiance stress on the photosynthetic performance

When light irradiance was increased 6-fold, an increase in the activation of the NPQ system was also observed (Figures 2.8 and 2.9). NPQ is the most important photoprotective mechanism and is triggered by the high pH gradient (ΔpH) across the thylakoid membrane induced by high light irradiance (Lambrev et al., 2012). Similarly, high irradiance stress resulted in decreased $\mathbf{F_V/F_0}$ values along with an increase in $\boldsymbol{\phi_{Do}}$ and $\mathbf{DI_0/RC}$ values, in a lower proportion than under salt or nitrogen limitation stress. Interestingly, although higher values of $\mathbf{V_J}$ were obtained, **N** decreased, indicating a decrease in the number of times Q_A was reduced until $\mathbf{F_M}$ was reached. These findings revealed a possible photoacclimation mechanism to reduce the photon flux that triggers the electron flow to proceed to the ETC (Ort and Melis, 2010).

This hypothesis is consistent with the reduced intracellular chlorophyll content (Figure 2.3), and therefore, the proximity of the $\mathbf{ET_0/RC}$ values to those obtained for the control culture. Even though irradiance levels were increased 6-fold and the absorbed energy flux (**ABS/RC**) and trapping ($\mathbf{TR_0/RC}$) increased accordingly, the electron transport flux remains as that in the control culture cells. Considering that the intracellular chlorophyll content decreases and growth is promoted when irradiance levels increase, it can be suggested that an apparent reduction in the antenna size was achieved (Al-Rashed et al., 2016), thus supporting the photoacclimation hypothesis. The direct consequence is the reduction in the photon flux that plays a role in the photochemical reactions of photosynthesis, thus reducing the electron pressure in the ETC generated when irradiance increases. Other researchers have described this photoacclimation strategy in cultures under oversaturated irradiance levels as a means to decrease non-photochemical quenching for reducing photooxidative damage in chloroplasts (Ort and Melis, 2010). This conclusion was similar to that obtained by Srilatha et al. (2019), who analyzed the effects of exposure for 48 h to high light irradiance on cultures of *Chlamydomonas reinhardtii* and reported faster growth of the microalga, which was promoted by microalgal acclimation to high irradiance levels through an increase in NPQ for excess light dissipation as a photoprotective mechanism.

4.3. Effects of Fe (III) stress on the photosynthetic performance

By analyzing the variations shown in Figure 2.3, we hypothesized that when Fe (III) is added to *C. onubensis* cultures, within a certain range, the antenna size can decrease to maximize the photosynthetic use of light. Thus, although the lower intracellular chlorophyll content results in lower values of **ABS/RC** (Table 2.4), greater photosynthetic efficiency is obtained with less absorbed light, indicating optimized photosynthetic use of light (Al-Rashed et al., 2016). This finding was consistent with the higher values of $\mathbf{F_V/F_0}$, $\mathbf{F_V/F_M}$, and $\boldsymbol{\phi_{Eo}}$, and also $\mathbf{PI_{ABS}}$, a parameter that integrates the previous ones (Figure 2.5). These results indicated that microalgal viability increased

when Fe (III) was added to *C. onubensis* cultures. The PCA results (Figure 2.7) showed that these parameters were positively correlated with the performance of Fe (III)-added cultures and perfectly represented the photosynthetic status of cultures under Fe (III) stress. Thus, we hypothesized that Fe (III)-added cultures generally have greater potential for the biochemical photoconversion of solar energy and improve the viability of the microalga (Swoczyna et al., 2019). Similarly, the lower values recorded for $\mathbf{V_J}$ and **N** suggested a decrease in pressure over the photosynthetic ETC, which is consistent with the greater efficiency of the photosynthetic use of absorbed light (Strasser et al., 2000). Additionally, the decrease in $\boldsymbol{\phi_{D_0}}$ along with the decrease in $\mathbf{DI_0/RC}$ after adding Fe (III) to *C. onubensis* cells indicated a reduction in the activation of NPQ mechanisms (Singh et al., 2022).

Few studies have investigated the effects of Fe on the photosynthetic performance of microalgae and plants. Most researchers have investigated the depletion of Fe during photosynthesis (Nagi et al., 2023) and the effects of other heavy metals, such as Pb, Cd, and Zn, among others (Gan et al., 2023; Singh et al., 2022), with a negative effect on the photosynthetic machinery and growth of the studied species. However, Meriot et al. (2024) studied the effects of adding Fe (II) to a newly isolated dinoflagellate from New Caledonia, *Heterocapsa cf. bohaiensis*, at a concentration of $1.79 \cdot 10^{-5}$ M Fe (II); the treatment decreased photosynthetic activity probably due to the disruption of the ETC at the Q_B reducing step. Nevertheless, in the present study Fe (III) was added to *C. onubensis* cultures at a concentration 100-fold greater than that added to *Heterocapsa cf. bohaiensis* cultures by Meriot et al. (2024); and our results revealed greater biomass productivity and greater photosynthetic performance in Fe (III)-added cultures, which could be interpreted as an outstanding natural ability of highly acidic-habitat microalgae to perform photosynthesis in acidic media under conditions that can be lethal to non-extremophiles.

Photosynthesis is the most Fe-requiring process in plants. Photosynthetic electron transfer chain converts light energy into chemical energy between photosystems II and I (PSII and PSI) via cytochrome (cyt) b6f in thylakoid membranes (Saito et al., 2021). During this process, part of the Fe taken by microalgae from the medium distributes into [4Fe-4S] cluster-containing PSI proteins and Fe-containing cyt b6f complexes. Consequently, Fe mediates light-driven electron transfer in microalgal cells (Briat et al., 2015; Hantzis et al., 2018). Fe−S cluster-dependent metabolism in microalgae is sensitive to disruption by oxygen because of the decreased bioavailability of ferric iron at neutral and basic pH, as well as due to the direct oxidation of sulfur intermediates and Fe−S clusters by ROS (Boyd et al., 2014). Nevertheless, Fe is more bioavailable at low pH, mainly because both ionic forms of iron, Fe (II) and Fe (III), are far more soluble (especially ferric iron) at low pH than at neutral or basic pH (Johnson et al., 2012). In this sense, this could justify why the addition of Fe (III) to *C. onubensis* cultures favors the electron transport chain activity in the microalga, therefore resulting in a higher photosynthetic efficiency.

4.4. Overall

Based on all these findings, it is worth mentioning the greater adaptability of this extremophilic microalga to the harsh abiotic stress conditions imposed. In contrast to other microalgal species, *C. onubensis* responds to Fe (III) stress by reducing its antenna size to maximize the photosynthetic use of light, resulting in a higher biomass productivity than that recorded in control cells. Similarly, this species can adapt to high irradiance levels by a photoacclimation mechanism that decreases the electron pressure in the ETC, which, in turn, increases biomass productivity. This mechanism is based on reducing the photon flux that proceeds to the ETC and enhancing the activity of the NPQ system as a protective mechanism to dissipate part of the excess energy. In contrast to other microalgae, although cultivation of *C. onubensis* under nitrogen limitation or salt stress significantly affects the activity of the photosynthetic chain, the photosynthetic efficiency recorded was close to those typically obtained for algal viable cultures.

These cellular strategies of acclimation can further determine the application of the highly acidic-habitat microalga *C. onubensis* as a model organism for studying biological adaptation associated with climate change. That is, extreme environments offer valuable insights into the effects of climate change on living organisms, as climate change is making environments harsher for organisms. Additionally, the microalga *C. onubensis* has been described to enhance the production of valuable metabolites with antioxidant and anti-inflammatory properties in cultures exposed to certain abiotic stress conditions (Robles et al., 2023). Thus, we speculate that the greater adaptability of the extremophilic microalga *C. onubensis* to imposed abiotic stress conditions can contribute to understanding the scientific value of extremely acidic environments for photosynthetic microorganisms and can also pave the way to use this microalga in areas relevant to society, such as animal and human nutrition, health, agriculture, and water treatment.

5. Conclusions

The findings of this Chapter suggested that exposure of *C. onubensis* to Fe (III) induced a physiological response characterized by a reduction in antenna size, leading to improved PSII quantum efficiency and enhanced electron transport, without activation of excess energy dissipation mechanisms. This response, uncommon among non-extremophilic species, reveals an optimized photoconversion strategy probably specific to acidotolerant microalgae. Under high irradiance, *C. onubensis* exhibited a photoacclimation response involving reduced intracellular chlorophyll content, moderate activation of the non-photochemical quenching (NPQ) system, and decreased electron pressure in the photosynthetic electron transport chain (ETC). This mechanism reduces the photons flux that proceeds to the ETC and enhances the activity of the NPQ system as a protective mechanism to dissipate part of the excess energy. This maintains photosynthetic performance and biomass productivity, highlighting a resilience strategy probably typically for extreme microalgae. In addition, despite significant impairment of PSII function under salt and nitrogen limitation ($\uparrow V_J$, $\downarrow \phi_{Eo}$, $\uparrow DI_0/RC$, ↑NPQ), *C. onubensis* maintains photosynthetic efficiency values close to the viability range. This indicates coordinated activation of protective mechanisms against ROS and partial preservation of the photosynthetic apparatus, supporting its utility as a model for stress tolerance in extreme environments.

6. Supplementary material

Statistical analysis Figure 2.5 and Table 2.4

Table S2.1. Selected technical fluorescence parameters normalized to the control culture of *C. onubensis* cultures as a function of abiotic stress factors on day 4 of cultivation.

	C	Fe (III)	Irradiance	Salt	–N
F_0	1^{a}	0.777^{b}	0.919^{c}	0.886^{c}	0.247^{d}
F_M	1^{a}	0.841^{b}	0.748^{c}	0.639^{d}	0.157^{e}
V_J	1^{a}	0.8^{b}	1.259^{c}	1.431^{d}	1.399^{cd}
F_M/F_0	1^{a}	1.082^{a}	0.814^{b}	0.721^{bc}	0.634^{c}
F_V/F_0	1^{a}	1.111^{b}	0.751^{c}	0.613^{d}	0.477^{e}
M_0	1^{a}	0.786^{b}	1.375^{c}	1.874^{d}	2.038^{d}
Area	1^{a}	0.783^{b}	0.575^{c}	0.637^{c}	0.174^{d}
S_M	1^{a}	0.906^{ab}	0.833^{b}	1.170^{c}	1.478^{d}
N	1^{a}	0.893^{a}	0.909^{a}	1.523^{b}	2.152^{c}
φ_{Po}	1^{a}	1.027^{a}	0.922^{ab}	0.852^{bc}	0.753^{c}
Ψ_0	1^{ab}	1.070^{a}	0.917^{b}	0.837^{c}	0.830^{c}
φ_{Eo}	1^{a}	1.099^{a}	0.846^{b}	0.712^{c}	0.625^{c}
φ_{Do}	1^{a}	0.924^{a}	1.230^{b}	1.385^{b}	1.577^{c}
PI_{ABS}	1^{a}	1.551^{b}	0.462^{c}	0.234^{d}	0.146^{d}
ABS/RC	1^{a}	0.960^{a}	1.181^{b}	1.534^{c}	1.934^{d}
TR_0/RC	1^{a}	0.985^{a}	1.089^{a}	1.305^{b}	1.456^{b}
ET_0/RC	1^{a}	1.054^{a}	1^{a}	1.093^{ab}	1.208^{b}
DI_0/RC	1^{a}	0.889^{a}	1.455^{b}	2.131^{c}	3.045^{d}

[a, b, c, d, e.] Different superscript letters indicate differences in treatments with a significance of $p < 0.05$.

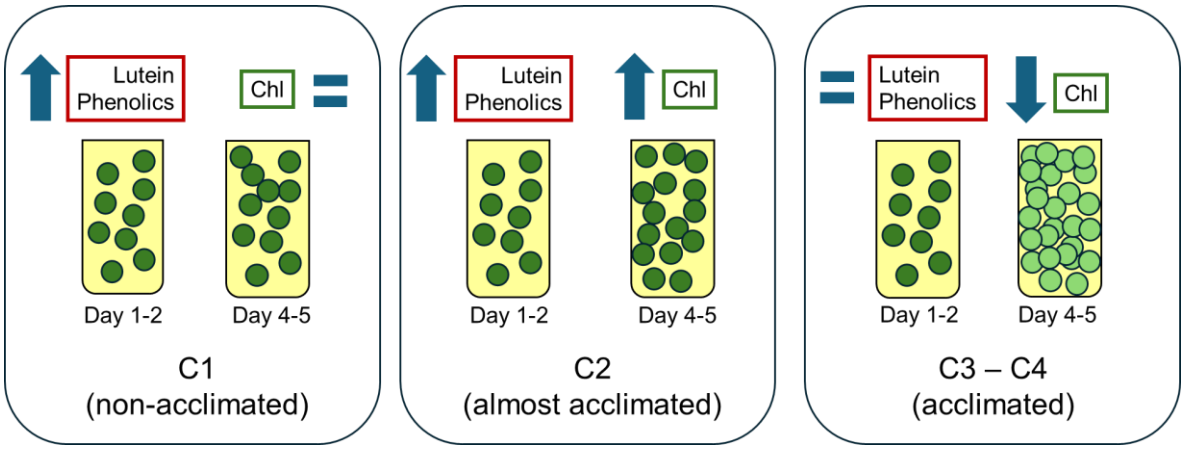
Lutein Phenolics
Chl
Day 1-2
Day 4-5
C1
(non-acclimated)
Lutein Phenolics
Chl
Day 1-2
Day 4-5
C2
(almost acclimated)
Lutein Phenolics
Chl
Day 1-2
Day 4-5
C3 – C4
(acclimated)

CHAPTER

3

Biomass and valuable molecule production by a highly acidic-habitat microalga in an air-fluidized system

Table of contents

Abstract: This study explores the repeated-batch production, in air-fluidized open bags, of the highly acidic habitat microalga *Coccomyxa onubensis*, isolated from the Tinto River, followed by extraction and determination of valuable antioxidant compounds, including carotenoids and polyphenols. Prior to the larger scale cultivation, a partial optimization of some of the crucial factors affecting *C. onubensis* growth (temperature, light irradiance and Fe (III)) was performed using a factorial design 3^3. The mathematical model predicted that the optimal condition for maximum biomass productivity was no addition of Fe (III) to *C. onubensis* cultures and growing the microalga under moderate levels of temperature and light irradiance (28.9 °C and 486 μmol photon·m^{-2}·s^{-1}). Accordingly, following this growth optimization, the results suggest that *C. onubensis* can be cultivated in an easy-to-operate air-fluidized bag system, achieving a maximum productivity of 0.17 g·L^{-1}·d^{-1}. Light irradiance was maintained constant. Therefore, light availability within the photic zone of *C. onubensis* cultures was primarily influenced by the dynamics of the repeated-batch cultivation cycles and the progressive increase in cell density though each cycle. Accordingly, several trends in the variation of antioxidants compounds were observed. On the one hand, at the beginning of the first cycle, the adaptation phase to the imposed conditions, light possibly causes oxidative stress in *C. onubensis* resulting in an increase in the content of lutein and phenolic compounds as a defense mechanism. On the other hand, when light availability decreases or the microalga gets acclimated to the imposed conditions, a decrease in chlorophyll antenna size seems to occur, representing a physiological acclimation of the microalga to the reduced light availability in high-cell density cultures as a strategy to maximize light absorption. The growth of *C. onubensis* in 30 L air-fluidized, open bags has proven stable and photosynthetically viable and with no growth of opportunistic species, which becomes advantageous for massive production.

Keywords: highly acidic-habitat microalga, growth-influencing factors, repeated-batch cultivation, air fluidized-system, antioxidants.

1. Introduction

Oxidative stress, resulting from the accumulation of reactive oxygen species (ROS) within the human cells, has been implicated in various pathological processes, including cardiovascular diseases, cancer, neurodegenerative disorders, and aging (Yoshihara et al., 2010). Oxygen, an essential element in the metabolism of aerobic organisms (Lourenço et al., 2019), can also trigger unfavorable reactions in living systems, such as ROS production (Halliwell, 2006). Antioxidants, as defined biologically, are natural or synthetic substances capable of preventing or delaying oxidative cellular damage caused by physiological oxidants. Specifically, they possess positive reduction potentials that allow them to neutralize ROS, reactive nitrogen species (RNS), and free radicals (Pérez-Gálvez et al., 2020). This has driven a significant increase in interest in health-promoting foods and natural products in recent years. An antioxidant-rich diet is considered one of the most practical and cost-effective strategies to mitigate the effects of aging. Consequently, food supplements, and also cosmetics, have become key research areas, particularly those based on novel natural sources with proven benefits to human health.

Within such a context, microalgae are valuable biological resources that align with these market demands due to their biochemical profile, which is rich in polyunsaturated fatty acids (PUFAs), carotenoids, and polyphenols. Additionally, they exhibit antioxidant, anticancer, and anti-inflammatory activities (Schüler et al., 2020). Among these bioactive compounds, polyphenols are of particular significance as natural antioxidants and anti-inflammatory molecules (Singla et al., 2019), encompassing more than 8,000 structurally diverse compounds. They can be broadly classified into flavonoids and non-flavonoids or further subdivided into 10 distinct classes based on their chemical structure (Natrah et al., 2007; Singla et al., 2019).

Microalgae can be integrated into efficient biotechnological processes to obtain extracts with potential bioactivity. In response to oxidative stress caused by both physical and chemical factors, microalgae have evolved metabolic pathways to produce antioxidant molecules as a protective mechanism. The presence of conjugated double bonds in their chemical structure not only contributes to pigmentation but also enhances their antioxidant capacity. Antioxidants neutralize and eliminate ROS through nucleophilic substitution reactions at these double bonds. Such reactions alter the electronic structure of the molecules, partially or completely modifying their ability to absorb radiation while still benefiting the organism through their antioxidant activity (Pérez-Gálvez et al., 2020). Several factors can induce the accumulation of these antioxidant compounds, depending on the microorganism. These include high-intensity photosynthetically active radiation (PAR) and ultraviolet radiation, the presence of metal cations in solution, or depletion of key nutrients such as nitrogen, sulfur, and phosphorus. The exposure to these stressors triggers a molecular signaling cascade that ultimately activates i.e. the expression of genes involved in carotenoid biosynthesis, particularly in the early stages of the pathway (Curcuraci et al., 2022).

Industrial-scale microalgae production has the potential to partially or entirely replace conventional chemical synthesis processes for health-promoting compounds

with biochemical synthesis pathways. Under specific conditions, these microorganisms can naturally generate antioxidants, making them a promising alternative to synthetic production. Furthermore, the biotechnological utilization of natural resources, such as microalgae, aligns with the principles of the circular economy, enhancing the sustainability of the process. Inspired by nature's cyclical model, the objective of using microalgae or their products is to maximize the use of biodegradable materials in consumer goods manufacturing, getting them returned to the environment without causing ecological harm at the end of their life cycle (Korhonen et al., 2018). Additionally, the production of microalgal biomass efficiently is a key prerequisite in the production process of valuable compounds from microalgae (Fuentes et al., 2020). For large scale cultivation, optimization of key growth-influencing factors is crucial to ensure light and nutrient availability and, therefore, the viability of the microalgal culture. Is that the reason why in this study a factorial design 3^3 was performed prior to cultivation at larger scale.

The microalga used in this study, *Coccomyxa onubensis* ACCV1 (*C. onubensis*), is a highly acidic-habitat species isolated from the Tinto River mining basin in southwestern Spain, Huelva. This environment is characterized by extreme acidity due to high proton concentrations derived from the chemical and biological oxidation of sulfides. Additionally, the acidic pH leads to elevated levels of dissolved metals in the water. Despite these harsh conditions, the ecosystem supports a diverse microbial community, with eukaryotic microalgae comprising 60 % of the river's biomass (Amils et al., 2014).

The habitat of *C. onubensis* is particularly rich in metals, with iron being one of the most abundant elements. While iron is essential for biological processes, excessive concentrations become highly toxic as they generate ROS via the Fenton reaction through electron exchange. The ability of *C. onubensis* to survive in such an extreme environment is largely due to its capacity to activate secondary metabolic pathways leading to the biosynthesis of unique and valuable antioxidant molecules. Among these bioactive compounds, carotenoids (primarily lutein), polyphenols and polyunsaturated fatty acids (PUFAs), such as linolenic and linoleic acids, are main representatives which have applications in both human and animal health (Navarro et al., 2016). Furthermore, the cultivation of *C. onubensis* at acidic pH offers a significant advantage for open-system production, as it naturally limits the growth of opportunistic contaminants (Fuentes et al., 2016).

For these reasons, *C. onubensis* was selected for this study to analyze the time-dependent evolution of target antioxidant molecules in suspended cell cultures as a function of irradiance levels, under cultivation in bags. In this context, light plays a fundamental role. As microalgae grow in an aqueous culture, their increasing total chlorophyll content leads to greater resistance to light penetration, particularly in later cultivation stages. Consequently, each cell in a dense culture spends more time in darkness and less time exposed to light. Since light is essential for both growth and the stimulation of antioxidant molecules accumulation, its limitation negatively impacts microalgal growth.

Accordingly, this study aimed to evaluate the effects of repeated-batch cultivation in air-fluidized bags on the productivity and antioxidant compound accumulation in *C. onubensis*. Cultures were maintained within an optical density (OD_{750}) range of 3 to 8, and growth, photosynthetic viability, and pigment content were assessed. As explained above, prior to cultivation at a larger scale than that of 0.5 L-bottles, an optimization of some of the crucial factors affecting *C. onubensis* growth (temperature, light irradiance and Fe (III)) was performed in flasks using a factorial design 3^3. From a sustainability perspective, this study is aligned to sustainable frameworks for microalgae biorefinery, enabling the production of high-value compounds while minimizing environmental impact.

2. Materials and methods

2.1. Microorganisms and culture composition

The microorganism used in this study was *Coccomyxa onubensis* ACCV1 (SAG 2510), a highly acidic-habitat and halotolerant microalga isolated from the acidic waters of the Tinto River (Huelva, Spain) in the sampling area at latitude 37.5851153° and longitude -6.550754°, by the Microalgae Biotechnology Unit (BITAL), of the Department of Chemistry "Professor Jose Carlos Vílchez Martín," from the Faculty of Experimental Sciences and CIQSO of the University of Huelva, Spain (Fuentes et al., 2016).

The microalga strain was kept in sterile agar plates prepared with K9 culture medium at pH 2.5 (Silverman & Lundgren, 1959). K9 medium was modified according to the following final composition, per liter: 2.29 g KNO_3, 0.5 g K_2HPO_4, 3.95 g K_2SO_4, 0.01 g $CaCl_2$, 0.41 g $MgCl_2$, 0.1 g KCl and 5 mL of Hutner solution (Hutner et al., 1950).

2.2. Optimization of growth-influencing factors: 3^3 factorial design

An optimization of the growth-influencing factors –temperature, light irradiance and Fe (III)– at three levels (low: L, medium: M and high: H) was performed on the growth of *C. onubensis*. Selected growth factors and their respective levels were selected based on both unpublished results of our group (BITAL) and also results published by Robles et al. (2023) and Vaquero et al. (2014). Selected levels and its respective abbreviations were temperature (T): 25 (LT), 30 (MT) and 35 °C (HT); light irradiance (L): 150 (LL), 300 (ML) and 600 (HL) μmol photon·m^{-2}·s^{-1} and Fe (III): 0 (LFe), 0.25 (MFe) and 2 mM (HFe) of Fe (III). The cultures were prepared through a standard mother culture in exponential phase and were inoculated with k9 medium at an initial biomass concentration of, approximately, 0.3 g·L^{-1} in 0.5 L round bottles. The pH of the *C. onubensis* cultures was maintained at 2.5 and Fe (III) was added in the form of $FeCl_3 \cdot 6H_2O$ (VWR, Belgium). The cultures were established in a culture room with temperature control. Light was supplied by white light fluorescent tubes for 24 hours, and the cultures were bubbled with air enriched with 2.5 % (v/v) CO_2.

2.3. Biomass production in air-fluidized bags

NPK-based culture medium was used for a larger-scale cultivation experiment. Thus, a previous adaptation of *C. onubensis* under NPK was performed in Schott glass bottles of 5L. The NPK-based culture medium was based on an industrial NPK-liquid fertilizer, specifically designed for the scaling of microalgae in our facilities (BITAL). The composition of the NPK-liquid fertilizer prepared with osmosis water was per liter: 1.5165 g KNO_3, 0.1497 g KH_2PO_4, 0.0039 g H_3BO_3, 0.0013 g $CuSO_4 \cdot 5H_2O$, 0.0433 g $FeSO_4 \cdot 7H_2O$, 0.0160 g $MnCl_2 \cdot 4H_2O$, 0.0022 g $(NH_4)_6Mo_7O_{24} \cdot 4H_2O$, 0.0045 g $ZnSO_4 \cdot 7H_2O$, 0.9766 g $CaCl_2$ and 3.7624 g $MgCl_2$.

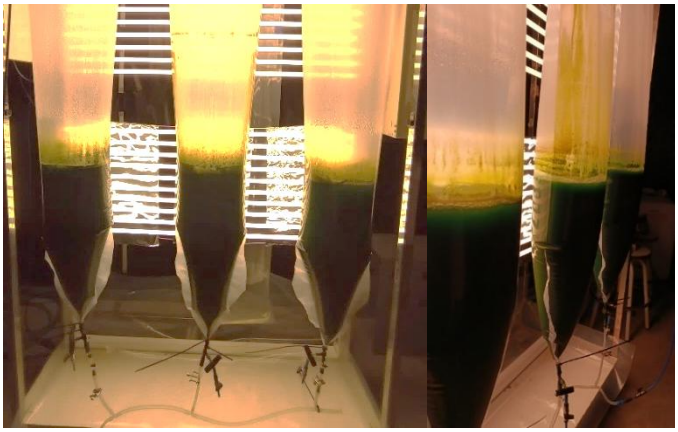

Figure 3.1 Bag cultivation system of the microalga *C. onubensis*.

As shown in Figure 3.1, the microalga *C. onubensis* was cultivated in triplicate using 30 L bags, with a maximum culture volume of 10 L. A repeated-batch cultivation approach was employed, operating under non-sterile conditions and maintaining cultures within an optical density range (measured at 750 nm) of approximately 3–8. All systems consisted of plastic culture bags (high-density polyethylene) with a width of 30 cm, and the cultures were operated as fluidized bed systems. The cultures were fluidized by bubbling a CO_2-air mix (2.5 % CO_2, v/v) through the gas inlet at the bottom of the bags. The cultures pH was maintained at 2.5 by addition of 40 % (v/v) H_2SO_4 when required. The room temperature was kept at 24 ± 4 °C and illumination was provided by white, fluorescent tubes (Philips 54W/830), delivering an average photosynthetically active radiation (PAR) intensity of approximately 700 µmol photons m^{-2} s^{-1} at the surface of the culture bags.

2.4. Growth and calculated parameters

Cell density of the microalga *C. onubensis* was determined by optical density measurements and by measuring the dry weight (dw) of the biomass contained in 2 mL of culture medium. Optical density was measured in a UV-Vis spectrophotometer model Evolution 201 (Thermo Fisher Scientific, Walthman, MA, USA) at wavelengths of 750 and 680 nm in plastic cuvettes and using distilled water as blank. The optical density data measured at 750 nm (OD_{750}) provides information on the turbidity of the culture, that is, the amount of biomass present in the culture. On the other hand, the data obtained at 680 nm (OD_{680}) reports on the relative turbidity due to the chlorophyll content of the culture.

Based on the dry weight data, different parameters were calculated for each cycle of repeated-batch cultivation, C_i and C_f being the initial and final cell concentration of each cycle of the repeated-batch cultivation, and t the duration of each cycle, expressed in days.

$$\text{Growth factor } (d^{-1}) = \frac{C_f/C_i}{t} \qquad (3.1)$$

$$\text{Specific growth rate } (d^{-1}) = \frac{\ln(C_f/C_i)}{t} \qquad (3.2)$$

$$\text{Productivity } (g\ L^{-1}\ d^{-1}) = \frac{C_f - C_i}{t} \qquad (3.3)$$

2.5. Photosynthetic viability

Photosynthetic viability was determined based on the chlorophyll fluorescence measurements, the maximum quantum yield (F_V/F_M) of Photosystem II (PSII) according to published methods (Schreiber, 2004). Quantum yield (Qy) was measured by placing dark-adapted culture samples of *C. onubensis* into the measuring chamber of portable pulse amplitude-modulated fluorimeter model AquaPEN AP-C 100 (Photon Systems Instruments, Drásov, Czech Republic). F_V represents the variable fluorescence and is calculated as $F_V = F_M - F_0$, being F_0 the minimum level of fluorescence observed after exposing cells to a non-actinic beam and acclimating them in the dark, while F_M represents the maximum fluorescence observed in cells after exposing them to a brief but saturating pulse of actinic light.

2.6. Chlorophylls and carotenoids determination

Chlorophyll and carotenoid content were determined in samples of *C. onubensis* as described by Cuaresma et al. 2012. Culture samples of 1 or 2 mL volume, were centrifuged at 3 *g* for 5 min, methanol was added to the pellet, and the mixture was placed in an ultrasound bath (60°C, 5 min) to weaken the microalgal cell wall. After another centrifugation step, the supernatant was collected and analyzed by UV/Visible spectrophotometry, model Evolution 201 (Thermo Fisher Scientific, Walthman, MA, USA). Modified Arnon's equations were used to calculate chlorophyll and carotenoid concentrations in the extracts. The extracts obtained were used to analyze the antioxidant capacity of the microalga and the determination of polyphenols compounds.

For specific carotenoid analysis and quantification, separation was performed by liquid chromatography (HPLC; Beckman System gold, Fullerton, CA, USA) using a C18 column (150 mm × 4.6 mm i.d., 5 µm, SunFire TM column; Waters, Milford, MA, USA) with a flow rate of 1 mL min^{-1} and injection extract volume of 40 µL. The applied gradient was the following (solvent A; ethyl acetate and solvent B; acetonitrile/water, 9:1 v/v): 0–16 min, 0–60% solvent A; 16–30 min, 60% A; 30–35 min, 100% A. In order to quantify, pigment standards supplied by DHI-Water and Environment (Denmark) were injected. Quantification of the selected pigments was based on a comparison of peak areas obtained from methanolic extracts of *C. onubensis* with those areas obtained from the injected standards.

2.7. Polyphenols determination

Total polyphenols were determined using the procedure described by Georgé et al. (2005). According to this, phenolic compounds were oxidized by the Folin-Ciocolteau reagent (Panreac, Spain), resulting in a blue color complex formation. The reaction was carried out in an alkaline medium; for this, sodium carbonate was added to the samples, and the absorbance was measured at 725 nm by UV-vis spectrophotometry model Evolution 201 (Thermo Fisher Scientific, USA). Total content of polyphenols was obtained using a calibration line from a standard solution of gallic acid 1-hydrate (Panreac, Spain) and was expressed as mg-eq· gallic acid·L^{-1} ($y = 0.0996 \cdot x - 0.0016$, $R^2 = 0.9999$).

Flavonoid compounds were determined by a spectrophotometric method described by (Liu et al., 2002). For this, the following reagents were used: $NaNO_2$, $AlCl_3 \cdot 6H_2O$ and NaOH. As an external standard, a 1 $g \cdot L^{-1}$ catechin stock, (+)-catechin hydrate (Sigma aldrich, Germany) in MilliQ water was used. The absorbance value was measured at 510 nm using UV-vis spectrophotometry model Evolution 201 (Thermo Fisher Scientific, USA). Total content of flavonoids was calculated by extrapolating the values obtained in the calibration line ($y = 0.0029 \cdot x - 0.0515$, $R^2 = 0.9985$).

2.8. Statistics

Unless otherwise stated, all data are presented as the mean of three replicates, and the standard deviations are shown in the corresponding figures and tables. The data from the different treatments were evaluated by constructing univariate statistical models and performing the analysis of variance (ANOVA) (confidence of 95% was considered for determining statistical significance). Significant differences were evaluated using Tukey's range test with a confidence level of 95% ($p \leq 0.05$), additional data in Table S3.2 to S3.8 of Supplementary Material section.

The effects of the growth-influencing factors on response variables in the separation process were assessed using pure error and considering a confidence interval of 95% for all variables using Statgraphics Centurion XVIII® (StatPoint Technologies, Inc., Warrenton, VA, USA) software. The effect of each factor on the response variables and their statistical significance was determined by the ANOVA and the standardized Pareto chart. Regression coefficients and p-Value of ≤ 0.05 are included in the Table S3.1 of Supplementary Material section.

3. Results

3.1. Optimization of growth-influencing factors: factorial 3^3

For large scale cultivation, optimization of key growth-influencing factors is crucial to ensure light and nutrient availability and, therefore, the viability of the microalgal culture. In the present study, we elucidated the effect of different factors –temperature, light irradiance and Fe (III)– with three levels in the growth of *C. onubensis*, by performing a factorial design (3^3). As explained in the Materials and Methods section, temperature levels were 25, 30 and 35 °C, light irradiance levels were 150, 300 and 600 µmol photon·m^{-2}·s^{-1} and Fe (III) levels were 0, 0.25 and 2 mM of Fe (III). Results for biomass productivity are shown in Figure 3.2.

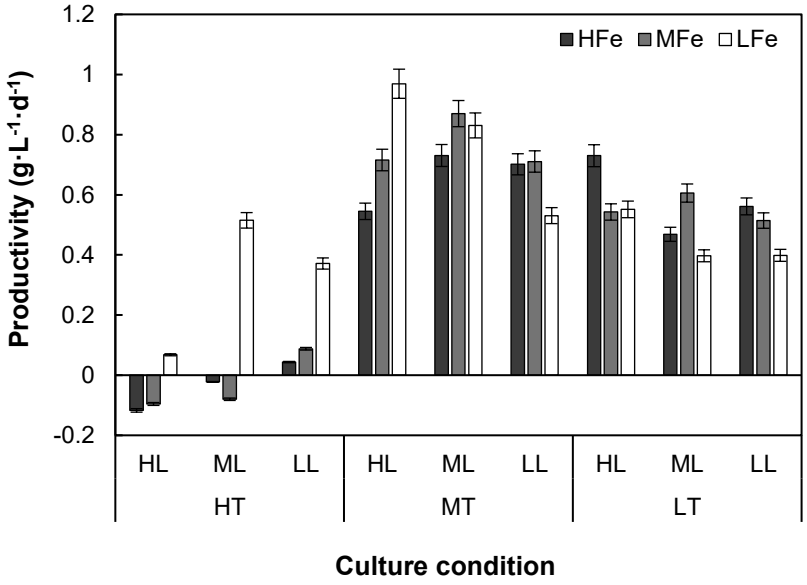

Figure 3.2. Effect of different factors –temperature (T), light irradiance (L) and Fe (III) (Fe)– with three levels –low (L), medium (M) and high (H)– in the biomass productivity of *C. onubensis*. Values for the levels of the different factors are given in the Materials and Methods section.

Figure 3.2 shows that temperature could be modulated to increase microalgal growth, i.e. the highest productivity values were obtained when cultivating *C. onubensis* at 30 °C (medium temperature, MT). Additionally, temperature seems to be a critical factor to *C. onubensis* growth as temperature equal or higher than 35 °C resulted in growth cessation. Regarding light irradiance and Fe (III) levels, generally, increasing light irradiance levels resulted in higher biomass productivity, whereas an opposite pattern appeared to occur when adding Fe (III) to *C. onubensis* cultures.

For a better analysis of the effect of the different factors in the growth of the microalga, the data were analyzed using factorial designs (3^3) based on response surface methodology (RSM), Pareto charts and main effect plot (Figure 3.3). The data analyzed in Figure 3.3 corresponds to day 4 of cultivation as it was the day when the greatest variations in the growth of the microalga were found.

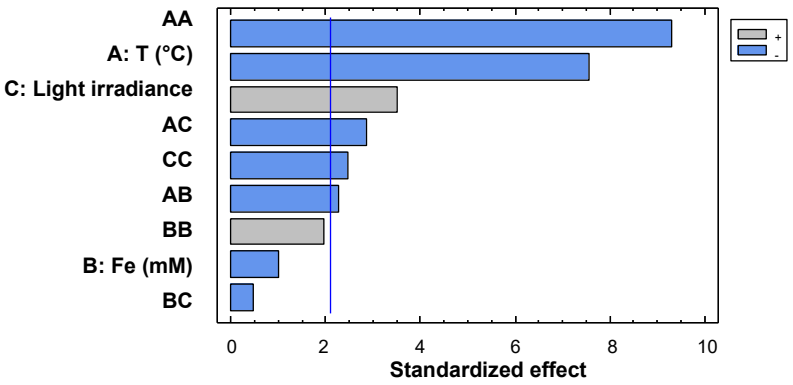

(**a**)

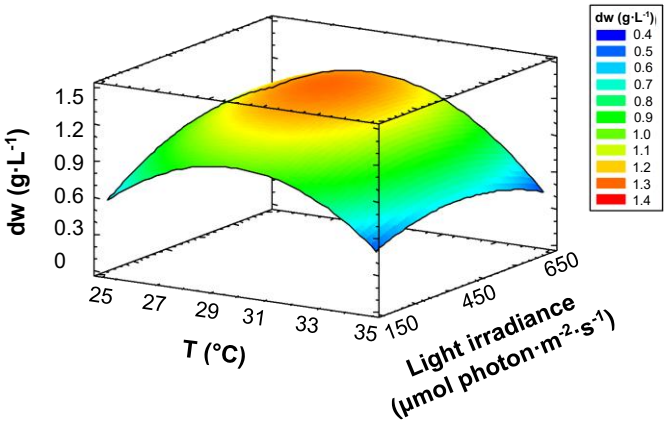

(**b**)

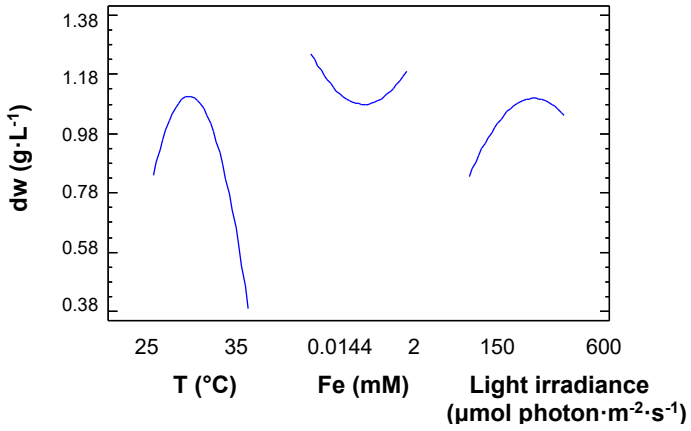

(**c**)

Figure 3.3. Pareto chart (**a**), RSM (**b**) and main effect plot (**c**) rationalizing the effect of each factor on the growth of *C. onubensis* obtained by estimating the biomass concentration through dry weight measurements. More details can be found in the Materials and Methods section. Hold value in contour plot corresponded to no-addition of Fe (optimal growth condition).

Figure 3.3 illustrates the Pareto chart (Figure 3.3a), RSM plot (Figure 3.3b) and main effects plot (Figure 3.3c) of *C. onubensis* after adjusting the effect of each factor (temperature, light irradiance and Fe (III)) on the biomass production. The Pareto chart (Figure 3.3a) revealed that factors such as temperature, light irradiance, quadratic

interaction of temperature–light and temperature–Fe (III) were statistically significant in the biomass production ($p \leq 0.05$). Light irradiance improved biomass production, whereas temperature and Fe (III) provided opposite results. On the other hand, the statistical software predicted a complete mathematical model, Equation (3.4), to estimate dry weight of the microalgal culture, expressed in $g \cdot L^{-1}$, with an R^2 value of 90.8717 %; this indicates that this model has a good fit (Table S1). In the equation, *T* is temperature in °C, *L* is light irradiance in μmol photon$\cdot m^{-2} \cdot s^{-1}$ and *Fe (III)* is iron concentration in the cultures, in mM.

$$\begin{aligned} dw\ (g \cdot L^{-1}) = &- 0.018644 \times T^2 + 0.141637 \times [Fe\ (III)]^2 - 0.00000280999 \times L^2 \\ &- 0.0155693 \times T \times [Fe\ (III)] - 0.0000887455 \times T \times L - 0.0000723699 \times [Fe\ (III)] \times L \\ &+ 1.12267 \times T + 0.179547 \times [Fe\ (III)] + 0.00530202 \times L - 16.2416 \end{aligned} \quad (3.4)$$

Furthermore, in Figure 3.3b (RSM) the color intensity increases with moderate levels of temperature and light irradiance. Thus, the mathematical model predicted that the optimal condition for maximum biomass productivity was no addition of Fe (III) to *C. onubensis* cultures and growing the microalga at 28.9 °C and 486 μmol photon$\cdot m^{-2} \cdot s^{-1}$ (Figure 3.3c).

3.2. Growth and antioxidant accumulation under repeated-batch cultivation.

This section analyzes the growth and photosynthetic viability of the highly acidic-habitat microalga *C. onubensis* under repeated-batch cultivation for efficient biomass production. Thus, based on the results obtained in section 3.1 and the estimations realized in the discussion section, light irradiance that reaches the cells was kept roughly constant at 700 μmol photon$\cdot m^{-2} \cdot s^{-1}$. The cultures were allowed to grow until they reached a maximum optical density (OD) of approximately 8, measured at 750 nm. Subsequently, they were diluted to a minimum OD of around 3, and this process was repeated over several cycles. As cell density increased, the amount of light reaching individual cells in the photic zone of each bag decreased. This was due to a self-shading effect, where the increasing cell concentration reduces light penetration, ultimately limiting growth (Richmond, 2003).

Following this cultivation strategy, Figure 3.4 presents the growth curves of *C. onubensis* under repeated-batch cultivation, assessed by OD at 750 and 680 nm (Figure 3.4a) as well as dry weight (dw) data (Figure 3.4b). Dry weight measurements indicate the total biomass present in a given culture volume, while OD_{750} reflects culture turbidity as an indirect measure of biomass concentration (Nielsen and Hansen, 2019). In contrast, OD_{680} provides an estimation of chlorophyll content in the cultures. As described earlier, repeated-batch cultivation consists of successive growth cycles, each of them initiated after culture dilution. Accordingly, Figure 3.4 is divided into four compartments, each of them corresponding to a dilution cycle, separated by dashed vertical lines.

Figure 3.4a shows that both OD_{750} and OD_{680} follow similar growth trends over time, with OD_{680} values consistently higher than OD_{750}, indicating the presence of chlorophyll-rich biomass. Additionally, growth exhibited a diminished rate during the first batch cycle (days 0–6). However, a cyclic, constant growth pattern emerged through

subsequent cycles showing no significant differences between them (Table S3.2 and S3.3 of Supplementary Material), suggesting a gradual adaptation of the cultures to the imposed experimental conditions. Similarly, by analyzing dry weight data in Figure 3.4b, the distinct growth pattern observed during the first cycle suggests an acclimation period to occur which is characterized by a reduced cell growth rate compared to subsequent cycles.

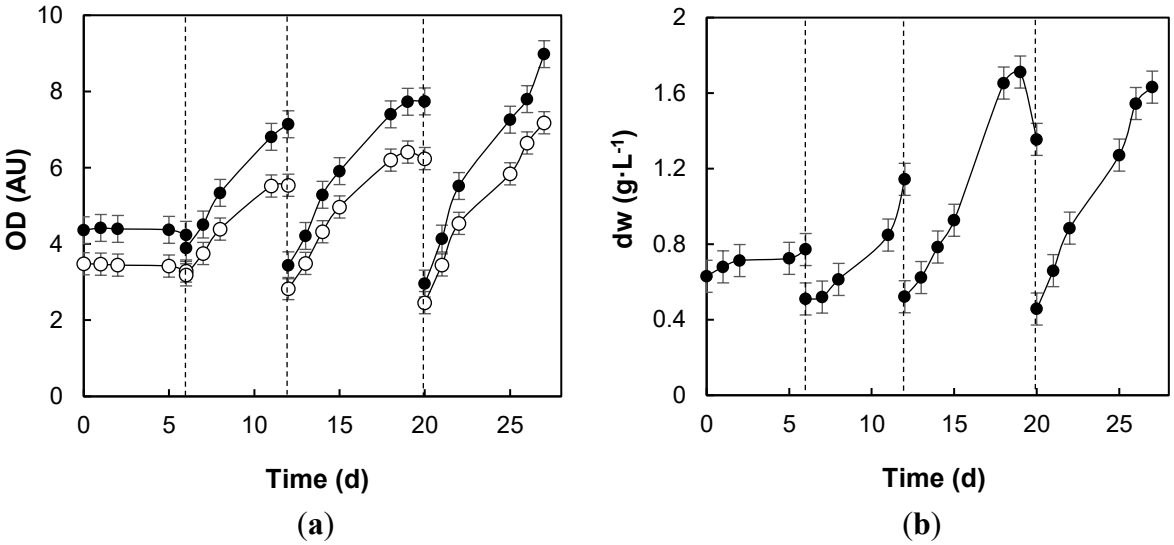

Figure 3.4. Growth curves of *C. onubensis* under several repeated-batch cultivation. (a) Optical density at 750 nm, OD_{750}, (-○-) and 680 nm, OD_{680}, (-●-) and (b) dry weight (dw) expressed as $g \cdot L^{-1}$. Dashed lines indicate that a new cultivation cycle has started.

The acclimation of the cultures to the imposed conditions was assessed through their growth factor, growth rates and productivity values calculated from dry weight data and presented in Table 3.1. The Table presents values of various growth-related parameters based on the time-dependent evolution of dry weight data for each cycle of repeated-batch cultivation of *C. onubensis*. Details regarding the calculation of each parameter can be found in the Materials and Methods section.

Table 3.1. Growth factors, specific growth rate and productivity values calculated based on the time-dependent evolution of dry weight data of repeated-batch cultivation of the microalga *C. onubensis.* Abbreviation (C): Cycle of repeated-batch cultivation. Values are means ± standard deviation (n = 3).

Batch culture cycle	Growth factor (d^{-1})	Specific growth rate (d^{-1})	Productivity ($g \cdot L^{-1} \cdot d^{-1}$)
C1	0.204^{a}	0.027^{a}	0.024^{a}
C2	0.374^{b}	0.131^{b}	0.106^{b}
C3	0.469^{c}	0.177^{c}	0.170^{c}
C4	0.510^{c}	0.172^{c}	0.168^{c}

$^{a, b, c.}$ Different superscript letters indicate differences in treatments with a significance of $p < 0.05$.

Table 3.1 shows a similar pattern in the evolution of these parameters throughout the repeated-batch cycles. Initially, the parameters exhibited lower values until the third cycle (C3) of repeated-batch cultivation, where the values stabilized and showed no significant differences. Additionally, the highest values recorded for the measured

parameters —0.51 d^{-1} growth factor, 0.17 d^{-1} specific growth rate, and 0.17 $g \cdot L^{-1} \cdot d^{-1}$ productivity— were obtained during the final cultivation cycle.

The results suggest an adaptative trend to the imposed conditions. The efficient production of a microalgal culture is linked to the photosynthetic viability of the cultured cells. Figure 3.5a illustrates the efficiency of photosystem II (PSII) performance, assessed through the quantum yield (Qy) parameter, in *C. onubensis* cultures under repeated-batch cultivation. Two trends are shown in the Figure: (i) the initial days of cultivation, cycle 1, characterized by a decline in Qy to values of about 0.6, and (ii) from cycle 2 onwards, where Qy remains roughly constant (Table S3.5 of Supplementary Material) at its highest level (approximately 0.7).

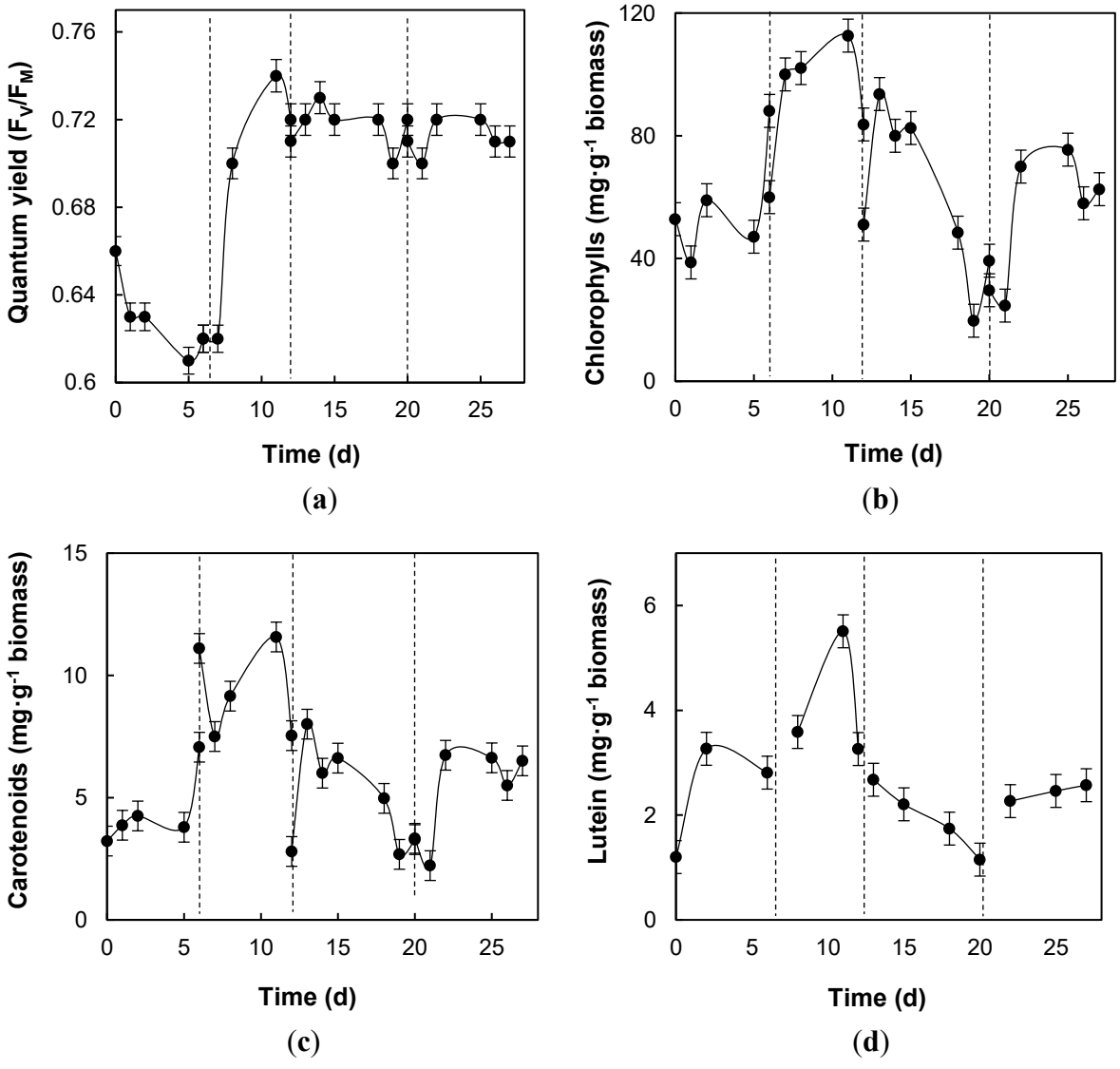

Figure 3.5. Photosynthetic viability of *C. onubensis* under repeated-batch cultivation. Maximum quantum yield (F_V/F_M) of photosystem II (PSII) (**a**), intracellular content of chlorophylls (**b**), carotenoids (**c**) and lutein (**d**) expressed as $mg \cdot g^{-1}$ biomass. Dashed lines indicate that a new cultivation cycle has started.

Figure 3.5b-d illustrates the temporal variation in intracellular chlorophyll and carotenoid concentrations in *C. onubensis* grown under repeated-batch cultivation. The figure delineates four distinct phases, each corresponding to a repeated-batch cycle. The

initial value for each cycle was recorded immediately after culture renewal. Figure 3.5b and 3.5c exhibit a pattern like that observed in the Qy data; specifically, after culture dilution a significative increase in intracellular chlorophyll and carotenoid content was detected (Table S3.6 and S3.7 of Supplementary Material), followed by a subsequent decline. The highest concentrations were recorded on day 11, second cycle, reaching 112.6 and 23.1 mg of chlorophylls and carotenoids per gram of biomass, respectively.

Figure 3.5d displays the intracellular concentration of lutein, the predominant carotenoid produced by *C. onubensis* (Robles et al., 2023), obtained from cultures of *C. onubensis* under repeated-batch cultivation. The figure reveals two distinct trends: (i) during the first two cycles, a similar trend to that obtained for Qy, chlorophylls and carotenoids was recorded, i.e. after culture dilution a significative increase in intracellular lutein content was detected (Table S3.8 of Supplementary Material), followed by a subsequent decline; and (ii) during the last two cycles, the intracellular lutein content appears to decrease across the cycles until its stabilization in the last cycle, when the culture has apparently acclimated to the imposed conditions. Noticeably, the highest intracellular lutein concentrations during the first cycle and the early part of the second cycle corresponded to low biomass concentrations, as shown in Figure 3.4.

The content of phenolic compounds was also analyzed in this study throughout repeated batch-cultivation cycles in *C. onubensis* cultures. The results are shown in Figure 3.6.

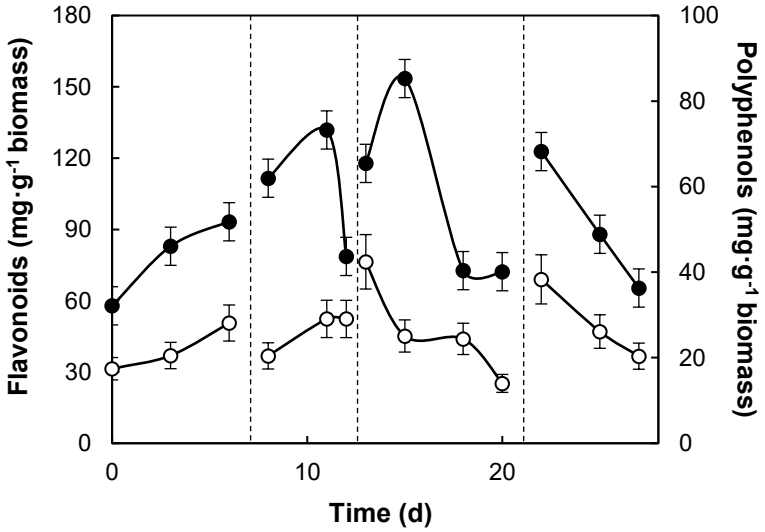

Figure 3.6. Phenolic compounds of the microalga *C. onubensis* under repeated-batch cultivation. Intracellular concentration of polyphenols (empty circles) and flavonoids (dark circles) expressed as mg g^{-1} biomass. Dashed lines indicate that a new cultivation cycle has started.

Figure 3.6 evaluates the time-dependent variation of polyphenol and flavonoid content in *C. onubensis* throughout the repeated batch-cultivation cycles. The figure again shows four distinct phases, each corresponding to a repeated-batch cycle. A pattern similar to that recorded for lutein was obtained. Nevertheless, the highest content of both phenolic compounds was obtained during the third cycle. Specifically, a significant increasing trend was obtained in the content of polyphenols and flavonoids from cycle 1 to 3 (Tables S3.9 and S3.10 of Supplementary Material), reaching maximum values during

the third cycle of, approximately, 42.5 and 153.5 $mg \cdot g^{-1}$ biomass, respectively. Additionally, as obtained in Figure 3.5 for Qy and photosynthetic pigments, the highest values in each cycle were obtained during the first 24-48 h of each cycle, followed by a decile at the end of each cycle. During the last cycle, the content of both flavonoids and polyphenols appeared to decrease once the culture had apparently acclimated to the imposed condition.

In summary, the growth and photosynthetic viability of the highly acidic-habitat microalga *C. onubensis* were analyzed under repeated-batch cultivation mode. Overall, the results evidenced that light irradiance greatly influences both growth and the stimulation of antioxidant molecules accumulation, particularly carotenoids.

4. Discussion

This study aimed to evaluate the effects of selected growth-influencing factors in *C. onubensis* using a factorial design (3^3) to optimize the microalgal response in repeated-batch cultivation mode on air fluidized bags. The effect of repeated batch-cultivation on the productivity and antioxidant compounds accumulation of the microalga was also evaluated. As explained above, cultures were maintained within an optical density (OD_{750}) range of 3 to 8, and growth, photosynthetic viability, and pigment and phenolic content were assessed.

4.1. Optimization of growth-influencing factors: factorial 3^3

As explained above, producing microalgal biomass efficiently is a key prerequisite in the production process of valuable compounds from microalgae (Fuentes et al., 2020). For large scale cultivation, optimization of key growth-influencing factors is crucial to ensure light and nutrient availability and, therefore, the viability of the microalgal culture. In this sense, this section analyzes the effect of three factors –temperature, light irradiance and Fe (III)– on the growth of the highly acidic-habitat microalga *C. onubensis*. Temperature and light irradiance were the factors that had the greatest influence on the biomass concentration of the microalga, whereas the influence of Fe (III) was not significant (Figure 3.2 and 3.3). Addition of Fe (III) had a negative influence on the growth of the microalga. However, Robles et al. 2023 (chapter 5 and 6 of this thesis) investigated the effect of adding Fe (III) to *C. onubensis* cultures as a unique factor and they found Fe (III) to significantly improve *C. onubensis* growth. Nevertheless, these two situations cannot be compared as this study compares the eventual synergistic effect of three factors in the growth of *C. onubensis*. For instance, the decrease in microalgal growth upon the addition of Fe (III) could be associated, to a greater or lesser extent, with variations in temperature and/or light irradiance. Therefore, the absence of significant differences in microalgal growth when including Fe (III) concentration as a variable in a 3^3 factorial experiment does not necessarily imply that Fe (III) has no effect on microalgal growth, as demonstrated by Robles et al. (2023).

Additionally, when analyzing the synergistic effect of the three factors on the microalgal growth, the mathematical model predicted that the optimal condition for maximum biomass production was no addition of Fe (III) to *C. onubensis* cultures and growing the microalga under moderate levels of temperature and light irradiance (28.9 °C and 486 μmol photon$\cdot m^{-2}\cdot s^{-1}$). Considering these growth-influencing factors as optimal, *C. onubensis* was grown under repeated-batch cultivation mode in air-fluidized bags. Light irradiance that reaches the cells depends on the depth of the culture. As this parameter values are higher in air-fluidized bags, light irradiance must be adjusted. In this sense, the average irradiance inside the culture (I_{av}) can be estimated through equation (3.5) described by Molina Grima et al. 1997, where I_0 is the light irradiance that reaches the microalgal culture surface, c_b is the biomass concentration of the microalgal culture, k_α is the extinction coefficient of biomass (which, generally, varies between 0.1 and 0.3 $m^2\cdot g^{-1}$) and L is the vessel optical path.

$$I_{av} = \frac{I_0}{c_b \times k_\alpha \times L} \times (1 - e^{-c_b \times k_\alpha \times L}) \qquad (3.5)$$

Considering the values obtained for the optimal growth condition of the factorial 3^3 (I_0 = 486.13 μmol photon·m^{-2}·s^{-1}, c_b = 1.29 g·L^{-1}, k_α = 0.18 m^2·g^{-1} and L = 0.08 m), the average irradiance inside the culture (I_{av}) was estimated as 26.08 μmol photon·m^{-2}·s^{-1}. Thus, the initial irradiance that reaches the culture surface (I_0) in the air-fluidized bags was estimated as, approximately, 700 μmol photon·m^{-2}·s^{-1} based on their optical path (L = 0.3 m) and the obtained average irradiance (I_{av}). For these reasons, several cycles of repeated batch-cultivation in air-fluidized bags were performed in *C. onubensis* cultures grown without extra addition of Fe (III), at moderate temperatures and at the optimal light irradiance estimated (700 μmol photon·m^{-2}·s^{-1}) for efficient biomass production.

4.2. Growth and antioxidant accumulation under repeated-batch cultivation

This section analyzes the growth and photosynthetic viability of the highly acidic-habitat microalga *C. onubensis* under repeated-batch cultivation. The data obtained suggest that *C. onubensis* can be cultivated under repeated-batch mode, achieving moderate productivity values in a highly acidic medium at pH 2.5. The repeated-batch cultivation process was operated for an additional cycle (data not shown) without significant variations in the growth parameters values. As previously explained, determination of dry weight provides information on the biomass concentration in a microalgal culture at a given cultivation time. However, this procedure requires at least 24 hours to yield accurate data. In contrast, optical density allows real-time monitoring of microalgal growth in liquid cultures, offering immediate measurements. Nevertheless, optical density cannot be considered a direct measure of biomass concentration. However, as shown in Figure 3.4, a similar pattern emerges when comparing optical density and dry weight values obtained for a growing *C. onubensis* culture. This suggests that optical density measurement, a more cost-effective and time-efficient procedure, can serve as a reliable proxy for growth assessment.

Furthermore, the analysis of Figure 3.4 indicates that growth stabilized between cycles 2 and 4 of the repeated-batch cultivation process. This observation is corroborated by the data presented in Tables S3.2 to S3.4 of the Supplementary Material, which shows no significant differences in the time-dependent growth evolution of the microalgal cultures under the aforementioned repeated-batch cycles. A given culture was considered acclimated when the time required to complete one cycle (from the initial to the final optical density) remained approximately constant across subsequent cycles under repeated-batch cultivation (Fuentes et al., 2016). This can be evaluated by analyzing the growth-related parameters presented in Table 3.1, which showed no significant differences between repeated-batch cycles 3 and 4. Furthermore, an assessment of the microalga's photosynthetic viability data in Figure 3.5 shows that Qy values felt within the range expected for photosynthetically viable cultures (0.6–0.7), as reported by Kühl et al. (2001). Thus, the adaptation of *C. onubensis* to grow under repeated-batch mode was achieved during the third dilution cycle, obtaining cultures photosynthetically efficient in air-fluidized bags in, approximately, 12 to 18 days.

The productivity values obtained for *C. onubensis* in the last cycles of the repeated-batch cultivation process (indoor) fall within the range of productivity values reported for commercially relevant microalgal species, including spp. from valuable genus such as *Chlorella* and *Tetraselmis*. For instance, Moheimani (2013) analyzed the growth of *Tetraselmis suecica* and *Chlorella* sp. in outdoor bag systems under moderate temperature, ranging from 20 to 35 °C, reporting productivity values of approximately 0.25 $g \cdot L^{-1} \cdot d^{-1}$ for *Tetraselmis suecica* and 0.3 $g \cdot L^{-1} \cdot d^{-1}$ for *Chlorella* sp. Abomohra et al. (2014) examined the growth of *Scenedesmus obliquus* in a semi-continuous bag cultivation system under a light intensity of 130 μmol photon $\cdot m^{-2} \cdot s^{-1}$ and moderate temperature ranging from 16 to 30 °C, reporting productivity values of approximately 0.14 $g \cdot L^{-1} \cdot d^{-1}$.

Interestingly, the microalgal productivity values mentioned above correspond to non-extremophilic species, whereas in this study they are compared with productivity values of the acidic environment microalga *C. onubensis*. The massive production of acidophilic microalgae (not exploited yet) has been reported to be hypothetically constrained by limited productivity, primarily due to the extreme pH conditions of the medium. These conditions force microalgal metabolism to expend energy in maintaining the proton gradient across the cell wall, thereby reducing the energy available for growth by approximately 10 % (Gross, 2000; Messerli et al., 2005). Nevertheless, the results of productivity obtained in this study with *C. onubensis* suggest that microalgae from highly acidic environments could be produced as efficiently as other non-extremophilic photosynthetic microorganisms. Additionally, extreme conditions are unsuitable for most microorganisms, allowing only the proliferation of extremophilic species that can withstand such harsh environments. Indeed, although acidophilic microalgae can coexist with prokaryotic microorganisms associated with their growth, the proliferation of exogenous biological contaminants is rare in long-term acidic cultures, as shown for a large culture of *C. onubensis* in a previous study by our team (Fuentes et al., 2020). Based on this, the main advantage of producing acidic environment microalgae, such as *C. onubensis*, is that the acidic pH of the culture medium inhibits the growth of non-acidotolerant microorganisms. The productivity data obtained for *C. onubensis* during the final cycles of repeated-batch cultivation (0.17 $g \cdot L^{-1} \cdot d^{-1}$) indicate that air-fluidized bag cultivation is a suitable system for its production.

Additionally, the increased OD_{680} values shown in Figure 3.4a compared to those at OD_{750} can be justified, as previously mentioned, since measurements at 680 nm are proportional to the chlorophyll content within the cell. In contrast, turbidity measurements at 750 nm do not correspond to any pigment maximum absorption wavelength (Schagerl et al., 2022), nor to those of the major macromolecules (e.g., proteins, nucleic acids). As described above, the highest optical density recorded in each repeated batch cycle (during the final 2–3 days of each cycle) exhibited a greater increase at 680 nm compared to the data obtained at 750 nm. This suggests that cellular chlorophyll content may increase as cell density rises in the culture. Thus, the intracellular chlorophyll variation of *C. onubensis* under repeated-batch cultivation was analyzed in Figure 3.5b. The evolution of intracellular chlorophyll content followed a

consistent pattern across all cycles, i.e. after dilution a significant increase in intracellular chlorophyll content was observed, followed by a subsequent decrease. When Figure 3.4 and 3.5b are analyzed together, it becomes evident that the decline in intracellular chlorophyll content begins in some cycles while the culture is still growing, indicating that sufficient nutrients are available.

In growing cultures illuminated with constant light irradiance on the culture surface, photon flux density availability decreases per cell. That is, the increasing cell density resulted in greater shading, limiting light availability for photosynthesis. This ultimately led to a slowdown in growth during the last days of each cycle, as shown in Figure 3.4. In response to it, the cells may reduce their chlorophyll content as a mechanism to enhance light penetration into the culture, allowing more photons to reach each cell per time unit, thereby counteracting the growth slowdown (Ort and Melis, 2010; Robles et al., 2023).

One of the findings of this chapter –specifically the decrease in chlorophyll content in cultures with higher cell density– may help explain the acclimation strategy of *Coccomyxa* in mining lakes. This strategy would involve counteracting the reduced light availability at depths of 8–10 meters below the lake surface, thereby enabling the microalga to bloom as long as other nutrients are sufficient. This interpretation is consistent with the findings of Sánchez-España et al. (2020).

To summarize, cells in less dense cultures experience greater photon availability. Conversely, as cultures become denser due to growth, excess pigments become unnecessary and the cells reduce their biosynthesis, including that of chlorophylls, to enhance photon capture (Ort and Melis, 2010). Within each cycle, the variation in cellular carotenoid content followed a similar pattern to that observed for chlorophylls (Figure 3.5c). Carotenoids, secondary pigments, play a key role in light capture, among other functions. Consequently, the intracellular increase in terpenoid content in low growth stages aligns with the well-known scenario of pigment accumulation channeling excess energy dissipation which could otherwise be detrimental to photosynthesis. Therefore, we propose that the observed decrease in the carotenoid content at the end of each cycle can be explained analogously to the reduction in chlorophylls. Specifically, this decrease may represent a mechanism by which cells increase light transmissivity in suspended cell cultures, thereby facilitating more efficient photon capture to more cells. Thus, a reduction in chlorophyll antenna size should result in an increased light absorption capacity of the culture, a behavior of *C. onubensis* that has been described by our group (Robles et al., 2023; Vaquero et al., 2016).

The increase in lutein content per cell observed during the initial cycles of repeated batch cultivation (Figure 3.5d) may be attributed to a potential response to stress by the microalga when exposed to the shifted conditions. The lutein content stabilized once the culture acclimated to the imposed conditions. A similar pattern was observed upon exposure of *C. onubensis* cells to Fe (III), suggesting a constitutive behavior for lutein of this microalga, given that lutein levels in Fe (III)-supplemented cultures did not significantly differ from those in control cultures (Robles et al., 2023).

Similarly, the variations obtained in polyphenols and flavonoids could also be attributed to the potential stress response of the microalga to the imposed conditions (Figure 3.6). That is, the greater availability of light during the first days of each cycle led to an increase in the intracellular concentration of reactive oxygen species (ROS), as described by Laloi et al. (2006), singlet oxygen being the first ROS to form. As a defense mechanism, microalgae have been described to respond to increased ROS levels by activating the production of antioxidants, especially PUFAs, polyphenols and carotenoids, among others (Das & Roychoudhury, 2014). The referred activation of antioxidants production would be consistent with the intracellular increase in lutein, polyphenols and flavonoids observed at the beginning of each repeated bath cycle, in coherence with the expected higher levels of ROS in cells exposed to greater irradiance upon culture dilution.

4.3. Strategies for efficient biomass production and accumulation of valuable molecules

The findings of this study underscore the importance of controlling the dynamics of phenolic compounds, chlorophyll and carotenoid accumulation during *C. onubensis* growth, which would be of relevance for planning mass production processes of this acidic habitat microalga. In this sense, several production strategies would be considered when cultivating *C. onubensis* under repeated-batch cultivation mode in air-fluidized bags depending on the growth stage and, therefore, light availability, as summarized in Figure 3.7.

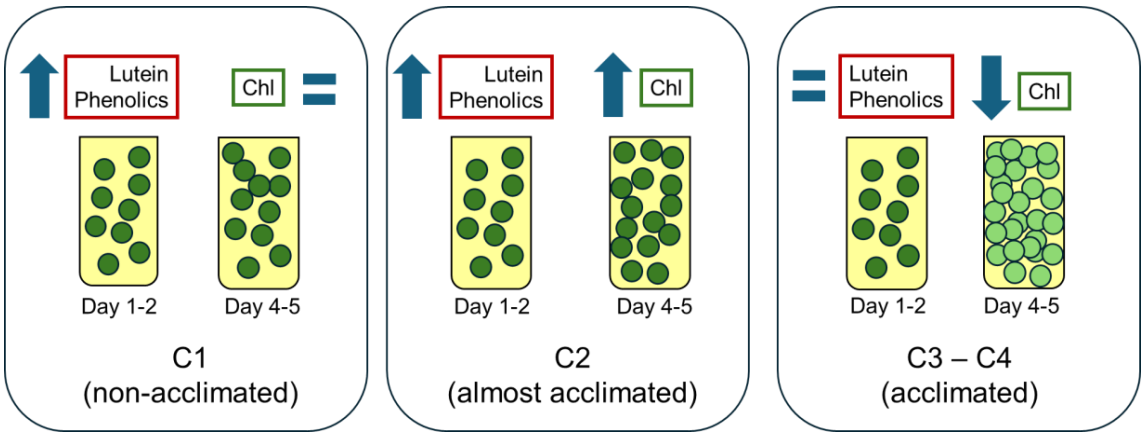

Figure 3.7. Schematic representation of the main changes in *C. onubensis* cells grown under repeated-batch cultivation mode in air-fluidized bags as a function of growth stage and light availability. Symbols: Cn (number of repeated-batch cycle) and Chl (Chlorophylls).

At the maximum level of light availability, i.e. at the beginning of the first cycles, the excess of light in *C. onubensis* would increase ROS content in the microalga, therefore, generating oxidative stress. The direct consequence of that fact is the increase in antioxidant compounds (lutein and phenolic compounds) as a defense mechanism to neutralize ROS species, therefore reducing the oxidative pressure caused by the excess light. Is that the possible reason why almost no growth was obtained in the microalgal cultures during the first cycle of repeated-batch cultivation. Nevertheless, during the second cycle of repeated-batch cultivation the growth of the microalga is enhanced, this could be

attributed to efficient functioning of the antioxidant mechanism and the photoacclimation of the microalga which includes shifted accumulation of photosynthetic pigments. Once the cultures are acclimated to the imposed conditions, the reduced stress results into lutein and phenolic content to fall to its constitutive values. The increase in the number of cells makes the culture experience a lower light availability. Consequently, a decrease in chlorophyll antenna size seems to occur, representing a physiological acclimation of the microalga to the reduced light availability in high-cell density cultures, to maximize light absorption.

In this sense, depending on the industrial objective several strategies could be suggested to address efficient biomass production. On the one hand, for efficient biomass production, the cultures should be kept acclimating for 3 or 4 subsequent cycles whereas the content of antioxidant compounds drop to its constitutive values. On the other hand, to produce an antioxidant-rich biomass just one or two cycles of repeated-batch cultivation would address increased contents of target molecules whereas biomass productivity would be lower due to the culture acclimation to the imposed conditions. Nevertheless, in case accumulation of antioxidants and moderate biomass productivity are required, a balance between both situations can be addressed during the second cycle of repeated-batch cultivation.

In addition, the findings of this study help partly explain the ecological relevance of *C. onubensis*, a unique acidic environment photosynthetic microorganism which is typically found in open acidic waters and in acidic lagoons of the Pyritic Belt in Huelva (Spain), mostly at highly exceeding one meter. Interestingly, according to the results shown and discussed in this study, this microorganism can adapt to low-light conditions by capturing light in deeper zones of the acidic water column. Subsequently, it can serve as primary nutrient source for sulphate-reducing bacteria when further decomposed in their natural habitat, as proposed by Sánchez-España et al. (2020).

5. Conclusions

The findings of this Chapter revealed that *Coccomyxa onubensis* demonstrated biomass productivity comparable to that of non-extremophilic microalgae under repeated-batch cultivation in open air-fluidized systems, validating its biotechnological potential for sustainable large-scale production under extreme environmental conditions. Despite the energetic constraints associated with growth in acidic environments (pH 2.5), *C. onubensis* achieved productivities up to 0.17 $g \cdot L^{-1} \cdot d^{-1}$, similar to those reported for industrially relevant genera such as *Chlorella* and *Tetraselmis*. These findings challenge the prevailing assumption that acidic conditions limit microalgal productivity and establish *C. onubensis* as a robust candidate for open-system cultivation with reduced risk of biological contamination. The accumulation of antioxidant compounds in *C. onubensis* is tightly regulated by intracellular light availability modulated by cell density during repeated-batch cultivation, reflecting efficient photoacclimation mechanisms. A transient increase in intracellular lutein, polyphenols, and flavonoids was observed during early cultivation cycles, likely triggered by oxidative stress due to excess light. As cultures acclimated and cell density increased, the content of these compounds declined, along with chlorophyll levels, suggesting a reduction in antenna size as a physiological response to maximize light utilization under self-shading conditions. Finally, this study establishes an effective operational model for biomass or antioxidant production in *C. onubensis* through repeated-batch cultivation, offering a tool for microalgal biorefinery within a circular bioeconomy framework. Depending on the industrial goal, cultivation strategies could be adapted: one or two cycles to maximize antioxidant accumulation at the expense of biomass, or three or more cycles to achieve higher biomass yields with reduced metabolite content. This physiological and biochemical plasticity enhances the versatility of *C. onubensis* as a production platform for environmentally sustainable biotechnological applications.

6. Supplementary material

Statistical analysis Figure 3.3

Table S3.1. Effect of different growth-influencing factors –temperature, light irradiance and Fe (III)– on the growth of *C. onubensis* obtained by estimating the biomass concentration through dry weight measurements.

Terms of the model	*Estimate*	*P-Value*
constant	-16.2416	
A: T (ºC)	1.12267	0.0000
B: Fe (mM)	0.179547	0.3313
C: Light (µmol photon·m^{-2}·s^{-1})	0.00530202	0.0027
AA	-0.018644	0.0000
AB	-0.0155693	0.0361
AC	-0.0000887455	0.0106
BB	0.141637	0.0646
BC	-0.0000723699	0.6340
CC	-0.00000280999	0.0239
Statistics for the goodness of fit of the model		
R^2	0.908717	
adjusted R^2	0.86039	
RSD	0.122643	
P	0.0771642	

Statistical analysis Figure 3.4

Table S3.2. Time-dependent evolution of growth, measured as optical density at 750 nm, under several repeated-batch cultivation in cultures of *C. onubensis*. Abbreviation: Cycles or period of repeated-batch cultivation (C).

Time (d)	**C1**	**C2**	**C3**	**C4**
0	3.48^{a}	3.19^{a}	2.83^{a}	2.46^{a}
1	3.47^{a}	3.75^{a}	3.49^{a}	3.45^{a}
2	3.44^{a}	4.39^{b}	4.32^{b}	4.54^{b}
5	3.42^{a}	5.52^{b}	5.70^{b}	5.84^{b}
6	3.29^{a}	5.54^{b}	6.2^{bc}	6.65^{c}
7			6.41^{a}	7.18^{a}
8			6.24^{a}	

$^{a, b, c}$ Different superscript letters indicate differences in treatments with a significance of $p < 0.05$.

Table S3.3. Time-dependent evolution of growth, measured as optical density at 680 nm, under several repeated-batch cultivation in cultures of *C. onubensis*. Abbreviation: Cycles or period of repeated-batch cultivation (C).

Time (d)	C1	C2	C3	C4
0	4.36^{a}	3.89^{ab}	3.44^{bc}	2.96^{c}
1	3.47^{a}	3.75^{a}	3.49^{a}	3.45^{a}
2	4.39^{a}	5.34^{b}	5.29^{b}	5.52^{b}
5	4.37^{a}	6.81^{b}	7.01^{b}	7.26^{b}
6	4.24^{a}	7.14^{b}	7.40^{bc}	7.80^{c}
7			7.73^{a}	8.98^{b}
8			7.74^{a}	

$^{a, b, c}$ Different superscript letters indicate differences in treatments with a significance of $p < 0.05$.

Table S3.4. Time-dependent evolution of growth, measured as dry weight, under several repeated-batch cultivation in cultures of *C. onubensis*. Abbreviation: Cycles or period of repeated-batch cultivation (C).

Time (d)	C1	C2	C3	C4
0	0.63^{a}	0.51^{a}	0.52^{a}	0.46^{a}
1	0.68^{a}	0.52^{a}	0.62^{a}	0.66^{a}
2	0.71^{ab}	0.61^{b}	0.78^{ab}	0.88^{a}
5	0.72^{a}	0.85^{b}	1.05^{c}	1.27^{c}
6	0.77^{a}	1.14^{b}	1.65^{c}	1.54^{c}
7			1.71^{a}	1.63^{a}
8			1.35^{a}	

$^{a, b, c}$ Different superscript letters indicate differences in treatments with a significance of $p < 0.05$.

Statistical analysis Figure 3.5

Table S3.5. Time-dependent evolution of photosynthetic efficiency, measured as Quantum yield, under several repeated-batch cultivation in cultures of *C. onubensis*. Abbreviation: Cycles or period of repeated-batch cultivation (C).

Time (d)	C1	C2	C3	C4
0	0.66^{a}	0.62^{b}	0.71^{c}	0.71^{c}
1	0.63^{a}	0.62^{a}	0.72^{b}	0.72^{b}
2	0.63^{a}	0.7^{b}	0.73^{c}	0.73^{c}
5	0.61^{a}	0.74^{b}	0.72^{c}	0.72^{c}
6	0.62^{a}	0.72^{b}	0.72^{b}	0.72^{b}
7			0.7^{a}	0.7^{a}
8			0.72^{a}	

$^{a, b, c}$ Different superscript letters indicate differences in treatments with a significance of $p < 0.05$.

Table S3.6. Time-dependent evolution of chlorophyll concentration under several repeated-batch cultivation in cultures of *C. onubensis*. Abbreviation: Cycles or period of repeated-batch cultivation (C).

Time (d)	C1	C2	C3	C4
0	52.82^{a}	124.37^{b}	51.06^{c}	29.65^{d}
1	38.72^{a}	100.62^{b}	93.60^{b}	24.65^{c}
2	59.63^{a}	102.06^{b}	80.73^{c}	69.95^{d}
5	47.10^{a}	112.64^{b}	82.52^{c}	75.48^{c}
6	78.29^{a}	83.69^{a}	48.42^{b}	58.72^{c}
7			19.72^{a}	62.59^{b}
8			39.28^{a}	

$^{a, b, c, d}$ Different superscript letters indicate differences in treatments with a significance of $p < 0.05$.

Table S3.7. Time-dependent evolution of carotenoid concentration under several repeated-batch cultivation in cultures of *C. onubensis*. Abbreviation: Cycles or period of repeated-batch cultivation (C).

Time (d)	C1	C2	C3	C4
0	6.45^{a}	22.20^{b}	5.59^{a}	6.67^{a}
1	7.74^{a}	15.54^{b}	16.01^{b}	4.44^{c}
2	8.53^{a}	18.30^{b}	12.73^{c}	13.46^{c}
5	7.58^{a}	22.14^{b}	13.23^{c}	13.25^{c}
6	14.13^{a}	15.07^{a}	9.94^{b}	11.72^{c}
7			5.36^{a}	13.01^{b}
8			6.57^{a}	

$^{a, b, c, d}$ Different superscript letters indicate differences in treatments with a significance of $p < 0.05$.

Table S3.8. Time-dependent evolution of lutein concentration under several repeated-batch cultivation in cultures of *C. onubensis*. Abbreviation: Cycles or period of repeated-batch cultivation (C).

Time (d)	C1	C2	C3	C4
0	1.19^{c}	3.59^{a}	2.67^{ab}	2.27^{bc}
2	3.26^{a}	5.51^{b}	2.21^{c}	2.46^{c}
5	2.81^{ab}	3.26^{a}	1.74^{b}	2.57^{ab}
7			1.15^{a}	

$^{a, b, c}$ Different superscript letters indicate differences in treatments with a significance of $p < 0.05$.

Table S3.9. Time-dependent evolution of polyphenol concentration under several repeated-batch cultivation in cultures of *C. onubensis*. Abbreviation: Cycles or period of repeated-batch cultivation (C).

Time (d)	C1	C2	C3	C4
0	17.427[a]	20.422[a]	42.42[b]	38.317[b]
3	20.510[a]	29.073[b]	25.078[bc]	26.118[c]
5	28.108[a]	29.053[a]	24.403[b]	20.358[c]
7			13.993[a]	

[a, b, c] Different superscript letters indicate differences in treatments with a significance of $p < 0.05$.

Table S3.10. Time-dependent evolution of flavonoid concentration under several repeated-batch cultivation in cultures of *C. onubensis*. Abbreviation: Cycles or period of repeated-batch cultivation (C).

Time (d)	C1	C2	C3	C4
0	57.837[a]	111.536[b]	117.769[b]	122.753[b]
3	82.9068[a]	131.836[b]	153.483[c]	87.937[a]
5	93.216[a]	78.618[b]	72.649[bc]	65.326[c]
7			72.207[a]	

[a, b, c] Different superscript letters indicate differences in treatments with a significance of $p < 0.05$.

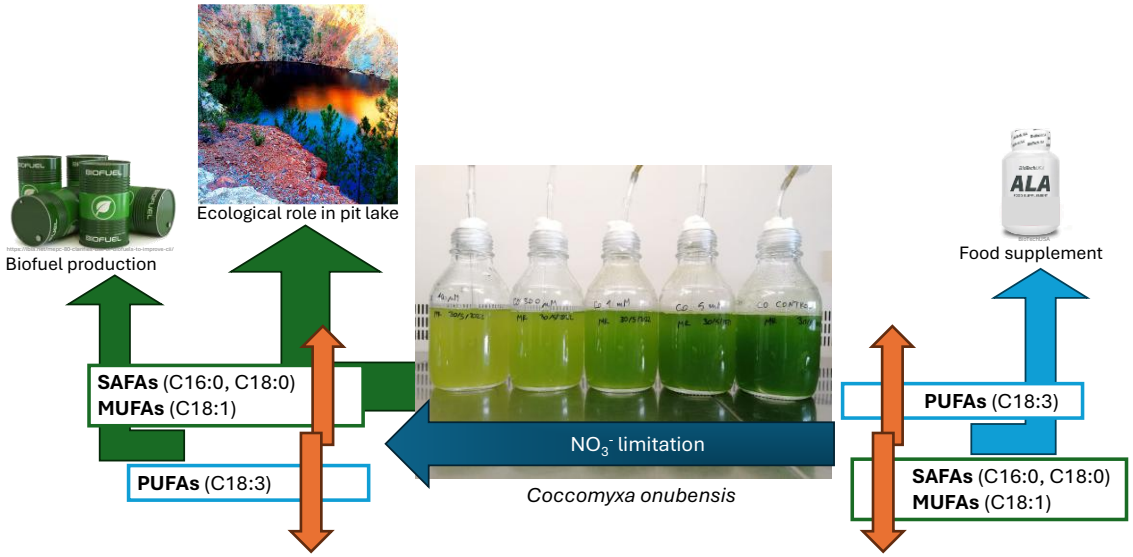
Ecological role in pit lake
Biofuel production
Food supplement
ALA
SAFAs (C16:0, C18:0)
MUFAs (C18:1)
PUFAs (C18:3)
NO3- limitation
Coccomyxa onubensis
PUFAs (C18:3)
SAFAs (C16:0, C18:0)
MUFAs (C18:1)

CHAPTER

4

Modulation of nitrogen-free molecules production in a highly acidic-habitat microalga under nitrogen limitation

Table of contents

Abstract: In microalgal cultures, nitrogen deprivation leads to a markedly reduced synthesis of nitrogen-rich molecules such as proteins and chlorophylls. This typically results in lower photosynthetic efficiency and, consequently, growth inhibition or cessation. However, under such stress conditions, metabolic energy may be redirected toward the synthesis of nitrogen-free biomolecules such as carbohydrates and lipids. This study aimed to investigate lipid biosynthesis and accumulation in the highly acidic-habitat microalga *Coccomyxa onubensis* (*C. onubensis*) under varying degrees of nitrogen limitation, achieved by adjusting nitrogen availability to 0.01, 0.3, 1, 5, and 26 mM (nitrogen-replete condition). The results confirmed the essential role of inorganic nitrogen in the growth and viability of *C. onubensis*, as nitrogen limitation led to decreased growth and photosynthetic performance. Nonetheless, nitrogen limitation significantly enhanced the accumulation of carbohydrates and lipids, with increases of 2.07-fold and 1.13-fold, respectively, at 0.01 mM NO_3^-. Fatty acid content progressively increased as nitrogen availability decreased, reaching its highest level—1.54-fold higher than the control—in cultures grown with the lowest nitrogen concentration (0.01 mM NO_3^-). A partial lipidomic analysis revealed that nitrogen limitation significantly increased the total content of saturated fatty acids (SAFAs), specifically C18:0 and C16:0, by 2.87- and 2.08-fold, respectively. Remarkably, the monounsaturated fatty acid (MUFA) C18:1 increased by 88-fold. Conversely, the polyunsaturated fatty acid (PUFA) C18:3 decreased by approximately 1.84-fold under nitrogen limitation. In contrast, cultures grown with 5 mM nitrate accumulated higher levels of C18:3 and lower levels of SAFAs and MUFAs. These findings suggest that manipulating nitrogen concentration in *C. onubensis* cultures can serve as an effective strategy to obtain fatty acid-enriched biomass tailored either for biofuel production or as a food supplement, depending on the desired degree of fatty acid unsaturation. Additionally, the results may indicate a potential ecological role for *C. onubensis* as a source of electron donors supporting bacterial growth in its natural habitat, such as acidic pit lakes, an aspect further discussed in this study.

Keywords: Microalgae, acidophiles, *Coccomyxa*, lipidomics, fatty acids, nitrogen limitation.

1. Introduction

The current energy model necessitates the development of alternative and sustainable energy sources, primarily due to the depletion of fossil fuel reserves and the high levels of CO_2 emissions associated with their use. As a result, alternative fuels—such as biodiesel derived from microalgae—are receiving increasing attention (Chisti, 2007). The growing industrial interest in microalgae is justified by their natural ability to produce a wide range of valuable compounds, including significant amounts of triacylglycerols (TAGs) and high-value biomolecules such as terpenoids, phenols, phytosterols, and long-chain polyunsaturated fatty acids (LC-PUFAs) (Schüler et al., 2017). Several studies have demonstrated that green microalgae are well-suited for biofuel production due to their high lipid content, which typically ranges from 20 to 50 % of their dry weight (Chisti, 2007; Spolaore et al., 2006). In addition, microalgae convert solar energy into biomass more efficiently than terrestrial plants, primarily due to their simple cellular structure and their growth in aqueous environments, which provide constant access to inorganic carbon—mainly in the form of bicarbonate—as well as other essential nutrients (Chacón-Lee and González-Mariño, 2010; Wijffels and Barbosa, 2010).

The suitability of vegetable oils for use in food, industrial applications, and fuel production largely depends on the fatty acid composition of their triacylglycerols (TAGs) (Bates and Browse, 2012). For example, polyunsaturated fatty acids (PUFAs) —such as linolenic acid (C18:3, ALA), eicosapentaenoic acid (C20:5, EPA), and docosahexaenoic acid (C22:6, DHA)— as well as polar lipids, are more suitable for use in nutraceutical formulations than those esterified in neutral lipids (Guedes et al., 2010). These fatty acids are essential because they cannot be produced within the human body (Saini et al., 2021). In addition, these compounds are considered pharmacologically relevant for both dietary and therapeutic applications. EPA and DHA are incorporated into various tissues, particularly into cell membranes, where they play a key role in modulating anti-inflammatory processes (Swanson et al., 2012). Alpha-linolenic acid (ALA) has a significant impact on the regulation of oxidative stress and the enhancement of mitochondrial function (Lopez-Maldonado et al., 2021). Thus, these PUFAs have been shown to be beneficial in the prevention or treatment of various diseases, including peripheral artery disease, coronary events, and in modulating anticoagulant activity (Serhan et al., 2008).

Short-chain fatty acids C14-C18 are more suitable for biodiesel production (Huang et al., 2010). C16:0 and C18:1 are considered the most common fatty acid components of biodiesel, with C18:1 being especially predominant. In addition, oleic acid (C18:1n-9c) has applications in the food industry due to its antiatherogenic and antithrombotic properties; it also increases the HDL/LDL cholesterol ratio and reduces platelet aggregation (Tonstad and Clifton, 2017). Olive oil, the primary dietary source of oleic acid, appears to exert protective anticancer effects and modulate the inflammatory response (Rodrigues et al., 2010). Due to their favorable properties, monounsaturated fatty acids (MUFAs) are preferred for biodiesel production. However, fuels containing a high proportion of polyunsaturated fatty acids (PUFAs) tend to exhibit poor oxidative

stability because their numerous double bonds are highly susceptible to autoxidation (Griffiths et al., 2012). This issue can be managed, for example, by selecting cultivation conditions that favor the differential production of monounsaturated and polyunsaturated fatty acids. In this context, microalgal biotechnology currently employs cultivation strategies aimed at activating metabolic pathways that modify biomass composition to meet specific objectives, such as enriching the biomass with antioxidant compounds or optimizing it for biodiesel production (Schüler et al., 2020). For example, the accumulation of carotenoids and long-chain polyunsaturated fatty acids (LC-PUFAs) has been shown to be stimulated under growth-promoting conditions or low light intensity, resulting in a biomass composition that is promising for nutraceutical applications (Guedes et al., 2010). However, triacylglycerols (TAGs) are enhanced in cultures subjected to non-optimal conditions, such as nutrient depletion, which typically occurs when cultures enter the stationary phase. This shift in biomass composition makes it more suitable for biodiesel production (Huang et al., 2010). Nitrogen deprivation leads to a reduced synthesis of nitrogen-rich molecules, such as proteins and chlorophylls. The direct consequence is a decrease in photosynthetic efficiency, resulting in growth limitation and eventual cessation (Markou et al., 2017). In this context, metabolic energy may be redirected toward the synthesis of energy-rich, carbon-rich biomolecules that lack nitrogen—such as carbohydrates and/or lipids—explaining the observed increase in TAG production.

Selecting microalgal strains suitable for mass cultivation and lipid production is essential for developing efficient production processes. *Coccomyxa onubensis* (*C. onubensis*), the strain used in this study, is an acidotolerant eukaryotic microalga isolated from acid mine drainage sites in the pyritic belt of the province of Huelva, Spain (Garbayo et al., 2012), characterized by the presence of high levels of cations in solution, of which Fe (II) and (III) and Cu (II) have a relevant quantitative presence (Amils et al., 2014). The adaptability of the microalga to the aforementioned extreme conditions, combined with the low nitrogen concentrations in its natural acidic habitat (as low as 0.05 mM nitrate) (Bottaro et al., 2025) makes *C. onubensis* a prominent candidate for this study. Therefore, this microalga serves as an example of a photosynthetic microorganism adapted to the extremely acidic waters and high dissolved metal concentrations characteristic of its natural environment. Based on the extreme acidic conditions of its habitat, a specific culture medium was developed in which *C. onubensis* proliferates at moderate growth rates and is notable for accumulating antioxidant molecules such as linoleic acid, linolenic acid, and lutein (Bermejo et al., 2018), which have been reported to display anti-inflammatory and antimicrobial activities (Montero-Lobato et al., 2018; Navarro et al., 2016).

Interestingly, *C. onubensis* has been found to dominate phototrophic communities in acidic pit lakes of the Iberian Pyrite Belt, being responsible for pronounced chlorophyll *a* blooms observed at depths of approximately 8 to 10 meters in several acidic pit lakes in southwestern Spain (Sánchez-España et al., 2020). This study aimed to gain insight into lipid accumulation under nitrogen (nitrate) limitation, which could help elucidate both the potential ecological role of *Coccomyxa* in acidic pit lakes and its

biotechnological potential for lipid production. The production of other valuable biomolecules was also analyzed, and the ecological significance of *C. onubensis* fatty acid composition as biochemically suitable nutrients for acidophilic bacteria is discussed.

2. Materials and methods

2.1. Biological material and culture conditions

The organism used for this work was, as described by Robles et al. (2023), the microalga *Coccomyxa onubensis* ACCV1 (SAG 2510), an acidotolerant and halotolerant microalga isolated from the acidic waters of the Tinto River (Huelva) in the sampling area at latitude 37.5851153° and longitude −6.550754°, by the Microalgae Biotechnology Unit (BITAL), of the Department of Chemistry "Professor Jose Carlos Vílchez Martín," from the Faculty of Experimental Sciences and CIQSO of the University of Huelva, Spain (Fuentes et al., 2016).

C. onubensis was grown in an optimized liquid culture medium, K9 (Silverman and Lundgren, 1959). The constituents of K9 (per liter) were as follows: 3.95 g K_2SO_4, 0.1 g KCl, 0.5 g K_2HPO_4, 0.41 g $MgCl_2$, 2.29 g KNO_3, 0.01 g $CaCl_2$, and 5 mL of Hutner traces, which were prepared as described in (Garbayo et al., 2012). *C. onubensis* cultures were prepared at an initial concentration of, approximately, 0.2 $g \cdot L^{-1}$, from a mother culture in the middle of the linear growth phase, the pH was adjusted to 2.5 and the cultures were subjected to different degrees of nitrogen limitation (added as KNO_3) from 26 mM (nitrogen-replete culture) to 0.01 mM. The cultures were established in a culture room at 25 °C ± 2. Light was supplied by white light fluorescent tubes, reaching the cultures at a constant light intensity of 150 µmol (photon)$\cdot m^{-2} \cdot s^{-1}$ for 24 h, and the cultures were bubbled with air enriched with 2.5 % (v/v) CO_2.

2.2. Growth and photosynthetic viability determination

Growth was followed, as described by Robles et al. (2023), by cell density and determined by measuring dry weight of the biomass present in 2 mL of culture medium. Dry weight was analyzed gravimetrically in a scale model CP225D (sartorius, Germany) by filtering 2 mL culture samples through 0.7 µm filters, MFV5 model (Anoia, Spain) and allowing the filters to dry for 24h in an oven at 100°C.

Photosynthetic viability was determined based on the measurement of chlorophyll fluorescence, the maximum quantum yield (F_V/F_M) of Photosystem II (PSII) according to published methodology (Schreiber, 2004). Quantum yield (Qy) was measured by subjecting cultured samples of *C. onubensis* to darkness for 15 min and then placing them in the measurement chamber of the AquaPEN AP-C 100 portable amplitude-modulated pulse fluorimeter (Photon Systems Instruments, Drasov, Czech Republic). F_V represents the variable fluorescence and is calculated as $F_V = F_M - F_0$, being F_0 the minimum level of fluorescence observed after exposing cells to a non-actinic beam and acclimating them in the dark, while F_M represents the maximum fluorescence observed in cells after exposing them to a brief but saturating pulse of actinic light.

2.3. Transmission electron microscopy

Transmission electron microscopical (TEM) observations was performed, as described by Robles et al. (2025), with the method described by Nishikawa et al. (2006) was performed. The microalgal cells were collected by centrifugation (1.5 *g*, 1 min) from

each culture (cultures treated with different Fe (III) concentrations, and control culture). The microalgal cells were fixed with 1 % glutaraldehyde in 0.1 M sodium cacodylate buffer (pH 7.4) for 2 h at 4 °C. The cells were then washed three times for 5 min using the same buffer. The samples were postfixed with 1 % osmium tetroxide in 0.2 M cacodylate buffer at 4 °C for 1 h. Samples were washed with the same buffer, dehydrated in a graded ethanol series, and embedded in Epon 812 (Electron Microscopy Science, USA). Ultrathin sections of 80–90 nm obtained by an ultramicrotome (Leica, Germany) and placed on copper grids were stained with aqueous 1 % (w/v) uranyl acetate and lead citrate. Transmission electron micrographs were observed with a JEM 1011 (Jeol Ltd., Japan) electron microscope using an accelerating voltage of 80 kV. Several photographs of entire cells and of local detailed structures were taken at random, analyzed, and compared to investigate the effect of different concentrations of Fe (III) on different subcellular structures.

2.4. Nitrogen determination

Nitrate was determined every day, as described by Dineshkumar et al. 2016, on supernatants of culture samples centrifuged at 3 *g* for 5 min. Supernatants were collected after filtration of samples through 0.45 µm syringe filters (Millipore®). Briefly, 0.85 mL of supernatants were mixed with 0.17 mL of 0.1 N HCl. The samples were mixed, and the absorbance was measured at 220 nm and 275 nm. Absorbance at 220 nm corresponds to nitrate and at 275 nm corresponds to nitrite. Nitrogen concentration was determined based on a calibration curve from a standard solution of nitrate, equation 4.1.

$$\text{Nitrogen (mM)} = 0.0027 \times (\text{Abs}_{220} - 2\text{Abs}_{275}) - 0.0842 \qquad (4.1)$$

2.5. Chlorophyll determination.

Chlorophyll content was determined as described by Cuaresma et al. (2012). Culture samples, containing 1 or 2 mL, were centrifuged at 3 *g* for 5 min, methanol was added to the pellet, and the mixture was placed in an ultrasound bath (60 °C, 5 min) to weaken the microalgal cell wall. After another centrifugation step, the supernatant was collected and analyzed by UV/Visible spectrophotometry. Modified Arnon's equations were used to calculate the chlorophyll concentrations in the extracts.

2.6. Lipids and fatty acids determination

Lipid content of the microalgal biomass was measured in lyophilized biomass samples as described by Südfeld et al. (2021). Briefly, 10 mg samples were extracted with chloroform:methanol (2:1, v/v). The extraction process was followed by solvent evaporation using an N_2 stream. Subsequently, lipid content was determined gravimetrically.

Fatty acid analysis was performed according to the following procedure (Robles et al., 2023). Once the acylglycerides were extracted, the corresponding fatty acids methyl-ester (FAME) were obtained through acid catalysis-mediated transesterification. The mixture was heated at 85 °C for 1 h, then cooled and washed with hexane and water.

FAMEs were obtained from the upper organic layer upon centrifugation (3 *g*, 10 min). FAMEs were separated and analyzed in a gas chromatograph system equipped with flame ionization detector (model 7890A, Agilent, California, USA). A 1-µL sample was injected into a silica capillary column (30 m, 0.32 mm id and 0.25-µm film thickness). Helium was used as carrier gas. The applied flow rate was 1.5 $mL \cdot min^{-1}$ and the split ratio 20:1. The injector and detector temperature values were 100 °C and 220 °C, respectively. The programmed oven temperature raised from 80 to 140 °C at 5 °C min^{-1}, followed by increase to 170 °C at 4 °C min^{-1} and then maintained for 2 min at 170 °C. Temperature was then increased to 190 °C at 1 °C min^{-1} and maintained for 2 min. The final temperature in the oven was 210 °C. Each one of the FAME peaks was identified by comparing retention times with those of mixed fatty acids standards (FAMEs Mix C4-C24 Supelco Analytical). Concentrations of FAMEs (ppm) were quantified by comparing their peak areas with those obtained from the standards of known concentration (Sigma Aldrich, St. Louis, MI, USA). Fatty acid composition was calculated as percentage of the total fatty acids in the volume of hexane. For quantification, tripentadecanoin was used as internal standard (Sigma Aldrich, St. Louis, MI, USA).

2.7. Carbohydrates

Carbohydrate content was determined by the method described by (DuBois et al., 1956). Freeze-dried biomass samples of about 15 mg of residue were used. The first stage of this protocol is acid hydrolysis. To do this, a positive control was prepared with 3 mg of glucose in triplicate. The corresponding volume of a 2.5 M HCl solution is added to each sample and positive control, 0.5 mL HCl/mg biomass. To break up the biomass, the tubes are placed in an ultrasound bath at 40 ºC for 10 minutes. Then, the samples were vortexed and incubated in a bath at 100.5 ºC for 3 hours. Afterwards, the samples were allowed to cool down to room temperature and were neutralized with the addition of the corresponding volume of a 2.5 M NaOH solution, 0.5 mL NaOH/mg biomass. Finally, the samples were centrifuged at 3 *g* for 5 min.

Then, 500 µL of 5 % phenol (v/v) and 2.5 mL of concentrated H_2SO_4 were added to each tube, incubated for 10 minutes at room temperature and then placed in a bath at 35 ºC for 30 minutes. Finally, the carbohydrate content of the samples was determined spectrophotometrically by measuring the absorbance at 483 nm, using distilled water as a blank. Total content of carbohydrates was determined by a calibration curve from a standard solution of glucose.

2.8. Statistics

Unless otherwise stated, all data are presented as the mean of three independent experiments replicates, and the standard deviations are shown in the corresponding figures and tables. The data from the different treatments were evaluated by constructing univariate statistical models and performing the analysis of variance (ANOVA) (confidence of 95% was considered for determining statistical significance). All analyses were performed using the Minitab 21 software.

3. Results

In nitrogen-limited cultures, metabolic energy can be stored in the form of carbohydrates and/or lipids. This study aimed to gain insight into fatty acid biosynthesis and accumulation in the highly acidic-habitat microalga *Coccomyxa onubensis* (*C. onubensis*) through a partial lipidomic approach. Cultures were incubated under varying concentrations of inorganic nitrogen—0.01, 0.3, 1, 5 and 26 mM nitrate (nitrogen repletion). The experimental design also allows a preliminary discussion on the potential ecological role of *Coccomyxa* sp. as a nutrient source for bacterial growth in the photic zone–chemocline interface of acidic pit lakes.

3.1. Effect of nitrogen limitation on growth and photosynthetic viability

This section analyzes the effect of nitrogen limitation (with nitrate as the sole nitrogen source) on the growth and photosynthetic viability of the highly acidic-habitat microalga, with the goal of determining the minimal nitrogen concentration range that supports photosynthetic growth. Figure 4.1 presents the time-dependent evolution of growth, measured as dry weight, and nitrate consumption in *C. onubensis* cultures as a function of the nitrate concentration supplied.

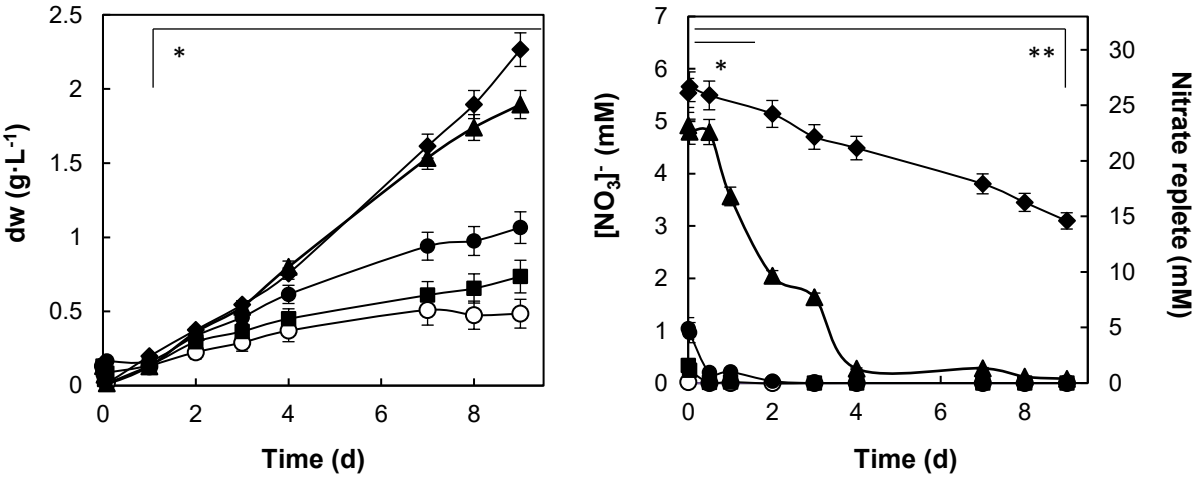

Figure 4.1. Effect of different degrees of nitrogen limitation on time-dependent evolution of (**a**) growth and (**b**) nitrate consumption in *C. onubensis* cultures. Right y-axis corresponds to nitrate-replete cultures. Legend symbols: 0.01 (-○-), 0.3 (-■-), 1 (-●-), 5 (-▲-) and 26 mM (nitrogen-replete culture) (-○-) NO_3^-. (*) Represents the significant differences of all treatments relative to the control cultures with 95 % confidence. (**) Represents the significant differences of consumption of nitrate replete concentration relative to the control cultures with 95 % confidence.

According to the figure, nitrate-limiting concentrations at or below 1 mM were depleted within approximately 1 to 2 days. Consequently, cultures of *C. onubensis* exhibited a significant growth reduction of roughly 53 to 78 % compared to nitrate-replete cultures. In contrast, cultures grown with 5 mM nitrate displayed a growth pattern similar to that of nitrate-replete cultures, with nitrate nearly fully consumed after approximately 4 to 5 days. However, beyond this point, a slight growth decline of about 16 % was observed.

Having established how nitrogen limitation (in the form of nitrate) affected the growth of *C. onubensis* and the rate of nitrate consumption, the effect of nitrate limitation on photosynthesis was subsequently analyzed. The results are presented in Figure 4.2.

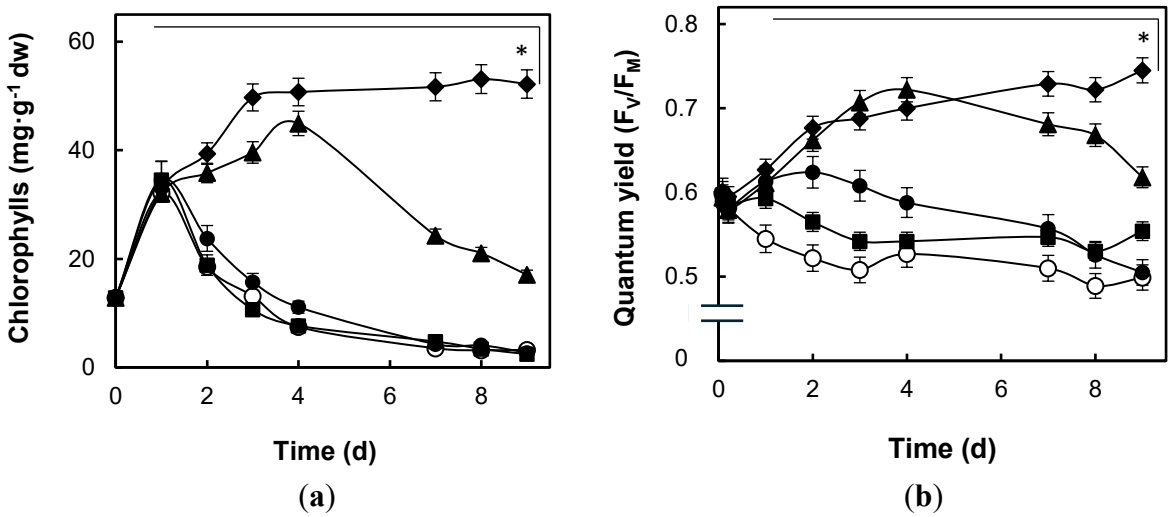

Figure 4.2. Effect of different degrees of nitrogen limitation on the intracellular chlorophyll content and photosynthetic efficiency of *C. onubensis* cultures. Time-dependent evolution of (**a**) intracellular chlorophyll concentration, and (**b**) maximal photosynthetic efficiency of photosystem II (Quantum yield, Qy). Symbols: 0.01 (-○-), 0.3 (-■-), 1 (-●-), 5 (-▲-) and 26 mM (nitrogen-replete culture) (-◆-) NO_3^-. (*) Represents the significant differences of all treatments relative to the control cultures with 95 % confidence.

Figure 4.2 shows changes in pigmentation and photosynthetic efficiency of *C. onubensis* cultures as nitrogen limitation increases. Intracellular chlorophyll content increased in all culture conditions until day 1 of cultivation. After this point, chlorophyll content in nitrogen-limited cultures declined significantly, becoming almost completely depleted over time. In contrast, the culture grown at 5 mM nitrate maintained intracellular chlorophyll levels comparable to the nitrogen-replete culture until day 4, after which chlorophyll content decreased sharply.

Consistent with nitrogen deficiency, Figure 4.2b illustrates a steep decline in the maximal photosynthetic efficiency of photosystem II (quantum yield, Qy) over time as nitrogen limitation intensified, with values dropping to the range of 0.5–0.6 in nitrogen-depleted cultures (0.01 to 1 mM nitrate). Conversely, the culture grown at 5 mM nitrate exhibited Qy values similar to those of the nitrogen-replete culture, showing only a slight decrease after day 7. Nonetheless, all Qy values for the 5 mM culture remained within the range of 0.6–0.7, which are typical for healthy cultures.

Physiological evidence of changes in cell viability under nitrogen limitation was complemented by morphological observations of cells from nitrogen-depleted cultures. Ultrastructural analysis of *C. onubensis* cells using transmission electron microscopy (TEM) revealed nitrogen deficiency-associated alterations. The results are presented in Figure 4.3. TEM images of cells from control cultures display a typical ultrastructural pattern characteristic of nutrient-replete conditions. Dark granules indicate metabolite

accumulation sites commonly found in metabolically active cells, whereas granules with a grayish or whitish appearance are typically associated with stressed cells. The figure shows a well-defined microalgal cell with a large chloroplast.

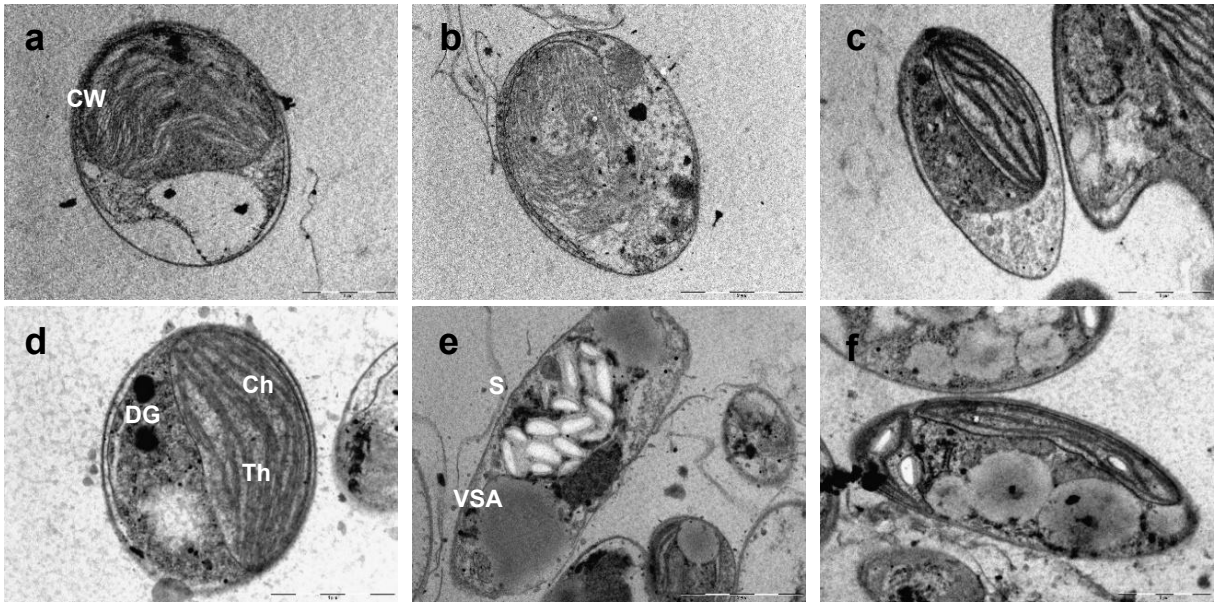

Figure 4.3. Effect of nitrogen limitation degree on cell ultrastructure of *C. onubensis* through transmission electron microscopy (TEM) images on days 1 (**a**, **b**, **c**) and 3 (**d**, **e**, **f**). Control culture, nitrogen replete, 26 mM (**a**, **d**); nitrogen limitation of 0.3 mM NO_3^- (**b**, **d**) and 0.01 mM NO_3^- (**c**, **f**). Abbreviations: Ch: chloroplasts, Th: thylakoids, CW: cell wall, DG: dark granules, VSA: vesicular activity, S: starch.

The ultrastructure of *C. onubensis* cells grown for 1 day at 0.3 mM nitrate (Figure 4.3b) was similar to that of the control culture, suggesting no apparent impact of nitrogen limitation on cellular ultrastructure within the first 24 hours. However, at the same nitrogen concentration after 3 days (Figure 4.3e), a notable accumulation of starch was observed, indicating that nitrogen depletion triggers starch biosynthesis.

Under more severe nitrogen limitation (0.01 mM nitrate on day 1; Figure 4.3c), cells exhibited lower thylakoid membrane density and increased spacing between membranes compared to the control, consistent with the chlorophyll reduction observed in *C. onubensis* under nitrogen-limited conditions (Figure 4.2a). As expected, prolonged nitrogen limitation led to complete nitrogen depletion, resulting in cells with markedly retracted chloroplasts and a substantial decrease in thylakoid density. Nonetheless, photosynthetic efficiency remained at moderate to high levels, suggesting a temporary adaptation of the photosynthetic machinery to the imposed stress. A circular vesicle-like structure, possibly corresponding to a lipid accumulation body, was also visible. This structure first appeared in cultures growing at 0.3 mM nitrate (Figure 4.3e) and appeared more prominent under more severe nitrogen limitation at 0.01 mM (Figure 4.3f).

Interestingly, a greater accumulation of starch was observed at 0.3 mM nitrate compared to 0.01 mM, possibly indicating that, as nitrogen limitation intensifies, carbon and energy reserves are redirected toward triacylglycerol accumulation—an energy storage form—through enhanced fatty acid synthesis and increased lipid droplet size.

As demonstrated, the level of nitrogen availability influences the cellular ultrastructure of the highly acidic-habitat microalga, including changes in the number and morphology of lipid-accumulating structures. The effects of varying degrees of nitrogen limitation on the accumulation of nitrogen-free molecules –specifically carbohydrates and lipids– are presented in the following section.

3.2. Effect of nitrogen limitation on energy storage molecules accumulation

Under nitrogen limitation, metabolic energy can be redirected toward the synthesis of nitrogen-free biomolecules, primarily carbohydrates and lipids. This section examines the effect of nitrogen limitation on the biomass composition of *C. onubensis* by analyzing the time-dependent evolution of intracellular energy storage compounds, specifically carbohydrates and lipids. A lipidomic approach was employed to assess changes in the fatty acid profile throughout the experimental period. The effects of nitrogen limitation on the intracellular carbohydrate, lipid, and fatty acid content of *C. onubensis* are presented in Figure 4.4.

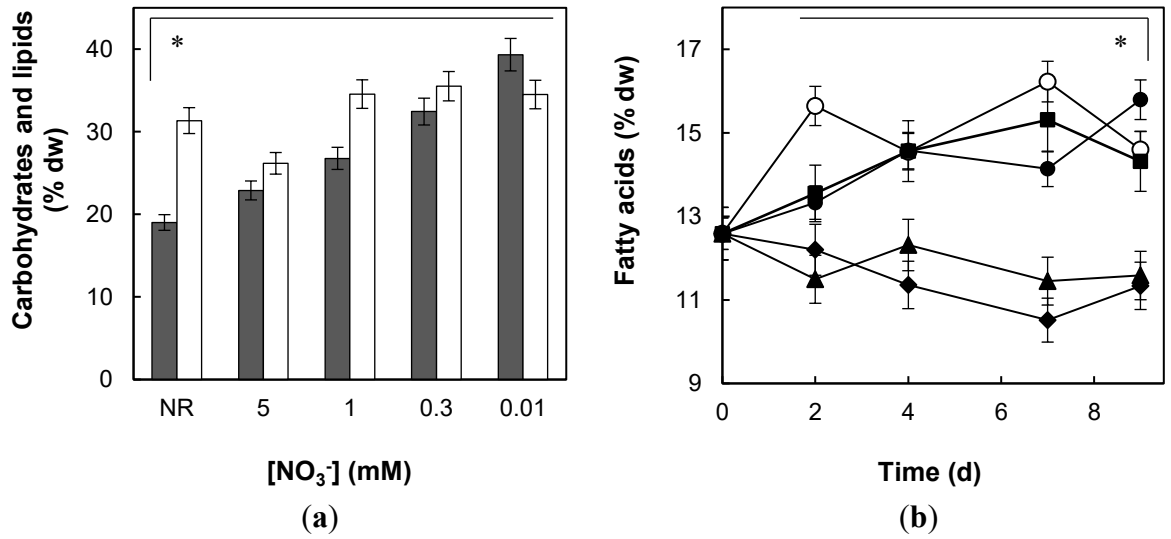

Figure 4.4. Effect of different degrees of nitrogen limitation on the production of nitrogen-free molecules in cultures of *C. onubensis*. (**a**) Intracellular content of carbohydrates (dark-grey bar) and lipids (white bar) from samples collected at day 9 of cultivation and (**b**) intracellular content of fatty acids. Symbols: 0.01 (-○-), 0.3 (-■-), 1 (-●-), 5 (-▲-) and 26 mM (nitrogen-replete culture) (-◆-) NO_3^-. (*) Represents the significant differences of all treatments relative to the control cultures with 95 % confidence.

According to Figure 4.4a, nitrogen limitation stimulated the accumulation of both carbohydrates and lipids, with their contents increasing by 2.07-fold and 1.13-fold, respectively, in nitrogen-depleted cultures. Similarly, Figure 4.4b shows that intracellular fatty acid content rise as nitrogen availability decreased. In cultures subjected to nitrogen-limiting conditions (0.01 to 1 mM nitrate), a consistent increase in both nitrogen-free biomolecules was observed, reaching maximum levels during the final days of cultivation (days 7–9), with values approximately 54 % higher than those of the nitrogen-replete culture.

In contrast, the time-dependent fatty acid profile of the culture grown at 5 mM nitrate closely resembled that of the nitrogen-replete condition, displaying a slight decreasing trend over time. To gain deeper insight into how nitrogen limitation affects fatty acid composition, the fatty acid profile was further analyzed. The results are shown in Figure 4.5, which presents the variations in the content of saturated and unsaturated fatty acids in *C. onubensis* cultures as a function of nitrogen concentration.

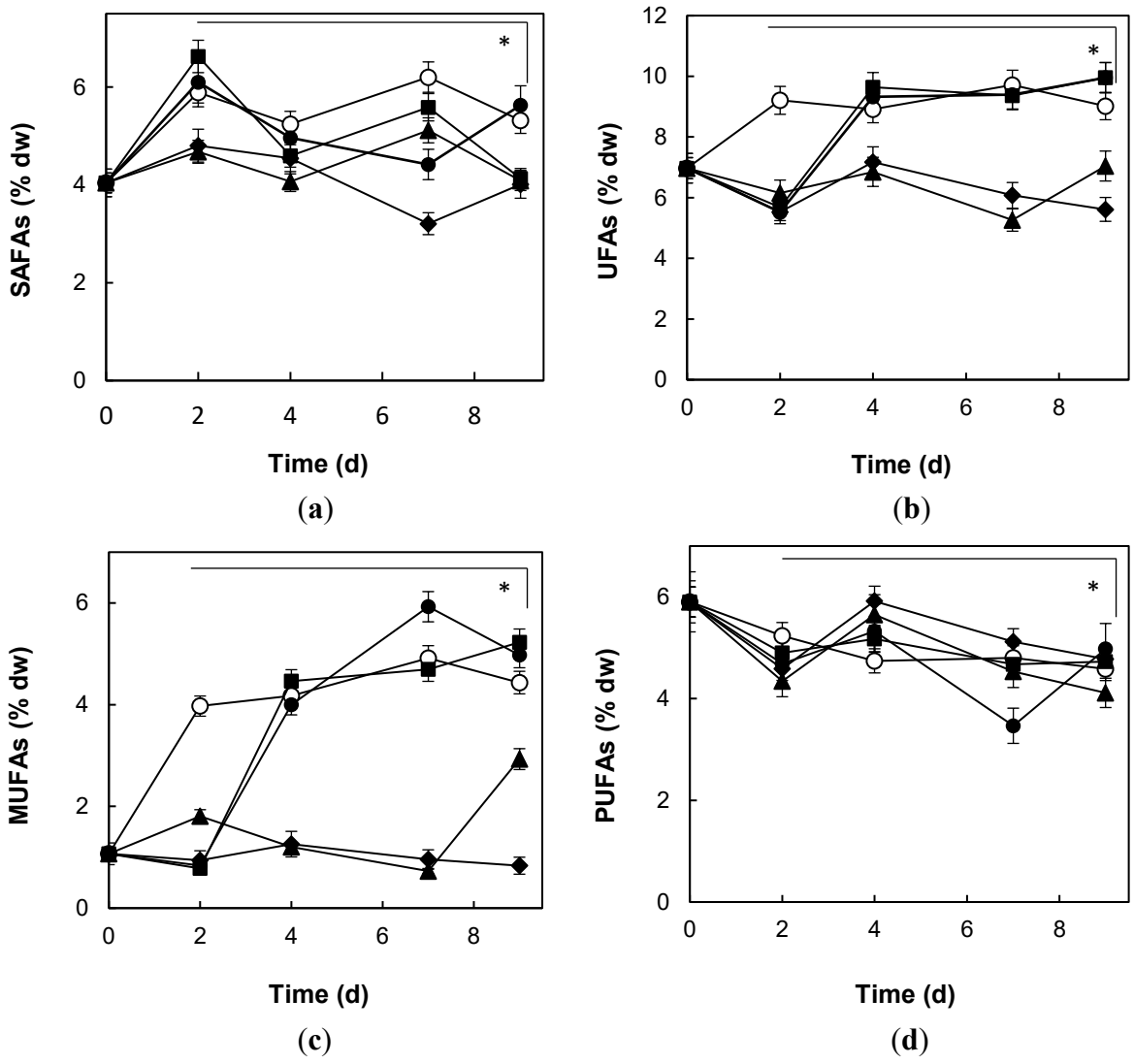

Figure 4.5. Effect of different degrees of nitrogen limitation on time-dependent evolution of intracellular content of (**a**) saturated (SAFAs), (**b**) unsaturated (UFAs), (**c**) monounsaturated (MUFAs) and (**d**) polyunsaturated (PUFAs) fatty acids of *C. onubensis* cultures. Legend symbols: 0.01 (-○-), 0.3 (-■-), 1 (-●-), 5 (-▲-) and 26 mM (nitrogen-replete culture) (-◆-) NO_3^-. (*) Represents the significant differences of all treatments relative to the control cultures with 95 % confidence.

Figure 4.5 illustrates the variation in the intracellular content of saturated and unsaturated fatty acids in *C. onubensis* cultures as a function of nitrogen concentration. In nitrogen-replete cultures, the time-dependent evolution of both saturated fatty acids (SAFAs) and unsaturated fatty acids (UFAs) remained relatively constant, with average values of 3.9 and 6.5 % dry weight (dw), respectively (Figures 4.5a and 4.5b). However, as nitrogen limitation intensified, a marked increase in both SAFAs and UFAs was

observed—approximately 48 and 55 % higher, respectively, than in nitrogen-replete cultures. These results suggest that nitrogen limitation activates carbon storage pathways in the highly acidic-habitat microalga, a point that will be further discussed.

Likewise, in nitrogen-replete cultures (Figures 4.5c and 4.5d), monounsaturated fatty acids (MUFAs) and polyunsaturated fatty acids (PUFAs) exhibited a nearly stable trend over time, with average values of approximately 0.73 and 5.11 % dw, respectively. As nitrogen availability decreased, a slight reduction in PUFA content (~20 %) was observed. In contrast, nitrogen depletion (0.01 to 1 mM nitrate) induced a significant increase in MUFA content –reaching up to 5.93 % dw– an 8.12-fold increase compared to the nitrogen-replete condition.

To provide a more comprehensive overview, the lipid profile of *C. onubensis* cultures was evaluated as a function of the degree of nitrogen limitation. Accordingly, the time-dependent evolution of the major fatty acids synthesized by *C. onubensis* was analyzed, with the most relevant results presented in Figure 4.6. The predominant fatty acids identified include palmitic acid (C16:0), stearic acid (C18:0), heptadecenoic acid (C17:1), oleic acid (C18:1), linoleic acid (C18:2), linolenic acid (C18:3), and docosadienoic acid (C22:2).

In general, cultures subjected to lower nitrogen availability accumulated higher levels of saturated fatty acids (SAFAs), particularly C16:0 and C18:0 (Figures 4.6a and 4.6b). Palmitic acid (C16:0) reached its peak concentration (4.43 % dw) in cultures grown with 0.01 mM nitrate on day 7, representing an increase of approximately 45 % compared to the nitrogen-replete condition. Conversely, the highest stearic acid (C18:0) level was observed at an early cultivation stage (day 2) in the 0.3 mM nitrate culture –with a value of around 1.5 % dw– roughly 50 % higher than that recorded for the nitrogen-replete culture.

Oleic acid (C18:1) content remained low in nitrogen-replete cultures (0.05–0.08 % dw), whereas nitrogen-depleted conditions induced a pronounced accumulation of this monounsaturated fatty acid (MUFA) (Figure 4.6c). Notably, in cultures with 0.01 mM nitrate, C18:1 content increased dramatically at early growth stages, reaching values up to 40-fold higher than those in nitrogen-replete conditions. At later stages, this accumulation became even more pronounced –with C18:1 levels reaching 5.28 % dw– an increase of approximately 88-fold compared to the replete culture, showing that nitrogen depletion could activates biosynthesis mechanisms of oleic acid.

Figures 4.6d–f illustrate the variation of polyunsaturated fatty acids (PUFAs) under nitrogen-limited conditions. A slight increasing trend was observed for linoleic acid (C18:2), and a more pronounced accumulation was evident for docosadienoic acid (C22:2) in nitrogen-depleted cultures. In contrast, linolenic acid (C18:3) exhibited a decreasing trend throughout the cultivation period in cultures grown under nitrogen limitation.

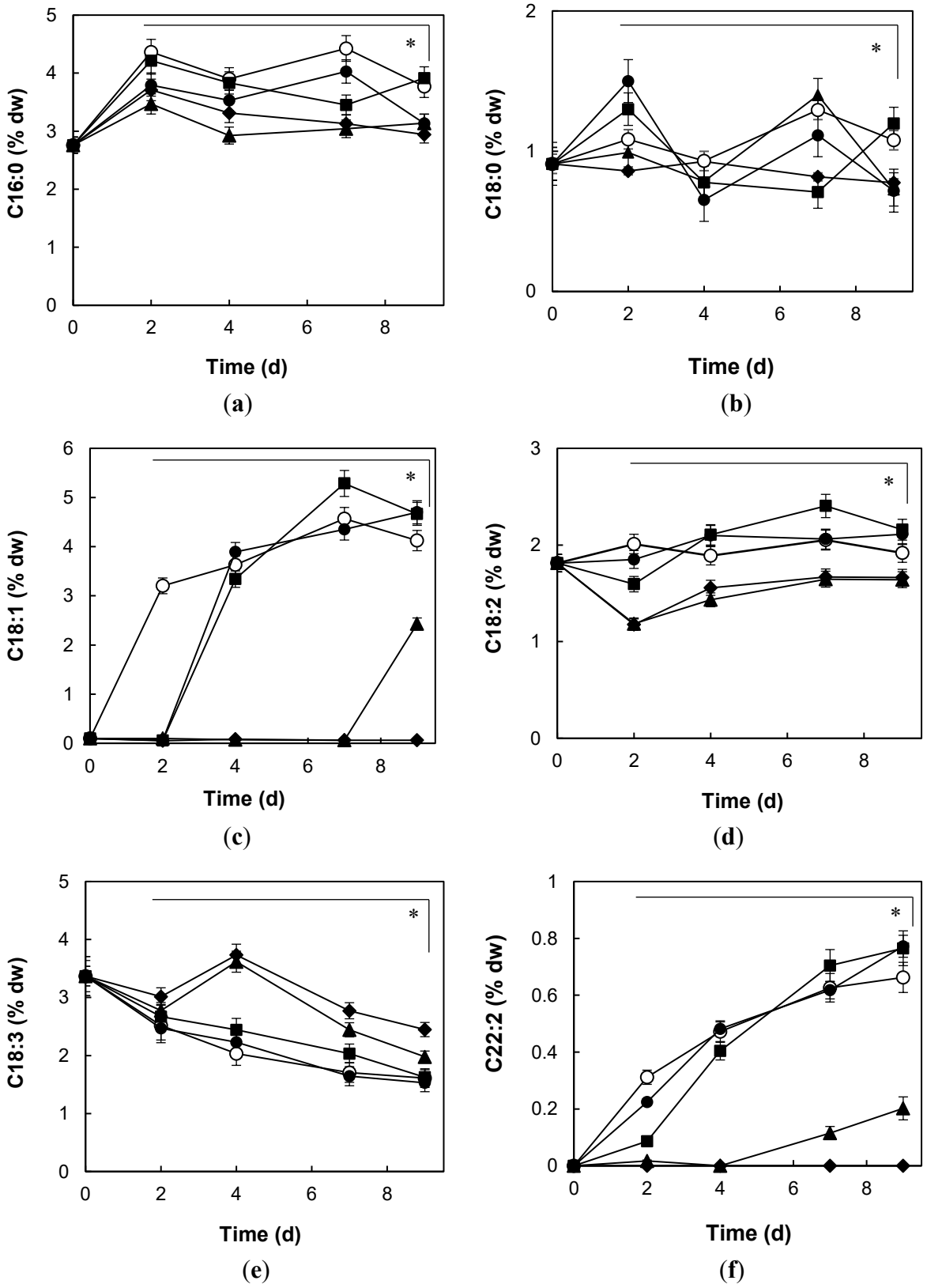

Figure 4.6. Effect of different degrees of nitrogen limitation on time-dependent evolution of intracellular content of saturated (SAFAs; (**a**) C16:0 and (**b**) C18:0), monounsaturated (MUFAs; (**c**) C18:1) and polyunsaturated (PUFAs; (**d**) C18:2, (**e**) C18:3 and (**f**) C22:2) fatty acids in *C. onubensis* cultures. Legend symbols: 0.01 (-○-), 0.3 (-●-), 1 (-■-), 5 (-▲-) and 26 mM (nitrogen-replete culture) (-◆-) NO_3^-. (*) Represents the significant differences of all treatments relative to the control cultures with 95 % confidence.

Interestingly, C22:2 was exclusively detected in nitrogen-depleted cultures, with the maximum content (approximately 0.7 % dw) observed at later cultivation stages in cultures grown with 1 mM nitrate. Under the same conditions –late-stage cultivation and 1 mM nitrate– C18:2 also reached its highest concentration, approximately 2.4 % dw, representing an increase of 44 % relative to the nitrogen-replete condition. Regarding C18:3, the highest values were observed in depleted cultures and those grown with 5 mM nitrate, with a maximum content of 3.62 % dw.

To better illustrate the shifts in fatty acid composition under nitrogen limitation, the relative proportions of each major fatty acid were calculated in relation to total fatty acid content and represented as percentages in Figure 4.7.

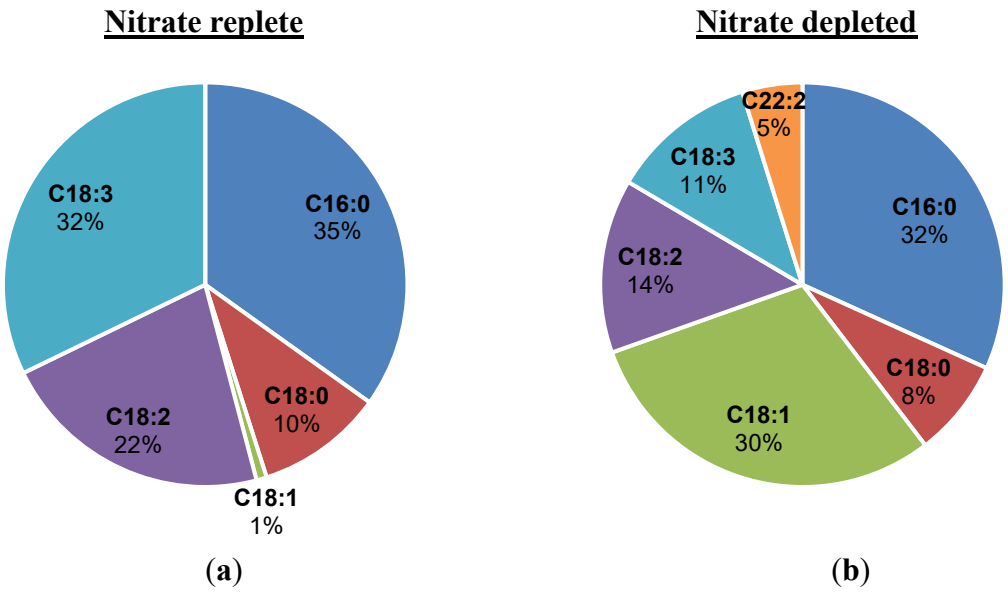

Figure 4.7. Fatty acid profile (% FA) of *C. onubensis* cultures as a function of nitrogen limitation: (**a**) nitrogen-replete medium and (**b**) 0.01 mM nitrate. Data represented correspond to day 9 of cultivation.

Figure 4.7 displays the fatty acid composition of *C. onubensis* cultures, expressed as a percentage of total fatty acids (% FA), under varying nitrogen concentrations. The results indicate that the relative abundance of palmitic acid (C16:0) and stearic acid (C18:0) remained nearly constant regardless of nitrogen availability. In contrast, oleic acid (C18:1) showed a pronounced increase, rising from approximately 1 % FA in nitrogen-replete cultures to nearly 30 % FA under nitrogen-depleted conditions. This increase was accompanied by a significant reduction in the content of linoleic acid (C18:2) and linolenic acid (C18:3), by approximately 36 and 65 %, respectively, under nitrogen-limited conditions. Additionally, consistent with the results shown in Figure 4.6, docosadienoic acid (C22:2) was only detected in nitrogen-depleted cultures, highlighting the influence of nitrogen availability on the biosynthesis of specific long-chain polyunsaturated fatty acids.

These findings suggest that manipulating nitrogen concentrations in the culture medium effectively modulates the fatty acid profile and abundance in *C. onubensis*. This opens the possibility of designing tailored cultivation strategies aimed at optimizing the production of specific fatty acids, depending on the intended industrial or nutritional

application. Such strategies, along with the productivity outcomes of nitrogen-limited cultures, are discussed in the following section.

In addition, the changes observed in the quantity and relative abundance of specific fatty acids in nitrogen-limited and starved cultures may provide insights into the potential ecological role of *Coccomyxa onubensis* biomass in the deep-water habitats of acidic pit lakes.

4. Discussion

4.1. Effect of nitrogen limitation on growth and photosynthetic viability

Nitrogen, typically supplied to cultures as an inorganic nitrogen compound, plays a crucial role in microalgal nutrition, being an essential element for the biosynthesis of chlorophylls, proteins, and nucleic acids. Consequently, nitrogen availability governs the rate and extent of microalgal growth. Furthermore, if cellular nitrogen demand exceeds the supplied nitrogen level, the biosynthesis of chlorophylls and proteins is partially or even completely inhibited, thereby compromising the photosynthetic viability and primary metabolism of the microalgal cells (Richmond, 2003). Specific metabolic responses are triggered to mitigate the effects of severe nitrogen limitation. For example, the reduction in photosynthetic energy and reducing power (ATP and NADPH) production leads to growth arrest under these conditions.

The specific nitrogen concentration that limits cell growth varies depending on the species and culture conditions. In this study, nitrate concentrations below 1 mM were completely consumed within approximately two days, resulting in growth arrest (Figure 4.1b) at biomass levels averaging around 0.2–0.3 g (dw)·L^{-1}.

Nevertheless, the biomass density of these nitrogen-depleted cultures continued to increase slightly for an extended period (Figure 4.1a), likely by utilizing intracellular traces of ammonium produced through the photorespiratory cycle (Hellebust and Ahmad, 1989). The remaining cell growth, as shown in the Results section, represents a key phase for accumulating and defining conditions that stimulate fatty acid production, as discussed further. The culture grown with 5 mM nitrate depleted its nitrogen content between days 4 and 5 of cultivation, which likely explains the decline in growth observed around day 7 compared to the nitrogen-replete culture. Accordingly, 5 mM nitrate was considered saturating for *C. onubensis* growth in batch mode, allowing moderate cell densities and suggesting the need to refresh (repeat) cultures before day 7. Conversely, nitrogen levels below 1 mM can be considered growth-limiting for this highly acidic-habitat microalga, with cultures entering nitrogen deprivation within 1 to 3 days.

Microalgae use nitrogen as an essential nutrient to build proteins, chlorophylls, and nucleic acids, among other molecules (Gonçalves et al., 2017). Low nitrogen availability limits the production of essential molecules such as chlorophylls (Figure 4.3a), which are crucial for light capture and conversion into chemical energy within the photosynthetic apparatus of the thylakoids. The physiological consequence of this limitation includes alterations in the photosynthetic efficiency of the microalgal cells. Photosynthetic efficiency, measured as Qy, should typically range between 0.6 and 0.7 in healthy microalgal cultures (Maxwell and Johnson, 2000). Although nitrogen-limited *C. onubensis* cultures approach the aforementioned Qy range, the reduced photosynthetic efficiency may result from a decreased turnover rate of photosystem II protein subunits due to the nitrogen deprivation experienced by the cells. Interestingly, regarding the design of cultivation processes using *C. onubensis* under nitrogen limitation, microalgal cultures subjected to nitrogen deprivation (after 2 days at nitrate

concentrations below 1 mM) remain photosynthetically viable for several days under these nutrient-limiting conditions.

Nitrogen limitation induces changes in the cell ultrastructure of *C. onubensis* cultures (Figure 4.3). Under nitrogen-limited conditions, chloroplast division is inhibited, leading to a reduction in the number of thylakoid membranes per chloroplast. Additionally, the synthesis of the D1 protein decreases, resulting in the production of fewer functional reaction centers (RCs) (Kolber et al., 1988). This observation is consistent with the retraction of chloroplasts and the increased spacing between thylakoid membranes observed in Figure 4.3. Nevertheless, photosynthetic efficiency is still maintained under nitrogen limitation (Figure 4.2), suggesting the activation of temporary adaptation mechanisms, including photosynthetic readjustment, in response to the imposed stress conditions.

Generally, in microalgae, starch accumulates rapidly following the onset of nitrogen limitation or other stress conditions, serving as a primary energy reserve, while storage lipid accumulation typically begins a few hours to days thereafter (Vitova et al., 2015). Accordingly, this study also demonstrated that carbon and energy reserves shift toward triacylglycerol or starch accumulation depending on the degree of nitrogen limitation. Specifically, greater starch accumulation was observed under moderate nitrogen limitation (0.3 mM), whereas under severe nitrogen depletion, increased vesicular activity was evident, indicating storage in a form with higher specific energy content through enhanced fatty acid synthesis and enlarged lipid droplets (Wan and Zhang, 2012). Most algae can produce both starch and lipids as energy reserves, with the relative proportions varying according to growth conditions. Typically, starch serves as the primary energy storage compound; however, the mechanisms underlying the shift from starch to triacylglycerol production (carbon partitioning) under specific conditions remain not fully understood (Vitova et al., 2015).

As discussed, varying nitrogen availability induces changes in the cell ultrastructure of the microalga, including modifications in the number and morphology of lipid-accumulating structures. Consequently, the biosynthesis and accumulation of these molecules are affected. In this sense, next section analyzes the effects of different degrees of nitrogen limitation on the production of nitrogen-free molecules, namely carbohydrates and lipids.

4.2. Effect of nitrogen limitation degree on energy storage molecules production

In a nitrogen-limited medium, the metabolic energy flux is partially diverted to the production of nitrogen-free biomolecules (carbohydrates and/or lipids) (Schüler et al., 2017). This strategy has been widely described as an energy-saving mechanism activated when nitrogen depletion negatively impacts the main cellular energy production pathways, namely photosynthesis and mitochondrial oxidative phosphorylation (Markou et al., 2017). The intracellular increase in carbohydrates and lipids observed under nitrogen limitation, as shown in Figure 4.4a, can be explained by this mechanism. Specifically, lipids and carbohydrates act as sources of energy and carbon, thereby not only ensuring cell survival but also providing the necessary energy

for processes related to cell division, such as DNA replication, nuclear division, cytokinesis, and cell formation and release (Vitova et al., 2015). In this context, the increase in both compounds can be attributed to the microalga's adaptive mechanisms for energy storage expressed under nitrogen-limiting conditions.

Under nitrogen limitation, photochemical activity of photosynthesis is reduced (Figure 4.2b), which leads to decreased availability of ATP and NADPH for nutrient assimilation. This reduction directly impacts cell growth negatively (Figure 4.2a). Nevertheless, although nitrogen-limited cultures become nitrogen-depleted within 2–3 days (Figure 4.1), they remain photosynthetically viable, allowing sustained reduction of $NADP^+$ to NADPH. This maintains the anabolic reducing power required for fatty acid biosynthesis induced by nitrogen depletion (Figure 4.4) and remains active for at least several days. Such a phenomenon has been previously reported in microalgae; for example, studies on *Schizochytrium* spp. under nitrogen starvation showed that the enzymes isocitrate dehydrogenase and malic enzyme provide the NADPH necessary for fatty acid biosynthesis, leading to enhanced lipid and DHA accumulation (Chen et al., 2022; Jiang et al., 2017). Other genes involved in assembling triacylglycerols were also upregulated in nitrogen-deprived cultures (Chen et al., 2022; Ren et al., 2017), proving the enhanced expression of several pathways in the response to nitrogen limitation or starvation.

Thus, the enhanced fatty acid biosynthesis observed in nitrogen-depleted microalgal cultures can be partially interpreted as a mechanism to dissipate excess reducing power generated under conditions of surplus light energy—such as in less dense cultures or when nutrient deficiency reduces the demand for reducing power in nutrient assimilation. Through this strategy, microalgae are able to store carbon and energy in the chemical form of fatty acids (Schüler et al., 2017). This reasoning aligns with the observed increasing trends in the fatty acid content of *C. onubensis* under nitrogen limitation (Figure 4.4b).

Nitrogen limitation induced changes in the saturated to unsaturated fatty acid ratio in *C. onubensis*, promoting a decreased abundance of unsaturated fatty acids. The saturation and unsaturation levels of fatty acids were analyzed based on the results presented in Figures 4.5 and 4.6. Data from both figures suggest that nitrogen limitation enhanced the biosynthesis of saturated fatty acids (SAFAs, C16:0 and C18:0) and monounsaturated fatty acids (MUFAs, C18:1) in *C. onubensis* cultures. The observed increase in unsaturated fatty acids (UFAs) under nitrogen limitation was mainly attributed to MUFAs. Concurrently, the polyunsaturated fatty acid (PUFA) C18:3 content decreased as nitrogen limitation intensified. Although increases in C18:2 and C22:2 were observed in nitrogen-depleted cultures, they did not compensate for the decline in C18:3, resulting in an overall decreasing trend in PUFA content. Overall, nitrogen limitation appears to trigger fatty acid accumulation, consistent with findings in other microalgal species, and alters the relative abundance of fatty acids, notably causing marked increases in oleic acid (C18:1) and docosadienoic acid (DDA, C22:2), alongside a significant decrease in linolenic acid (C18:3).

There are two main pathways for TAG synthesis: (1) *de novo* synthesis by the Kennedy pathway and (2) acyl editing reactions involving carbon flux from membrane lipids (Li-Beisson et al., 2013; Poddar et al., 2020). The *de novo* synthesis results in a high content of saturated (such as C16:0/C18:0) and monounsaturated (such as C16:1/C18:1) acyl chains in TAG (Krzemińska et al., 2023). However, recycling membrane lipids through acyl editing reactions results in higher levels of PUFAs in TAG (Bates and Browse, 2012). In these reactions, fatty acids can be further desaturated when they are part of the phosphatidylcholine (PC) pool, an important membrane lipid (Li-Beisson et al., 2013). For instance, the common PC-modified FAs found in membrane and storage lipids C18:1-PC could be desaturated to C18:2 and then C18:3 (Bates and Browse, 2012).

Nitrogen limitation seems to enhance the *de novo* fatty acids pathway in *C. onubensis* cultures, based on the increase of saturated (C16:0 and C18:0) and monounsaturated (C18:1) fatty acids. These results are coherent with those obtained by Martin et al. (2014), who studied the effect of nitrogen depletion (0.5 mM NO_3^-) on fatty acids in *Nannochloropsis* sp. and compared it with a nitrogen-replete culture (5 mM nitrate), observing a significant increase in the levels of C18:1, C16:1, and C16:0. This increase in these fatty acids was attributed to an enhancement in the *de novo* synthesis of these fatty acid species. Similarly, Krzemińska et al. (2023) studied the effect of different degrees of nitrogen limitation in the microalga *Eustigmatos calaminaris*, observing an increase in the content of C18:1 and C16:0 at 0.375 $g \cdot L^{-1}$ $NaNO_3$ compared to nitrogen-replete cultures (1.5 $g \cdot L^{-1}$). It was also suggested that the increase in C18:1 content is associated with *de novo* synthesis of this fatty acid and not solely with the degradation of polar lipids. These findings are consistent with results from studies on other *Coccomyxa* strains. For example, nitrogen starvation in *Coccomyxa subellipsoidea* led to an increase in triacylglycerol (TAG) species containing C18:0 fatty acids, which was also presumably attributed to enhanced *de novo* fatty acid synthesis (Allen et al., 2015).

As reported above, *de novo* fatty acid biosynthesis produces saturated fatty acids (C16:0 and C18:0), which can then undergo desaturation by plastid or endoplasmic reticulum (ER) desaturases (DES) and elongation by various elongases (ELO), resulting in fatty acids with different degrees of unsaturation and chain lengths (Santin et al., 2021) (Figure 4.7). Therefore, a more precise strategy to alter fatty acid composition involves targeting the desaturation and elongation processes by selectively modulating elongases and/or desaturases. For example, stearoyl-ACP desaturase (SAD), a Δ9-desaturase, catalyzes the conversion of stearic acid (C18:0) into oleic acid (C18:1ω9). Overexpression of this enzyme, combined with repression of the Δ12-desaturase responsible for converting oleic acid (C18:1) into linoleic acid (C18:2), could potentially lead to increased accumulation of oleic acid under nitrogen limitation (Rismani-Yazdi et al., 2012). These results are consistent with those obtained in this study and may explain the enhanced accumulation of oleic acid under nitrogen limitation in the microalga *C. onubensis*. It is noteworthy that the C18:1 content reached 5.28 % dry weight under nitrogen limitation, which is significantly higher compared to several

Chlorella strains with the highest reported fatty acid productivity, where C18:1 content ranged from 0.14 to 2.59 % dry weight (Hempel et al., 2012). In addition, Zanella and Vianello, 2020 compares the C18:1 content of *Nannochloropsis* sp. and other microalgal strains, with values ranging between 0.1 and 3.39 % dry weight. Similarly, cultivation of *C. onubensis* at 5 mM nitrate yielded an α-linolenic acid (ALA) content as high as 3.62 % dry weight, which exceeds the range reported for several *Chlorella* strains with high fatty acid productivity, where ALA content ranged from 0.19 to 0.67 % dry weight (Hempel et al., 2012).

The novelty of our analysis of fatty acid biosynthesis in *C. onubensis* under nitrogen-limiting conditions lies in the unexpected production of docosadienoic acid (DDA, C22:2). This diene is extremely rare in microalgae, with its presence previously reported only at relatively low concentrations, around 3 % of total fatty acids measured as fatty acid methyl esters (FAMEs) (Ruiz-Marin et al., 2019). The biosynthetic pathway for C22:2 in microalgae has not yet been described. Studies from the 1980s conducted in plants such as meadowfoam, *Arabidopsis*, and *Brassica* suggested that the biosynthesis of C22:2 follows the pathway of C20:0, C20:1, and C22:1, proposing that the diene may be synthesized through enzymatic desaturation of C22:1 (Pollard and Stumpf, 1980) This hypothesis was unequivocally demonstrated by Marillia et al. (2002) using somatic soybean embryos heterologously expressing the Δ5-desaturase enzyme from *Limnanthes*.

In microalgae, C20 fatty acids typically contain three or four double bonds (C20:3 and C20:4) and are synthesized through the catalytic action of desaturases and elongases acting on C18:2 and C18:3, respectively (Blasio and Balzano, 2021). Thus, in accordance with established fatty acid biosynthesis pathways in microalgae, it is plausible to hypothesize that the synthesis of C22:2 in *C. onubensis* occurs through successive desaturation and elongation steps—requiring NADH input—starting from C18:1 and C18:2 (see Figure 4.7). This hypothesis is supported by the sustained intracellular levels of C18:2 observed during incubation, which may serve as a biochemical intermediate toward C22:2 synthesis, potentially driven by the overaccumulation of C18:1. This is also consistent with the reduction in C18:3 levels observed in this study.

Further transcriptomic and proteomic analyses are needed to clarify the differential expression of genes involved in unsaturated fatty acid biosynthesis under nutrient-limited conditions. Such studies could help identify key enzymes in the C22:2 biosynthetic pathway and determine its specific role within the broader network of unsaturated fatty acid metabolism. The physiological role of C22:2 remains unclear. However, substantial scientific evidence indicates that cis-13,16-docosadienoic acid (C22:2) acts as a potent inhibitor of topoisomerases and interferes with DNA polymerase activity in *in vitro* studies (Yonezawa et al., 2006). Inhibition of topoisomerases and polymerases typically leads to the arrest of DNA replication and the activation of cellular stress responses, which often culminate in cell death. Throughout this process, the integrity of the cell membrane becomes progressively compromised, resulting in the release of intracellular metabolites into the surrounding medium, including partially

degraded enzymes, free fatty acids, nucleic acid fragments, phenolic compounds, and other cellular constituents.

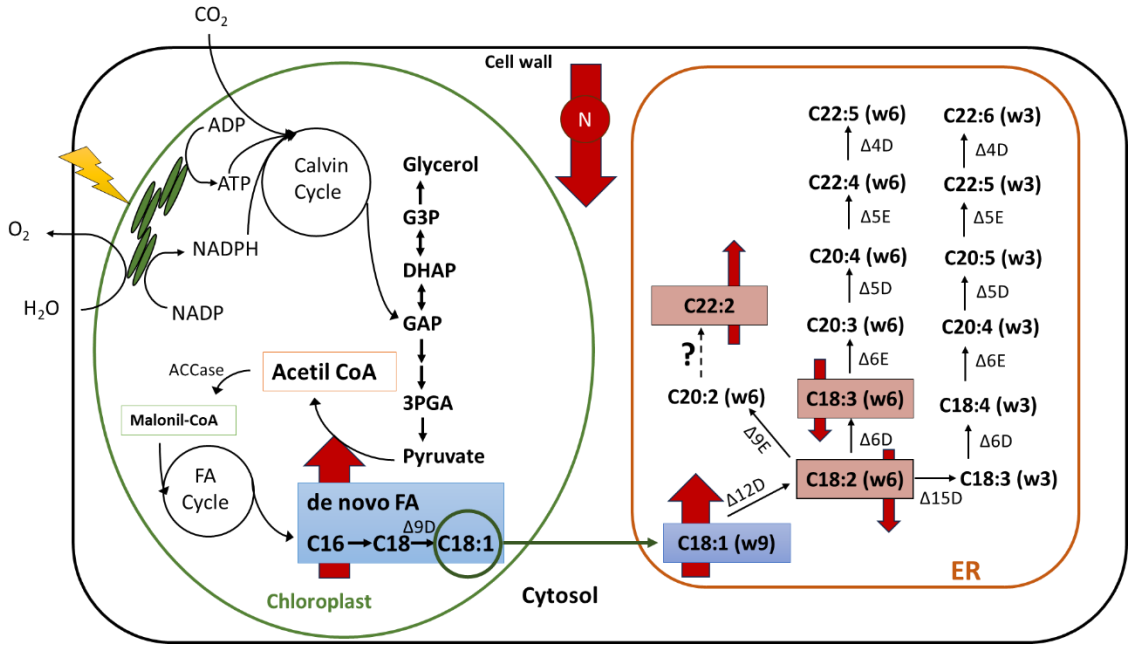

Figure 4.7. Proposed mechanism under nitrogen limitation. Symbols: ER: endoplasmatic reticulum, N: nitrogen, ADP: Adenosine diphosphate, ATP: Adenosine triphosphate, NADPH: Nicotinamide adenine dinucleotide phosphate reduced, $NADP^+$: Nicotinamide adenine dinucleotide phosphate oxidated, G3P: Glycerol-3-phosphate, DHAP: Dihydroxyacetone phosphate, GAP: Glyceraldehyde phosphate, PGA: Phosphoglyceric acid, ACCase: Acetyl-CoA carboxylase, FA: Fatty acid, C16: Palmitic acid, C18: Stearic acid, C18:1 (w9): oleic acid, C18:2: linoleica cid, C18:3: linolenic acid, C20:3: Eicosatrienoic acid, C20:4: Arachidonic acid, C20:5: Eicosapentaenoic acid (EPA), C20:2: Eicosadienoic acid, C22:2: Docosadienoic acid, C18:3: α-Linolenic acid (ALA), C18:4: Stearidonic acid, C20:4: Arachidonic acid, C20:5: Eicosapentaenoic acid (EPA), C22:5: Docosapentaenoic acid (DPA), ΔnD: Δn desaturase, ΔnE: Δn elongase.

From a biotechnological perspective, the results demonstrate that modulation of the degree of nitrogen limitation enables the definition of two distinct cultivation strategies. Specifically, under nitrogen-deprived conditions, the increase in saturated fatty acids (C16:0 and C18:0), and more notably the substantial rise in the monounsaturated fatty acid C18:1, renders the biomass composition more suitable for biodiesel production. These conditions appear to particularly enhance the *de novo* synthesis of fatty acids in *C. onubensis*, as supported by the increased total fatty acid content observed under such conditions (Figure 4.4b). Additionally, the reduced content of polyunsaturated fatty acids (PUFAs), particularly C18:3 (α-linolenic acid, ALA), further improves the lipid profile for applications such as biodiesel production.

On the other hand, cultivation under 5 mM nitrate resulted in an ALA (α-linolenic acid) content as high as 3.62 % of dry weight. As noted in the Introduction section, ALA plays a significant role in regulating oxidative stress and enhancing mitochondrial function, which is the primary site of its biological activity (Lopez-Maldonado et al., 2021). In addition, the reduced content of SAFAs and MUFAs contributes to making the biomass composition more suitable for use as a food supplement rich in unsaturated

fatty acids. Therefore, these cultivation strategies may guide the potential applications of *C. onubensis* biomass.

From an industrial application perspective, the biosynthesis of the unsaturated fatty acid docosadienoic acid (DDA) in *C. onubensis* under nitrogen-deprivation conditions is particularly noteworthy. DDA accumulates up to 1 % of the dry biomass weight, suggesting that this microalga, under the specified incubation conditions, could serve as a promising starting point for further exploration of DDA production. The significant proportion of this uncommon diene is of industrial interest due to the stability provided by its non-conjugated double bonds. DDA is valuable in the production of estolides, which are precursors for hydroxylated fatty acid feedstocks and for the synthesis of various high-value organic compounds used as lubricants and slip-type antiblocking agents in plastic film manufacturing (Burg and Kleiman, 1991; Cahoon et al., 2000; Marillia et al., 2002). DDA has been found to display noticeable antitumor, antioxidant and anti-inflammatory functions which can be of applied relevance (Chen et al., 2021).

This discussion becomes particularly relevant within the framework of microbial ecology, especially regarding the activity of sulfate-reducing bacteria (SRB) in the acidic lagoon waters of pyrite mining areas. As elegantly described by Diez-Ercilla et al. (2014), sulfide precipitation in the chemocline of acidic pit lakes (PITs) appears to be associated with the activity of sulfate-reducing bacteria (SRB), which likely depends on the availability of organic carbon compounds originating from the photic zone. Previous studies have identified *Coccomyxa* as the dominant photosynthetic eukaryotic species in the deep photic zone, near the lower boundary of the redoxcline, in acidic pit lakes of the Iberian Pyrite Belt in southwestern Spain, particularly in the province of Huelva (Sánchez-España et al., 2020). According to the aforementioned reference, the abundance of *Coccomyxa onubensis* in the deep waters of the redoxcline zone leads to a characteristic deep chlorophyll maximum. Consequently, *C. onubensis* could represent the most abundant source of organic carbon in the chemocline, thereby fulfilling the nutrient requirements of sulfide-producing bacteria in these deep waters. Notably, the inorganic nitrogen concentration at depths of 8–10 m in the acidic pit lakes of the Iberian Pyrite Belt (Huelva) is below 5 $mg \cdot L^{-1}$, which is significantly lower than the inorganic nitrogen saturation level for *C. onubensis* (above 5 mM) observed in artificial culture media. This low nitrogen availability was simulated in the present study through laboratory experiments of *C. onubensis* cultivation under nitrogen-limited conditions, aiming to mimic the biomass density to light irradiance ratio present at those depths. As described in the Results section, under such growth-limiting conditions, *C. onubensis* increases its intracellular fatty acid and starch content, becoming enriched in reducing power molecules that could serve as electron donors for the biosulfidogenesis activity of sulfate-reducing bacteria.

Based on the discussion above, it should be reasonable to hypothesize that nitrogen limitation experienced by *C. onubensis* in the deeper layers (8–10 m) of the chemocline in the acidic lagoons of the Iberian Pyrite Belt (Huelva, Spain) (Sánchez-España et al., 2020) triggers a cascade of biochemical events in the microalga. These processes may be directed towards the accumulation of reducing power, primarily in the form of fatty

acids and polysaccharides, ultimately facilitating programmed cell death and the subsequent release of molecular components. This release would supply essential nutrients to anaerobic prokaryotes inhabiting the mesocline, thereby sustaining sulfur-based reductive metabolic processes such as sulfidogenesis.

5. Conclusions

The findings of this Chapter suggested that *C. onubensis* develop metabolic strategies to acclimate to nitrogen limitation conditions. Although nitrate concentrations below 1 mM were completely consumed within approximately two days, the biomass density of these nitrogen-depleted cultures continued to increase slightly for an extended period. The remaining cell growth represents a key phase for accumulating and defining conditions that stimulate fatty acid production. This chapter also demonstrated that carbon and energy reserves shift toward triacylglycerol or starch accumulation depending on the degree of nitrogen limitation. Specifically, greater starch accumulation was observed under moderate nitrogen limitation (0.3 mM), whereas under severe nitrogen depletion an increased storage of fatty acid synthesis and enlarged lipid droplets was obtained. From a biotechnological perspective, the results demonstrate that modulation of nitrogen limitation enables the definition of two distinct cultivation strategies. Specifically, cultures grown with 5 mM nitrate accumulated higher levels of C18:3 and lower levels of SAFAs and MUFAs. On the other hand, under nitrogen-deprived conditions, the increase in saturated fatty acids (C16:0 and C18:0), and more notably the substantial rise in the monounsaturated fatty acid C18:1, renders the biomass composition more suitable for biodiesel production. These conditions appear to particularly enhance the *de novo* synthesis of fatty acids in *C. onubensis*, as supported by the increased total fatty acid content observed under such conditions. Additionally, the reduced content of polyunsaturated fatty acids (PUFAs), particularly C18:3 (α-linolenic acid, ALA), further improves the lipid profile for applications such as biodiesel production. Additionally, the results may indicate a potential ecological role for *C. onubensis* as a source of electron donors supporting bacterial growth in its natural habitat, such as acidic pit lakes.

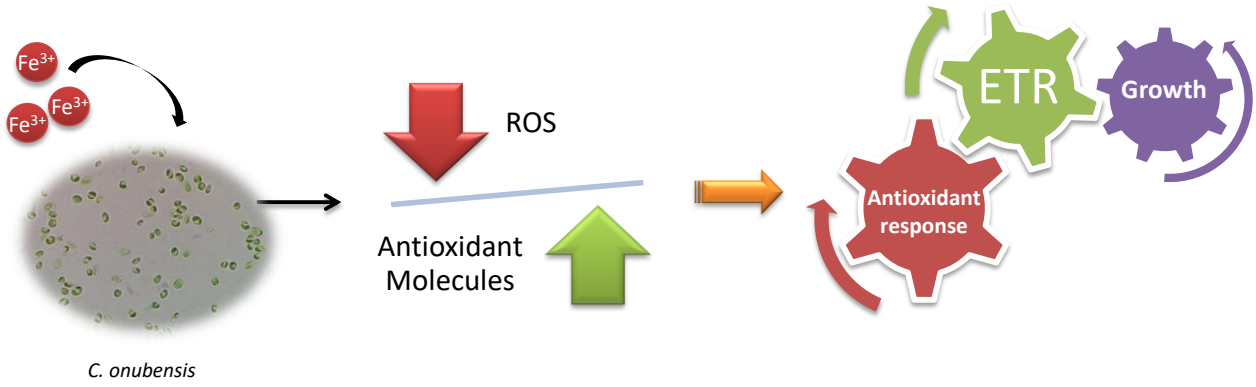
Fe3+
Fe3+
Fe3+
ROS
Antioxidant
Molecules
ETR
Growth
Antioxidant
response

C. onubensis

5

CHAPTER

Modulation of antioxidant production in a highly acidic-habitat microalga exposed to Fe (III).

Table of contents

Abstract: *Coccomyxa onubensis* (*C. onubensis*) is a highly acidic-habitat microalga isolated from Tinto River (Huelva) which contains high levels of metal cations in solution, mainly Fe (II) and (III), and Cu (II). Fe is more bioavailable at low pH because Fe (II) and Fe (III) are far more soluble at acidic pH, especially Fe (III). For this reason, this study aims to evaluate both physiological and biochemical responses of *C. onubensis* when subjected to Fe (III)-induced stress. Changes in growth, photosynthetic viability and antioxidant responses to the induced oxidative stress were determined. The results suggest that the addition of moderate Fe (III) levels to *C. onubensis* cultures results in improved growth and photosynthetic viability. Increases in the intracellular levels of the enzyme superoxide dismutase (SOD) and flavonoids, used as antioxidant response biomarkers, point at Fe (III)-mediated oxidative stress induction to occur. The apparent decrease in the content of other phenolic molecules and polyunsaturated fatty acids might be understood as a sign of antioxidant molecules involvement in reactive oxygen species (ROS) scavenging. In conclusion, the noticeable antioxidant capacity displayed by *C. onubensis* allows the use of moderate Fe (III) levels to trigger accumulation of valuable antioxidant molecules without affecting microalgal growth.

Keywords: Antioxidants; oxidative stress; Fe; reactive oxygen species; photosynthesis.

1. Introduction

Microalgae in nature are usually subjected to abiotic stress, which may be due to changes in the salinity of the environment, temperature variation, ultraviolet radiation, lack of nutrients or presence of metal cations, among other factors. Under these extreme conditions, microalgae produce certain metabolites to maintain homeostasis by minimizing the impact of stress. Some of these metabolites produced to counteract stress have commercial value (Paliwal et al., 2017), including terpenoids, phenolic compounds, polyunsaturated fatty acids (PUFAs) and even polysaccharides, among others. PUFAs, particularly long-chain omega-3 fatty acids, are highly susceptible to oxidation, as their double bonds are targeted by reactive oxygen species (ROS), producing lipoperoxides. Carotenoids are antioxidant molecules and microalgae increase their intracellular concentration to eliminate excess free radicals derived from oxidative stress (Ferrat et al., 2003). Polyphenols quench free radicals, and this chemical capacity has evidenced their efficiency in cellular protection against oxidative stress. Flavonoids display a range of cell functions including acting as redox transfer moieties and UV radiation dissipation. The above-mentioned biomolecules share common applications based on their proven antioxidant capacity; for instance, PUFAs, carotenoids and phenolic compounds have been reported to display biological activities valuable to human health, including anticancer, antioxidant and anti-inflammatory capacities (Goiris et al., 2014; Montero-Lobato et al., 2018). Therefore, incubation conditions for microalgae cultures leading to the accumulation of these molecules would be highly useful to efficiently design biotechnological processes to obtain extracts with potential bioactivity.

Coccomyxa onubensis (*C. onubensis*) is an acidotolerant eukaryotic microalga (Garbayo et al., 2012), isolated from acid mine drainages of the pyrite belt in the province of Huelva, Spain, characterized by the presence of cations in solution, of which Fe (II) and (III) and Cu (II) have a relevant quantitative presence (Amils et al., 2014). It has been shown that the extremely acidic conditions of the Tinto river basin are not just the product of 5,000 years of mining activity in the area, but principally the consequence of an active underground bioreactor that obtains its energy from the sulphur minerals of the Iberian Pyrite Belt (Amils et al., 2014). The bio-oxidation of pyrite produces a sulfate-enriched acidic solution (pH between 0.8 and 3) that prevents ferric iron precipitation, contrary to what occurs in neutral conditions (Fernández-Remolar et al., 2003). Under these extreme acidic conditions, ferric iron concentrations as high as 30 $g \cdot L^{-1}$ may be recorded (Fernández-Remolar et al., 2004). *C. onubensis* is an example of a photosynthetic microorganism adapted to the extreme acidic pH waters and high levels of solved metals of that environment. Under certain cultivation conditions, *C. onubensis* stands out for accumulating antioxidant molecules such as linoleic and linolenic acid and lutein (Bermejo et al., 2018), among others, which have been reported to display anti-inflammatory and antimicrobial activities (Navarro et al., 2017).

Fe is essential in microalgae for redox processes, being an essential component of S-Fe clusters of proteins involved in electron transport reactions; on the other hand, Fe also triggers oxidative stress addressing the cell metabolism to synthesize antioxidant

molecules such as polyphenols or carotenoids and to express the synthesis of antioxidant enzymes. Thus, Fe is generally toxic to life at high concentrations as it can interact with active centers of enzymes or interfere in redox processes (Eid et al., 2017). Its intracellular presence, in both forms as Fe (II) and Fe (III), produces the well-known Fenton reaction (see reaction 5.1) (Fenton, 1894), giving rise to ROS that would act in molecular signaling to activate the expression of genes responsible for antioxidant molecules and enzymes production (Rana and Prajapati, 2021).

$$Fe\ (II) + H_2O_2 \longrightarrow Fe\ (III) + HO^{\bullet} + HO^{-} \quad (5.1)$$

In this sense, the intracellular presence of Fe (II) or Fe (III) results in the production of ROS which are detrimental to microalgal viability. ROS are unavoidably produced in the cell, displaying an important function as signaling molecules (Lamers et al., 2008). An imbalance of ROS causes strong oxidative damage as they react with proteins, lipids and nucleic acids to produce their oxidation. ROS originates from electron transport processes, the photosynthetic electron transport chain being a major electron source. Superoxide radical ($O_2^{\bullet-}$), besides singlet oxygen, is usually the first ROS to be formed. An intensive activity of the photosynthetic electron transport chain favors molecular oxygen (O_2) to accept a single electron (Das and Roychoudhury, 2014). When $O_2^{\bullet-}$ is reduced by a second electron, hydrogen peroxide (H_2O_2) is produced. $O_2^{\bullet-}$ and H_2O_2 undergo transformation into the more reactive and toxic form, •OH (Halliwell, 2006). This oxygen species causes oxidative damage in cell membranes as •OH groups attack the double bonds of phospholipids giving rise to epoxy groups which promote stronger membrane lipids hydrocarbon chains interaction, thus addressing membrane fluidity losses. Moreover, •OH can also attack DNA nitrogen bases, giving rise to mutations that seriously impair cell life (Das and Roychoudhury, 2014).

Additionally, at high concentrations, Fe is one of the metals heading the molecular signaling that induces the expression of genes encoding the following antioxidant enzymes: ascorbate peroxidase, superoxide dismutase (SOD), dehydroascorbate reductase and catalase (Pikula et al., 2019; Pinto et al., 2003). SOD is a metalloprotein responsible for catalyzing the transformation of $O_2^{\bullet-}$ into H_2O_2. In prokaryotes, Mn-SOD and Fe-SOD can be found, while in eukaryotes Cu/Zn-SOD stands out (Okamoto et al., 1996; Pinto et al., 2003).

We hypothesize that modulating oxidative stress by Fe (III) in acidophilic or acidotolerant microalgal cultures, adapted to cope with oxidative conditions, might address increased productivity of antioxidant molecules (flavonoids, other phenolic compounds, PUFAs and/or carotenoids). The photochemical activity of *C. onubensis* stressed cells, as demonstrated in Chapter 2, is less negatively affected than that of common microalgae under similar conditions, which is also coherent to previous reports referring to the strong antioxidant enzymatic response of *C. onubensis* subjected to oxidative stress (Bermejo et al., 2018). Thus, this study analyzes the microalgal growth and antioxidant response of *C. onubensis* to Fe-mediated stress, attempting to find a suitable balance between stress and growth to trigger accumulation of antioxidant molecules while preventing culture productivity from decaying.

2. Materials and methods

2.1. Biological material and culture conditions

The organism used for this study was the microalga *Coccomyxa onubensis* ACCV1 (SAG 2510) (Figure 5.1a), an acidotolerant and halotolerant microalga, isolated from the acidic waters of the Tinto River (Huelva) in the sampling area at latitude 37.5851153° and longitude -6.550754°, by the Microalgae Biotechnology Unit (BITAL), of the Department of Chemistry "Professor Jose Carlos Vílchez Martín," from the Faculty of Experimental Sciences and CIQSO of the University of Huelva, Spain (Fuentes et al., 2016).

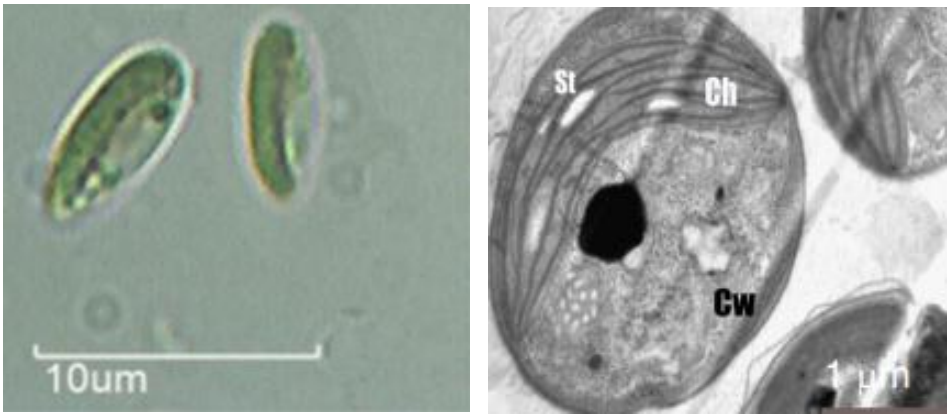

(**a**) (**b**)

Figure 5.1. *C. onubensis*: light, 100x amplification (**a**) and transmission electron microscopy (TEM) (**b**), scale bar 1 µm (x 30,000). Abbreviations: Ch, Chloroplasts; St, Starch grains; Cw, Cell wall.

Morphological studies carried out using electron microscopy techniques (Figure 5.1b) allowed us to determine that *C. onubensis* is an unicellular microalga with an ellipsoidal shape that has a cell wall and a size of approximately 3 µm in length and 2 µm in width. It has a large chloroplast that partially surrounds the nucleus and occupies more than half of the cell volume. The nucleus has an approximate size of 1 µm in length and 1 µm in width, while the nucleolus has a diameter of approximately 0.15-0.25 µm, both are located in the central zone of the cell.

C. onubensis was grown in an optimized liquid culture medium, K9 (Silverman and Lundgren, 1959). The constituents of K9 (per liter) were as follow: 3.95 g K_2SO_4, 0.1 g KCl, 0.5 g K_2HPO_4, 0.41 g $MgCl_2$, 2.29 g KNO_3, 0.01 g $CaCl_2$ and 5 mL of Hutner traces, which were prepared as described in (Garbayo et al., 2012), containing a Fe concentration of 17.98 µM. Fe was used in this study because is more bioavailable at low pH, mainly because both ionic forms of iron, Fe (II) and Fe (III), are far more soluble (especially ferric iron) at low pH than at neutral or basic pH (Johnson et al., 2012). In this way, *C. onubensis* cultures were prepared at an initial concentration of, approximately, 0.2 $g \cdot L^{-1}$, from a mother culture in the middle of the linear growth phase, the pH was adjusted to 2.5 and the cultures were subjected to different concentrations of Fe (III), added in the form of $FeCl_3 \cdot 6H_2O$ (VWR, Belgium) from 0 mM (control culture) to 2 mM. The cultures were established in a culture room at 25 ºC ± 2. Light was supplied by white light fluorescent tubes, reaching the cultures at a constant light

intensity of 150 µmol (photon)·m^{-2}·s^{-1} for 24 hours, and the cultures were bubbled with air enriched with 2.5 % (v/v) CO_2.

2.2. Light and Transmission Electron Microscopy

Photomicrographs of *C. onubensis* were taken using an Olympus BX-61 microscope (Olympus, Tokyo, Japan) with a CCD Colour-View-II camera (Soft Imaging System, Germany) and the CellSens analysis imaging system (Olympus, Japan). For transmission electron microscopical observations, the algal cells were collected by centrifugation (1.5 *g*, 1 min). The algal cells were fixed with 1 % glutaraldehyde in 0.1 M sodium cacodylate buffer (pH 7.4) for 2 h at 4 ºC. The cells were then washed three times for 5 min using the same buffer. The samples were postfixed with 1 % osmium tetroxide in 0.2 M cacodylate buffer at 4 ºC for 1 h. Samples were washed with the same buffer, dehydrated in a graded ethanol series, and embedded in Epon 812 (Electron Microscopy Science, USA). Ultrathin sections of 80–90 nm obtained by an ultramicrotome (Leica, Germany) and placed on copper grids, were stained with aqueous 1 % (w/v) uranyl acetate and lead citrate. Transmission electron micrographs were observed with a JEM 1011 (JEOL Ltd., Japan) electron microscope using an accelerating voltage of 80 kV. All chemicals used for histological preparation were purchased from Electron Microscopy Sciences.

2.3. Growth and photosynthetic viability

Productivity, the increase in biomass in a culture over time, was calculated in Equation 5.1.

$$\text{Productivity } (g \cdot L^{-1} \cdot d^{-1}) = \frac{C_t - C_0}{t_t - t_0} \qquad (5.1)$$

where C_t and C_0 represent the cell density for times *t* and zero. Cell density was determined by measuring the dry weight (dw) of the biomass contained in 2 mL of culture medium.

Photosynthetic viability was determined based on the chlorophyll fluorescence measurements, the maximum quantum yield (F_V/F_M) of Photosystem II (PSII) according to published methods (Schreiber, 2004). Photobiochemical parameters were determined through the OJIP protocol. Culture samples were diluted so that all Chl fluorescence measurements (Chl, chlorophyll) were done on samples with the same cell concentration, OD_{750} = 0.2 (OD_{750}, optical density at 750 nm). Quantum yield (Qy) was measured by placing *C. onubensis* culture samples into the measuring chamber of portable pulse amplitude modulated fluorimeter model AquaPEN AP-C 100 (Photon Systems Instruments, Czech Republic). F_V represents the variable fluorescence and is calculated as $F_V = F_M - F_0$, being F_0 the minimum level of fluorescence observed after exposing cells to a non-actinic beam and acclimating them in the dark, while F_M represents the maximum fluorescence observed in cells after exposing them to a brief but saturating pulse of actinic light.

2.4. Chlorophyll and carotenoid determination

Chlorophyll and carotenoid content were determined as described by Cuaresma et al. (2012). Culture samples, containing 1 or 2 mL, were centrifuged at 3 *g* for 5 min, methanol was added to the pellet, and the mixture was placed in an ultrasound bath (60 °C, 5 min) to weaken the microalgal cell wall. After another centrifugation step, the supernatant was collected and analyzed by UV/Visible spectrophotometry. Modified Arnon's equations were used to calculate chlorophyll and carotenoid concentrations in the extracts. The extracts obtained were used to analyze the antioxidant capacity of the microalga and the determination of polyphenols compounds.

For specific carotenoid analysis and quantification, separation was performed by liquid chromatography (HPLC; Beckman System gold) using a RP-18 column with a flow rate of 1 $mL \cdot min^{-1}$ and injection extract volume of 40 µL. The applied gradient was the following (solvent A; ethyl acetate and solvent B; acetonitrile/water, 9:1 v/v): 0–16 min, 0–60 % solvent A; 16–30 min, 60 % A; 30–35 min, 100 % A. In order to quantify, pigment standards supplied by DHI-Water and Environment (Denmark) were injected. Quantification of the selected pigments was based on comparison of peak areas obtained from methanolic extracts of *C. onubensis* with those areas obtained from the injected standards.

2.5. Antioxidant capacity

Antioxidant capacity of the methanolic extracts of microalga was determined by the modified version of the DPPH (2,2-diphenyl-1-picryl-hydrazyl-hydrate) free radical method described by Brand-Williams et al. (1995). The antioxidant capacity was determined by the decrease in absorbance at 515 nm of a methanolic solution of DPPH in the presence of the different methanolic samples of the microalga. A concentrated solution of DPPH (Sigma aldrich, Germany) in methanol of approximately 0.4 $g \cdot L^{-1}$ was prepared and diluted with methanol to obtain an absorbance around 0.8. Next, 950 µL of the diluted DPPH solution was made to react with 50 µL of the methanolic sample. The absorbance at 515 nm at time 0 was then measured in a UV-vis spectrophotometer model Evolution 201 (Thermo Fisher Scientific, USA) in a glass cuvette, using methanol as a blank.

Subsequently, the samples were allowed to stand for 30 minutes at room temperature and the absorbance of the sample at 515 nm was measured after that time. Trolox (Fisher Scientific, USA) was used as an external standard. The antioxidant capacity was determined through the difference in absorbance at time 0 and 30 min and was expressed as µmol eq-Trolox$\cdot g^{-1}$ biomass ($y = -0.6536 \cdot x + 1.1429$, $R^2 = 0.9949$).

2.6. Polyphenols determination

Total polyphenols were determined using the procedure described by Georgé et al. (2005). According to this, phenolic compounds were oxidized by the Folin-Ciocolteau reagent (Panreac, Spain), resulting in a blue color complex formation. The reaction was carried out in an alkaline medium; for this, sodium carbonate was added to the samples, and the absorbance was measured at 725 nm by UV-vis spectrophotometry model Evolution 201 (Thermo Fisher Scientific, USA). Total content of polyphenols was

obtained using a calibration line from a standard solution of gallic acid 1-hydrate (Panreac, Spain) and was expressed as mg-eq· gallic acid·L^{-1} ($y = 0.0996 \cdot x - 0.0016$, $R^2 = 0.9999$).

Flavonoid compounds were determined by a spectrophotometric method described by (Liu et al., 2002). For this, the following reagents were used: $NaNO_2$, $AlCl_3 \cdot 6H_2O$ and NaOH. As an external standard, a 1 g·L^{-1} catechin stock, (+)-catechin hydrate (Sigma aldrich, Germany) in MilliQ water was used. The absorbance value was measured at 510 nm using UV-vis spectrophotometry model Evolution 201 (Thermo Fisher Scientific, USA). Total content of flavonoids was calculated by extrapolating the values obtained in the calibration line ($y = 0.0029 \cdot x - 0.0515$, $R^2 = 0.9985$).

2.7. Superoxide dismutase activity determination

Superoxide dismutase (SOD) activity was tested as described by Mccord and Fridovich, (1969), monitoring the inhibition of nitroblue-tetrazolium (NBT) staining at 530 nm due to the decrease in superoxide associated with SOD activity. NBT reduced superoxide anion and resulted in a pink color that can be measured at 530 nm. Each unit of SOD was defined as the amount of enzyme required to inhibit 50 % of the reaction of superoxide anion with NBT.

The first stage consisted in the preparation of the algal crude extract, for which algal cultures were harvested during the exponential growth phase by centrifugation at 3 *g* model Eppendorf centrifuge 5702 (Fisher scientific, USA). The pellet was resuspended in 2 mL of extraction buffer per g of fresh weighted pellet. The SOD-extraction buffer contained 50 mM P-Buffer + 1 mM PMSF + 0.1 mM EDTA + 1 % PVP. Pellet was washed 3 times with the extraction buffer and cells were disrupted, for which the ball mill method model mm 400 (Retsch, Germany) was used applying 10 cycles of 30 seconds with a 1-minute rest between them. Next, the mixture was spined for 10 minutes in a refrigerated centrifuge at 4 °C at 16,000 g model FC5816R (Ohaus, USA).

The enzyme activity was determined spectrophotometrically, following the consumed H_2O_2 decay at 530 nm (ε=2.8 $mM^{-1} \cdot cm^{-1}$) and 25 °C. The reaction mixture contained, per milliliter: 0.1 Tris-HCl 500 mM, 0.5 EDTA 10 mM, 0.05 Xanthene 10 mM, 0.05 NBT 1 mM and 0.04 µL Xanthene Oxidase. A blank sample was prepared accordingly replacing NBT with demi water. One unit, U, of activity represents the enzyme required to consume H_2O_2, at 1 $\mu mol \cdot min^{-1}$. Specific activity of SOD was calculated considering the difference absorbance between the sample and blank expressed as a U·mg^{-1} of proteins.

2.8. Proteins determination

Proteins content was determined spectrophotometrically by the Lowry quantification method, by interpolation on a bovine serum albumin (BSA) standard curve, measured at 580 nm (Lowry et al., 1951). Reagent A (2 g Na_2CO_3 in 100 mL NaOH 0.1 M), reagent B (0.1 g $CuSO_4 \cdot 5H_2O$ in 10 mL H_2O) and reagent C (0.2 g $KNaC_4H_4O_6 \cdot 4H_2O$ in 10 mL H_2O) were prepared. Crude extracts prepared for SOD activity were diluted with SOD-extraction buffer. More details of SOD reagent can be found in section 2.7 of Material and Methods. Next, 5 mL of reagent D (reagent A:B:C 100:1:1 v/v) was added to each

sample, and a dark incubation for 15 minutes was performed. It was followed by the addition of 0.5 mL of reagent E (Folin-Ciocalteau reagent diluted with H_2O (1:3) and dark incubation for 30 minutes. The calibration curve was prepared from aqueous solutions obtained from 0-277 $\mu g \cdot L^{-1}$ of BSA (Sigma Aldrich, USA). Finally, the protein content of the samples was determined spectrophotometrically with absorbance measurement at 580 nm, using distilled water as a blank. Quantification of proteins was based on interpolation on the standard curve ($y = 0.031x + 0.0504$, $R^2 = 0.9952$).

2.9. Lipids and fatty acids determination

Lipid composition was measured in lyophilized biomass samples as described by (Südfeld et al., 2021). Briefly, 10 mg of sample was extracted with chloroform:methanol (2:1, v/v). The extraction process was followed by solvent evaporation using a N_2 stream. Subsequently, lipid content was determined gravimetrically.

The fatty acid analysis was performed according to the following procedure. Once the acylglycerides were extracted, the corresponding fatty acids methyl-ester (FAME) were obtained through acid catalysis-mediated transesterification. The mixture was heated at 85 °C for 1 h, then cooled and washed with hexane and water. The FAMEs were separated by centrifugation (3 *g*, 10 min). FAMEs were separated and analyzed in a gas chromatograph system equipped with flame ionization detector (model 7890A, Agilent, California, USA). A 1-µL sample was injected into a silica capillary column (30 m, 0.32 mm id and 0.25-µm film thickness). Helium was used as carrier gas. The applied flow rate was 1.5 $mL \cdot min^{-1}$ and the split ratio 20:1. The injector and detector temperature values were 100 °C and 220 °C, respectively. The programed oven temperature raised from 80 to 140 °C at 5 °C min^{-1}, followed by increase to 170 °C at 4 °C min^{-1} and then maintained for 2 min at 170 °C. Temperature was then increased to 190 °C at 1 °C min^{-1} and maintained for 2 min. The final temperature in the oven was 210 °C. Each one of the FAME peaks was identified by comparing retention times with those of mixed fatty acids standards (FAMEs Mix C4-C24 Supelco Analytical). Concentrations of FAMEs (ppm) were quantified by comparing their peak areas with those obtained from the standards of known concentration (Sigma Aldrich, USA). Fatty acid composition was calculated as a percentage of the total fatty acids in the volume of hexane. For quantification, tripentadecanoin was used as internal standard (Sigma aldrich, USA).

2.10. Statistics

Unless otherwise indicated, the presented data are the means of three independent experiments and the standard deviations are represented in the corresponding figures and tables. The data from the different treatments was analyzed with univariate statistical models using analysis of variances (ANOVA) with a confidence of 95 %. The analysis was performed using Minitab 17 software.

3. Results

Fe (III), as already described, plays a determining role in physiological processes of microalgae and is an inducer of the antioxidant response through its direct participation in the Fenton reaction. The effect that the addition of Fe (III) can exert on the productivity and photosynthetic viability of *C. onubensis* along with the accumulation of antioxidant molecules was analyzed. The molecules selected for the study are of nutraceutical value and were described to display anti-inflammatory activity.

3.1. Abiotic stress on cell growth and photosynthetic viability

Initially, the effect of Fe (III) on the growth and photosynthetic viability of cultures of the highly acidic-habitat microalga was analyzed in order to determine the range of Fe (III)-sublethal concentrations. Fe (III) was supplemented to *C. onubensis* cultures from 0 to 2 mM. The effect of Fe (III) on the growth of *C. onubensis* throughout the experiment is shown in Figure 5.2 based on biomass dry weight data.

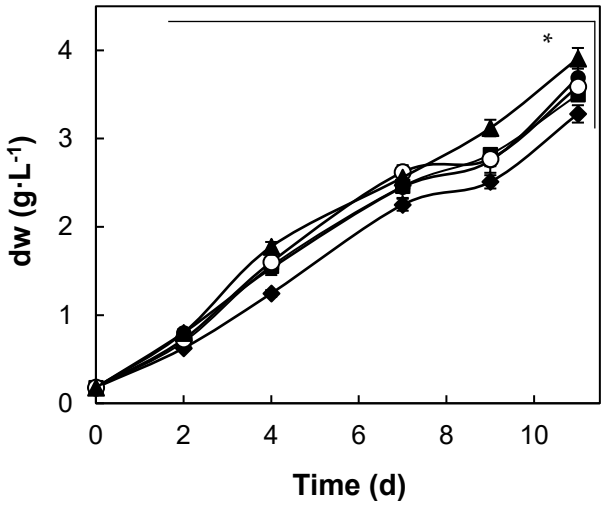

Figure 5.2. Time-dependent evolution of growth (dry weight, dw) in cultures of *C. onubensis* subjected to different concentrations of Fe (III). Symbols for Fe (III) concentration: 0 (-◆-), 0.25 (-■-), 0.5 (-●-), 1 (-○-) and 2 (-▲-) mM. Fe (III) 0 mM corresponds to the standard culture medium (control culture). (*) Represents the significant differences of all treatments with respect to the control culture with 95% confidence.

Figure 5.2 shows a continuous increasing trend in biomass concentration for all the cultures, the increase being larger as Fe (III) increases. For better visualization, the differences in growth as a function of Fe (III) concentration were determined based on their productivities (Figure 5.3a). In turn, Figure 5.3a shows that an increase in Fe (III) resulted in increased productivity of the cultures, reaching a maximum value of 0.35 $g \cdot L^{-1} \cdot d^{-1}$ (17 % higher than that of the control culture) in the 2 mM Fe (III)-added culture. Additionally, the physiological status of the microalgal cultures is connected with the photosynthetic cellular viability, which can be determined as the photosynthetic efficiency of photosystem II (PSII), measured as Quantum yield (Qy), and the chlorophyll (Chl) concentration of the cultures (Figure 5.3b).

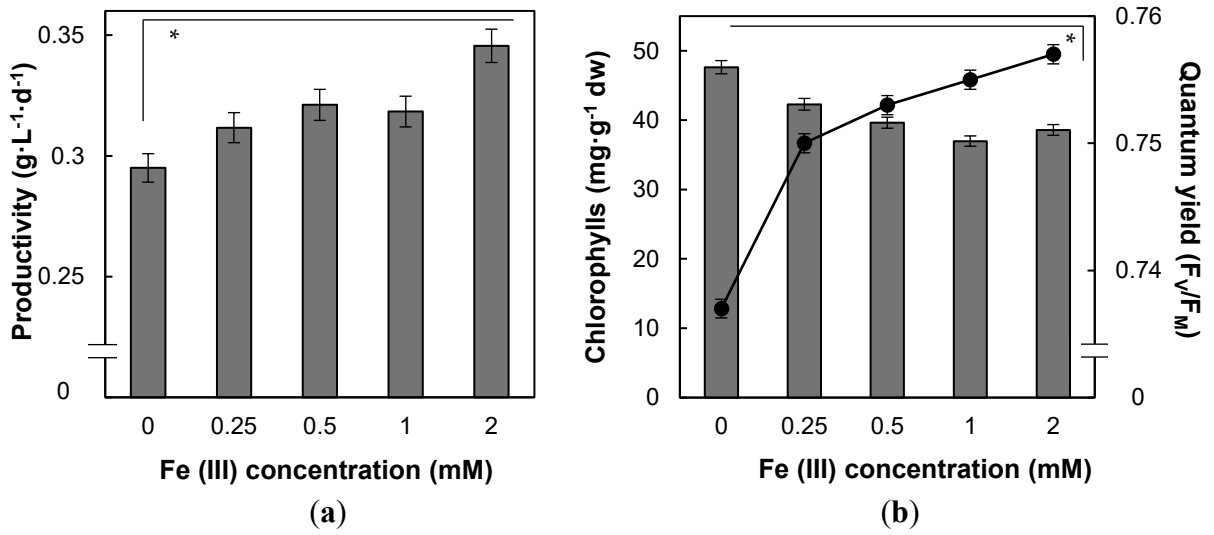

Figure 5.3. (**a**) Microalgal productivity, (**b**) intracellular chlorophyll concentration (bars) and maximal photosynthetic efficiency of photosystem II (Quantum yield, solid circles), as a function of the Fe (III) concentration in cultures of the microalga *C. onubensis*. Data corresponds to day 4 of cultivation, Procedure details are provided in the Materials and Methods section. (*) Represents the significant differences of all treatments with respect to the control culture with 95 % confidence.

Figure 5.3b shows the effect of Fe (III) on the photosynthetic viability of *C. onubensis* cultures. As shown, the increase in Fe (III) concentration resulted in a progressive decrease of the intracellular concentration of chlorophyll, which became 19 % lower for 2 mM Fe (III) culture compared to the control culture. Conversely, a higher efficiency in the photochemical process at PSII was achieved as Fe (III) increased, this value being 27 % higher in the 2 mM Fe (III) culture than that of the control culture. Similarly, by analyzing the time-dependent variation of the intracellular chlorophyll concentration as a function of the Fe (III) concentration (Figure S5.1 of Supplementary Material), a decrease in the cell chlorophyll content is observed with increased Fe (III) concentrations in cultures of *C. onubensis*. Chl a and Chl b were also determined along the experiment time in cultures exposed to Fe (III) (Figure S5.2 of Supplementary material), showing decreased contents of both Chl a and Chl b along the experiment time (from day 0 to 9) in cells exposed to increased Fe (III) levels.

For a better understanding of the Fe (III) role during the photochemical process, samples of Fe (III)-added cultures were subjected to Chl fluorescence analysis. Table 5.1 illustrates some selected parameters, which were calculated based on the OJIP Chl fluorescence signals. The selected photochemical parameters of *C. onubensis* express specific electron and energy fluxes per reaction center (RC), as described in the Table legend. Among the parameters listed, the net closing rate of RCs during illumination (M_0) decreased as Fe (III) increases, being 22 % lower for the highest Fe (III) concentration tested. The electron transport flux per RC (ET_0/RC) increased by 5.4 % for the 2 mM Fe (III) culture with respect to the control culture, while the trapping energy flux per RC (TR_0/RC) remained almost stable. ABS/RC expresses the absorption flux per RC, related to apparent antenna size which decreased slightly when Fe (III) is added to the cultures, becoming 4 % lower for the 2 mM Fe (III) culture with respect to the control culture. The dissipated energy flux per RC (DI_0/RC) decreased as Fe (III)

increases, being 11 % lower for the 2 mM Fe (III) culture with respect to the control culture.

Table 5.1. JIP parameters calculated based on the OJIP Chl fluorescence signals for the microalga *C. onubensis* as a function of the Fe (III) concentration. M_0, net closing rate of RC during illumination; ABS/RC, absorption flux per RC; TR_0/RC, trapping energy flux per RC; ET_0/RC, electron transport flux per RC; DI_0/RC, dissipated energy flux per RC.

Parameter	Fe (III) concentration				
	0 mM	**0.25 mM**	**0.5 mM**	**1 mM**	**2 mM**
M_0	0.210±0.009	0.235±0.011	0.177±0.071*	0.172±0.007*	0.164±0.007*
ABS/RC	1.095±0.047	1.029±0.043*	1.018±0.046*	1.034±0.045*	1.051±0.047*
TR_0/RC	0.807±0.032	0.771±0.034*	0.766±0.032*	0.805±0.036	0.795±0.035
ET_0/RC	0.597±0.023	0.594±0.025*	0.603±0.026	0.611±0.027	0.629±0.025
DI_0/RC	0.288±0.011	0.257±0.004	0.252±0.005	0.254±0.003	0.256±0.010

(*) Represents the significant differences of all treatments with respect to the control culture with 95 % confidence.

The results obtained seem to evidence the expected Fe (III) involvement in photosynthetic redox processes. In addition, Fe (III) is directly involved in the so-called Fenton reaction which triggers the production of reactive oxygen species within the cell. Therefore, the antioxidant response of the microalga to cope with the oxidative stress generated through the addition of Fe (III) to the cultures was analyzed.

3.2. Antioxidant cell response as a function of the Fe (III) concentration

As described in the Introduction section, superoxide dismutase (SOD) is one of the key enzymes in the defense mechanisms against oxidative stress. The following figure shows the evolution of SOD activity as a function of the Fe (III) concentration supplied to *C. onubensis* cultures.

Figure 5.4a shows the evolution of the specific SOD activity as a function of the Fe concentration added to cultures of the microalga *C. onubensis*. As shown, incubation under increasing Fe (III) concentrations resulted in increased specific SOD activity levels, this being maximal for the culture supplied with 1 mM Fe (III), approximately 62 % higher than that of the control culture. Figure 5.4b shows the changes of the total cellular protein concentration as a function of the Fe (III) concentration added to *C. onubensis* cultures. According to the Figure, as Fe (III) increased, a slight decrease in cell protein concentration was found, this being minimal for the 1 mM culture, 18 % lower than that value obtained from the control culture.

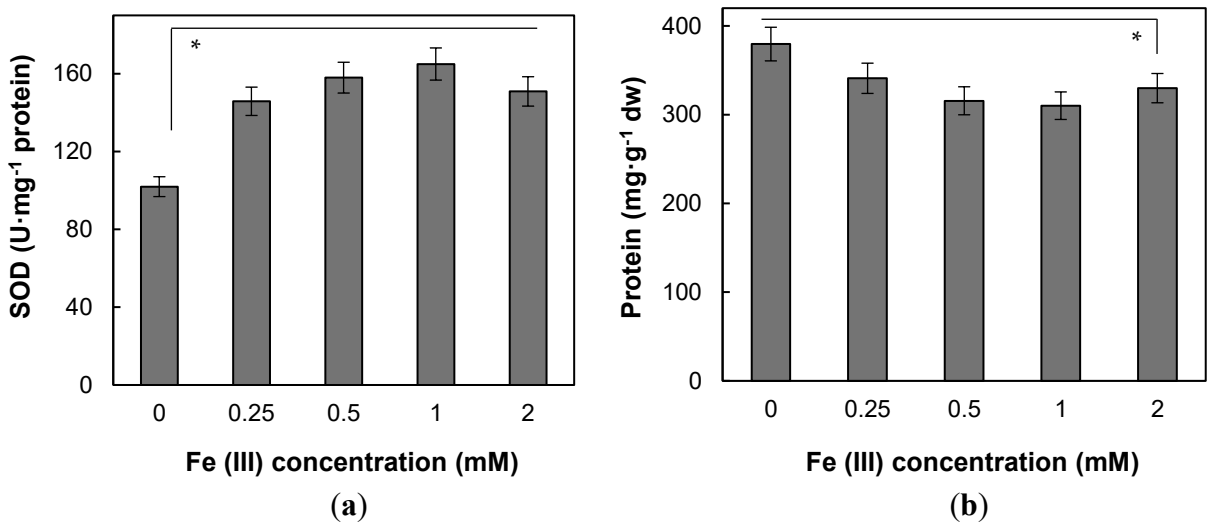

Figure 5.4. Effect of Fe (III) on the SOD enzyme activity (**a**) and total cell protein content (**b**) of *C. onubensis* cultures. The data presented corresponds to day 11 of cultures incubation in Fe (III), last day of experiment. More details are provided in the Material and Methods section. (*) Represents the significant differences of all treatments with respect to the control culture with 95 % confidence.

The results suggest an increasing expression of the antioxidant biochemical response under increased Fe-mediated oxidative pressure, in parallel to an apparently less active protein biosynthesis which seems not to compromise the photosynthetic viability, as shown in Figure 5.3 and Table 5.1. In this study, the non-enzymatic antioxidant response was also analyzed as a function of Fe (III) concentration added to the *C. onubensis* cultures (Figure 5.5).

Figure 5.5a represents the antioxidant capacity of culture samples of the highly acidic-habitat microalga cultures subjected to different Fe (III) concentrations. As shown, Fe induced changes in the antioxidant capacity of the microalga. The increase in Fe (III) concentration caused a decrease in the antioxidant capacity which was 22 % lower for the culture with the maximum Fe (III) concentration tested –2 mM– at day 2 of experiment, with respect to the control culture.

The Fe-dependent decrease in antioxidant capacity should accordingly indicate a reduction in the antioxidant molecules pool of *C. onubensis* upon a long-term exposition to the metal. As shown in Figure 5.5b, polyphenol content in the cells apparently decreased as the Fe concentration increased, with minimum values for the 2 mM Fe (III) culture, approximately 30 % lower than those for the control culture. On the other hand, the intracellular flavonoid content tends to increase as the Fe concentration increased, reaching a maximum value for the maximum Fe (III) concentration tested –2 mM–, this being 8 % higher with respect to the control culture. The cell content of polyphenol compounds and flavonoids remained roughly unaltered during the first 24 h of experiment, then starting to decrease (polyphenols) and increase (flavonoids) slightly, respectively, from day 2. For this reason, Figure 5.5b shows the averaged content of both molecules in the above-referred time period, from day 2 to 9.

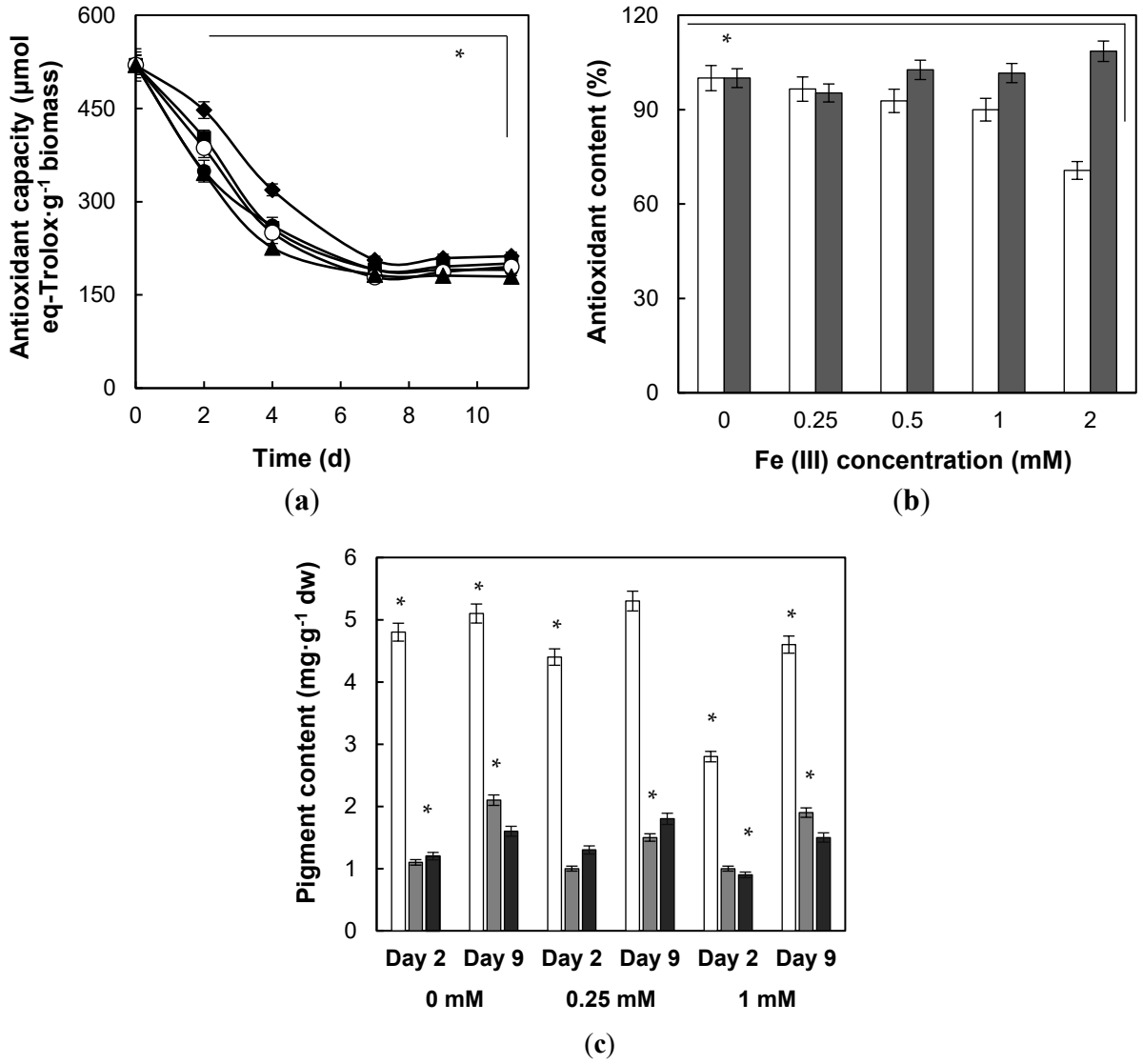

Figure 5.5. Effect of Fe (III) concentration on the non-enzymatic antioxidant response of *C. onubensis* cultures. (**a**) Antioxidant capacity. Symbols for Fe (III) concentration: 0 (-◆-), 0.25 (-■-), 0.5 (-●-), 1 (-○-) and 2 (-▲-) mM; (**b**) Average antioxidant content between days 2 and 9 of cultivation: polyphenols (empty bar) and flavonoids (black bar). 100 % of polyphenols and flavonoids corresponds to an average content of 17.50 and 94.06 mg·g^{-1} biomass, respectively; (**c**) Pigment content: lutein (empty bar), neoxanthin (grey bar) and beta-carotene (black bar) for day 2 and 9 of cultivation. Procedure details are provided in the Materials and Methods section. (*) Represents the significant differences of all treatments with respect to the control culture with 95 % confidence.

Figure 5.5c shows the variation in the content of the majority carotenoids of *C. onubensis* produced during the days 2 and 9 of cultivation as a function of the Fe (III) concentration. Short term cultivation, 48 h, resulted in a slight decrease in the lutein content compared to control culture, as Fe (III) concentration increases, while under long term cultivation a recovery of that content was obtained. Slight differences were found in neoxanthin and beta-carotene in Fe-added cultures. Nevertheless, under long term cultivation an increase of about 30-50 % was obtained for neoxanthin and beta-carotene. Day 2 of experiment was taken as a reference, based on the fact that the carotenoid content in control cultures did not change in the first 24-48 h days and the relevant variation in Fe (III)-supplemented cultures occurred from day 2.

The results obtained show that Fe (III) has a direct effect in the enzymatic and non-enzymatic antioxidant responses of the microalga. The main trend inferred from the results leads to an imbalanced variation of the majority antioxidant molecules.

3.3. Triggering the accumulation of fatty acids and lipids

In this section, the effect of Fe (III) on the accumulation of lipids and fatty acids in the microalga *C. onubensis* as a response to the imposed oxidative stress was analyzed.

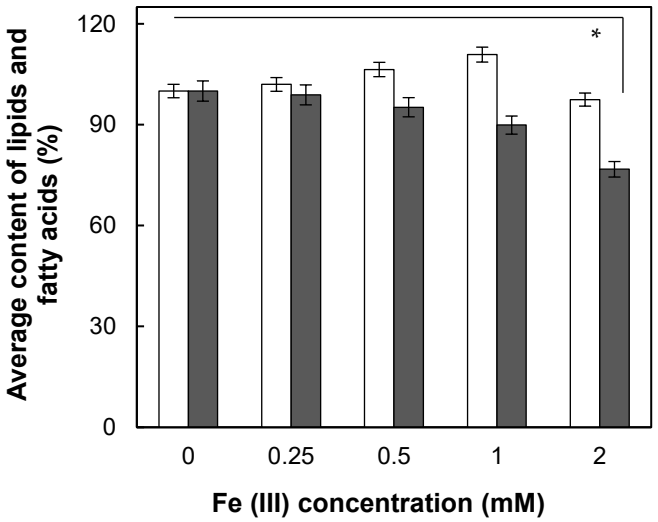

Figure 5.6. Effect of Fe (III) concentration on the average content of lipids (empty bars) and fatty acids (grey bars) of the microalga *C. onubensis* between days 2 and 9 of cultivation. 100 % of average content of lipids and fatty acids corresponds to 31.52 and 12.63 $mg \cdot g^{-1}$ biomass, expressed as percentage, respectively. Procedure details are provided in the Materials and Methods section. (*) Represents the significant differences of all treatments with respect to the control culture with 95 % confidence.

Figure 5.6 shows the variation in the cell content of lipids and fatty acids in *C. onubensis* biomass samples as a function of the Fe (III) concentration of the cultures. According to the Figure, the cell lipid content for cultures grown in the presence of Fe shows a slight increase as Fe (III) increased, being maximal for the 1 mM Fe (III) culture, approximately 11 % higher than that of the control culture. On the other hand, the cell content of total fatty acids tended to decrease when the Fe (III) concentration increases, the lowest fatty acids content (23 % lower than that content in control culture samples) being reached in the culture with the maximum Fe (III) concentration –2 mM–.

As discussed further in this study, ROS neutralizing role of unsaturated fatty acids might partly explain their apparent content variation in cultures exposed to Fe (III). Consequently, the fatty acids profile of *C. onubensis* samples from cultures exposed to Fe (III) was carefully analyzed. Results are shown in Figure 5.7.

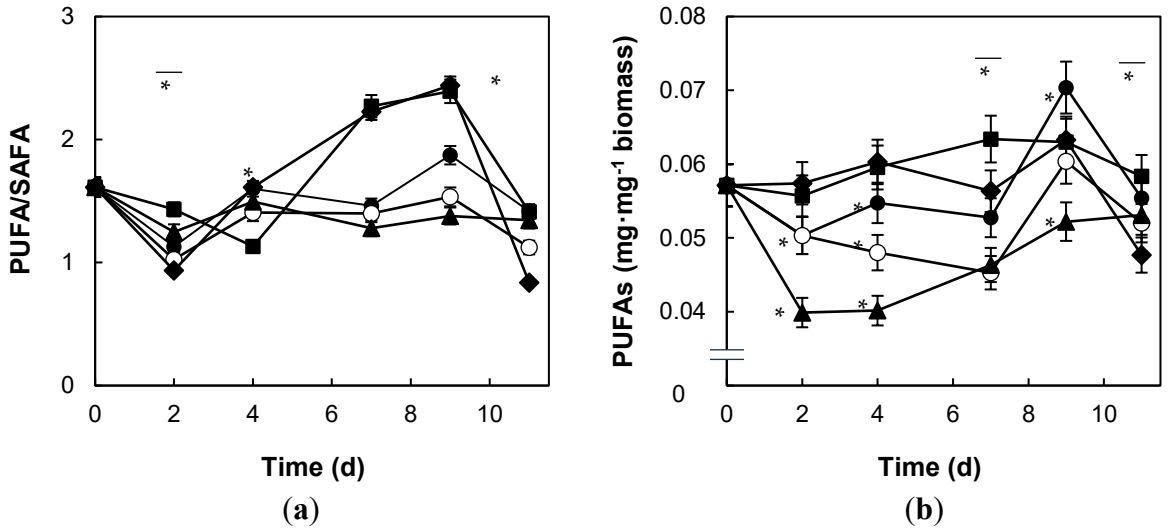

Figure 5.7. Effect of Fe (III) concentration on the fatty acids saturation level of the microalga *C. onubensis.* SAFA: saturated fatty acids; PUFA: polyunsaturated fatty acids. Symbols: 0 (-◆-), 0.25 (-■-), 0.5 (-●-), 1 (-○-) and 2 (-▲-) mM Fe (III). Procedure details are provided in the Materials and Methods section. (*) Represents the significant differences of all treatments with respect to the control culture with 95 % confidence.

Figure 5.7 shows the time-dependent evolution of the cell content of unsaturated fatty acids in *C. onubensis* cultures as a function of the Fe concentration. According to the Figure, the ratio of polyunsaturated fatty acids to saturated fatty acids (PUFA/SAFA) tended to remain roughly stable for several days after the experiment started up. From day 4, an increase in the PUFA/SAFA ratio was obtained in the control culture and in the culture added with 0.25 mM of Fe (III), while under increasing Fe (III) concentrations the ratio remained almost stable.

Specifically, the abundance of polyunsaturated fatty acids (PUFAs) was analyzed in Figure 5.7b. The cell PUFA content tended to decrease during the first days of incubation as the concentration of Fe supplied to the cultures increases, except for the 0.25 mM culture which presented similar values to those of the control culture. From the point of view of the physiological significance of the results, those data obtained during the early growth phase, until day 3-4 of cultivation, should be more relevant to the final conclusions of the study, as all the microalgal cells were experiencing most of the total Fe (III) concentration added to the cultures, unlike at later stages of growth, above day 7 of cultivation.

The maximum cell fatty acids content accumulated by *C. onubensis* as a function of the Fe (III) concentration was analyzed, and the main data are shown in Table 5.2. Table 5.2 shows the maximum cell content of fatty acids, expressed as a percentage with respect to the biomass dry weight, obtained from *C. onubensis* culture samples. The data corresponds to the accumulation of main fatty acids as a function of the Fe concentration. The data exceeding those obtained from control culture samples are highlighted in bold. According to the Table, the presence of increased Fe (III) concentrations in *C. onubensis* cultures resulted, on the one hand, in a decreased content of saturated fatty acids C16:0 and C18:0. On the other hand, in the case of unsaturated fatty acids, an increase was observed for low concentrations of Fe (III), while as Fe

concentration increased the unsaturated content tended to decrease. It is worth noting that the C18:2 and C18:3 fatty acids, which correspond to omega 6 and omega 3 series, respectively, reached maximum values in Fe (III) added cultures: at 0.5 mM, C18:2 content became 48 % higher than that value obtained in the control culture, and at 0.25 mM C18:3 concentration was 36 % higher than that of the control culture.

Table 5.2. Maximum average fatty acids content of *C. onubensis* cells incubated in Fe (III)-added culture medium. Fatty acids: palmitic acid (C16:0), hexadecatrienoic acid (C16:3), heptadecenoic acid (C17:1), stearic acid (C18:0), oleic acid (C18:1), α-linoleic acid (C18:2) and α-linolenic acid (C18:3). Data are expressed as a percentage of mg of fatty acid per mg of biomass dry weight. The data exceeding those obtained from control culture samples are highlighted in bold.

Fatty acid	Fe (III) concentration				
	0 mM	**0.25 mM**	**0.5 mM**	**1 mM**	**2 mM**
C16:0	4.35±0.17	4.02±0.17*	3.18±0.14*	3.49±0.15*	3.02±0.12*
C16:3	0.72±0.04	0.71±0.03	**0.82**±0.04*	0.62±0.02*	0.65±0.03*
C17:1	1.10±0.06	**1.55**±0.06*	1.03±0.04*	**1.12**±0.05	0.80±0.03*
C18:0	1.44±0.04	0.83±0.04*	0.96±0.04*	1.11±0.05*	0.80±0.03*
C18:1n9	1.08±0.03	**1.10**±0.05*	1.04±0.05*	0.88±0.04*	0.88±0.04*
C18:2n6	2.49±0.11	**2.70**±0.12*	**3.77**±0.16*	2.28±0.09*	2.30±0.10*
C18:3n3	3.42±0.15	**4.67**±0.20*	3.17±0.14*	3.24±0.14*	2.56±0.12*

(*) Represents the significant differences of all treatments with respect to the control culture with 95 % confidence.

Saturated fatty acids are adequate to obtain biodiesel, while fatty acids from the omega-3 and omega-6 families are considered essential in nutrition and have a high value in human health. In this way, the decrease in saturated fatty acids C16:0 and C18:0 under low Fe levels, together with the increase in polyunsaturated fatty acids from the omega 6 and omega 3 families, C18:2 and C18:3, respectively, would result in fatty acids, rich microalgal biomass that could be suitable as supplement for animal nutrition and/or the design of functional foods.

4. Discussion

4.1. Abiotic stress on cell growth and photosynthetic viability

Fe plays a key role in the cellular biochemistry of microalgae due to its redox properties and the involvement in fundamental processes such as photosynthesis, respiration, nitrogen fixation, and DNA synthesis (Estevez et al., 2001; Hardie et al., 1983). Our results in *C. onubensis* are in good agreement with this fact showing that Fe (III), added to the cultures in a certain concentration range, stimulates the growth of the acidotolerant microalga (Figure 5.2 and 5.3). The range of Fe (III) concentrations used in this study is still below toxic levels, since the highest concentration of Fe (III) added to the cultures resulted in the highest biomass productivity of the microorganism.

Photosynthesis is the most Fe-requiring process in plants. Photosynthetic electron transfer chain converts light energy into chemical energy between photosystems II and I (PSII and PSI) via cytochrome (cyt) b6f in thylakoid membranes (Saito et al., 2021). During this process, part of the Fe taken by microalgae from the medium distributes into [4Fe-4S] cluster-containing PSI proteins and Fe-containing cyt b6f complexes. Consequently, Fe mediates light-driven electron transfer in microalgal cells (Briat et al., 2015; Hantzis et al., 2018). Fe−S cluster-dependent metabolism in microalgae is sensitive to disruption by oxygen because of the decreased bioavailability of ferric iron at neutral and basic pH, as well as due to the direct oxidation of sulfur intermediates and Fe−S clusters by reactive oxygen species (Boyd et al., 2014). Fe is more bioavailable at low pH, mainly because both ionic forms of iron, Fe (II) and Fe (III), are far more soluble (especially ferric iron) at low pH than at neutral or basic pH (Johnson et al., 2012). In addition, in the acidic natural habitat of *C. onubensis*, Fe (III) is by far the predominant form of iron, due to the rapid, natural oxidation of Fe (II) to Fe (III) in the aerobic, photic zone (Sánchez-España et al., 2020).

In this study the microalga *C. onubensis* is cultivated under acidic conditions with a supplement of Fe (III). The higher Fe (III)-bioavailability under acidic conditions should result in increased Fe (III)-intracellular levels, including Fe (III) presence in inorganic Fe-S clusters. In this sense, the results obtained for the photobiochemical parameters (Table 5.1) show that the addition of Fe (III) to the cultures favors the electron transport flux (ET_0) while the net closing rate of RC (M_0) decreases. As $M_0 = TR_0 – ET_0$ and the trapping energy flux per RC (TR_0) remains almost stable, the reduction in net closing rate of RC means that the electron transport chain (ETC) should be more active while Fe is added. The increase in the efficiency of PSII (Figure 5.2b) together with the enhancement obtained in the ETC (Table 5.1) allow us to suggest that photosynthesis in *C. onubensis* becomes stimulated by moderated concentrations of Fe (III) (0.25-2 mM).

Fe-mediated increased photosynthetic capacity addresses faster growth of *C. onubensis*. In batch cultures, this fact led to a faster increase in cell turbidity which could favor the cells to experience light limitation. Thus, the subsequent reduction in the chlorophyll cell content (Figure 5.3b and S5.1) should be understood as a light-capturing apparatus adaptation strategy to reduce the shadowing effect among the cells (Ort and Melis, 2010). This fact is in good agreement with the values obtained for the

photobiochemical parameters determined in Fe-exposed cultures, shown in Table 5.1. For instance, the decrease in absorption per reaction center rate (ABS/RC) and dissipated energy per reaction center (DI_0), could be understood as a mechanism to minimize light use efficiency losses in a light-limited culture. In this scenario, the decreased chlorophyll cell content could be interpreted as an apparent reduction of the antenna size per cell, expressed to increase light capture. Accordingly, the decreased Chl b contents along the experiment time (from day 0 to 9) shown in Figure S5.2b for cells exposed to increased Fe (III) levels is in line with the discussion. As published, a reduction of chlorophyll b can result in a reduction of light harvesting complex proteins stability which become degraded. This fact results in the reduction of the apparent optical cross section of the light harvesting antenna (Friedland et al., 2019). The same reduction effect in the antenna size is hypothesized based on the results obtained in our experiments for *C. onubensis* cultures exposed to Fe (III). This strategy has been described by other authors in cultures under oversaturating light irradiance as a mean to decrease the non-photochemical quenching, aimed at reducing photooxidative damage in the chloroplasts (Ort and Melis, 2010). For practical purposes at large scale, addition of Fe (III) to *C. onubensis* cultivation systems might be considered to modulate cell growth and chlorophyll cell content.

4.2. Antioxidant response as a function of the Fe (III) concentration

Antioxidant molecules and enzymes are commonly synthesized in microalgae to cope with oxidative stress and help maintain the homeostatic balance in the cultures. The results obtained showed that the presence of Fe (III) in *C. onubensis* cultures triggers biochemical responses which are typically expressed as a defense mechanism against ROS; particularly, the increased activity of the enzyme superoxide dismutase (Figure 5.4a) evidenced Fe (III)-mediate increased oxidative stress. At higher concentrations of Fe (III), the expression of genes encoding the activity of antioxidant enzymes is induced, including ascorbate peroxidase, superoxide dismutase, dehydroascorbate reductase and catalase (Pikula et al., 2019; Pinto et al., 2003). Nevertheless, the enzyme superoxide dismutase has a constitutive presence according to scientific information (Al-Rashed et al., 2016) and is involved in the cellular antioxidant response, being responsible for catalyzing the transformation of $O_2^{\bullet-}$ into H_2O_2 (see reaction 5.2).

$$2\ O_2^{\bullet-} + 2H^+ \longrightarrow 2\ H_2O_2 + O_2 \quad (5.2)$$

ROS have been described to cause protein oxidation during oxidative stress (Das and Roychoudhury, 2014). In this way, the decrease in the protein content observed as the Fe (III) concentration increases (Figure 5.4b), could theoretically be assigned to the damage caused by the greater activity of ROS generated by the oxidative stress caused by the addition of Fe to the cultures. However, it should be emphasized that this decrease in protein content of *C. onubensis* is compatible with the increase in growth observed in the presence of Fe (III). That is, as described later, to overcome the shadowing effect generated by the increasing number of cells, an apparent reduction of the antenna size per cell was hypothesized. This should be accompanied by a reduction in the protein

content and thus in the light harvesting complex proteins, in coherence with the obtained results.

The slightly increased photosynthetic electron flux (ET_0, Table 5.1) should result in slightly increased reduced ferredoxin pool required as physiological electron donor to assimilatory enzymes, including GOGAT (glutamate synthase) for nitrogen assimilation leading to aminoacid biosynthesis (Sanz-Luque et al., 2015). Accordingly, also photosynthetically produced NAD(P)H availability for assimilatory metabolism should be enhanced. This is in good agreement with the enhanced growth data obtained in Fe (III)-added cultures. In this context, the slightly lower protein content of Fe (III)-added cultures might be, partly, a consequence of a more intensive carbohydrate and/or lipid biosynthesis in Fe (III)-added cultures (the latter shown in Figure 5.6), thus shifting the protein to carbohydrate and lipid ratio in favor to the latter molecules, among others (Depraetere et al., 2015).

The non-enzymatic antioxidant system of the microalga was also analyzed as a function of the Fe (III) concentration added to cultures (Figure 5.5). The results obtained apparently evidenced lower antioxidant capacity for cell extracts from Fe (III)-supplemented cultures (Figure 5.5a). There is a certain decrease in said capacity as a direct function of the added Fe (III) concentration and, particularly, during the first days of cultivation, when most of the Fe (III) could presumably be bioavailable. The apparently lower antioxidant capacity should correspond to cultures under weaker oxidative stress. Nevertheless, the increase in the SOD activity (Figure 5.4a) as the Fe (III) concentration increase might be a sign of a more active antioxidant response of the microalga, though a more extensive analysis of other antioxidant enzymes (ascorbate peroxidase, glutathione reductase, catalase, among others) is required to define the antioxidant response more accurately. This scenario is coherent with a greater involvement of polyphenols in ROS neutralizing reactions (Figure 5.5b), which would explain their apparent decreased content in presence of Fe (III).

Thus, conversely to what many times is accepted, an apparent lower antioxidant capacity might be compatible with the decrease of the chemically active antioxidant form of antioxidant molecules which can eventually be not detected through their specific standard determination methods. For instance, maximal absorption wavelengths for carotenoid and phenol compounds can shift due to double bound oxidation through reaction with oxidizing agents, as elegantly described by Payne et al. (2019). This would affect chromatographic retention times and maximal light absorption of target compounds, then proving the complexity to accurately determine any antioxidant molecule content in the extracts. Indeed, the decrease in the lutein content when Fe (III) is more bio-available together with the lutein content recovery obtained under long term cultivation (Figure 5.5c) suggests eventual regulation mechanisms of the microalga in response to the oxidative stress generated. In this sense, lutein content in *C. onubensis* seems to be constitutive as the contents in Fe (III)-added cultures tend to reach almost to the same high value, 4-5 $mg \cdot g^{-1}$ dw.

Flavonoids increase their intracellular content in the presence of Fe (III), which in principle allows us to suggest a direct relationship between the generation of oxidative

stress and the expression of the biosynthesis of these molecules in acidophilic microalgae. Flavonoids are considered a secondary system for the elimination of ROS present in the Fenton reaction already mentioned in the Introduction section. These molecules also help eliminate oxidative species formation risk caused by excess energy from photosynthesis (Fini et al., 2011), through the so-called auxiliary electron transport (AET) pathways (Nikkanen et al., 2021). AET pathways are comprised of electron sinks which function as efficient release valves for excessive electrons in the ETC, any of them with ability to reduce O_2 to H_2O—without the concomitant production of ROS—known as the Mehler-like reaction (Allahverdiyeva et al., 2013), a sort of chloroplast respiration. Thus, flavonoids seem to be relevant to the antioxidant response of *C. onubensis*.

4.3. Stimulation of the accumulation of fatty acids and lipids

As commented in the above section, Fe has strong prooxidative properties (Guerin et al., 2003), and microalgae such as *C. onubensis*, which grow naturally in the presence of high concentrations of this metal, could express antioxidant responses in Fe (III)-rich media. In response to this stress, terpenoid compounds (carotenoids) and unsaturated fatty acids tend to accumulate in microalgae (Granado-Lorencio et al., 2009), thus an increase in lipid concentration would be expected in the highly acidic-habitat microalga cultures treated with Fe. The results obtained are coherent with this reasoning (Figure 5.6). Nevertheless, our results evidence a slight decrease in the cell content of fatty acids in Fe (III)-added cultures. We cannot offer a clear explanation to this fact, though the decrease in fatty acids might be linked to the use of stored energy in stressed cultures (Alishah Aratboni et al., 2019).

As discussed in the Introduction section, Fe is an essential bioelement but highly toxic in high concentrations due to its ability to exchange electrons with various substrates, giving rise to ROS. The generation of hydroxyl radicals produces oxidative stress by reacting with lipids, proteins and nucleic acids, resulting in irreversible damage to cell structures (Das and Roychoudhury, 2014). Some of these damages include loss of permeability by the lipid membrane, when the hydroxyl radical reacts with the unsaturated fatty acids of membrane phospholipids and thus the unsaturated character of membrane lipids, which is required to keep membrane fluidity, gets lost (Halliwell, 2006).

The results obtained are coherent with this fact (Figure 5.7). As the concentration of Fe increases, the cell content of unsaturated fatty acids decreases in response to the oxidative stress produced. Thus, ROS are expected to react with unsaturated fatty acids which partially loss their unsaturation level through lipid peroxidation, giving rise to conjugated dienes, lipids with peroxyl radicals, and hydroperoxides (Smirnoff, 2000). However, the decreased rate in membrane unsaturated fatty acids in *C. onubensis* does not lead to a loss of cell activity, quite the contrary according to the growth results obtained in the presence of increasing concentrations of Fe (III).

The variation in the fatty acids profile for the microalga *C. onubensis* when subjected to Fe (III) was analyzed in Table 5.2. Saturated fatty acids are used to obtain biodiesel, while fatty acids from the omega-3 and omega-6 families are considered

essential and have a high value in human health. In this way, the decrease in saturated fatty acids C16:0 and C18:0 together with the increase in polyunsaturated fatty acids of the omega 6 and omega 3 family, C18:2 and C18:3, respectively, for cultures treated with an Fe (III) concentration of 1 mM or lower, would result in a supplement suitable for animal nutrition and/or generation of functional food. According to these results, oxidative stress by moderate Fe (III) concentrations favors the biosynthesis of essential polyunsaturated fatty acids, probably benefiting from a moderate activity of generation and action of ROS.

4.4. Overall

It should be noted here that while the levels of Fe (III) added to the culture medium favor growth (Figure 5.2), the levels of antioxidant molecules seem to decrease, in the case of phenolic compounds. The growth stimulated by Fe (III) is compatible, during the first days of incubation, with a retracted synthesis of thylakoid membranes as evidenced, among other factors, by the lower intracellular concentration of chlorophyll (Figure 5.3b) and protein (Figure 5.4a) in cultures with Fe (III). This situation is also compatible with an increase in the efficiency of PSII (Figure 5.3c), which allows us to postulate that this decrease in the microalgae's antenna size would have an evident regulatory function aimed at maximizing the use of light in grown cultures, as inferred from photobiochemical parameters through the increase in ET values and decrease in ABS (Table 5.1).

Numerous proteins involved in electron transfer and reductive biosynthetic reactions in microalgae contain or require Fe, as presented in Figure 5.8. The consequence of that could be an imbalance in the energy that generates through the ETC. The excess energy generated could react with oxygen to produce ROS through the flavodoxin $NADP^+$ reductase (FNR). Especially, the generation of hydroxyl radical through the Fenton reaction could cause oxidative damage in functional biomolecules. The result of that is the activation of defense mechanisms such as the increase in SOD activity (Figure 5.4a) and the apparent decrease in the antioxidant capacity of the microalga as it is shown with the decrease in polyphenols and PUFAs (Figure 5.5 to 5.7). On the other hand, the increase in flavonoids, as mentioned before, could be a mechanism to efficiently release excessive electrons in the electron transport chain (ETC) (Table 5.1), by neutralizing oxygen species—without the concomitant production of ROS.

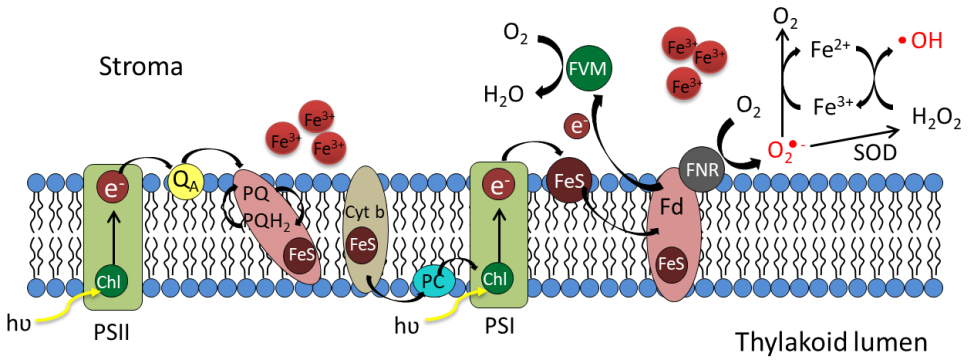

Figure 5.8. Schematic mechanism proposed for the oxidative stress induction linked to the photosynthetic chloroplast electron transport chain when Fe (III) is added. PSII: photosystem II; PSI: photosystem I; Chl: Chlorophyll; Q_A: Quinone A; PQ: Plastoquinone; PQH_2: Plastoquinol; FeS: Iron/sulfur cluster belonging to redox proteins; Cyt b: cytochrome b6f; PC: Plastocyanin; FVM: like-flavonoid molecules; Fd: ferredoxin; FNR: ferredoxin-$NADP^+$ reductase; SOD: superoxide dismutase.

The decrease in the intracellular content of phenolic and terpenoids compounds are hypothesized to be also consistent in this study to a major interaction of these molecules in ROS neutralization. The oxidative biochemical consequences of the Fenton reaction are forced in the presence of Fe (III) and are described in detail in the literature (Rana and Prajapati, 2021). Consequently, an increase or decrease in the antioxidant capacity and/or in the content of certain antioxidant biomolecules in cultures with Fe (III) could be the result of the balance between the chemical oxidative pressure generated by the ROS against these molecules (responsible for its apparent decrease) and the biosynthetic activity stimulated under the applied stress conditions (responsible for its potential intracellular increase).

5. Conclusions

The findings of this Chapter revealed that the addition of Fe to cultures of the microalga *C. onubensis* at appropriate concentrations promotes microalgal cell growth. Fe (III) causes oxidative stress in *C. onubensis*, as a defense mechanism, the microalga produces an increase in the intracellular levels of the enzyme SOD and flavonoids, while the content of other phenolic and terpenoid molecules suffers from an apparent decrease. It is suggested that the latter could be related to any of the following aspects: (i) constitutive presence of some of the aforementioned molecules, particularly carotenoids; (ii) net negative balance between biosynthesis and the participation of said molecules in ROS neutralization reactions; (iii) molecules modification by ROS reactivity, which gives rise to changes in molecular features required for e.g. spectrophotometric detection, like the case of polyphenols. The increase in Fe (III) concentrations in the microalga *C. onubensis* impacts on the cell content of unsaturated fatty acids, i.e., oxidative stress by Fe (III), in moderate concentrations, favors the biosynthesis of essential polyunsaturated fatty acids, particularly linoleic and linolenic acids. This could probably be a consequence of a moderate PUFA involvement in ROS neutralization, in addition to moderate ROS generation. Overall, this study offers insight to understand the antioxidant response features of acidophilic/acidotolerant microalgae which can be further useful to design large scale production of antioxidant molecules enriched microalgal biomass.

6. Supplementary material

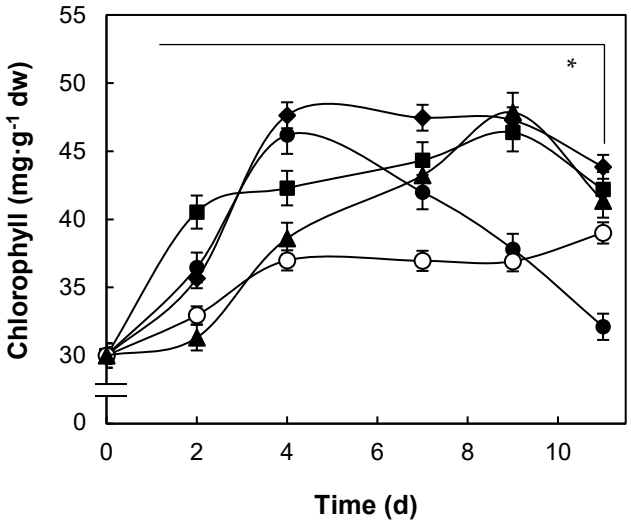

Figure S5.1. Time-dependent evolution of intracellular chlorophyll concentration, expressed as mg·g^{-1} dw, in cultures of *C. onubensis* subjected to different concentrations of Fe (III). Symbols for Fe (III) concentration: 0 (-◆-), 0.25 (-■-), 0.5 (-●-), 1 (-○-) and 2 (-▲-) mM. The indication Fe (III) 0 mM corresponds to the standard culture medium (control culture). (*) Represents the significant differences of all treatments with respect to the control with 95% confidence.

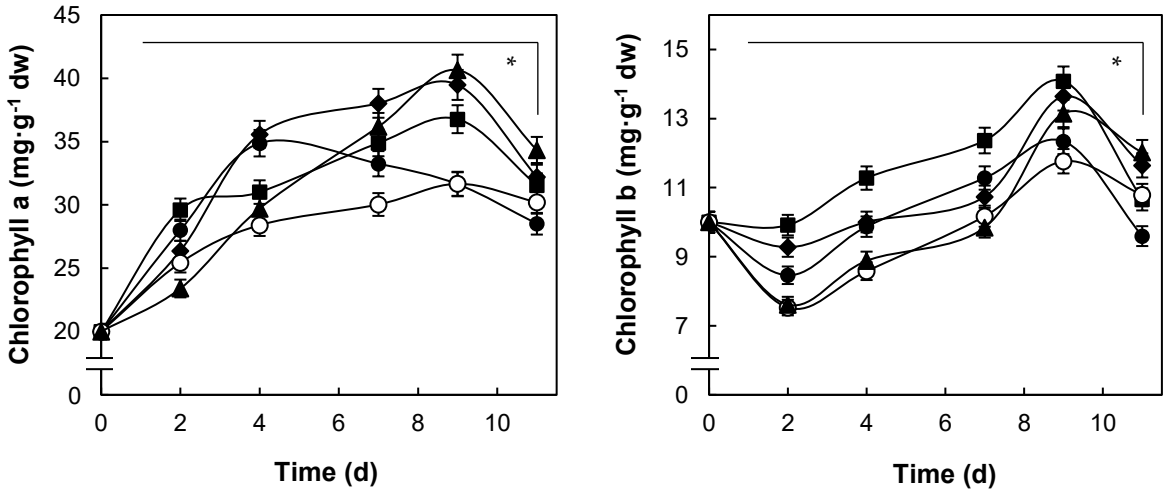

(**a**) (**b**)

Figure S5.2 Time-dependent evolution of intracellular concentration of (**a**) chlorophyll a and (**b**) chlorophyll b, expressed as mg·g^{-1} dw, in cultures of *C. onubensis* subjected to different concentrations of Fe (III). Symbols for Fe (III) concentration: 0 (-◆-), 0.25 (-■-), 0.5 (-●-), 1 (-○-) and 2 (-▲-) mM. The indication Fe (III) 0 mM corresponds to the standard culture medium (control culture). (*) Represents the significant differences of all treatments with respect to the control with 95% confidence.

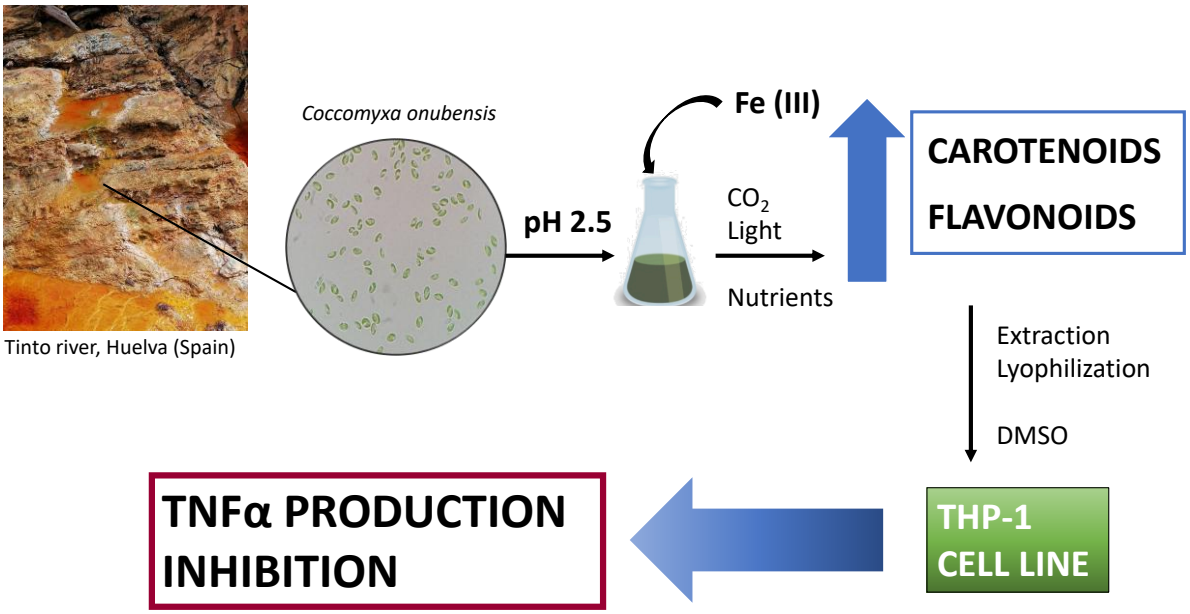
Tinto river, Huelva (Spain)
Coccomyxa onubensis
pH 2.5
Fe (III)
CO_2
Light
Nutrients
CAROTENOIDS
FLAVONOIDS
Extraction
Lyophilization
DMSO
THP-1
CELL LINE
TNFα PRODUCTION
INHIBITION

6

CHAPTER

Anti-inflammatory activity of antioxidant-enriched biomass of a highly acidic-habitat microalga.

Table of contents

Abstract: *Coccomyxa onubensis* (*C. onubensis*) is an acidotolerant microalga isolated from the extremely acidic Tinto River (Huelva), which contains high levels of metals in solution, mainly Fe and Cu. This makes *C. onubensis* a potentially suitable candidate to cope with high levels of oxidative stress by increasing the levels of certain molecules and enzymes, which helps them elicit an adequate antioxidant biochemical response. Thus, *C. onubensis* is a promising source of bioactive compounds which exhibit *in vitro* anti-inflammatory activity, including fatty acids, (poly)phenolic compounds and carotenoids. In this study, the correlations between the antioxidant response and anti-inflammatory activity of cell extracts obtained from Fe (III)-stressed microalgal cultures were analyzed. The results suggested a direct relationship between the antioxidant capacity of the microalgal extracts and Fe (III) concentration in the culture medium. Consequently, the production of some of the target antioxidant molecules, including carotenes, xanthophylls and (poly)phenols, increased. The levels of these molecules increased the most in cell extracts obtained from microalgal cultures at 0.25 mM of Fe (III), which was correlated with a 50 % increase in the inhibition of the production of pro-inflammatory interleukin TNFα in THP-1 differentiated human macrophages. Nevertheless, Fe (III) concentration had no significant effect on the inhibition of the production of other pro-inflammatory interleukins (IL-6 and IL-1β), whereas *C. onubensis* extracts obtained from cultures exposed to varying levels of both light irradiance and Fe (III) influenced the production of these cytokines. Accordingly, it can be hypothesized that the synergistic interaction between Fe (III) concentration and light irradiance in *C. onubensis* cultures may enhance the anti-inflammatory activity of *C. onubensis* extracts, which are enriched in valuable antioxidant molecules. Overall, this study highlighted the utility of a microalgal species from a highly acidic environment as a novel, natural source of anti-inflammatory agents, based on its ability to cope with the oxidative conditions of its habitat.

Keywords: Acidotolerant microalga; Anti-inflammatory activity; Phenolics and carotenoids; Coccomyxa; Oxidative stress; Metals; pro-inflammatory interleukins.

1. Introduction

Microalgae are a valuable source of natural antioxidants that can benefit human health. The antioxidants accumulated by microalgae, including unsaturated fatty acids, terpenoids, (poly)phenolic compounds, and phytosterols, can mitigate inflammatory symptoms (Araújo et al., 2020; Gallego et al., 2022). Therefore, culture conditions that facilitate the accumulation of antioxidant molecules can be used to develop biotechnological processes to produce cell extracts with high anti-inflammatory activity (Montero-Lobato et al., 2018). For this, extremophilic microorganisms can play a key role, i.e., the ability of these microorganisms to adapt to the harsh conditions of their habitats partly depends on the expression of secondary metabolic pathways, leading to the biosynthesis of unique molecules. Among these molecules, terpenoids, such as astaxanthin and lutein, (poly)phenolic compounds (e.g. caffeic and gallic acids), polyunsaturated fatty acids, and sterols (Ruiz-Domínguez et al., 2023) are important as they have anti-inflammatory effects. Therefore, microalgal extracts that contain them are valuable for applications in human health care (Navarro et al., 2016).

C. onubensis is a highly acidic-habitat microalga (Garbayo et al., 2012), isolated from the Tinto River in the province of Huelva, Spain. This river has a highly acidic aquatic environment and contains dissolved metals, such as Fe (II and III) and Cu (II), at concentrations that are normally toxic to living forms. Despite these harsh conditions, the Tinto River has a wide variety of microorganisms (Fernández-Remolar et al., 2004). *C. onubensis* is adapted to the environment to tolerate pH values as low as 2.5 (Garbayo et al., 2012). This ability of microalgae to adapt to the acidic environment might be due to the impermeability of the plasma membrane to protons, among other reasons. This allows the cells maintaining a neutral cytoplasmic pH, also supported by a highly active ATP-synthase activity that pumps protons out of the cell. This leads to the maintenance of high proton concentrations in the extracellular medium, considerably increasing the osmotic pressure that also confers moderate halotolerance to acidotolerant microalgae (Gimmler et al., 1988; Gross, 2000). Maintaining a neutral intracellular pH in an acidic environment requires energy, which reduces the energy available for growth (Messerli et al., 2005). Low energy levels, along with the low availability of dissolved inorganic carbon in acidic water, may limit biomass productivity in large production processes. However, in an acidic environment, microalgae have developed strategies to compensate for this low inorganic carbon availability by evolving mechanisms to improve carbon uptake (Vaquero et al., 2013). This allows these extremophilic microorganisms, such as *C. onubensis*, to show moderate levels of productivity in acidic liquid cultures.

The membrane adaptability to the acidic environment might also partly explain the capability of *C. onubensis* to grow in high concentrations of Fe (III) (as high as 30 $g \cdot L^{-1}$) in its natural habitat (Fernández-Remolar et al., 2004). Fe is necessary for microalgae as it plays a key role in cellular biochemistry due to its redox properties (Gao et al., 2022). However, Fe becomes highly toxic at high concentrations due to its oxidative action through the Fenton reaction, which leads to the production of reactive oxygen species (ROS). This reaction (see reaction 6.1) consists of an oxidation process catalyzed by

transition metals, usually iron, in which highly ROS, such as the hydroxyl radical ($HO^{\bullet}$), are generated from hydrogen peroxide (H_2O_2) (Gulcin and Alwasel, 2023).

$$Fe\ (II) + H_2O_2 \longrightarrow Fe\ (III) + HO^{\bullet} + HO^{-} \qquad (6.1)$$

The generation of hydroxyl radicals increases oxidative stress due to their reaction with lipids, proteins, and nucleic acids. The reaction between ROS and membrane lipids results in the loss of membrane permeability due to the partial saturation of unsaturated fatty acids of phospholipid molecules (Halliwell, 2006). Additionally, ROS can damage DNA, triggering genetic mutations that can lead to cell death (Ávila-Román et al., 2023). Microalgae respond to oxidative stress by inducing the activity of different antioxidant systems, including an increase in the activity of enzymes such as superoxide dismutase (SOD), catalase (CAT), glutathione peroxidase (GPX), and ascorbate peroxidase (APX), and the synthesis of low-molecular-weight antioxidant compounds, mainly glutathione, carotenoids, (poly)phenolic compounds, and flavonoids (Montero-Lobato et al., 2018).

Thus, microalgae biotechnology allows us to obtain cell extracts rich in antioxidants molecules which can be used to improve human and animal health (Navarro et al., 2016). For instance, (poly)phenolic compounds and carotenoids directly interfere with the transcription of TNFα (tumor necrosis factor-α), an inflammatory cytokine commonly used in assays to evaluate anti-inflammatory activity in suitable cell lines (*in vitro*), such as THP-1 (Araújo et al., 2020; Gallego et al., 2022) (Figure 6.1). TNFα is used in anti-inflammatory activity assays of microalgal and algal extracts (Araújo et al., 2020; Ávila-Román et al., 2023). Nuclear factor kappa B (NF-κB) belongs to a family of inducible transcription factors and plays various evolutionarily conserved roles in the immune system (Gómez-Chávez et al., 2021). High levels of ROS induce the generation of oxidative stress inside cells. During exposure to oxidants, IκB (inhibitors of NF-κB) proteins bound to NF-κB are rapidly phosphorylated, leading to their ubiquitin-mediated proteasomal degradation and release from NF-κB (Linnewiel-Hermoni et al., 2014). Then, NF-κB is translocated to the nucleus where it binds to DNA sequences and activates the expression of pro-inflammatory cytokines (Gómez-Chávez et al., 2021). TNFα is, generally, the first pro-inflammatory cytokine to be synthesized; next interleukins (ILs) such IL-1β and IL-6 are released (Ávila-Román et al., 2021; Ott et al., 2007). Thus, these pro-inflammatory cytokines are crucial signaling molecules that initiate and amplify the inflammatory response, a key part of the body's immune system's defense against pathogens and tissue damage (Bhol et al., 2024).

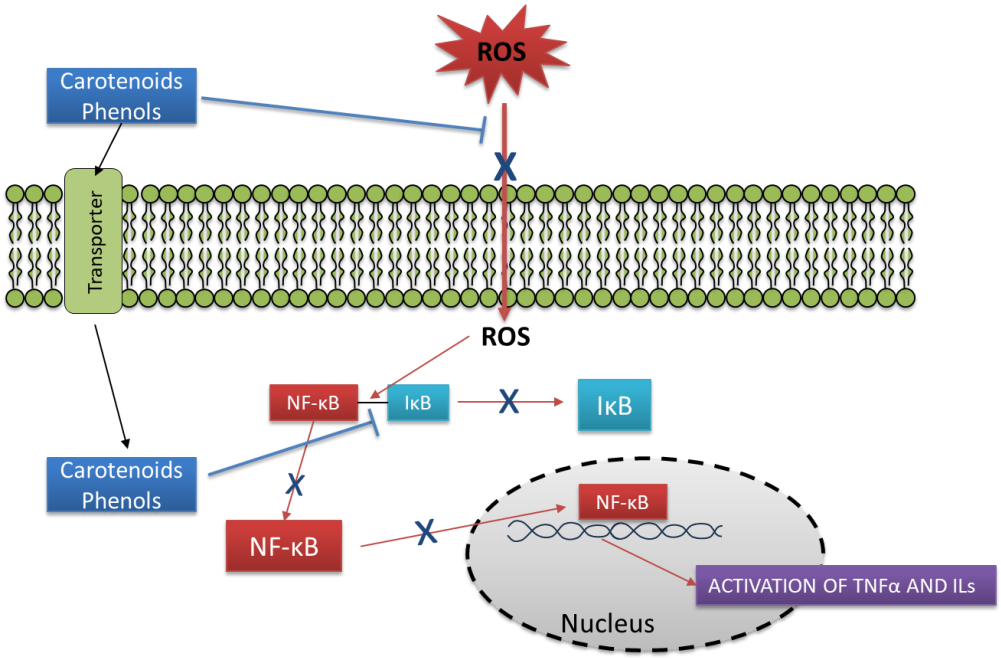

Figure 6.1. A schematic representation of the mechanism underlying the anti-inflammatory effect of (poly)phenolic compounds and carotenoids through interaction with the transcription of TNFα (tumor necrosis factor-α); ROS: reactive oxygen species, NF-κB: transcription factor of TNFα, ILs: interleukins and IκB: inhibitor of NF-κB.

To summarize, *C. onubensis* can adapt to its environment (acidic pH and high concentrations of heavy metals) by activating metabolic pathways that promote the accumulation of antioxidant compounds, which have biotechnological applications (Montero-Lobato et al., 2018; Navarro et al., 2016). This ability of *C. onubensis* to adapt makes it a suitable model system for this study. In this study, we found a relationship between the antioxidant capacity of *C. onubensis* cells (that modulates oxidative stress levels), triggered by Fe (III), and the anti-inflammatory capacity of cell extracts rich in carotenoids and (poly)phenolic compounds.

2. Materials and methods

2.1. Microalgal strain and culture conditions

The organism used for this work was the microalga *Coccomyxa onubensis* ACCV1 (SAG 2510), an acidotolerant and halotolerant microalga isolated from the acidic waters of the Tinto River (Huelva) in the sampling area at latitude 37.5851153° and longitude −6.550754°, by the Microalgae Biotechnology Unit (BITAL), of the Department of Chemistry "Professor Jose Carlos Vílchez Martín," from the Faculty of Experimental Sciences and CIQSO of the University of Huelva, Spain (Fuentes et al., 2016).

C. onubensis was grown in an optimized liquid culture medium, K9. The constituents of K9 (per liter) were as follows: 3.95 g K_2SO_4, 0.1 g KCl, 0.5 g K_2HPO_4, 0.41 g $MgCl_2$, 2.29 g KNO_3, 0.01 g $CaCl_2$, and 5 mL of Hutner traces, which were prepared as previously described (Garbayo et al., 2012), containing a Fe (II) concentration of 17.98 µM. Fe is more bioavailable at low pH than at neutral or basic pH, Fe (III) was used in this study because it is more soluble than Fe (II) (Johnson et al., 2012). *C. onubensis* cultures were prepared at an initial concentration of, approximately, 0.2 $g \cdot L^{-1}$, from a mother culture in the middle of the linear growth phase, the pH was adjusted to 2.5 and the cultures were subjected to different Fe (III) concentrations, added in the form of $FeCl_3 \cdot 6H_2O$ (VWR, Belgium) from 0 mM (control culture) to 2 mM. The cultures were established in a culture room at 25 °C ± 2. Light was supplied by white light fluorescent tubes, reaching the cultures at a constant light intensity of 150 µmol (photon)$\cdot m^{-2} \cdot s^{-1}$ for 24 h, and the cultures were bubbled with air enriched with 2.5% (v/v) CO_2. Similarly, the synergistic effect of Fe (III) concentration and different light irradiances was studied by combining three light irradiance levels (30, 150 and 400 µmol of photon$\cdot m^{-2} \cdot s^{-1}$) under low (0 mM) and moderate (0.25 mM) Fe (III) concentration.

2.2. Growth and photosynthetic viability determination

Growth was followed by measuring optical density (OD) of the cultures at 750 nm in a Cary 60 UV–Vis spectrophotometer (Agilent Technologies, USA) equipped with temperature control system adjusted to 25 °C. The OD_{750} data expressed in absorption unit (UA) provided the information of culture turbidity, which is proportional to the amount of biomass present in the culture (Shuler and Kargi, 2005). In addition, dry weight of the biomass contained in 2 mL of culture medium was analyzed.

Photosynthetic viability was determined based on the measurement of chlorophyll fluorescence, the maximum quantum yield (F_V/F_M) of Photosystem II (PSII) according to published methodology (Maxwell and Johnson, 2000). Quantum yield (Qy) was measured by subjecting cultured samples of *C. onubensis* to darkness for 15 min and then placing them in the measurement chamber of the AquaPEN AP-C 100 portable amplitude-modulated pulse fluorimeter (Photon Systems Instruments, Drasov, Czech Republic). F_V represents the variable fluorescence and is calculated as $F_V = F_M - F_0$, being F_0 the minimum level of fluorescence observed after exposing cells to a non-actinic beam and acclimating them in the dark, while F_M represents the maximum fluorescence observed in cells after exposing them to a brief but saturating pulse of actinic light.

2.3. Transmission electron microscopy

For transmission electron microscopical observations, the method described by Nishikawa et al. (2006) was performed. The microalgal cells were collected by centrifugation (1,957×g, 1 min) from each culture (cultures treated with different Fe (III) concentrations, and control culture). The microalgal cells were fixed with 1 % glutaraldehyde in 0.1 M sodium cacodylate buffer (pH 7.4) for 2 h at 4 °C. The cells were then washed three times for 5 min using the same buffer. The samples were postfixed with 1 % osmium tetroxide in 0.2 M cacodylate buffer at 4 °C for 1 h. Samples were washed with the same buffer, dehydrated in a graded ethanol series, and embedded in Epon 812 (Electron Microscopy Science, USA). Ultrathin sections of 80–90 nm obtained by an ultramicrotome (Leica, Germany) and placed on copper grids were stained with aqueous 1% (w/v) uranyl acetate and lead citrate. Transmission electron micrographs were observed with a JEM 1011 (Jeol Ltd., Japan) electron microscope using an accelerating voltage of 80 kV. Several photographs of entire cells and of local detailed structures were taken at random, analyzed, and compared to investigate the effect of different concentrations of Fe (III) on different subcellular structures.

2.4. Chlorophyll and carotenoid determination

Chlorophyll and carotenoid content were determined as described by Robles et al. (2023). Culture samples, containing 1 or 2 mL, were centrifuged at 3 *g* for 5 min, methanol was added to the pellet, and the mixture was placed in an ultrasound bath (60 °C, 5 min) to weaken the microalgal cell wall. After another centrifugation step, the supernatant was collected and analyzed by UV/Visible spectrophotometry. Modified Arnon's equations were used to calculate chlorophyll and carotenoid concentrations in the extracts. The extracts obtained were used to analyze the antioxidant capacity of the microalga and the determination of (poly)phenol and flavonoids compounds, see section 2.5 to 2.6. In addition, methanolic extracts were evaporated using a N_2 stream and resuspended in DMSO to 10 $\mu g \cdot mL^{-1}$ of extract to analyze the anti-inflammatory activity exerted of *C. onubensis* extracts on THP-1 Mac cells, see section 2.7.

For specific carotenoid analysis and quantification, separation was performed by liquid chromatography (HPLC; Beckman System gold) using an RP-18 column with a flow rate of 1 mL/min and injection extract volume of 40 µL. The applied gradient was the following (solvent A; ethyl acetate and solvent B; acetonitrile/water, 9:1 v/v): 0–16 min, 0–60 % solvent A; 16–30 min, 60 % A; 30–35 min, 100 % A. For quantification, pigment standards supplied by DHI-Water and Environment (Denmark) were injected. Quantification of the selected pigments was based on comparison of peak areas obtained from methanolic extracts of *C. onubensis* with the areas obtained from the injected standards. Xanthophylls pools were determined as the summatory between lutein and neoxanthin concentration and, carotene pool corresponds to the sum between α- and β-carotene.

2.5. Antioxidant capacity

Antioxidant capacity of the methanolic extracts of microalga was determined by the modified version of the DPPH (2,2-diphenyl-1-picryl-hydrazyl-hydrate) free radical method described by Brand-Williams et al. (1995). The antioxidant capacity was determined by the decrease in absorbance at 515 nm of a methanolic solution of DPPH in the presence of the different methanolic samples of the microalga. A concentrated solution of DPPH (Sigma aldrich, Germany) in methanol of approximately 0.4 $g \cdot L^{-1}$ was prepared and diluted with methanol to obtain an absorbance around 0.8. Next, 950 µL of the diluted DPPH solution was made to react with 50 µL of the methanolic sample. The absorbance at 515 nm at time 0 was then measured in a UV-vis spectrophotometer model Evolution 201 (Thermo Fisher Scientific, USA) in a glass cuvette, using methanol as a blank.

Subsequently, the samples were allowed to stand for 30 minutes at room temperature and the absorbance of the sample at 515 nm was measured after that time. Trolox (Fisher Scientific, USA) was used as an external standard. The antioxidant capacity was determined through the difference in absorbance at time 0 and 30 min and was expressed as µmol eq-Trolox$\cdot g^{-1}$ biomass ($y = -0.6536 \cdot x + 1.1429$, $R^2 = 0.9949$).

2.6. (Poly)phenols and flavonoids determination

Total polyphenols were determined using the procedure described by Georgé et al. (2005). According to this, phenolic compounds were oxidized by the Folin-Ciocolteau reagent (Panreac, Spain), resulting in a blue color complex formation. The reaction was carried out in an alkaline medium; for this, sodium carbonate was added to the samples, and the absorbance was measured at 725 nm by UV-vis spectrophotometry model Evolution 201 (Thermo Fisher Scientific, USA). Total content of polyphenols was obtained using a calibration line from a standard solution of gallic acid 1-hydrate (Panreac, Spain) and was expressed as mg-eq· gallic acid$\cdot L^{-1}$ ($y = 0.0996 \cdot x - 0.0016$, $R^2 = 0.9999$).

Flavonoid compounds were determined by a spectrophotometric method described by (Liu et al., 2002). For this, the following reagents were used: $NaNO_2$, $AlCl_3 \cdot 6H_2O$ and NaOH. As an external standard, a 1 $g \cdot L^{-1}$ catechin stock, (+)-catechin hydrate (Sigma aldrich, Germany) in MilliQ water was used. The absorbance value was measured at 510 nm using UV-vis spectrophotometry model Evolution 201 (Thermo Fisher Scientific, USA). Total content of flavonoids was calculated by extrapolating the values obtained in the calibration line ($y = 0.0029 \cdot x - 0.0515$, $R^2 = 0.9985$).

2.7. Anti-inflammatory activity in THP-1 differentiated macrophages (THP-1 Mac)

THP-1 cell line, kindly given by Dr. Nuno Santos (CBME, University of Algarve, Faro), was cultured according to ATCC instructions in RPMI Growth Medium (RPMI 1640 with L-Glutamine (Gibco, Waltham, MA, USA), 10 % heat-inactivated Fetal Bovine Serum (FBS, Biowest, Nuaillé, France), 1 % Pen-Strep (P/S, Gibco), at 37 °C in a humidified atmosphere containing 5 % CO_2. THP-1 macrophage differentiation (THP-

1 Mac) was achieved by culturing cells in 25 ng·mL^{-1} of phorbol 12-myristate 13-acetate (PMA) (Sigma-Aldrich, St. Louis, MO, USA) in complete RPMI for 48h.

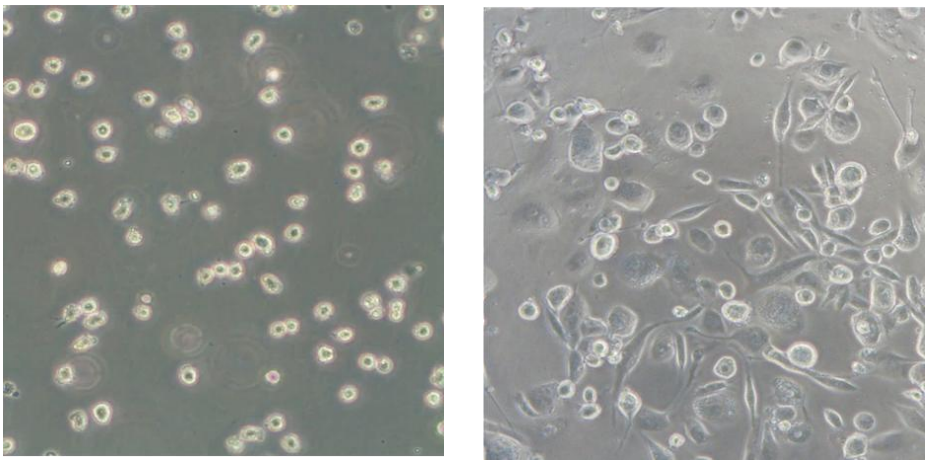

(**a**) (**b**)

Figure 6.2. Human acute leukemia monocytic cell line, THP-1 (**a**) and 80-90 % transformation into macrophage (**b**). Photographs, gently provided by Javier Ávila (Farmolap, University of Seville) have been taken with an inverted microscope with a 10X objective.

THP-1 Mac cells viability exposed during 48h to 10 µg·mL^{-1} of *C. onubensis* extracts from Fe (III)-added cultures, was determined using the CellTiter 96 cell proliferation assay (Promega, Madison, WI, USA), following manufacturer's instructions. The anti-inflammatory potential of *C. onubensis* extracts from Fe (III)-added cultures, was evaluated in 1x10^6 THP1-Mac cells, plated in 96 well plates with 200 µL media, by pre-treatment of the cells with 10 µg·mL^{-1} of each extract during 24 h, followed by inflammation stimulation with LPS (100 ng·mL^{-1}) (Sigma-Aldrich) for additional 24 h. THP-1 Mac cells without any treatment were used as non-inflamed control cells, and THP-1 Mac cells only exposed to LPS were used as positive inflammatory control. Cell culture media were collected for quantification of TNFα, IL-6 and IL-1β levels by ELISA (R&D Systems, Minneapolis, MN, USA) according to manufacturer's recommendations. The % of TNFα inhibition was calculated using the following formula: ([TNFα in LPS condition] – [TNFα in testing extracts + LPS condition]/ [TNFα in LPS condition]) x 100. The same expression was used to calculate the percentage (%) of IL-6 and IL-1β inhibition.

2.8. Statistics

Unless otherwise stated, all data are presented as the mean of three replicates and the standard deviations are shown in the corresponding figures and tables. The data from the different treatments were evaluated by constructing univariate statistical models and performing the analysis of variance (ANOVA) (confidence of 95 % was considered for determining statistical significance). Tukey's test was also applied to identify significant differences between all the treatments studied, without reference to a specific control. Detailed results are presented in Tables S6.1-S6.10 of Supplementary Material section. All analysis was performed using the Minitab 22 software.

3. Results

As described in the Introduction section, an increase in the antioxidant capacity of microalgal extracts could result in a higher anti-inflammatory activity. This would enable planning strategies to produce microalgal biomass with higher antioxidant content and, therefore, anti-inflammatory activity by inducing oxidative stress in the microalgal cells. Thus, we studied the anti-inflammatory activity of *C. onubensis* extracts as a function of the concentration of Fe (III) added to the cultures. We also evaluated the correlations between the anti-inflammatory activity and the antioxidant capacity of the extracts. Similarly, the synergistic effect of Fe (III) concentration and different light irradiances was studied by combining three light irradiance levels (30, 150 and 400 μmol of photon·m^{-2}·s^{-1}) under low (0 mM) and moderate (0.25 mM) Fe (III) concentration. The results were expected to reveal the contribution of the antioxidant compounds produced by the highly acidic-habitat microalga *C. onubensis* to the reduction of lipopolysaccharide (LPS)-induced inflammatory response in THP-1 differentiated macrophages (THP-1 Mac) human cells. The anti-inflammatory effects of *C. onubensis* extracts were analyzed and discussed as a function of key target antioxidant molecules that accumulated in the microalgal cells and were present in the extracts tested (carotenes, xanthophylls, and total (poly)phenolic compounds).

3.1. Effect of Fe (III) concentration on the growth and viability

C. onubensis is a highly acidic-habitat microalga (Garbayo et al., 2012), isolated from the Tinto River in the province of Huelva, Spain. An acidic environment containing Fe (III) concentrations as high as 30 g·L^{-1} (Fernández-Remolar et al., 2004). First, the growth and photosynthetic viability of the microalga *C. onubensis* were evaluated as a function of Fe (III) concentration, to determine the range of sublethal concentrations of Fe (III) (Figure 6.3).

A time-dependent increase in the microalgal cell density (measured as OD at 750 nm) was found to be significative (Table S6.1 of Supplementary Material) in Fe (III)-added cultures with respect to control cells (Figure 6.3a). The maximum cell density was reached in the culture grown at the highest Fe (III) concentration tested (2 mM). The photosynthetic efficiency of photosystem II (quantum yield) in the microalgal cultures supplemented with Fe (III) is shown in Figure 6.3b. This data provided information on the efficiency of the use of light by microalgal cells. A significative increase (Table S6.2 of Supplementary Material) in quantum yield was recorded under increased Fe (III) concentrations; the highest quantum yield was recorded on day 3 of cultivation, which was approximately 3 % higher than the obtained in control culture cells.

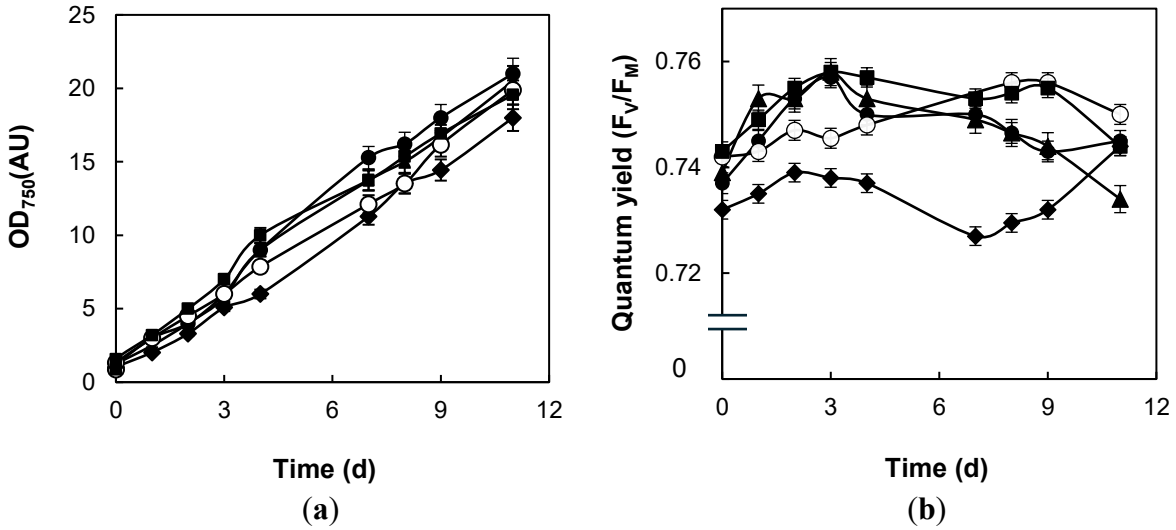

Figure 6.3. Time-dependent evolution of **(a)** growth, measured as OD_{750}, and (**b**) the maximum photosynthetic efficiency of photosystem II (quantum yield, F_V/F_M) as a function of the concentration of Fe (III): 0 (-◆-), 0.25 (-●-), 0.5 (-▲-), 1 (-○-), and 2 (-■-) mM in cultures of the acidotolerant microalga *C. onubensis*. Data are the mean ±SD of three replicates.

At the concentrations tested, Fe (III) induced changes in the growth and photosynthetic viability of the microalga. This might have affected the ultrastructure of the microalga, including changes in the number and appearance of lipid accumulating structures. These changes may also influence the anti-inflammatory activity exerted by the microalgal extracts on THP-1 Mac cells, as carotenoids and unsaturated fatty acids are antioxidant lipids that accumulate in microalgal cells. Such ultrastructural modifications in cells were analyzed through transmission electron microscopy (TEM) using cell samples obtained from cultures supplemented with Fe (III) (Figure 6.4). The control culture (Figure 6.4a) showed dark granules, which represent the accumulation or secretion of molecules that are typical of cellular activity in metabolically active cells, unlike the grayish and whitish granules that appear in stressed cells. The figure shows a unicellular microalga with a well-defined, regular, and spherical membrane, stable cytoplasm, and a typical large thylakoid-dense chloroplast that occupies approximately half of the total cell volume.

However, as Fe (III) concentration increased, the cell wall became thicker, which increased the rigidity of the cell membrane. Also, the increase in Fe (III) concentration led to the disorganization of cellular structures, as revealed by the widely separated (Figure 6.4d) and unstructured thylakoid membranes (Figure 6.4e). Additionally, black spots appeared in stressed cells and between thylakoid membranes, as shown in Figure 6.4d. We also observed mucilage in Figure 6.4e, which appeared as a viscous membrane-like structure around the algal membrane. Two cells undergoing cell division exhibiting the phenotype of cells under stress are illustrated in Figure 6.4e.

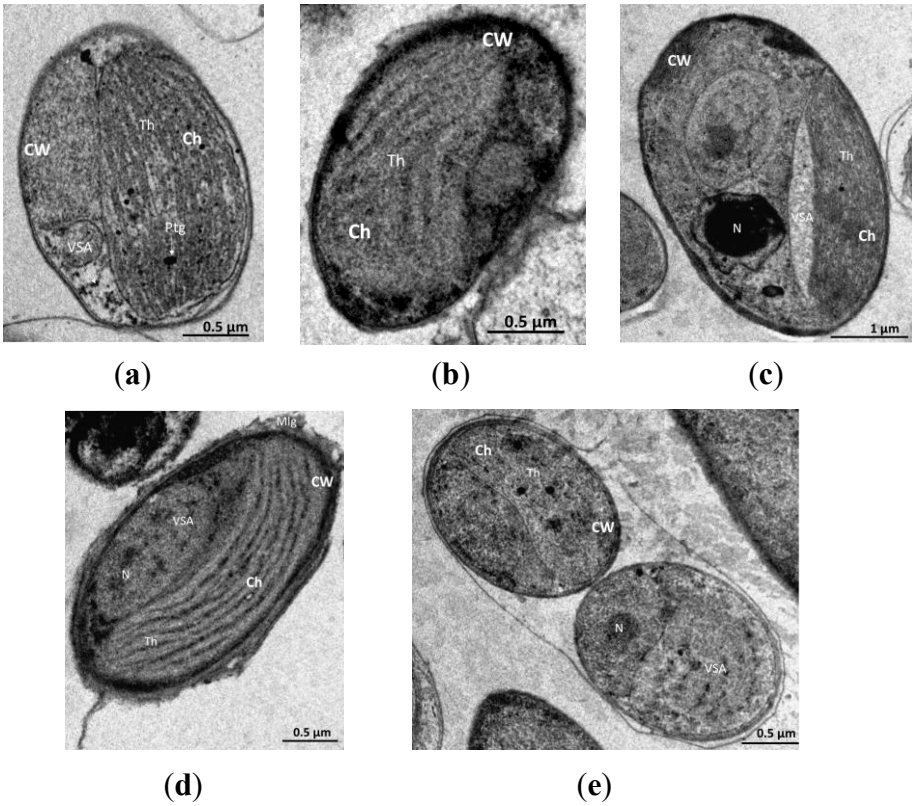

Figure 6.4. Effect of Fe (III) concentration on the ultrastructure of the microalga *C. onubensis* through transmission electron microscopy (TEM) images at day 4 of cultivation. (**a**) Control culture without Fe (III) supplement; cultures supplied with Fe (III) at concentrations of (**b**) 0.25 mM, (**c**) 0.5 mM, (**d**) 1 mM, and (**e**) 2 mM. Abbreviations: Ch: chloroplasts, Th: thylakoids, CW: cell wall, VSA: vesicular activity, N: nucleus, and Mlg: mucilage.

The results showed that Fe (III) was involved in the generation of oxidative stress in cells. This led to an increase in the antioxidant response of the microalga. Thus, an increase in the accumulation of antioxidant molecules, previously shown to modulate inflammatory reactions in cell lines (*in vitro*) (Araújo et al., 2020), was also expected. Based on this speculation, we next assessed the non-enzymatic antioxidant responses of *C. onubensis* to cope with the oxidative stress generated in cultures to which Fe (III) was added.

3.2. Non-enzymatic antioxidant response and anti-inflammatory activity

The antioxidant capacity of the microalgal extracts was analyzed and correlated with their anti-inflammatory activity as a function of Fe (III) concentration. The anti-inflammatory activity was evaluated in THP-1 Mac cells and expressed as the percentage of TNFα inhibition, which reflected the capacity of each extract to decrease the production of TNFα in LPS-treated THP-1 Mac cells (Figure 6.5). The cytotoxic effects of *C. onubensis* methanolic extracts obtained from Fe (III)-added cultures were tested; none of the tested extracts altered the viability of THP-1 Mac cells (Figure S6.1 of Supplementary Material).

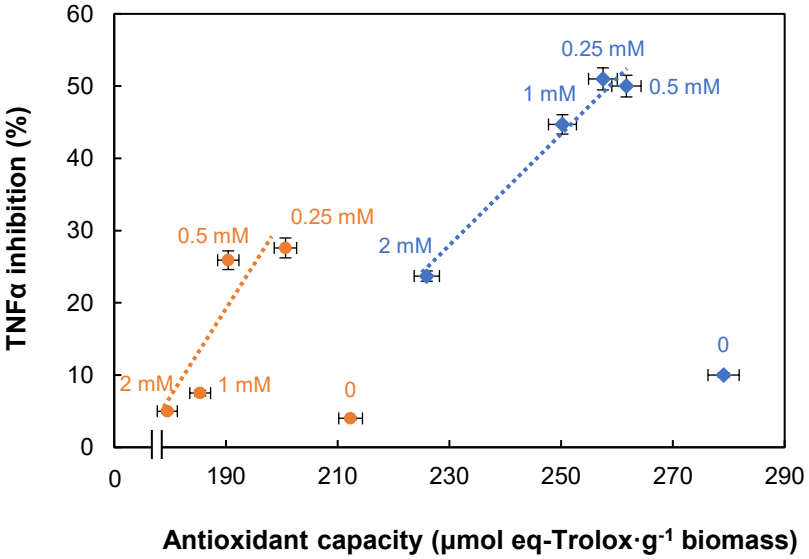

Figure 6.5. Antioxidant capacity and anti-inflammatory activity exhibited by *C. onubensis* culture extracts as a function of Fe (III) concentration in the culture medium, after 4 days (blue rhombus) and 11 days (orange circle) of exposure to Fe (III). Antioxidant capacity was measured as the capacity of the extracts to react with the DPPH radical. Anti-inflammatory activity was measured as the inhibition percentage of TNFα released by THP-1 MoM cells exposed to *C. onubensis* extracts. Further details are presented in the Materials and Methods section. Data are the mean ±SD of three replicates.

In the early growth stage (day 4; Figure 6.5), the antioxidant capacity unexpectedly showed a significant decrease as Fe (III) concentration increased (Table S6.3 of Supplementary Material); the antioxidant capacity was the lowest for the 2 mM Fe (III) culture. Similarly, for the late cultivation stages (day 11), the antioxidant capacity of Fe (III)-added cultures was slightly lower than that of the control culture, irrespective of the concentration of Fe (III) present. Contrary to the pattern recorded in antioxidant capacity, we found a significant increase in anti-inflammatory activity (Table S6.4 of Supplementary Material), as determined by higher inhibition in the production of TNFα, in Fe (III)-added culture extracts compared to the control culture extracts and irrespective of the growth stage. The strongest inhibition of TNFα of, about, 50 % was found in the early growth cultivation period (day 4) and at the lowest Fe (III) concentration added (0.25 and 0.5 mM), while control culture extracts on same cultivation period exerted 10 % inhibition of TNFα.

The variation in antioxidant capacity and anti-inflammatory activity as a function of Fe (III) concentration showed that the target antioxidant molecules of *C. onubensis* cultures were involved in ROS neutralization reactions, this is further analyzed in Figure 6.6. The antioxidant capacity (Figure 6.6a) decreased irrespective of the concentration of the target antioxidant molecules. As represented in Figure 6.5, the highest antioxidant capacity was found in cultures that were not exposed to Fe (III). Nevertheless, a different pattern was found for anti-inflammatory activity (Figure 6.6b), in which the highest values corresponded to the highest concentrations of the antioxidant molecules.

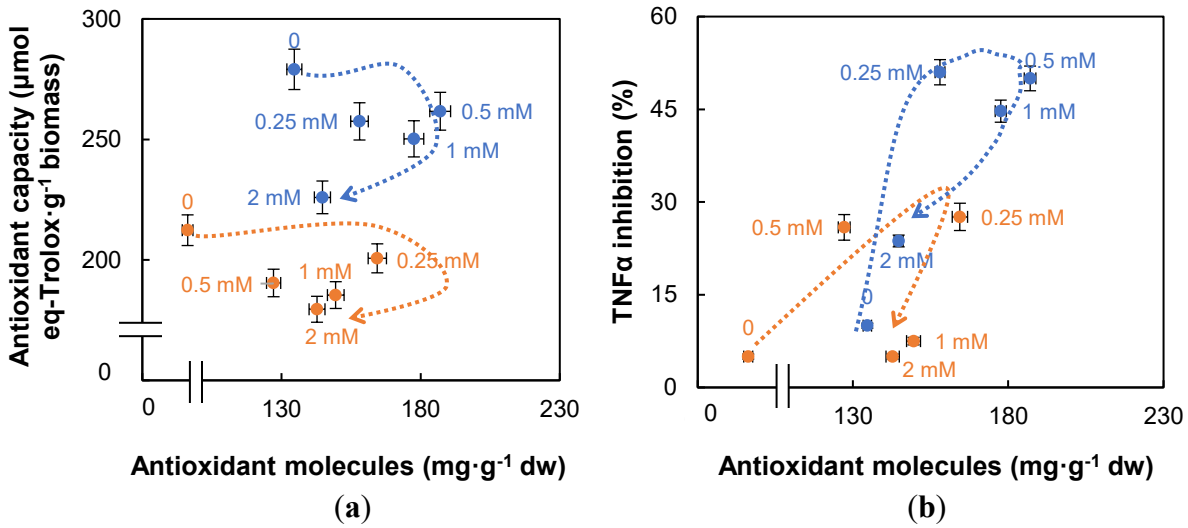

Figure 6.6. Analysis of the correlation between target antioxidant molecules (carotenes, xanthophylls, (poly)phenols, and flavonoids) and (**a**) the antioxidant capacity or (**b**) the anti-inflammatory activity in *C. onubensis* extracts, as a function of Fe (III) concentration in the microalga after 4 days (blue rhombus) and 11 days (orange circle) of exposure to Fe (III). Data are the mean ±SD of three replicates.

The overall contribution of the target antioxidant molecules to cope with Fe (III)-induced stress was evaluated by plotting the concentration data of each target molecule in the extract versus the total antioxidant capacity of the extracts (Figure 6.7a, 6.7b, 6.8a, and 6.8b). Similar graphs were plotted to assess the contribution of each target molecule to the anti-inflammatory effects of *C. onubensis* cell extracts on the THP-1 Mac cells (Figure 6.7c, 6.7d, 6.8c, and 6.8d). A similar pattern was obtained by plotting either (poly)phenols, carotenes, or xanthophylls against the total antioxidant capacity and anti-inflammatory activity of the extracts; i.e., only under (i) short-term exposure (day 4) at low Fe (III) levels or (ii) long-term exposure (day 11) at high Fe (III) levels, the intracellular levels of these antioxidant molecules presented similar or significantly higher values than in control cultures (Table S6.5 to S6.8 of Supplementary Material). This pattern was similar to that recorded for the antioxidant capacity of the microalga, i.e., an increase in Fe (III) concentration and/or exposure time significantly decreased the content of carotenes, xanthophylls, and polyphenols thus resulting in a decrease in the antioxidant capacity of the microalgal extracts (Figure 6.7a, 6.7b and 6.8a).

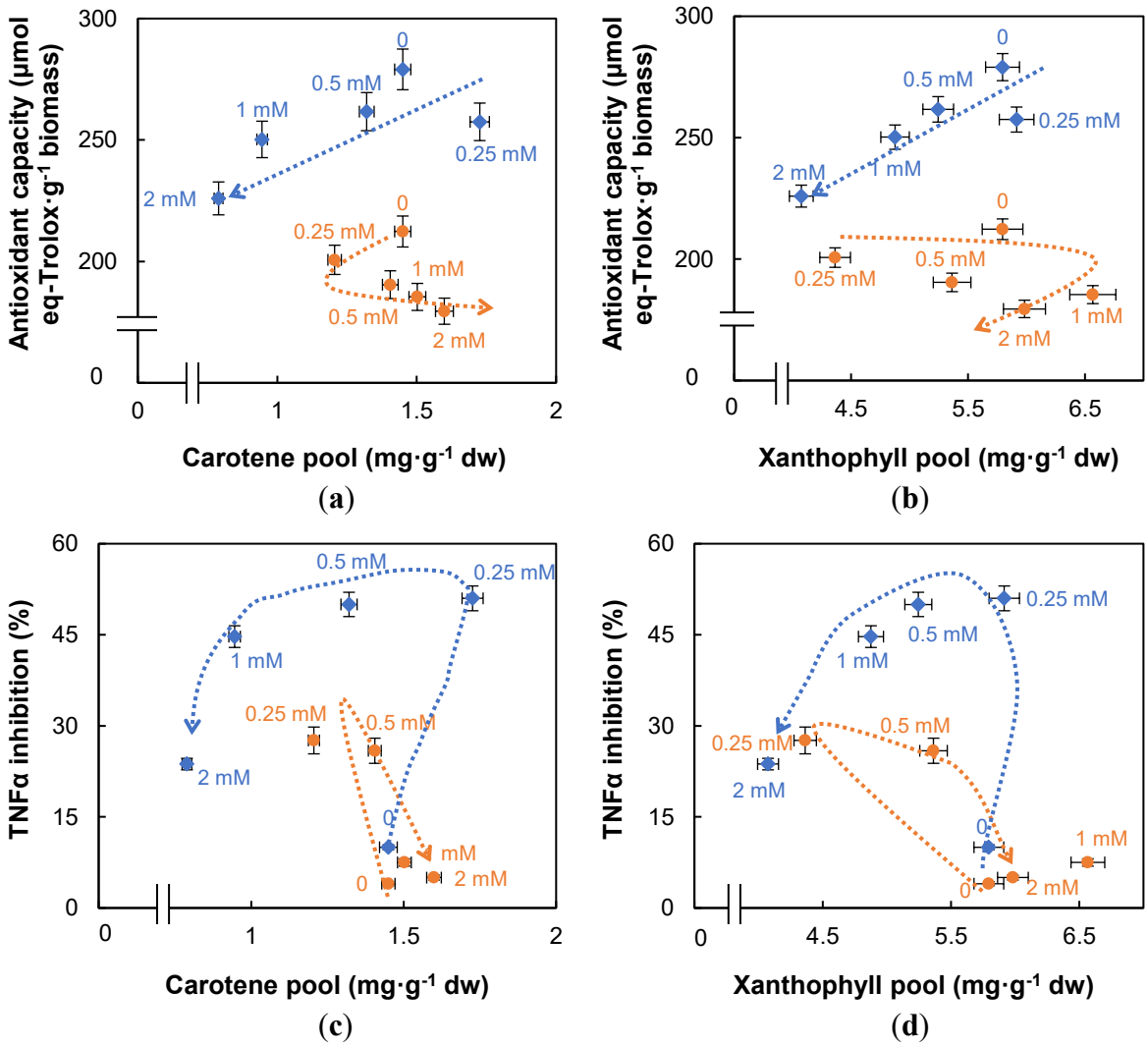

Figure 6.7. Analysis of the correlations of carotene (**a**, **c**) and xanthophyll (**b**, **d**) with the antioxidant capacity (**a**, **b**) and anti-inflammatory activity (**c**, **d**) as a function of Fe (III) concentration in *C. onubensis* after 4 days (blue rhombus) and 11 days (orange circle) of exposure to Fe (III). Data are the mean ±SD of three replicates.

We found a different pattern for the anti-inflammatory effect on THP-1 Mac cells (Figure 6.7c and 6.7d). In this case, the highest anti-inflammatory activities (blue line) were recorded in the microalgal cultures that were exposed to low Fe (III) levels (0.25 and 0.5 mM) for a short duration. However, the differences in the intracellular content of carotenes, xanthophylls, and (poly)phenols between the above-mentioned conditions and the control culture were minimal.

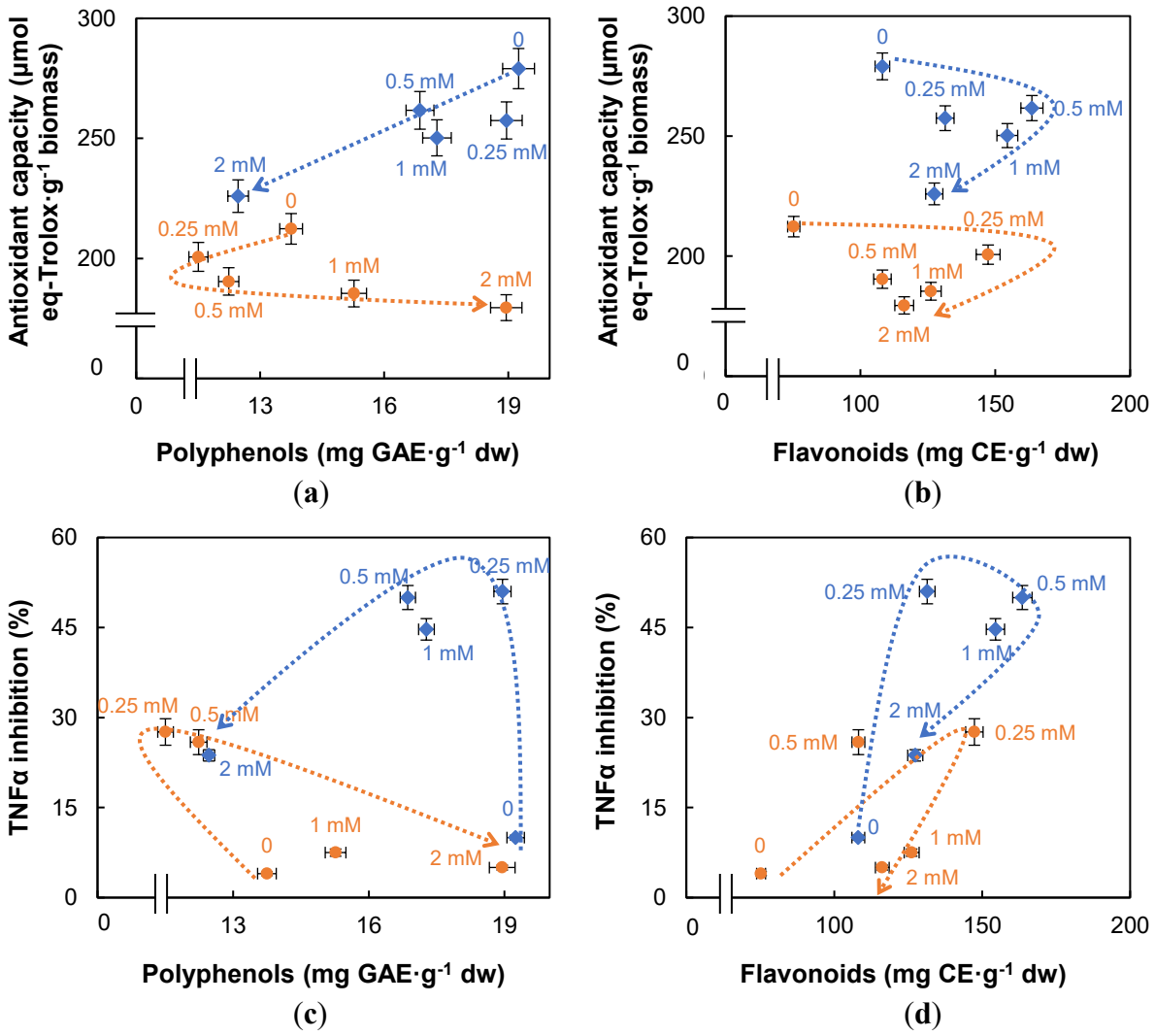

Figure 6.8. Analysis of the correlations of (poly)phenols (**a**, **c**) and flavonoids (**b**, **d**) with the antioxidant capacity (**a**, **b**) and anti-inflammatory activity (**c**, **d**) as a function of Fe (III) concentration in *C. onubensis* after 4 days (blue rhombus) and 11 days (orange circle) of exposure to Fe (III).

In contrast, the flavonoid content (Figure 6.8b) increased significantly in *C. onubensis* cells as Fe (III) concentration increased (up to 0.5–1 mM) (Table S6.9 of Supplementary Material); however, the antioxidant capacity in extracts of Fe (III)-added cultures was lower than in control culture extracts. The anti-inflammatory activity was also represented against the flavonoid content (Figure 6.8d), i.e., the highest concentration of flavonoids was found in cultures grown under low Fe (III) concentrations in the early growth stage. Under these conditions, *C. onubensis* extracts also showed the highest anti-inflammatory activity, which suggested that the flavonoids of *C. onubensis* play a more important role in inhibiting inflammation, compared to the contribution of carotenoids and phenolic compounds.

The production of other pro-inflammatory interleukins (IL-6 and IL-1β) was also evaluated as a function of Fe (III) concentration. Additionally, the synergistic effect of varying Fe (III) concentration and light irradiance levels was also investigated (Figure 6.9).

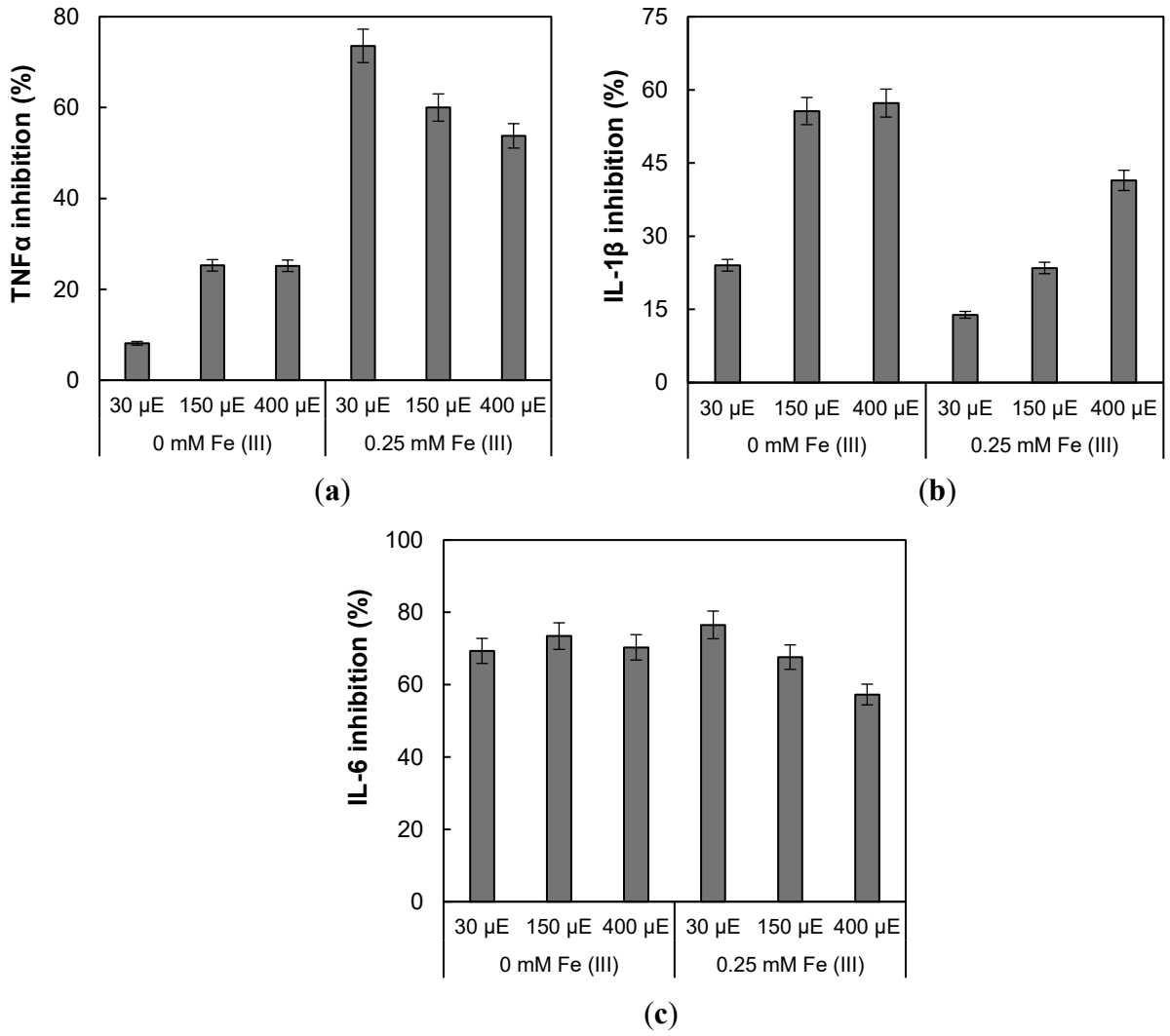

Figure 6.9. Effect of different Fe (III) and light irradiance levels on the anti-inflammatory capacity of *C. onubensis* extracts by measuring the inhibition in the production of TNFα (**a**), IL-1β (**b**) and IL-6 (**c**) in THP-1 stressed cells treated with *C. onubensis* extracts. Procedure details in Materials and Methods section.

C. onubensis cell extracts from cultures with different Fe (III) concentrations showed no significant differences in the inhibition of the production of IL-6 and IL-1β in THP-1 stressed cells. However, as also shown in Figure 6.5, *C. onubensis* extracts from cultures grown under 0.25 mM Fe (III) concentration resulted in a higher inhibition of TNFα production. In contrast, different levels of light irradiance influenced the production of these pro-inflammatory interleukins. No significant differences were found in IL-6 inhibition when combining different light irradiance levels under no-addition of Fe (Table S6.10 of Supplementary Material), whereas under higher Fe (III) levels a slight increasing trend in the inhibition of IL-6 was observed as light irradiance decreases. Nevertheless, IL-6 inhibition ranged from 60 to 75 % while the greatest changes were obtained when analyzing IL-1β inhibition varying from 13 to 60 %. That is, increased light irradiance led to greater inhibition of IL-1β irrespective of the Fe (III) concentration of *C. onubensis*. The highest inhibition was found under no-addition of

Fe and light irradiance equal or higher than 150 μmol photon·m^{-2}·s^{-1} of, approximately, 60 % of inhibition.

The results obtained suggest that Fe (III) and light irradiance in cultures of *C. onubensis* could be adjusted to increase the potential of the microalgal extracts to inhibit the production of pro-inflammatory interleukins: TNFα, IL-6 and IL-1β, thus enhancing their anti-inflammatory capacity. Nevertheless, the next section will focus on a more in-depth investigation of the anti-inflammatory activity of Fe (III)-added culture and its relationship with the antioxidant capacity and antioxidant molecules of the extracts, aiming at analyzing the antioxidant molecules that could have a greater effect on the increasing levels of anti-inflammatory activity obtained in the microalgal extracts.

4. Discussion

4.1. Effect of Fe (III) concentration on the growth and viability

The results suggested that Fe (III) concentration of up to 2 mM can slightly increase the growth of *C. onubensis* (Figure 6.3a). Photosynthetic efficiency is a relevant parameter for studying the toxic effects of Fe (III) on microalgae (Lysenko et al., 2020). Photosynthetic efficiency was determined by evaluating the quantum yield (Qy), which provides information on the efficiency of the photochemical events in photosystem II (PSII). The Qy values recorded were within 0.6 – 0.7 (Figure 6.3b), which is typical for healthy cells (Maxwell and Johnson, 2000). This finding indicated that the Fe (III) concentration range selected for this study was below the lethal concentration range for the microalga. Additionally, the Fe (III) concentrations selected increased the photosynthetic viability of *C. onubensis*. This finding agreed with the notion that Fe plays a key role in the cellular biochemistry of microalgae due to its redox properties and its participation in fundamental processes, such as photosynthesis, respiration, nitrogen fixation, and DNA synthesis (Gao et al., 2022). Our results indicate that modulating Fe (III) levels in the culture medium can yield incubation conditions that are optimum for the growth and photosynthetic viability of *C. onubensis*, as also demonstrated in Chapters 2 and 5.

Changes in the growth and photosynthetic viability of *C. onubensis* due to an increase in Fe (III) concentration can affect their ultrastructure at the cellular level, including modification of the number and appearance of lipid accumulating structures. Cell ultrastructure photographs (Figure 6.4) showed that the membrane fluidity of Fe (III)-exposed cells decreased, as determined by an increase in the thickness of the cell wall (Figure 6.4b-e). This might be a protective mechanism to prevent the entry of Fe (III) in the cell, thus minimizing oxidative stress (Ejaz et al., 2023). An increase in vesicular activity due to an increase in Fe (III) concentration indicated the accumulation of molecules inside the cells. Vesicular activity is not only related to the abundance of vesicles but also to the dilated cisternae of the smooth endoplasmic reticulum, which accumulates compounds synthesized *de novo* (Wan and Zhang, 2012). The smooth endoplasmic reticulum does not have associated ribosomes, and it is involved in key cell functions, such as lipid synthesis and detoxification (Miller and Zachary, 2017), which might include the toxic effects of Fe (III). Some studies have reported the presence of small black globules close to thylakoids in chloroplasts from plants grown in the presence of different stressors (Giacomelli et al., 2006). In this study, black spots occurred between the chloroplasts of Fe (III)-stressed cells, which might be related to the accumulation of lipidic compounds. Some researchers have found tocopherols and other lipid isoprenoid-related metabolites in the plastids of stressed cells (Laizet et al., 2004).

The ultrastructure of cells from cultures exposed to the highest Fe (III) concentration tested showed a more intense vesicular activity (Figure 6.4d-e). Additionally, nucleolar activity was found in the nucleus, which implied that the cells synthesized molecules that protected these cells against the originated stress (Miller and Zachary, 2017; Wan

and Zhang, 2012). The appearance of mucilage in stressed cells indicates that the cells are either about to divide or are under stress (Holzinger and Pichrtová, 2016). Related to the latter, Figure 6.4e, shows two cells undergoing cell division that exhibit the phenotype of a stressed cell. Consequently, analysis of the microalgal cell ultrastructure in Fe (III)-exposed cultures showed that low-intensity oxidative stress might promote cell division under the tested conditions; this finding was also confirmed by an increase in the optical density of Fe (III)-stressed cultures (Figure 6.3).

4.2. Non-enzymatic antioxidant response and anti-inflammatory activity

Although Fe plays a key role in living beings, it can be highly toxic at high concentrations as it can undergo redox reactions with various molecules in the cell and can also produce reactive oxygen species (ROS) through the Fenton reaction. Thus, adding Fe (III) can directly lead to oxidative stress, which can activate the response of the microalgal antioxidant system to balance ROS production. However, the results showed a decrease in the level of antioxidant capacity of Fe (III)-exposed microalgal cultures, which was inversely correlated with the anti-inflammatory effects of the microalgal extracts in THP-1 Mac cells (Figure 6.5).

The anti-inflammatory effects exerted by control culture cell extracts of the highly acidic-habitat microalga *C. onubensis* on THP-1 Mac cells were not noticeable, with a maximum value of 10 % TNFα inhibition, which was similar to the values obtained for other microalgal species tested under standard conditions, despite the scarcity of studies on this topic (Gallego et al., 2022). However, cell extracts from *C. onubensis* cultures exposed to Fe (III) exerted anti-inflammatory effects that were quantitatively similar to the effects reported in a few microalgal species. Although the experimental approach followed was different from that described in our study, Gallego et al. (2022) investigated the anti-inflammatory effects of *Haematococcus pluvialis*, *Isochrysis lutea*, *Nannochloropsis oceanica*, and *Porphyridium cruentum* extracts on LPS-stimulated THP-1 cells, measured as the level of secretion of TNFα. The researchers found that only *N. oceanica* extracts induced a significant reduction in TNFα secretion levels compared to that recorded in control cultures (LPS-induced TNFα secretion), with up to 48 % inhibition of secretion. Similarly, Tzachor et al. (2021) studied the anti-inflammatory effects of *Spirulina* extracts obtained from the biomass produced under different conditions of light quality and irradiance; they found a maximum reduction of 40 % in TNFα secretion levels in LPS-stimulated human monocytes. *Spirulina* is considered to be a “super-food”, particularly due to its beneficial effects on human health, including antioxidant, anti-inflammatory, and immunomodulatory effects. However, systematic studies on its anti-inflammatory effects on humans, indicated by a reduction in TNFα, IL-6, and CRP levels, are lacking (Calella et al., 2022).

The anti-inflammatory effects on THP-1 Mac cells by extracts of *C. onubensis* obtained by exposing cultures to Fe (III) showed a 50 % reduction in TNFα secretion. This finding suggested that acidophilic microalgae might be excellent natural sources of anti-inflammatory compounds, partly because of their ability to adapt to oxidative stress due to the accumulation of a large number of anti-inflammatory molecules. Additionally,

the anti-inflammatory capacity of microalgal extracts could be improved by modulating oxidative stress during biomass production.

Assessing the content of the free radical DPPH, which is widely used to evaluate the ability of compounds to act as free-radical scavengers and hydrogen suppliers (Ávila-Román et al., 2023), is a rapid, simple, and inexpensive method for testing antioxidant capabilities. The antioxidant capacity of microalgal extracts obtained from Fe (III)-exposed cultures was lower than the antioxidant capacity of control cultures (Figure 6.5). However, those extracts showed a higher capacity to mitigate pro-inflammatory reactions, measured as the TNFα content released in the THP-1 Mac cell. These results were similar to those obtained by Barone et al. (2021), who showed that the antioxidant response of the tested microalgal species decreased after exposure to 0.5 mM H_2O_2. This decrease in the antioxidant capacity in the referred study indicated the role of the activity of the enzymatic antioxidant system in the neutralization of ROS. Similarly, results obtained by our group under similar conditions showed an increase in SOD activity in *C. onubensis* extracts obtained from cultures exposed to different Fe (III) concentrations, with activity values approximately 60 % higher than those recorded in control cultures (Robles et al., 2023, chapter 5). However, considering that Fe (III) induces an enzyme-based antioxidant response in *C. onubensis,* in this study, we aimed to more comprehensively understand the non-enzymatic antioxidant system that contributes to the anti-inflammatory activity of the microalgal extracts. For this, we analyzed the variation in the content of the target antioxidant molecules in *C. onubensis* cultures as a function of the added Fe (III) and correlated it with the antioxidant capacity and anti-inflammatory activity exerted by the microalgal extracts (Figure 6.6, 6.7, and 6.8).

As shown in Figure 6.6, the findings suggested that the microalgal extracts obtained from Fe (III)-exposed cultures contain molecules that can mitigate inflammatory responses, but these molecules may not exert antioxidant effects, as previously described, i.e., molecules involved in the antioxidant response of *C. onubensis* to cope with Fe (III) stress-derived ROS might not act against DPPH, and thus, they may not reflect the antioxidant capacity of the microalga. This might be the case for (poly)phenols and carotenoids (terpenoids), which are strong antioxidant scavengers of ROS (Montero-Lobato et al., 2018), whose content in *C. onubensis* extracts from Fe (III)-stressed culture cells generally decreased, compared to cell extracts from control culture (Figure 6.7 and 6.8). Thus, we hypothesized that the actual content and antioxidant capacity of (poly)phenols and carotenoids might be underestimated.

In relation with the later, the OH groups in the phenol structure, which must react with ROS to exhibit ROS-scavenging activity, are also required to react with DPPH. Gulcin and Alwasel (2023) studied the interaction between the DPPH radical and the (poly)phenolic group in usnic acid, which has two -OH units. They inferred that the withdrawal of H atoms from the (poly)phenolic -OH groups by a reactive radical species is a thermodynamically favorable chemical transformation, which can occur under high oxidative pressure. This is also coherent with the lower antioxidant capacity obtained in Fe (III)-added cultures of microalgal extracts and the proposed structural changes in

(poly)phenols. Therefore, part of the (poly)phenolic content in the microalgal extracts, especially in extracts from Fe (III)-stressed cultures, would not be acting in reducing chemically the DPPH molecule; thus, resulting in an apparent lower antioxidant capacity, as obtained for extracts with high Fe (III) levels.

However, (poly)phenols and carotenoids (terpenoids) can decrease the inflammatory response measured in terms of LPS-induced secretion of TNFα by THP-1 macrophages (Araújo et al., 2020; Gallego et al., 2022). Linnewiel-Hermoni et al. (2014) reported that carotenoid-oxidized derivatives, but not the intact carotenoid structures, can mediate the inhibition of NF-κB. Moreover, derivatives that contain α,β-unsaturated carbonyl groups interact with higher affinity with the active site of NF-κB following the Michael addition reaction (Linnewiel-Hermoni et al., 2014). This concept provides insights into new approaches to studying the anti-inflammatory potential capacity of natural compounds, which also explains our findings of considerably lower antioxidant capacity and higher anti-inflammatory activity in extracts from microalgal cell cultures exposed to high levels of Fe (III)-induced oxidative stress.

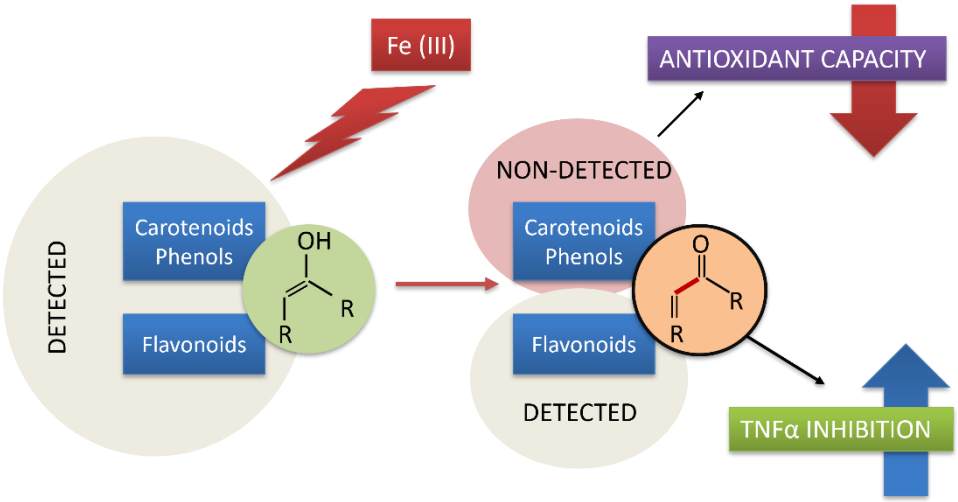

Figure 6.10. A schematic representation of the mechanism underlying the oxidative Fe (III) stress-derived structural changes in antioxidant molecules produced by *C. onubensis*, and illustration of the subsequent effect on the antioxidant capacity and anti-inflammatory activity exerted by its extracts.

Consequently, we hypothesized that structural changes in target antioxidant molecules after reacting with ROS might explain the observed reduction in antioxidant capacity and increase in anti-inflammatory activity. This hypothesis was supported by the results presented in Figure 6.7 and 6.8 and schematically represented in Figure 6.10, i.e., the data obtained allowed us to suggest the existence of a direct relationship between these structurally oxidized compounds and the increase in anti-inflammatory activity. This hypothesis matched the results reported by Havaux (2014); ROS, especially singlet oxygen, produced in chloroplasts under stress, can oxidize β–carotene, leading to the production of various oxidized derivatives, such as β–cyclocitral or β–ionone, containing α,β-unsaturated carbonyl groups. Similarly, after reacting with ROS, (poly)phenolic compounds and xanthophylls may lose their hydroxyl groups to form α,β-unsaturated carbonyl groups (Hunyadi, 2019; Rajashekar, 2023). These structural changes can cause the actual contents of the carotenoids identified by HPLC to be

underestimated (Figure 6.7), based on the changes in polarity. As (poly)phenolic compounds are determined spectrophotometrically based on the reaction of their hydroxyl groups with the Folin-Ciocolteu reagent (Pérez et al., 2023), fewer hydroxyl groups in (poly)phenolic compounds might be available for that reaction, which might result in lower levels of detection.

Additionally, these proposed structural changes might favor the (bio)synthesis of derived molecules containing α,β-unsaturated carbonyl groups; the active domain of NF-κB may have a higher affinity for these groups, as discussed above. Thus, the expression of TNFα might be inhibited, resulting in a higher anti-inflammatory activity of the extracts.

In contrast to the pattern obtained with carotenes, xanthophylls, and (poly)phenols, the measurement procedure of flavonoids might not be affected by reaction with ROS, as a direct correlation was found between the flavonoid content and anti-inflammatory activity (Figure 6.8d). This occurred probably because the determination of flavonoids is mediated by the oxidation of (poly)phenolic ring-hydroxyl groups to the carbonyl groups, which are also involved in the formation of Al (III)-flavonoid chelates, detected by spectrophotometry (Shraim et al., 2021). The transformation of hydroxyl groups into carbonyl groups in flavonoids by reacting with ROS does not hinder their detection. This fact explained why a significant increase in flavonoid content was recorded under moderate levels of Fe (III)-induced oxidative stress in *C. onubensis* cultures.

To summarize, the information obtained in this study can improve our understanding of the role of the target antioxidant molecules analyzed (carotenes, xanthophylls, (poly)phenols, and flavonoids) in neutralizing ROS to alleviate the oxidative stress generated by Fe (III) in cultures of the highly acidic-habitat microalga *C. onubensis*. We also found a relationship between an increase in the oxidative status of the microalga and an increase in the capacity of the microalgal extracts to mitigate the inflammatory response of THP-1 Mac cells. Structural changes have been proposed in xanthophylls, (poly)phenols, and flavonoids when reacting with ROS, consisting of oxidation of their hydroxyl groups to α,β-unsaturated carbonyl groups forming their respective derivative molecules. In the case of β–carotenes, these structural changes could be caused by bond breakage, leading to the formation of some oxidized products, such as β–cyclocitral or β–ionone, containing α,β-unsaturated carbonyl groups. These molecular changes could accordingly explain the lower detection of these molecules based on their chemical interference with the analytical determination procedure. Additionally, the suggested loss of hydroxyl groups could explain the decrease in their reactivity with the DPPH radical, which decreased the antioxidant capacity of the extracts. Flavonoids are an exception to this behavior; the possible oxidation of their hydroxyl groups seems to not interfere with their quantification procedure.

However, the proposed increase in α,β-unsaturated carbonyl groups of target antioxidant molecules due to an increase in the Fe (III)-mediated oxidative status of the microalgal cells is suggested to promote a stronger interaction with the active domain of NF-κB; thus, inhibiting the expression of the pro-inflammatory cytokine TNFα. In line with the results and discussion of this study, the algal meroditerpenoid amentadione,

an α,β-unsaturated carbonyl terpenoid (carotenoid derivative), was found by some researchers to inhibit NF-κB signaling pathways. Their findings strongly suggest that amentadione is a novel anti-inflammatory factor with high therapeutic potential (Araújo et al., 2020). The presence of the α,β-unsaturated carbonyl structure in amentadione strongly suggests that this group is a key chemically active moiety, which confers anti-inflammatory activity to carotenoids and phenolic compound-oxidized derivatives.

Therefore, Fe (III)-mediated induction of oxidative stress can be used to produce cell extracts with an enhanced capacity to reduce inflammatory responses by increasing the synthesis of antioxidants, such as terpenoids, (poly)phenolic compounds, and flavonoids. However, Figure 6.9 showed that increasing Fe (III) concentration had no significant differences in the inhibition of the production of other pro-inflammatory interleukins (IL-6 and IL-1β) in THP-1 stressed cells, suggesting that different molecules are responsible for inhibiting the production of other interleukins. In contrast, *C. onubensis* extracts obtained from cultures exposed to different levels of light irradiance influenced the production of these pro-inflammatory interleukins. By analyzing the synergistic effect of Fe (III) concentration and light irradiance in *C. onubensis* cultures, two strategies could be developed to increase the anti-inflammatory activity of the microalgal extracts. On the one hand, moderate levels of light irradiance (150 μmol photon·m^{-2}·s^{-1}) and Fe (III) (0.25 mM) on the highly acidic-habitat microalga *C. onubensis* enabled the production of biomass extracts with a higher inhibition in the production of the pro-inflammatory interleukins TNFα and IL-6. On the other hand, the highest inhibition in the production of IL-6 was found under low Fe concentration and light irradiance equal or higher than 150 μmol photon·m^{-2}·s^{-1}. Accordingly, it could be hypothesized that the synergistic effect of Fe (III) concentration and light irradiance in *C. onubensis* cultures could enhance the anti-inflammatory activity in *C. onubensis* extracts. Although our findings were limited to the action of microalgae in a highly acidic environment, Fe (III)-based stress may have broader applicability in other microalgal species.

5. Conclusions

The findings of this Chapter revealed that *C. onubensis* is a promising source of bioactive compounds that exhibit *in vitro* anti-inflammatory activity, including fatty acids, (poly)phenolic compounds and carotenoids. Nevertheless, based on the harsh conditions of its natural habitat, this study demonstrated that the addition of moderate Fe (III) concentrations to the microalgal cultures enhanced the antioxidant and anti-inflammatory capacity of microalgal extracts. The results suggested a direct relationship between the antioxidant capacity of the microalgal extracts and Fe (III) concentration in the culture medium. Nevertheless, opposite correlations were found for antioxidant and anti-inflammatory capacities, measured as TNFα inhibition in THP-1 Mac cells. Consequently, this study proposes that Fe (III)-induced oxidative stress might result in derivative antioxidants, which are potentially more effective as anti-inflammatories. Conversely, these derivative antioxidants could not be properly detected neither could be acting to reduce DPPH, thereby resulting in an apparently lower measured antioxidant capacity in the microalga. This concept provides insights into new experimental approaches to studying the anti-inflammatory potential capacity of natural compounds, which also explains our findings of considerably lower antioxidant capacity and higher anti-inflammatory activity in extracts from microalgal cell cultures exposed to high levels of Fe (III)-induced oxidative stress. Additionally, Fe (III) concentration had no significant effect in the inhibition of the production of other pro-inflammatory interleukins (IL-6 and IL-1β), while *C. onubensis* extracts obtained from cultures exposed to different levels of both light irradiance and Fe (III) influenced the production of these pro-inflammatory interleukins. Accordingly, it could be hypothesized that the synergistic effect of Fe (III) concentration and light irradiance in *C. onubensis* cultures could enhance the anti-inflammatory activity in *C. onubensis* extracts which are enriched in valuable antioxidant molecules. Overall, the obtained results highlight the utility of microalgal species from a highly acidic environment as a novel, natural source of anti-inflammatory molecules, based on its ability to cope with the oxidative conditions of its habitat.

6. Supplementary material

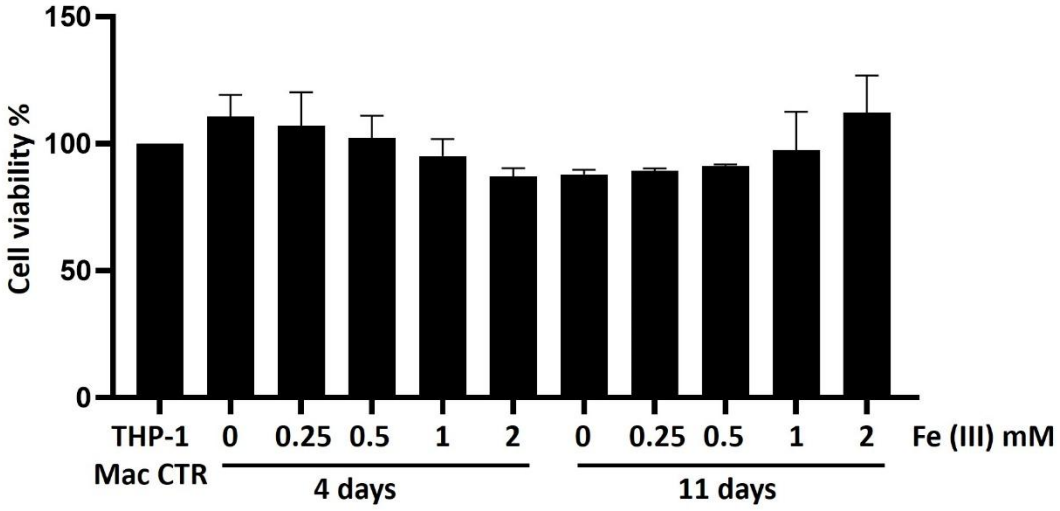

Figure S6.1. Viability of THP-1 macrophage cells (THP-1 Mac) exposed for 48h to 10 μg·mL^{-1} of *C. onubensis* methanolic extracts, obtained from cultures treated with different concentrations of Fe (III) (from 0 mM to 2 mM) for 4 and 11 days. THP-1 Mac CTR corresponds to non-treated cells. Graph shows mean ±SD of triplicate measurements. One-way Anova and multiple comparisons with the Dunnett's test demonstrate no statistical significance for any tested extract relative to THP-1 Mac CTR cells.

Statistical analysis Figure 6.3

Table S6.1. Time-dependent evolution of growth, measured as dry weight (dw), as a function of Fe (III) concentration in cultures of the acidotolerant microalga *C. onubensis*.

Time (d)	C	0.25 mM	0.5 mM	1 mM	2 mM
0	1.028^{a}	1.166^{b}	1.218^{c}	1.314^{d}	1.57^{e}
1	2.03^{a}	3^{b}	2.5^{c}	3^{b}	3.2^{d}
2	3.3^{a}	4^{b}	4^{b}	4.5^{c}	5^{d}
3	5.09^{a}	6^{b}	5.76^{c}	6^{b}	7^{d}
4	6^{a}	9^{b}	9^{b}	7.86^{c}	10^{d}
7	11.28^{a}	15.28^{b}	13.72^{c}	12.12^{d}	13.76^{e}
8	13.52^{a}	16.2^{b}	15^{c}	13.52^{a}	15.36^{d}
9	14.44^{a}	18^{b}	16.68^{c}	16.16^{d}	16.92^{e}
11	18^{a}	21^{b}	20.5^{c}	19.88^{d}	19.56^{e}

$^{a, b, c, d, e.}$ Different superscript letters indicate differences in treatments with a significance of $p < 0.05$.

Table S6.2. Time-dependent evolution of the maximum photosynthetic efficiency of photosystem II (Quantum yield, Fv/Fm) as a function of Fe (III) concentration in cultures of the acidotolerant microalga *C. onubensis*.

Time (d)	C	0.25 mM	0.5 mM	1 mM	2 mM
0	0.732[a]	0.737[b]	0.739[c]	0.742[d]	0.743[e]
1	0.735[a]	0.745[b]	0.753[c]	0.743[d]	0.749[e]
2	0.739[a]	0.753[b]	0.753[b]	0.747[c]	0.755[d]
3	0.738[a]	0.757[b]	0.758[c]	0.745[d]	0.758[c]
4	0.737[a]	0.75[b]	0.753[c]	0.748[d]	0.757[e]
7	0.727[a]	0.75[b]	0.749[c]	0.753[d]	0.753[d]
8	0.729[a]	0.746[b]	0.746[b]	0.756[d]	0.754[e]
9	0.732[a]	0.743[b]	0.744[c]	0.756[d]	0.755[e]
11	0.744[a]	0.745[b]	0.734[c]	0.75[d]	0.744[e]

[a, b, c, d, e.] Different superscript letters indicate differences in treatments with a significance of $p < 0.05$.

6

Statistical analysis Figure 6.5-6.8

Table S6.3. Antioxidant capacity exerted by *C. onubensis* cultures extracts as a function of the Fe (III) concentration in the culture medium, after 4 and 11 days exposure to Fe (III).

Time (d)	C	0.25 mM	0.5 mM	1 mM	2 mM
4	279.066[a]	257.473[b]	261.68[c]	250.232[d]	225.947[e]
11	212.313[a]	200.643[b]	190.45[c]	185.39[d]	179.501[e]

[a, b, c, d, e.] Different superscript letters indicate differences in treatments with a significance of $p < 0.05$.

Table S6.4. Anti-inflammatory activity measured as inhibition percentage of TNFα release by THP-1 MoM cells exposed to *C. onubensis* extracts as a function of the Fe (III) concentration in the culture medium, after 4 and 11 days exposure to Fe (III).

Time (d)	C	0.25 mM	0.5 mM	1 mM	2 mM
4	10[a]	51[b]	50[c]	44.7[d]	23.7[e]
11	4[a]	27.6[b]	25.9[c]	7.5[d]	4.9[e]

[a, b, c, d, e.] Different superscript letters indicate differences in treatments with a significance of $p < 0.05$.

Table S6.5. Antioxidant pool obtained by *C. onubensis* cultures extracts as a function of the Fe (III) concentration in the culture medium, after 4 and 11 days exposure to Fe (III).

Time (d)	C	0.25 mM	0.5 mM	1 mM	2 mM
4	134.622[a]	158.024[b]	187.016[c]	177.567[d]	144.704[e]
11	96.265[a]	164.424[b]	127.164[c]	149.491[d]	142.765[e]

[a, b, c, d, e.] Different superscript letters indicate differences in treatments with a significance of $p < 0.05$.

Table S6.6. Carotene pool obtained by *C. onubensis* cultures extracts as a function of the Fe (III) concentration in the culture medium, after 4 and 11 days exposure to Fe (III).

Time (d)	C	0.25 mM	0.5 mM	1 mM	2 mM
4	1.45[a]	1.726[b]	1.321[c]	0.946[d]	0.789[e]
11	1.45[a]	1.206[b]	1.405[c]	1.502[d]	1.599[e]

[a, b, c, d, e.] Different superscript letters indicate differences in treatments with a significance of $p < 0.05$.

Table S6.7. Xantophyll pool obtained by *C. onubensis* cultures extracts as a function of the Fe (III) concentration in the culture medium, after 4 and 11 days exposure to Fe (III).

Time (d)	C	0.25 mM	0.5 mM	1 mM	2 mM
4	5.795[a]	5.915[b]	5.245[c]	4.876[d]	4.074[e]
11	5.795[a]	4.364[b]	5.364[c]	6.567[d]	5.982[e]

[a, b, c, d, e.] Different superscript letters indicate differences in treatments with a significance of $p < 0.05$.

Table S6.8. Polyphenol content obtained by *C. onubensis* cultures extracts as a function of the Fe (III) concentration in the culture medium, after 4 and 11 days exposure to Fe (III).

Time (d)	C	0.25 mM	0.5 mM	1 mM	2 mM
4	19.248[a]	18.957[b]	16.864[c]	17.275[d]	12.466[e]
11	13.747[a]	11.504[b]	12.237[c]	15.265[d]	18.951[e]

[a, b, c, d, e.] Different superscript letters indicate differences in treatments with a significance of $p < 0.05$.

Table S6.9. Flavonoid content obtained by *C. onubensis* cultures extracts as a function of the Fe (III) concentration in the culture medium, after 4 and 11 days exposure to Fe (III).

Time (d)	C	0.25 mM	0.5 mM	1 mM	2 mM
4	108.129[a]	131.426[b]	163.586[c]	154.47[d]	127.374[e]
11	75.273[a]	147.351[b]	108.158[c]	126.156[d]	116.232[e]

[a, b, c, d, e.] Different superscript letters indicate differences in treatments with a significance of $p < 0.05$.

Statistical analysis Figure 6.9

Table S6.10. Inhibition in the production of TNFα, IL-1β and IL-6 in THP-1 stressed cells treated with *C. onubensis* extracts as a function of different Fe (III) and light irradiance levels.

	0 mM Fe (III)			0.25 mM Fe (III)		
	30 µE	**150 µE**	**400 µE**	**30 µE**	**150 µE**	**400 µE**
TNFα	8.110[a]	25.271[b]	25.175[b]	73.576[c]	60.034[d]	53.775[d]
IL-6	69.34[a]	73.45[b]	70.33[a]	76.53[c]	67.632[a]	57.286[d]
IL-1β	24.047[a]	55.652[b]	57.293[b]	13.896[c]	23.493[a]	41.445[d]

[a, b, c, d, e.] Different superscript letters indicate differences in treatments with a significance of $p < 0.05$.

Atacama dessert
- hyper-aridity
- extreme solar irradiance
- high day/night temperature

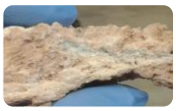

Gympsus rock
Protect harsh conditions

Chroococcidiopsis sp. cell aggregate
Protect harsh conditions

Ultrasound treatment
Diseggregate cells providing greater light and nutrient availability

IMPROVED BIOMASS PRODUCTIVITY

Tinto river, Huelva (Spain)

Elliptochloris sp.

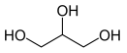

Glycerol

Mixotrophic growth
Acidic conditions (pH 2.5) limit growth of opportunits

IMPROVED FATTY ACID PRODUCTIVITY

7

CHAPTER

Assessment of growth and accumulation of valuable molecules in other photosynthetic extremophiles

Table of contents

Abstract: In addition to *Coccomyxa*, in this thesis we have explored specific characteristics of the cultivation of two other extremophilic microalgae, *Chroococcidiopsis* sp. (cyanobacterium from endolithic, hyper-arid environment, Atacama) and *Elliptochloris* sp. (microalga from hyper-acidic habitat, Tinto River). The aim was to obtain initial key information of their production, as a first step toward the analysis of their biotechnological potential. Atacama Desert is one of the driest deserts in the world due to the extremely scarce rainfall, low level of relative humidity and extremely high incident solar radiation. To survive these conditions and reduce the cell exposure to the incident UV radiation, *Chroococcidiopsis* sp. grows in the form of aggregates, diminishing the associated photo-oxidative damage. However, this adaptation strategy can reduce the availability of both light and nutrients to the growing cells. This study showed that the modulation of low-frequency ultrasound pulses was efficient in disaggregating *Chroococcidiopsis* sp. aggregates, improving light and nutrient availability to the cells and, therefore, the growth of the cyanobacterium. Depending on species, other strategies could be considered for improving biomass production. This has been tested with another (non-aggregating) highly acidic-habitat microalga, *Elliptochloris* sp., isolated by our team, Microalgae Biotechnology Unit (BITAL) at University of Huelva. Photoautotrophic algal cultivation is challenging due to the shadowing effect produced by an increase in the number of cells; under such circumstances, mixotrophic growth might be an efficient alternative. We grew cultures of the autochthonous acidotolerant microalga *Elliptochloris* sp. on crude technical glycerin or glucose bubbled with either only air or air containing 2.5 % (v/v) CO_2. We found that CO_2 strongly influenced the production of *Elliptochloris* sp., as higher growth occurred in mixotrophy with CO_2-enriched air compared to that with only air. Mixotrophy with CO_2-enriched air enabled reaching higher biomass productivity and facilitated an increase in the relative abundance of saturated fatty acids. Nevertheless, mixotrophy with only air resulted in an increase of both saturated and unsaturated fatty acids, but biomass productivities were lower. These results, along with the limited biological contamination facilitated by the low pH, suggest that this microalga might be attractive for large-scale production within the circular economy model.

Keywords: extremophilic microalgae, biomass productivity, aggregates, ultrasound pulses, mixotrophy, fatty acids.

1. Introduction

The study of extremotolerant microorganisms allows us to understand the limits of the conditions in which life is possible, thus providing answers to fundamental questions about the origin, distribution, and evolution of life (Varshney et al., 2015). In addition, the adaptation capacity of extremotolerant microorganisms to the harsh conditions of their habitats is partly based on the expression of secondary metabolic pathways leading to the biosynthesis of unique, valuable molecules with applications in human and animal health. These molecules include highly antioxidant phenolic compounds, peptides, indole derivates and terpenes, among other valuable biomolecules groups (Dumorné et al., 2017; Raddadi et al., 2015).

In addition to *Coccomyxa*, in this thesis we have explored specific characteristics of the cultivation of two other extremophilic microalgae, *Chroococcidiopsis* sp. and *Elliptochloris* sp. The aim was to obtain initial information of their production, as a first step toward the analysis of their biotechnological potential.

1.1. Chroococcidiopsis sp.

In particular, the genus *Chroococcidiopsis* sp. is known for its extremotolerant character and capability to adapt to polyextreme environments such as extreme aridity, high salinity, high and low temperatures, and ionizing radiations. The cyanobacterium was isolated from the endolithic habitat of gypsum rocks of the hyper-arid Atacama Desert (north Chile) (Wierzchos et al., 2015). This desert is one of the most challenging polyextreme environments on Earth due to its hyper-aridity, extreme solar irradiance, both ultraviolet radiation (UVR) and photosynthetic active radiation (PAR), high day/night temperature fluctuations and in some cases high salinity (Wierzchos et al., 2018). The high solar radiation in the Atacama Desert makes photosynthesis difficult due to the photo-oxidative damage suffered by the species growing in that habitat (Solovchenko and Merzlyak, 2008).

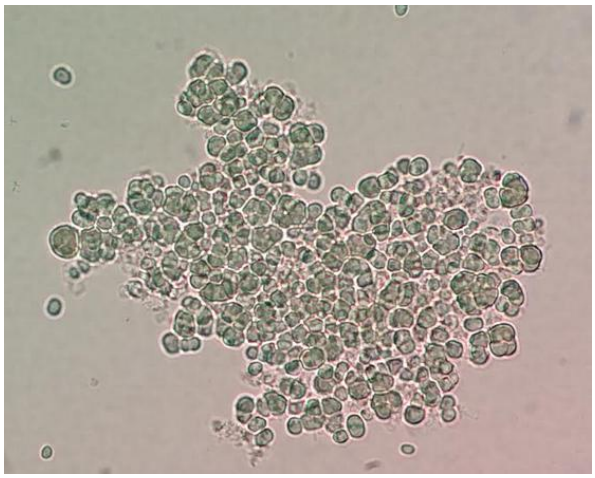

Figure 7.1. Picture of *Chroococcidiopsis* sp. taken under the optic microscope (augmentation, 40x).

To overcome these conditions, *Chroococcidiopsis* sp. produces a layer of exopolysaccharides (EPS) that surround the cells allowing them to retain some water

and create a more humid endolithic environment to live (Singh et al., 2019), thereby promoting photosynthesis. This EPS layer favors the formation of cellular aggregates (Figure 7.1) (Das et al., 2018), allowing the cyanobacteria to dissipate part of the light received, eventually reducing the oxidative damage (Flemming and Wingender, 2010). To achieve this, the cells accumulate the UV-filtering phenolic molecule scytonemin within the outermost EPS sheath (Casero et al., 2020; Vítek et al., 2014).

As a cyanobacterium, *Chroococcidiopsis* strains can be of biotechnological interest also due to the potential accumulation of valuable pigments including phycobiliproteins (Montero-Lobato et al., 2020; Vítek et al., 2014). However, despite the above-referred advantage of the aggregates, the cell morphological configuration in aggregates can limit their growth due to the lowered availability of light and nutrients reaching the central cells of the aggregates compared to the peripheral ones (Conradi et al., 2019). As a result, growth can occur at different rates within each cell aggregate, depending on each cell position and availability of light and nutrients. According to it, one of the hypotheses of this work is that avoiding aggregation could improve the productivity of the cyanobacterium, eventually increasing the production and even extraction yields of valuable molecules. The strategies and intensity used to keep cells disaggregated should guarantee the cells viability, which would potentially address improved nutrient availability. Consequently, cell growth would be enhanced, which could hypothetically facilitate large-scale production.

The rationale behind our work is minimizing the energy of the ultrasound pulses applied to cyanobacterial aggregates in liquid cultures to that required to splitting the cyanobacterial outer polysaccharide sheath over the cell membrane while avoiding cell disruption, thus promoting cell disaggregation. Based on this concept, we studied in culture flasks the efficacy of low-frequency ultrasound in cell disaggregation as a treatment to eventually improve the productivity of the *Chroococcidiopsis* sp. liquid cultures.

1.2. Elliptochloris sp.

Additionally, other strategies could be considered for efficient biomass production. This has been tested with another highly acidic-habitat microalga, *Elliptochloris* sp., isolated by our team, Microalgae Biotechnology Unit (BITAL) at University of Huelva. During photoautotrophic growth, microalgal biomass and lipid production might be limited by the reduction in light availability. That is, during the production of microalgae at high cell densities, the shadowing effect among cells might lead to growth photolimitation (Vaquero et al., 2014). As an alternative to photoautotrophic growth, some microalgal species can use organic carbon sources (OCS) and perform mixotrophic or heterotrophic growth. The process yields metabolic energy since OCS can directly follow a carbon-oxidation metabolic route. This process slightly decreases the importance of energy production by light-dependent growth, which is limited by the lower availability of light in dense algal cultures (D'Imporzano et al., 2017).

The fixing of CO_2 while assimilating OCS is defined as mixotrophic growth. Several microalgal species can grow mixotrophically, including *Chlorella*, *Chlorococcum*,

Haematococcus, *Nannochloropsis*, *Navicula*, *Phaeodactylum*, and *Nitzschia* (Perez-Garcia and Bashan, 2015). The most commonly used OCS during mixotrophic growth at laboratory scale are glucose and acetate (Paranjape et al., 2016). However, these carbon sources are not suitable for industrial-scale production as they are expensive (Li et al., 2007). Glycerol, a by-product of biodiesel production, can be obtained at a lower price (Vivek et al., 2017). Thus, the large-scale production of microalgae based on glycerol can reduce production costs while increasing the added value of glycerol through its conversion into oil as a raw material for advanced biofuel (da Silva et al., 2009).

The use of an extra OCS supports activities in the cell related to metabolic energy production through the oxidation of the carbon source, schematically represented in Figure 7.2. Additionally, using OCS promotes fatty acid biosynthesis in the chloroplast (Poddar et al., 2020). Glycerol can be transported to the cytosol by passive diffusion and then be phosphorylated and converted into glycerol-3-phosphate (G3P), which is involved in triacylglyceride (TAG) synthesis. Also, glucose is phosphorylated to glucose-6-phosphate (G6P), which is converted first into fructose-6-phosphate (F6P) and, subsequently, into G3P (Chen et al., 2017).

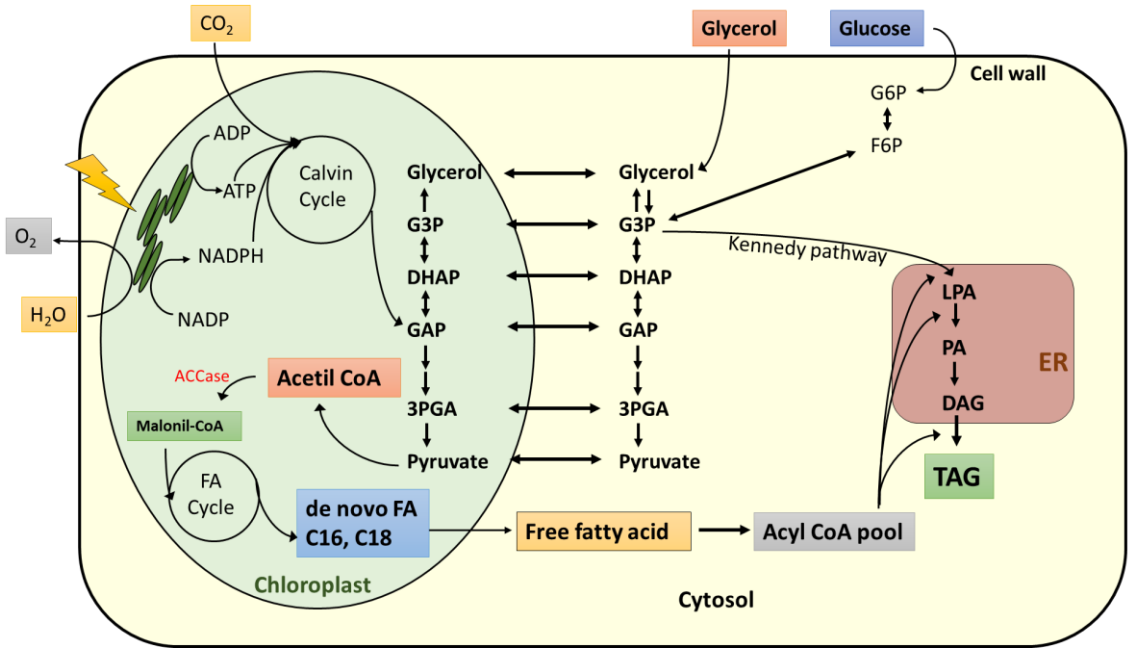

Figure 7.2. A schematic representation of the mechanism underlying the incorporation of an organic carbon source (OCS) in a microalgal cell and production of metabolic energy through its oxidation. Symbols: ADP: adenosine diphosphate, ATP: adenosine triphosphate, NADP, NADPH, FA: fatty acid, TAG: triacylglyceride, G3P: glycerol-3-phosphate, DHAP: dihydroxyacetone phosphate, GAP: glyceraldehyde phosphate, 3PGA: 3-phosphoglycerate, G6P: glucose-6-phosphate, F6P: fructose-6-phosphate, LPA: lysophosphatidic acid, PA: phosphatidic acid, DAG: diacylglycerol, ER: endoplasmic reticulum.

Bacterial contamination is a serious concern when microalgae are cultivated in a medium containing OCS, as microalgae have a growth rate one order of magnitude lower than their competitors (Abiusi et al., 2022). This is why the interest in extremophilic microalgae has increased in the last few years. Extreme conditions are not

suitable for all microorganisms, allowing only the growth of the extremophilic microorganisms that can cope with these harsh conditions. Based on these facts, the autochthonous highly acidic-habitat microalga *Elliptochloris* sp. isolated from Tinto River (Huelva) was selected for this study. The relevance of *Elliptochloris* sp. arises from its ability to grow in extreme acidic environment as fast as other non-extremophilic microalgae which grow at a near-neutral pH. Published information on the growth of *Elliptochloris* strains under controlled conditions is limited. However, the growth rates of *Elliptochloris* sp. (0.17-0.25 $g \cdot L^{-1} \cdot d^{-1}$, unpublished data) are in the range of those obtained by Chunzhuk et al. (2023) for a non-extremophilic *Elliptochloris subsphaerica* and other non-extremophilic microalgae (0.12-0.37 $g \cdot L^{-1} \cdot d^{-1}$).

In this study, the production of the highly acidic-habitat microalga *Elliptochloris* sp. in photoautotrophic and mixotrophic conditions was analyzed. Studies performed by Cuaresma et al. (2011) on the acidotolerant microalga, *C. onubensis*, revealed that glucose was the only organic carbon source which enabled reaching biomass concentration values similar to those obtained in photoautothrophic cultures; based on that, glucose was selected as carbon source for this study. In addition, technical glycerin was selected as a carbon source to promote the circular economy, i.e. the insertion of an industrial by-product in the metabolic pathway of the microalga. The supplemented glycerin was obtained in the process of advanced biodiesel production. This way, the added value of glycerin could be enhanced due to its application in the production of valuable microalgal biomolecules, such as fatty acids; for instance, glycerin might be re-used as an organic carbon source for microalgal biofuel production or as food supplements. The selected carbon sources were supplemented at 5 mM, based on studies conducted by Martínez et al. (1997) and Chojnacka and Noworyta (2004), who reported a glucose concentration of 3–5 mM to be the carbon saturation limit for the growth of microalgae in batch culture. This study provided insights into the growth and production of lipids by a microalgal strain recently isolated from a highly acidic environment. Our findings provided information on biotechnological strategies related to the production and application of extremophiles.

2. Materials and Methods

2.1. Biological material and cultivation conditions

The cyanobacterium *Chroococcidiopsis* sp. was isolated from the gypsum rock fragments of the Atacama Desert, (23°53′S, 068°08′W and 2,720 m a.s.l.) located in the north-south trending depression of the Cordon de Lila range, in northern Chile. The isolated cyanobacterium was supplied by researchers from the (National Museum of Natural Sciences, CSIC, Madrid) to the Microalgae Biotechnology Unit (BITAL), of the Department of Chemistry "Professor Jose Carlos Vílchez Martín," from the Faculty of Experimental Sciences of the University of Huelva. *Chroococcidiopsis* sp. was cultivated at pH 7 in a sterile culture medium BG11, which is widely used for the growth of freshwater green algae and cyanobacteria (Richmond, 2003). The constituents of BG11 (per liter) were as follows: 1.5 g $NaNO_3$; 0.04 g $KH_2PO_4 \cdot 3H_2O$; 0.075 g $MgSO_4 \cdot 7H_2O$; 0.036 g $CaCl_2 \cdot 2H_2O$; 0.006 g citric acid; 0.006 g ferric ammonium citrate; 0.222 µg $ZnSO_4.7H_2O$; 0.079 µg $CuSO_4 \cdot 5H_2O$; 1.81 µg $MnCl_2 \cdot 4H_2O$; 2.86 µg H_3BO_3; 0.391 µg $Na_2MoO_4 \cdot 2H_2O$: 0.049 µg $Co(NO_3)_2 \cdot 6H_2O$; 0.001 g Na_2EDTA. The cultures were grown in an algal cultivation room at 25 °C illuminated with white fluorescent light of 50–60 µmol photon $m^{-2} \cdot s^{-1}$, bubbled with a mix of CO_2 in the air (2.5 %, v/v), which was the only used carbon source.

Elliptochloris sp. was isolated from the Tinto River, in the north of the Huelva province (site GPS coordinates: 37.72326, –6.55081) by the Microalgae Biotechnology Unit (BITAL), of the Department of Chemistry "Professor Jose Carlos Vílchez Martín," from the Faculty of Experimental Sciences of the University of Huelva. Samples taken from the location were transferred to a sterile k9 culture medium (Silverman and Lundgren, 1959) prepared on agar in Petri dishes. Green spots were transferred from the agar plates to the k9 liquid culture medium. Liquid cultures were checked periodically in an optical microscope CX40 (Olympus, UK). Based on morphological observations, only one microalga species was found in the samples taken, and subsequently, DNA was extracted from cell pellets in the liquid culture for identification. The isolated *Elliptochloris* sp. was cultivated at pH 2.5 in sterile k9 culture medium originally used for bacteria and modified for acidophilic microalgae. Changes to k9 medium included modification of nitrogen source, replacing ammonia by nitrate, and Hutner solution (Hutner et al., 1950) was added to satisfy trace elements needs. Trace elements Hutner solution was prepared as described in Garbayo et al. (2012). The k9 medium was prepared according to the following composition: 3.95 g of K_2SO_4, 0.1 g of KCl, 0.5 g of K_2HPO_4, 0.41 g of $MgCl_2$, 2.29 g of KNO_3, 0.01 g of $CaCl_2$, and 5 mL of Hutner traces; distilled water was added to make the final volume 1 L and pH was set at 2.5 by the addition of 40 % (v/v) H_2SO_4.

2.2. Identification of Elliptochloris sp.: DNA extraction, PCR amplification, sequencing and phylogenetic analysis

Cell samples from a liquid culture of *Elliptochloris* sp. were harvested by centrifugation, and 5 replicates for DNA extraction were used. Genomic DNA extraction was done by

using the Quick-DNA™ Fecal/Soil Microbe MiniPrep kit (Zymo Research). The protocol was adapted by disrupting the cells in a cell mill for 30 seconds at 30 Hz twice using glass beads tubes. The supernatant obtained was used for DNA purification, which was performed according to standard procedures. A sequence of the 18S rDNA was amplified using a pair of conserved, universal primers for eukaryotes: NS1 (forward primer) and NS2 (reverse primer) (Hillis and Dixon, 1991). PCR was run by using iTaq Universal SYBR BIORAD (Bio-Rad Laboratories, Inc.). The PCR product was purified using the E.Z.N.A. Cycle Pure Kit purchased from OMEGA Bio-Tek (Norcross, GA, USA). Sanger sequencing was performed by Secugen S.L. (Madrid, Spain). The sequence was analyzed using the BlastN software against the non-redundant database available in GenBank (http://www.ncbi.nlm.nih.gov/blast/Blast/cgi) with a cutoff of 1×10^{-5}.

The nucleotide sequence of the 18S rDNA of the acidophilic strain was aligned with the sequences of *Elliptochloris* sp. The phylogenetic tree was deduced from all available positions of the 18S rDNA gene sequence by Neighbor-Joining methods (Saitou and Nei, 1987). The bootstrap consensus tree inferred from 1,000 replicates (Felsenstein, 1985) represented the evolutionary history of the analyzed taxa. Evolutionary distances were calculated using the Jukes-Cantor method (Jukes and Cantor, 1969) and were in units of the number of base substitutions per site. A total of 255 positions were identified in the final dataset. All phylogenetic analyses were performed using the MEGA 11 program (Tamura et al., 2021).

2.3. Experimental design for photoautotrophic and mixotrophic growth analysis of Elliptochloris sp.

Photoautotrophic and mixotrophic cultures were grown in batch cultivation mode for 16 days and were prepared from a repeated-batch culture in the middle of the exponential growth phase (OD_{750} value around 5). Cultures of 0.4 L were prepared in 0.5 L round bottles using k9 culture medium at a pH of 2.5, at an initial cell concentration measured as OD_{750} of, approximately 0.7. pH of the cultures was checked daily and adjusted with 40 % (v/v) H_2SO_4 to 2.5. The cultures were established in a culture room at 25 ± 2 °C with continuous mixing by magnetic stirring and at a continuous light intensity of 150 µmol (photon)·m^{-2}·s^{-1} for 24 h under white light fluorescent tubes. The photoautotrophic and mixotrophic cultures were bubbled with either air alone or air containing 2.5 % (v/v) CO_2. A flowmeter was connected to air supply and CO_2 pipes to adjust the proportion of both gases bubbled into the cultures. Only those cultures supplemented with CO_2-enriched air (2.5 % v/v) and no additional carbon sources were called “photoautotrophic cultures” in this study. The organic carbon sources selected for mixotrophic cultivation were glucose (D (+)-glucose, anhydrous compound, VWR) and glycerin, at a concentration of 5 mM. In this study, residual technical glycerin from biodiesel production was used. Two types of residual technical glycerin were added to the cultures separately. Purity of both technical glycerin sources is around 80 % in glycerol and their MONG (matter organic non-glycerol) is in the range 1–2 %. One of them was obtained from vegetal residues while the other was obtained from Used

Cooking Oil residues (UCO). Both glycerin types were supplied by BioOils Huelva S.L., a biodiesel production company located in Palos de la Frontera (Huelva, Spain). Three replicates of each culture condition were performed.

2.4. Experimental design for ultrasound treatment of Chroococcidiopsis sp.

Chroococcidiopsis sp. cultures or samples were subjected to ultrasound pulses of a given intensity and variable duration at the beginning of each experiment, in order to promote disaggregation of cell clusters before performing further experiments or measuring other parameters. Cultures (0.25 L in 0.5 L Erlenmeyer flasks) or culture samples (15 mL in Falcon tubes) were added to the BG11 culture medium to reach an initial optical density between 0.5 and 0.7, measured at 750 nm, and subjected to 180 W ultrasound pulses using a model Ultrasons H-D bath (Selecta, Spain) for a variable duration ranging from a few seconds (data of each specific experiment is given in the Results section) to 10 min. In the test performed to study the effect of ultrasound pulses on the growth and viability of *Chroococcidiopsis* sp., the cultures were incubated in the microalgal culture room under the conditions indicated above. Microscope images were acquired using an optical microscope model CX40 (Olympus, UK) with an objective of 10x or, in some cases, 40x to test the effect of ultrasound treatment on cell disaggregation.

7

2.5. Growth and photosynthetic viability determination

Growth of both species, *Chroococcidiopsis* sp. and *Elliptochloris* sp. was determined by measuring the optical density (OD) at 750 nm of 1 mL culture samples, in a Cary 60 UV–Vis spectrophotometer (Agilent Technologies, USA) equipped with temperature control system adjusted to 25 °C. The OD_{750} data provided information on culture turbidity, which is proportional to the amount of biomass present in the culture (Shuler and Kargi, 2005). Additionally, dry weight of biomass was analyzed gravimetrically in an analytical balance, model CP225D (sartorius, Germany). Culture samples (2 mL) were filtered through 0.7 µm filters, MFV5 model (Anoia, Spain), the filters were dried for 24h in an oven at 100°C and the remaining dry residue was further weighed.

The relative optical density for ultrasound experiment with *Chroococcidiopsis* sp. was expressed as a percentage according to the following expression:

$$\text{Relative optical density (\%)} = \frac{OD_{750}t_i - OD_{750}t_0}{OD_{750}t_0} \cdot 100$$

where OD_{750} is the optical density at 750 nm; t_0 is the time zero for a sample not subjected to ultrasound treatment, while t_i corresponds to the ultrasound-treated samples at time zero.

The maximal specific growth rate was calculated during the early-mid exponential phase, where cell density showed an increase with time according to the following logarithmic expression:

$$\mu = \ln (C_t/C_0)/t$$

where C_t and C_0 represented the cell density for times t and zero, respectively, and µ represented the specific growth rate, expressed in d^{-1}. In this study, the optical density at

750 nm was used as an indirect measure of the biomass density, while the above equation was used to calculate the specific growth rates.

Photosynthetic viability of both species was determined based on the measurement of chlorophyll fluorescence, the maximum quantum yield (F_V/F_M) of Photosystem II (PSII), following published methods (Schreiber, 2004). Quantum yield (Qy) was measured in an AquaPEN AP-C 100 portable pulse amplitude-modulated (PAM) fluorimeter (Photon Systems Instruments, Drasov, Czech Republic), at 620 nm of actinic light. Each culture sample (1 mL) was pre-incubated in the dark for 15 min, and subsequently placed in the measurement chamber of the AquaPEN fluorimeter. F_V represents the variable fluorescence and is calculated as $F_V = F_M - F_0$, being F_0 the minimum level of fluorescence observed after exposing cells to a non-actinic beam and acclimating them in the dark, while F_M represents the maximum fluorescence observed in cells after exposing them to a brief but saturating pulse of actinic light.

2.6. Lipids and fatty acids analysis

Lipid content of the microalgal biomass was measured in lyophilized biomass samples as described by Südfeld et al. (2021). Briefly, 10 mg samples were extracted with chloroform:methanol (2:1, v/v). The extraction process was followed by solvent evaporation using an N_2 stream. Subsequently, lipid content was determined gravimetrically.

Fatty acid analysis was performed according to the following procedure (Robles et al., 2023). Once the acylglycerides were extracted, the corresponding fatty acids methyl-ester (FAME) were obtained through acid catalysis-mediated transesterification. The mixture was heated at 85 °C for 1 h, then cooled and washed with hexane and water. The FAMEs were separated by centrifugation (1,000 g, 10 min). FAMEs were separated and analyzed in a gas chromatograph system equipped with flame ionization detector (model 7890A, Agilent, California, USA). A 1-µL sample was injected into a silica capillary column (30 m, 0.32 mm id and 0.25-µm film thickness). Helium was used as carrier gas. The applied flow rate was 1.5 $mL \cdot min^{-1}$ and the split ratio 20:1. The injector and detector temperature values were 100 °C and 220 °C, respectively. The programmed oven temperature raised from 80 to 140 °C at 5 °C min^{-1}, followed by increase to 170 °C at 4 °C min^{-1} and then maintained for 2 min at 170 °C. Temperature was then increased to 190 °C at 1 °C min^{-1} and maintained for 2 min. The final temperature in the oven was 210 °C. Each one of the FAME peaks was identified by comparing retention times with those of mixed fatty acids standards (FAMEs Mix C4-C24 Supelco Analytical). Concentrations of FAMEs (ppm) were quantified by comparing their peak areas with those obtained from the standards of known concentration (Sigma Aldrich, St. Louis, MI, USA). Fatty acid composition was calculated as percentage of the total fatty acids in the volume of hexane. For quantification, tripentadecanoin was used as internal standard (Sigma Aldrich, St. Louis, MI, USA).

2.7. Statistics

Unless otherwise stated, all data are presented as the mean of three replicates and the standard deviations are shown in the corresponding figures and tables. The data from

the different treatments were evaluated by constructing univariate statistical models and performing the analysis of variance (ANOVA) (confidence of 95 % was considered for determining statistical significance). All analyses were performed using the Minitab 21 software.

3. Results

3.1. Effect of ultrasound treatment on the aggregation of the extremotolerant cyanobacterium Chroococcidiopsis sp. for improving growth

Our study aimed to evaluate the efficacy of low-frequency ultrasound (LFU) in cell disaggregation as a treatment to promote the growth of the extremotolerant cyanobacterium *Chroococcidiopsis* sp. in liquid cultures. This goal should be achieved by optimizing the ultrasound pulse duration in order to simultaneously limit the impact of the LFU treatment to the cell cluster disaggregation while avoiding any negative effect on the cell viability, in order to keep the cultures viable. According to the previous studies detailed in the Introduction section, the use of LFU pulses could help in disaggregating cellular aggregates of microalgae suspended in a liquid medium (Phull et al., 1997). Accordingly, we hypothesized that using ultrasound on the cyanobacterial cultures could allow greater accessibility of light and nutrients into the cultivated cells. Consequently, if there is no negative effect on the cell viability by the ultrasound, an improvement in growth could be expected which might be further advantageous for an eventual production process at a larger scale.

To verify whether the proposed hypothesis is valid, we performed a test to analyze whether the application of ultrasound pulses had any effect on the aggregation state of *Chroococcidiopsis* sp. culture samples in a liquid medium. Based on the obtained results, a second test was performed to study the effect of ultrasound on the growth and viability of *Chroococcidiopsis* sp. subjected to different durations of ultrasound pulse.

To test the expected ultrasound-mediated disaggregation effect in cyanobacterial aggregates, culture samples were subjected to LFU pulses of different duration. The evolution of the aggregation state of treated samples was assessed by following variations in optical density of the samples and comparing the obtained data with those of the non-treated samples. Procedure details are described in the Materials and Methods section.

Figure 7.3 shows the variation in the relative optical density, plotted versus the ultrasound pulse duration in culture samples of *Chroococcidiopsis* sp. Details of the relative optical density meaning are provided in the Materials and Methods section. The curve (Figure 7.3a) shows a linear increasing trend for ultrasound pulse duration lower than 3 min, after which a constant maximum value of relative optical density is reached. Accordingly, the optical microscopic pictures of *Chroococcidiopsis* sp. samples (Figure 7.3b) showed an increase in cellular disaggregation as increasing the ultrasound pulse duration, resulting in the maximum disaggregation after an ultrasound pulse duration of 3 min.

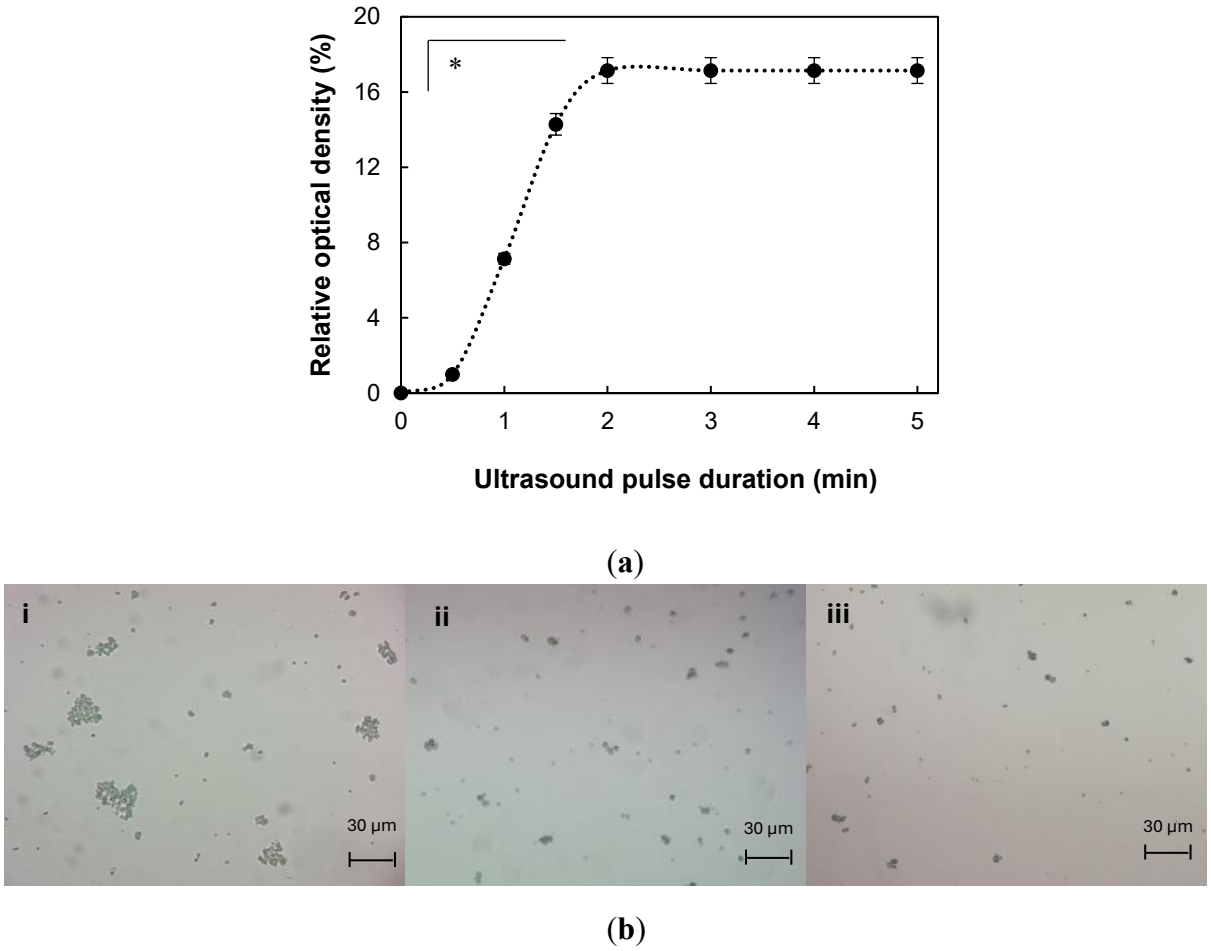

Figure 7.3. Variations in the relative optical density as a function of ultrasound pulse duration, expressed as a percentage, where 0.7 is the relative optical density (750 nm) value at time zero (**a**); Images of *Chroococcidiopsis* sp. obtained using the optical microscope (bright field) (**b**), for culture sample not subjected to ultrasound pulses (**i**), culture sample after ultrasound pulses of 3 (**ii**) and 5 min (**iii**). (*) Represents the significant differences of all treatments relative to the control cultures with 95 % confidence.

Once quantifying the impact of the pulse duration on the aggregation state of the cyanobacterial cell clusters, next figure analyzes the eventual impact of the ultrasound treatment on cyanobacterial growth and cell viability, measured as Quantum yield. Our results were useful in discussing the suggested hypothesis of enabling greater availability of nutrients and light to disaggregated cultures. Hence, we subjected the cultures to different durations of ultrasound pulses (Figure 7.4) according to the procedure described in the Materials and Methods section.

The variations in the maximal specific growth rate of *Chroococcidiopsis* sp. subjected to different durations of ultrasound pulse are shown in Figure 7.4a. According to the figure, specific growth rate of control culture and cultures subjected to ultrasound for 2 min began at a rate of 0.12 d^{-1}, approximately. From that ultrasound time on, a slight increase was observed in the growth rate of the cultures subjected to a pulse of 4 and 6 min duration, respectively, showing the highest value of approximately 0.13 d^{-1}, which was 14 % higher than the control rate.

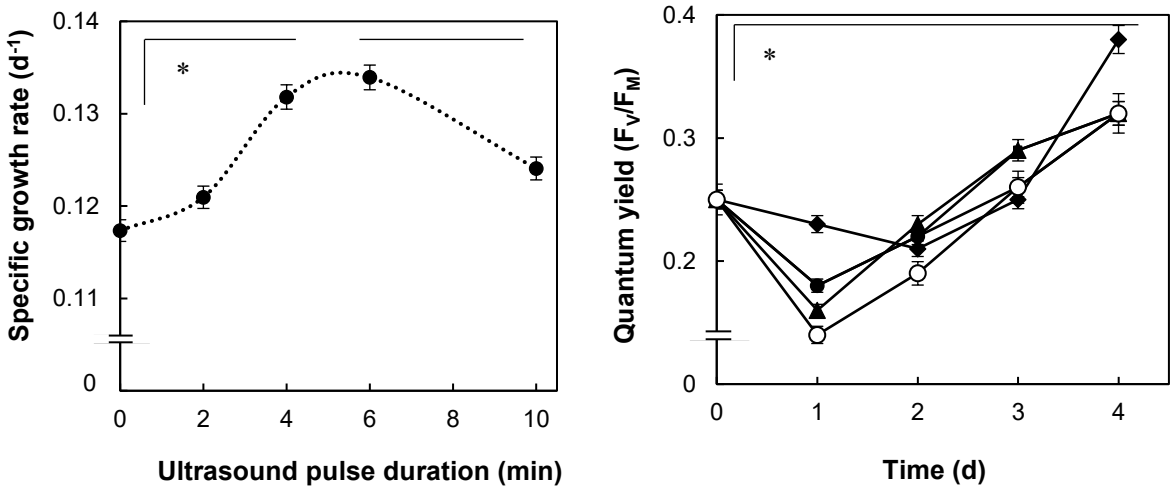

Figure 7.4. Effect of ultrasound pulse duration on the specific growth rate (**a**) and on the maximal photosynthetic efficiency of photosystem II (Quantum yield, F_V/F_M) along the cultivation time (**b**). Culture not subjected to ultrasound treatment (-♦-), and cultures subjected to ultrasound pulses of 2 min (-■-), 4 min (-▲-), 6 min (-●-), and 10 min (-○-). Error bars indicate standard deviation of three independent measurements. Procedure details are provided in the Materials and Methods section. (*) Represents the significant differences of all treatments relative to the control cultures with 95 % confidence.

Stable and productive growth is associated with the photosynthetic capability of cells and cell aggregates. To verify whether the application of ultrasound pulses did not cause the losses in cell viability of cyanobacterial cultures, the variations in the time-dependent evolution of the photochemical activity taking place in photosystem II (PSII) was analyzed in the samples of *Chroococcidiopsis* sp. cultures subjected to different durations of ultrasound pulses (Figure 7.4b). Details of the Quantum yield measurement and their meanings are provided in the Materials and Methods section. According to the Figure, the light photochemical usage by ultrasound-treated cultures seems to have the same efficiency as the control culture since the values obtained were between 0.2 and 0.4, which are typical of photosynthetically active cultures of cyanobacteria (Schuurmans et al., 2015; Zijffers et al., 2010). Only the early values of Quantum yield of ultrasound treated cultures, varying between 0.14 and 0.18, were considered lower than the expected values of healthy cyanobacterial cells.

Ultrasound treatment seems to have a positive effect on growth and viability of *Chroococcidiopsis* sp. This could partly be justified with the increase in the disaggregation state obtained. This hypothesis is discussed further in this Chapter (Discussion section).

3.2. Phylogenetic approach, and mixotrophic cultivation of the highly acidic habitat microalga Elliptochloris sp. for improving growth and lipid production

Elliptochloris sp. was isolated from the Tinto River, in the north of the Huelva province (site GPS coordinates: 37.72326, –6.55081) by the Microalgae Biotechnology Unit (BITAL), of the Department of Chemistry "Professor Jose Carlos Vílchez Martín," from the Faculty of Experimental Sciences of the University of Huelva. BLAST analysis of

18S rDNA sequences of the isolated microalga was performed to produce significant alignments (query cover, 99 %) with the sequences obtained from the isolated extremophilic microalga. The results indicated the presence of significant homology (> 80 %) with 17 sequences; 15 of them (approx. 90 %) belonged to the genus *Elliptochloris,* and only two belonged to the genus *Chloroidium*. The microscope images of the algae in culture collections showed robust morphological similarities with the isolated *Elliptochloris* species from Tinto River (Figure S7.1 of Supplementary Material). Based on the identification approach, we placed the isolated species into the genus *Elliptochloris*. A phylogenetic analysis showed that the isolated species could be included in the green algal class *Trebouxiophyceae*. In the 18S rDNA tree (Figure 7.5), *Elliptochloris* sp. was placed close to *Coccomyxa onubensis* and *Pseudococcomyxa simplex*, which also belong to the class *Trebouxiophyceae.*

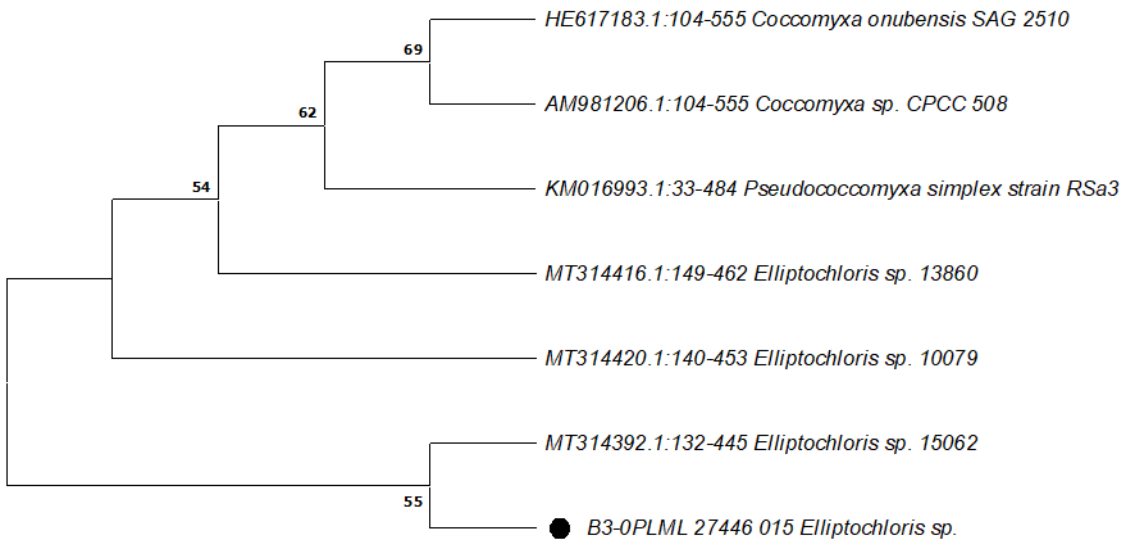

Figure 7.5. Molecular phylogeny of *Elliptochloris* sp. based on 18S rDNA gene sequence comparisons of the genus Elliptochloris. More details in Materials and Methods section.

In photoautotrophic cultures, an increase in the number of cells led to a shadowing effect among cells, which limits growth due to a reduction in available light (Richmond, 2003). The use of an organic carbon source (OCS) can satisfy the energy requirements for growth; thus, photosynthetically produced energy demand can decrease significantly. Based on this, mixotrophic growth of the highly acidic-habitat microalga *Elliptochloris* sp. bubbled with either air alone or air containing 2.5 % (v/v) CO_2 was analyzed and compared to photoautotrophic growth.

The time-dependent evolution of the growth of *Elliptochloris* sp. as a function of the carbon source is shown in Figure 7.6. The figure growth curves obtained were completed in about 16 days and showed a typical linear growth shape rather than the typical sigmoidal growth pattern with exponential and stationary phase. The growth curves obtained for mixotrophic cultivation bubbled with CO_2-enriched air (Figure 7.6a) showed less steep trends than those obtained for the photoautotrophic culture. Conversely, the curves obtained from cultures subjected to mixotrophic cultivation

bubbled with air alone (Figure 7.6b) showed steeper trends than those obtained for the culture grown only on air. That is, the growth rates obtained under these conditions were approximately 80 % lower than those obtained for the photoautotrophic culture bubbled with CO_2-enriched air.

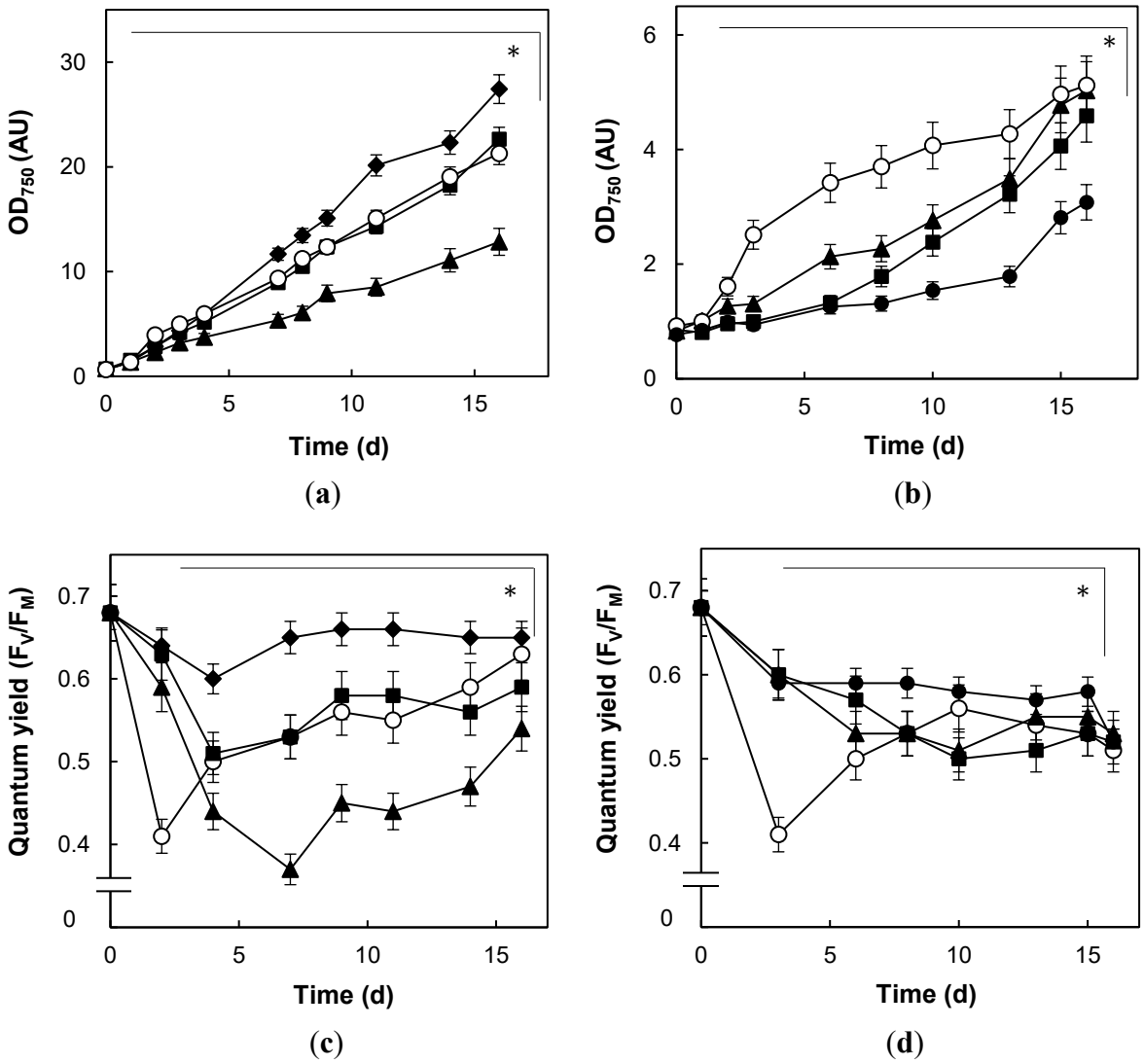

Figure 7.6. Growth curves and photosynthetic efficiency of PSII, measured as maximum quantum yield (F_V/F_M), of the acidotolerant microalga *Elliptochloris* sp. as a function of the carbon source in cultures bubbled with CO_2 (**a**,**c**) or air alone (**b**,**d**). Symbols represent: Photoautotrophic (-◆-), technical glycerin from vegetal residues (-■-) and from UCO residues (-▲-), glucose (-○-) and air (-●-). (*) Represents the significant differences of all treatments with respect to the photoautotrophic culture with 95 % confidence.

As reported above, the use of an OCS can satisfy the energy requirements for growth; thus, photosynthetically produced energy demand can decrease significantly. Based on that, the effect of the carbon source on photosynthetic efficiency is shown in Figure 7.6c and 7.6d, based on the Quantum yield (Qy) data of *Elliptochloris* sp. Cultures grown mixotrophically showed a decrease in the Qy values till 0.4–0.5 during the first few days of growth, i.e., up to the middle of the linear phase, day 4 of cultivation. After that, all mixotrophic cultures showed higher Qy values of about 0.6.

As reported in the Introduction section, the use of an OCS in microalgae promotes fatty acid biosynthesis in the chloroplast. Thus, we investigated the effect of using additional OCS –glycerin or glucose– bubbled with either air alone or air containing 2.5 % (v/v) CO_2 on the production of lipids and fatty acids in *Elliptochloris* sp.

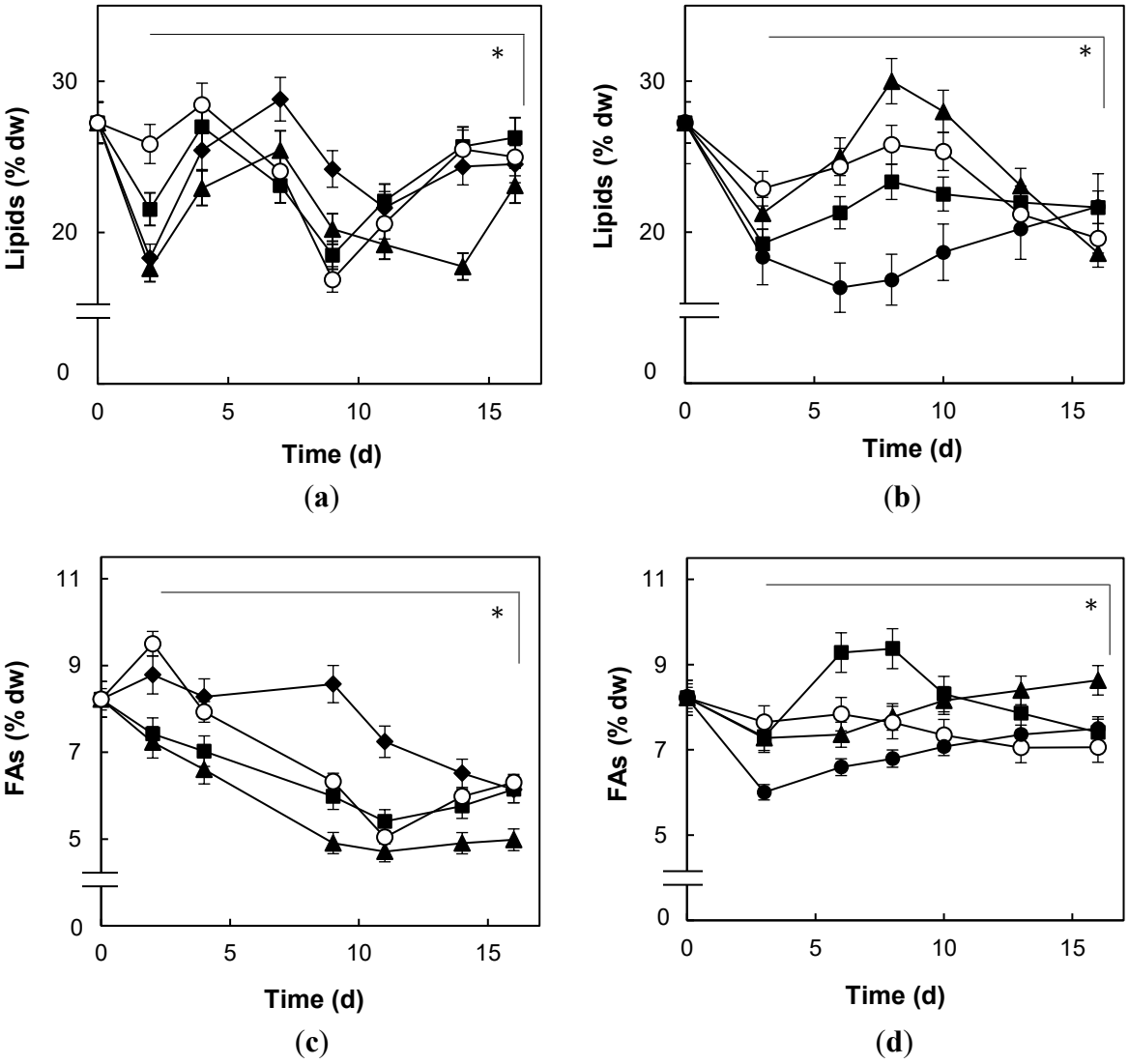

Figure 7.7. Intracellular content of lipids and fatty acids (FAs) produced for the microalga *Elliptochloris* sp. as a function of the carbon source in cultures bubbled with CO_2 (**a**, **c**) or air alone (**b**, **d**). Symbols represent: Photoautotrophic (-◆-), technical glycerin from vegetal residues (-■-) and from UCO residues (-▲-), glucose (-○-) and air (-●-). (*) Represents the significant differences of all treatments with respect to the photoautotrophic culture with 95 % confidence.

The evolution of intracellular lipids and fatty acids (FAs) as a function of the carbon source for cultures of *Elliptochloris* sp. is shown in Figure 7.7. We found that the intracellular lipid content in cultures grown mixotrophically and bubbled with CO_2-enriched air (Figure 7.7a) remained within a range of about 20 to 30 % of the total biomass and varying within this range along the culture incubation time. These variations are significant and could be related with metabolic adjustments in response to variations in key growth parameters along the batch-mode incubation, e.g. light availability due to increased cell density and, decreased availability of key nutrients by

the end of the curve (Alishah et al., 2019). A similar pattern was recorded for mixotrophically grown cultures bubbled with air alone (Figure 7.7b), except for the culture grown with technical glycerin obtained from UCO residues; this culture showed an increase in the intracellular lipid content of about 40 % during the first few days of growth, day 6–8 of cultivation, followed by a decrease in the lipid content to initial levels in the later stages obtaining a content of, approximately, 22 % dw. Under this condition, the highest content of intracellular lipids was obtained by day 8, approximately, 30 % dw, 48 % higher than that recorded in the photoautotrophic culture.

The intracellular content of fatty acids showed a different trend depending on whether the cultures grew mixotrophically bubbled with air alone or CO_2-enriched air. Cultures grown mixotrophically with CO_2-enriched air (Figure 7.7c) showed a decrease in the intracellular concentration of about 25–40 % FAs until, approximately, day 10 of cell culture; after that day the FA content remained unchanged, approximately, 6 % dw. In contrast, the intracellular FA content of cultures grown mixotrophically bubbled with air alone (Figure 7.7d) increased moderately after the first days of cultivation, day 3; and the highest data, approximately 9.3 % dw, 26 % higher than that obtained for the photoautotrophic culture, were obtained from the culture grown with technical glycerin obtained from vegetal residues. The composition of specific FAs of biomass samples from the different cultures was also analyzed (Figure 7.8).

The content of saturated fatty acids (SAFAs) increased about 20 % in the mixotrophic cultures bubbled with CO_2-enriched air (Figure 7.8a) till day 4 (approximately), obtaining values of, approximately, 2.3 % dw. Then, the content of SAFAs acids decreased considerably about 30–40 %. The intracellular content of UFAs (Figure 7.5c) decreased about 30–50 % till day 9 of cultivation, and then, their content remained unchanged of, approximately, 3.36 % dw. The changes in the content of these compounds in mixotrophic cultures bubbled with air alone were different. In general, the content of SAFAs (Figure 7.8b) increased moderately about 10–20 %, obtaining the highest value, approximately, 2.5 % dw, on day 8 from the culture grown with the technical glycerin from vegetal residues. However, the content of UFAs remained constant throughout the culture in almost all conditions (Figure 7.8d), approximately, 4.5 % dw. In contrast, in photoautotrophic cultures, the content of UFAs remained stable during the first few days of growth till day 9 of cultivation of, approximately, 5 % dw, that the content decreased about 30 % and was lower than that recorded in mixotrophic cultures.

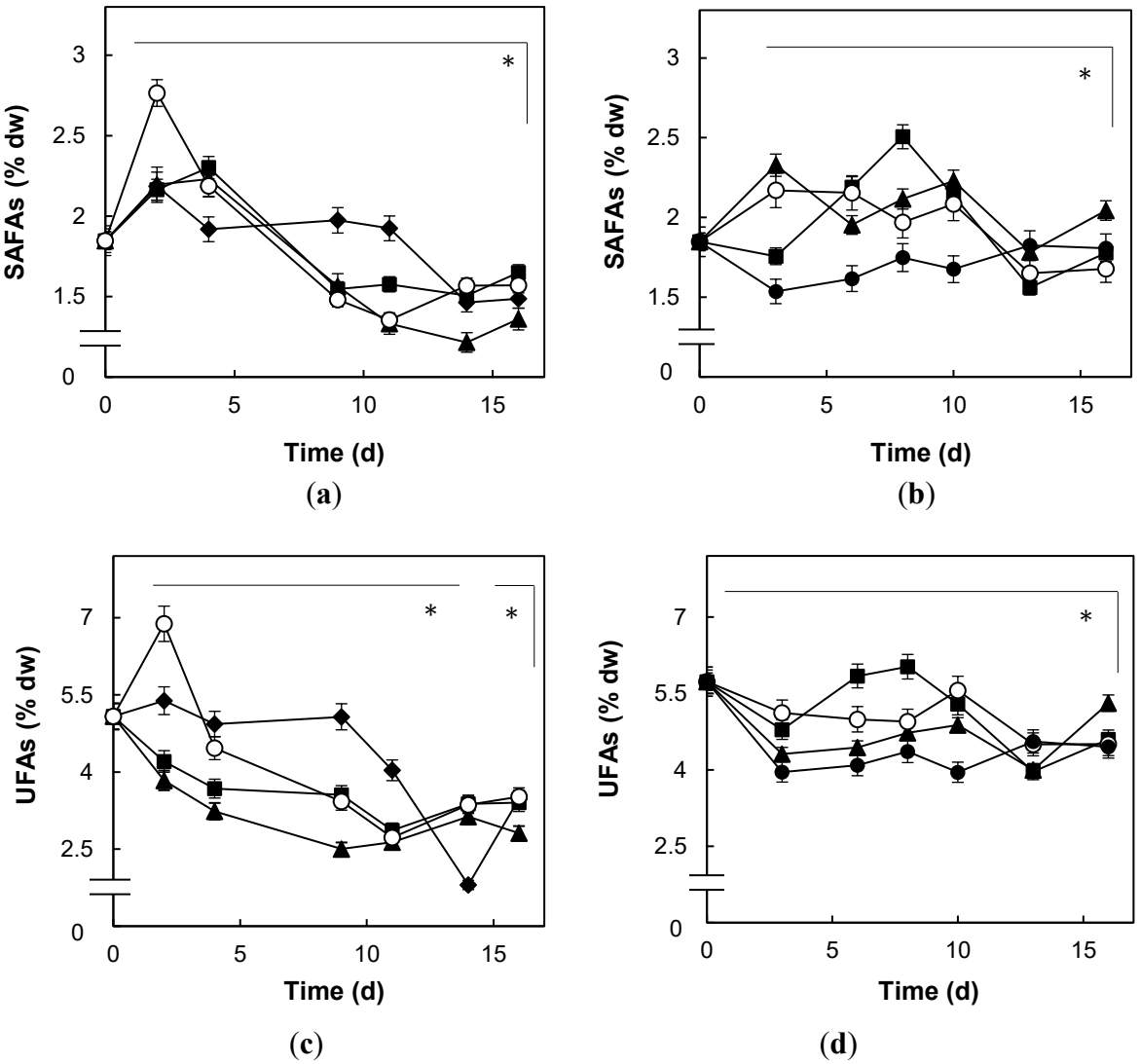

Figure 7.8. Time-dependent evolution of saturated (SAFAs) and unsaturated (UFAs) fatty acids content produced by the microalga *Elliptochloris* sp. as a function of the carbon source in cultures bubbled with CO_2 (**a**, **c**) or air alone (**b**, **d**). Symbols represent: Photoautotrophic (-◆-), technical glycerin from vegetal residues (-■-) and from UCO residues (-▲-), glucose (-○-) and air (-●-). (*) Represents the significant differences of all treatments with respect to the photoautotrophic culture with 95 % confidence.

Cultivation of *Elliptochloris sp.* cells with an OCS in presence or absence of CO_2 influences microalgal growth and the fatty acid profile. The main variations obtained as a function of the carbon source are commented and discussed in the discussion section.

4. Discussion

4.1. Effect of ultrasound treatment on the aggregation of the extremotolerant cyanobacterium Chroococcidiopsis sp. for improving growth

The development of cyanobacterial blooms in water bodies imparts undesirable characteristics to the water due to the potential presence of toxins (Rajasekhar et al., 2012). Several chemical and physical methods have been used to control the blooms, but have limitations in terms of pollution and application on a large scale (Lee et al., 2001). The application of ultrasound pulses to cyanobacterial suspensions has shown efficacy in controlling aggregates (Joyce et al., 2010; Wu et al., 2011). Ultrasound treatment can lead to structural and functional disruption of cyanobacterial cells (Phull et al., 1997) and its use as a treatment option to control cyanobacterial blooms has been under consideration in recent decades. However, only a few works have addressed the potential of ultrasound to improve microalgal growth (Joyce et al., 2014). This might be useful for species which grow forming aggregates, then eventually requiring higher energy inputs for agitation and having less light and nutrients availability. The rationale behind our work is minimizing the energy of the ultrasound pulses applied to cyanobacterial aggregates in liquid cultures. The aim is to use only the energy required to split the cyanobacterial outer polysaccharide sheath over the cell membrane while avoiding cell disruption, thus promoting cell disaggregation. Based on this concept, we studied in culture flasks the efficacy of low-frequency ultrasound (LFU) in cell disaggregation as a treatment to eventually improve the productivity of the extremotolerant cyanobacterium *Chroococcidiopsis* sp. liquid cultures.

The results indicated a direct relationship between the duration of the applied ultrasound pulses and the increase in the optical density value of ultrasound-treated samples. We attribute this relationship to the disaggregation caused by the ultrasound treatment in the cell aggregates, which was evidenced by the optical microscopic photographs (Figure 7.3b). In a more disaggregated sample of liquid culture, the cell suspension becomes homogeneously distributed with an increase in the number of single cells and smaller aggregates. An increased density of cell entities in the ultrasound-treated samples interferes with the light passage in the spectrophotometer cuvette, resulting in a higher spectrophotometer reading, so-called turbidity (Figure 7.3a). The key aspect of this work is that a minimum ultrasound pulse time that ensures cell disaggregation, of about 3 min, could be defined.

As expected, our data supported the positive impact of modulated ultrasound pulses on the growth of *Chroococcidiopsis* sp. cultures. The ultrasound-mediated cultures increased disaggregation evidenced by the optical microscopic observations. This led *Chroococcidiopsis* sp. cells to experience greater light and nutrient accessibility in liquid cultures, cells that previously occupied inner positions in the large *Chroococcidiopsis* sp. cell clusters before the ultrasound treatment. The data obtained on the efficiency of the photochemical processes, in turn, demonstrated that the ultrasound treatment with the optimized duration of the pulse did not affect cell viability, i.e. the photosynthetic efficiency (Qy) values obtained were within the range of values typical for cyanobacteria

in liquid cultures (Schuurmans et al., 2015). The decrease in the Qy data after the first 24 h (Figure 7.4b) is a common situation for the cultures adapting to the new conditions. Additionally, in this study, we hypothesized that the initial decrease in Qy for ultrasound-treated cultures was due to the cells being more disaggregated. Therefore, the cells experienced a more intense light exposure compared to the cells in non-disaggregated cell clusters, which needed to acclimatize to the newly experienced light conditions. Such acclimatization process can be temporarily linked to a less productive photochemical yield of the photosynthetic light fixation process (Richmond, 2003). The sudden increase in the light intensity experienced by the individual cells derived from the ultrasound-mediated disaggregation of *Chroococcidiopsis* sp. could be the reason behind the Qy decrease, and the later increase of Qy to regular values is on favor of this argument.

The natural aggregation of *Chroococcidiopsis* sp. can favor the economy of the harvesting process since larger particle size eases sedimentation or flocculation techniques, saving energy costs compared to centrifugation (Fasaei et al., 2018). However, additional energy costs may be required to keep cultures of large size aggregates in liquid medium homogeneously mixed (Montero-Lobato et al., 2020). Meanwhile, since the light and nutrients in principle may be less accessible to the inner cells of the aggregates, maximal biomass productivity cannot be achieved as well. In this sense, two possible cultivation strategies could be discussed for the eventual effective production of *Chroococcidiopsis* sp. at a pilot scale which would help in deciding production conditions that can lead to savings in process costs.

4.2. Phylogenetic approach, and mixotrophic cultivation of the highly acidic habitat microalga Elliptochloris sp. for improving growth and lipid production

As indicated in the Materials and Methods section, *Elliptochloris* sp. was isolated from Tinto River. The so-called “red river” is one of the most extensive examples of extreme acidic environments, exhibiting low pH values in the range of 1.7 to 3.1 and presence of cations in solution, of which Fe (II) and (III) and Cu (II) have a relevant quantitative presence (Amils et al., 2014; Fernández-Remolar et al., 2003).

Elliptochloris is a genus of *Chlorophyta* similar to *Chlorella* and is closely related to the genus *Coccomyxa* (Darienko et al., 2016). Members of this group have spherical and elliptical cells, possess bilobed chloroplasts with or without pyrenoid, and produce two types of auto-spores, which are used for a unique type of reproduction (Darienko et al., 2016; Eliáš et al., 2008; Gustavs et al., 2011). This genus was first described by Tschermak-Woess (1988) based on the species *E. bilobata*. Species belonging to this genus are widely distributed throughout the world. They are found in terrestrial habitats in free-living form or as a photobiont with lichens (Darienko et al., 2016). Members of the genus *Elliptochloris* are difficult to identify because of their flexible phenotype and lack of characteristic features. According to Gustavs et al. (2011), algae belonging to this group contain high concentrations of ribitol, a type of polyol, which plays a protective role and helps these microorganisms adapt to extreme environments. Our experience with *Elliptochloris* sp. cultures allowed us to state that this strain is able to grow at around neutral pH, thus it behaves as an acidotolerant strain. Previous

experiments (data not published) of growth at pH between 2.5 to 7 showed slight differences in biomass productivity as a function of the pH value. Nevertheless, the highest productivity was obtained at pH 4. Microscopic observations revealed increased presence of a fungus at around neutral pH. Further communities' abundance analysis would be required for understanding any eventual relationship between the strain of this study and any other associated community.

As this study intended to grow *Elliptochloris* sp. in a majoritarian form, a pH of 2.5 was selected as it allows obtaining moderate productivities whilst growth of any associated and non-associated microorganism is neglected. Because of this species ability to grow under acidic conditions which limits the growth of opportunist heterotrophic organisms in the presence of an organic carbon source, we selected it to conduct this study.

As observed in Figure 7.6, *Elliptochloris* sp. growth curve shows a linear growth shape rather than the typical sigmoidal growth pattern with exponential and stationary phases. Biomass concentration was not low enough to obtain a clear and visible adaptation phase, and the duration of this experiment was not long enough to obtain a stationary phase. The observed linear growth, rather than exponential growth, is the result of each cell having fewer photons per unit of time as long as growth progresses. The reason is that the light intensity provided to the cultures does not vary throughout growth, while there is an increase in the number of cells in the culture. In this way, a shielding effect of some cells on others occurs, limiting the availability of light for each cell (Richmond, 2003). The lower light availability per unit of time results in a lower activity of photosynthesis, therefore a lower rate of production of NADPH and ATP, necessary for cell growth. However, this lower light bioavailability does not seem to affect growth significantly. The reason is that the growth rates of *Elliptochloris* sp., around 0.8 $g \cdot L^{-1} \cdot d^{-1}$ (data not published), are in the range of those recorded for Chunzhuk et al. (2023) for a non-extremophilic *Elliptochloris subsphaerica* and other non-extremophilic microalgae (Richmond, 2003). Microalgal blooms have been described to occur at a depth of 8-10 m below of the acidic lakes in the Pyritic Belt of Huelva (Spain) surface (Sánchez-España et al., 2020) where only PAR radiations of low wavelengths PAR are available to the microalgal cells. Thus, this natural behavior is coherent with the linear growth phase obtained for *Elliptochloris* sp. regardless of light intensity availability.

The results obtained in Figure 7.6 showed that *Elliptochloris* sp. could assimilate an OCS. This was inferred by comparing the growth patterns of mixotrophic cultures supplemented with an OCS and bubbled with air to those of cultures supplied only with air. Our findings indicated that CO_2 strongly influenced the growth rate of *Elliptochloris* sp. Thus, the growth patterns obtained when supplementing the cultures with an OCS can be improved greatly by supplementing the cultures with CO_2. However, the maximum growth rate was recorded in cultures grown under photoautotrophic conditions. This finding showed that adding an OCS to cultures growing under conditions of standard light intensity and CO_2 concentration could partly slow down the growth of *Elliptochloris* sp. Mixotrophic growth is a commonly used strategy to

counteract the slow growth in photoautotrophic cultures because of the limited availability of light. However, adding an extra OCS affects the growth of some species negatively, probably because assimilating the extra carbon source might lead to temporary metabolic imbalances, resulting in the partial inhibition of growth (Paranjape et al., 2016). This might occur due to the combination of two biochemical events, including slow uptake rates and/or assimilation of the OCS and, low photosynthetic activity (Markou et al., 2021).

Generally, an increase in CO_2 concentrations increases the photosynthesis rate in microalgae (Martínez and Orús, 1991), which leads to a greater production of carbohydrates and biomass. This finding matched the increase in the growth and photosynthetic efficiency of the photoautotrophic cultures when compared with the culture supplied with only air (Figure 7.6). The PSII photosynthetic efficiency of healthy cultures should be around 0.6 – 0.7, which generally indicates that the culture is not under stress and is viable (Maxwell and Johnson, 2000; Zijffers et al., 2010). Some of the Qy values obtained in mixotrophic cultures were significantly below 0.6, even when supplemented with CO_2 which, as reported above, led to an increase in the photosynthesis rates. This finding could be justified by the lower photosynthesis-related energy needs for nutrient assimilatory reduction, as most of the anabolic energy needs can be obtained by oxidizing the OCS added to the culture medium (Castillo et al., 2021). These processes can lead to the partial inhibition (or downregulation) of the light energy bioconversion cell machinery, which might be indicated by a decrease in the photosynthetic efficiency of PSII. Consequently, resulting in a lower reading of the Quantum yield parameter, which matches the findings of our study. As the OCS was only supplied at the beginning of the experiment, the increase in the Qy values for mixotrophic cultures from the middle of the linear growth phase occurred probably because of the lower bioavailability of the OCS.

As shown above, for cultures supplemented with an OCS, part of the light energy fixed through photosynthesis in the form of NAD(P)H may not be utilized for the assimilation of nutrients (Figure 7.6); under such conditions, this excess chemical energy might be oxidized by reactive oxygen species (ROS) formed in the chloroplast (Hasanuzzaman et al., 2020). One of the metabolic capacities of microalgae to dissipate excess reducing power, i.e., chemical energy from the photosynthetic fixation of light energy, is to divert excess NAD(P)H to the synthesis of triacylglycerides (TAG); using this strategy, they can store carbon and energy in the chemical form of fatty acids (Schüler et al., 2017). Additionally, part of the acetyl-CoA derived from the oxidative degradation of the OCS can be diverted to the production of fatty acids using excess NAD(P)H (Poddar et al., 2020). The use of excess NAD(P)H might help in maintaining the balance between the reduced and oxidized forms of this coenzyme ($NAD(P)H/NAD^+$) in cells.

Based on this fact, the excess energy from light and organic carbon provided to the cultures in mixotrophic cultures probably led to the overproduction of NADPH. Consequently, the production of ROS could be stimulated, therefore, increasing oxidative stress. This could be the case of the mixotrophic cultures bubbled with only

air, in which a part of the photosynthetic energy produced could not be utilized for fixing CO_2. This might lead to an excess production of NADPH for the available CO_2, which as presented in Figure 7.7d was stored in the form of fatty acids to maintain the balance between NADPH and $NADP^+$ levels in the cells. Conversely, mixotrophic cultures bubbled with CO_2-enriched air had lower photosynthetic efficiency (Figure 7.6c), which might decrease the production of NADPH. Therefore, the decrease in the intracellular fatty acid content in mixotrophic cultures bubbled with CO_2-enriched air (Figure 7.7c) could be justified by the lower production of NADPH through photosynthetic process, as needs of reducing power decrease if OCS are available by the cells.

The ratio of the saturated to unsaturated fatty acid content was constant throughout the experiment and independent of the carbon source used (Figure S7.2 of Supplementary Material). Thus, the addition of CO_2 did not affect the ratio of total saturated to unsaturated fatty acids. Then, by analyzing the total content of saturated and unsaturated fatty acids, we found that the air-bubbled mixotrophic cultures generally produced greater intracellular content of both saturated and unsaturated fatty acids than photoautotrophic cultures. This was shown in Figure 7.8 and Figure S7.3 of Supplementary Material. Figure S7.3 resumes the average relative variation with respect to photoautotrophic cultures of total saturated (black bar) and unsaturated (white bar) fatty acid content throughout the cultivation period in any of the mixotrophic conditions tested. The figure shows that the use of OCS and air alone enhanced the accumulation of fatty acids (dry biomass basis).

Additionally, the changes described suggested that the behavior of mixotrophic cultures of *Elliptochloris* sp. under high CO_2 throughout the growth phase was similar to that of cultures exposed to oxidative stress, irrespective of whether OCS was added. We found that the content of unsaturated fatty acids decreased. This might occur partly because of the involvement of unsaturated fatty acids in the neutralization of ROS, which leads to a decrease in the level of unsaturation due to lipid peroxidation. This led to the production of conjugated dienes, lipids with peroxyl radicals, and hydroperoxides (Smirnoff, 2000). The slight increase in saturated fatty acid content in these cultures was consistent with a greater expression of reducing power dissipation mechanisms, which helped maintain the $NAD(P)H/NAD(P)^+$ ratio in the cells and decrease oxidative stress (Schüler et al., 2017).

The growth of aerobic opportunist heterotrophs is limited under the extreme pH conditions in which *Elliptochloris* sp. thrives. In fact, the referred eventual advantage was already proven for *Coccomyxa onubensis*, a highly acidic environment strain isolated by our lab from Tinto river, when grown under non-sterile conditions in an outdoor tubular PBR (Fuentes et al., 2020). Due to these reasons, *Elliptochloris* sp., a highly acidic-habitat microalga, is a promising candidate as a novel bioresource for the production of microalgal biomass within the circular economic model. Regarding costs and sustainability, the value of crude technical glycerin might increase when it is used as a carbon source for synthesizing fatty acids (raw material for biodiesel production). We found similar results when glycerin was added as a carbon source to cultures of the acidotolerant autochthonous microalga *Elliptochloris* sp.

5. Conclusions

The findings of this Chapter revealed the significant potential of extremophilic photosynthetic microorganisms for efficient biomass production and accumulation of valuable molecules. On the one hand, several strategies could be performed to increase *Chroococcidiopsis* sp. growth. Low-frequency ultrasound is effective in producing disaggregation of *Chroococcidiopsis* sp. cells clusters, making it an effective way according to our results. Disaggregation increases the homogeneity of suspension cultures, reducing the energy requirements for culture agitation. In addition, cyanobacterial growth has been proven greater in disaggregated cultures, based on a demonstrated greater availability of light and, expectedly, nutrients. Overall, the adequate modulation of LFU pulses to cyanobacterial aggregated cultures should be considered as a valuable strategy to improved growth and save agitation energy costs. On the other hand, the use of CO_2 along with technical glycerin affects growth and fatty acid production in the autochthonous acidotolerant microalga *Elliptochloris* sp. We suggest two cultivation strategies for the effective production of *Elliptochloris* sp. First, mixotrophy in CO_2-enriched air allows higher biomass productivity, but metabolic imbalances can decrease the content of fatty acids and increase the relative abundance of saturated fatty acids. Second, mixotrophy in air alone can increase the content of both saturated and unsaturated fatty acids but biomass productivity decreases. These strategies can further determine the application of *Elliptochloris* sp. for biofuel or production of food supplements. Overall, the results presented in this chapter demonstrate the significant potential for enhancing the growth of extremophilic photosynthetic microorganisms, which have traditionally been regarded as less efficient for biomass production compared to non-extremophilic species. Intensive research into their physiology, biochemistry, genomics, proteomics, and process engineering is expected to reveal their considerable biotechnological potential.

6. Supplementary material

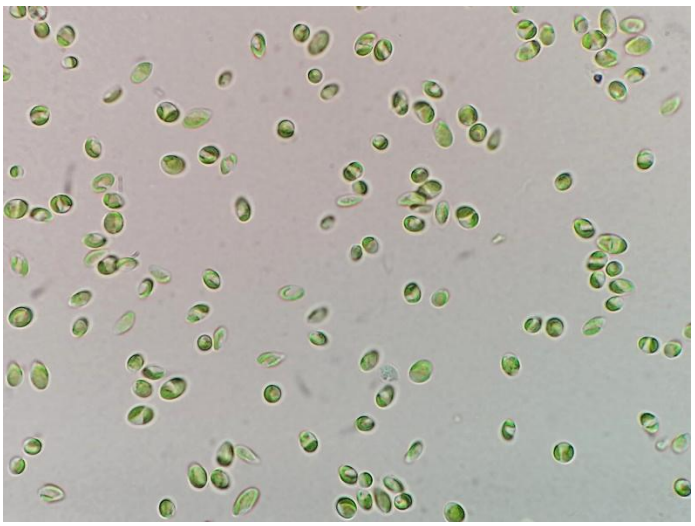

Figure S7.1. Picture of *Elliptochloris* sp. taken under the optic microscope (magnification, 100x).

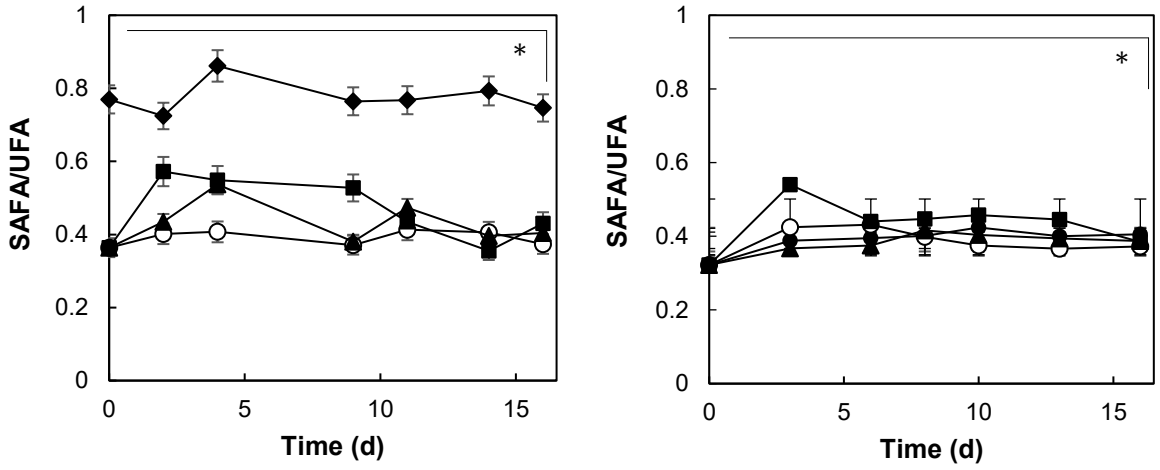

Figure S7.2. Time-dependent evolution of the saturated/insaturated fatty acids ratio produced by the microalga *Elliptochloris* sp. as a function of the carbon source in cultures bubbled with CO_2 (a) or air alone (b). Symbols represent: Photoautotrophic (-◆-), technical glycerin from vegetal residues (-■-) and from UCO residues (-▲-), glucose (-○-) and air (-●-). (*) Represents the significant differences of all treatments with respect to the photoautotrophic culture with 95% confidence.

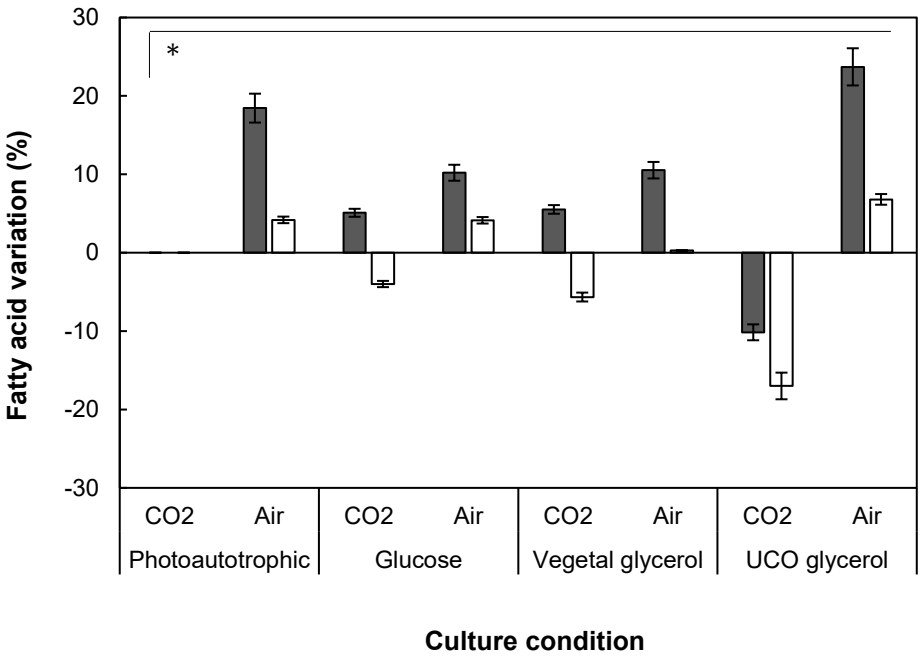

Figure S7.3. Relative variation, with respect to photoautotrophic cultures, of total saturated (black bar) and unsaturated (white bar) fatty acid content, expressed as a percentage, of *Elliptochloris* sp. biomass throughout the cultivation period in any mixotrophic condition. The presented values represent the fatty acid content variation, in percentage, between the start and the end part of the experiment (values at time zero, and average values in the period day 13-day 16). In the graph, data 0 of photoautotrophic culture corresponds to an average content of saturated and unsaturated fatty acids of -20.141 and -25.594 %, respectively. (*) Represents the significant differences of all treatments with respect to the photoautotrophic culture with 95% confidence.

Statistical analysis Figure 7.6

Table S7.1. Growth of *Elliptochloris* sp. as a function of carbon source in CO_2 bubbled cultures.

Time (d)	Photoautot. CO_2	Glycerin Veg.	Glycerin UCO	Glucose
0	0.63^{c}	0.69^{b}	0.72^{a}	0.64^{c}
1	1.39^{b}	1.53^{a}	1.36^{c}	1.34^{d}
2	2.84^{b}	2.84^{b}	2.29^{c}	3.95^{a}
3	4.36^{b}	4.19^{c}	3.20^{d}	4.99^{a}
4	5.95^{a}	5.15^{b}	3.72^{c}	5.96^{a}
7	11.66^{a}	8.94^{c}	5.38^{d}	9.36^{b}
8	13.44^{a}	10.49^{d}	6.08^{b}	11.21^{c}
9	15.10^{a}	12.34^{b}	7.92^{c}	12.34^{b}
11	20.14^{a}	14.32^{c}	8.51^{d}	15.10^{b}
14	22.32^{a}	18.24^{b}	11.08^{d}	19.04^{c}
16	27.42^{a}	22.64^{b}	12.84^{d}	21.28^{c}

[a, b, c, d.] Different superscript letters indicate differences in treatments with a significance of $p < 0.05$.

Table S7.2. Growth of *Elliptochloris* sp. as a function of carbon source in air bubbled cultures.

Time (d)	Photoautot. air	Glycerin Veg.	Glycerin UCO	Glucose
0	0.77^{d}	0.85^{b}	0.83^{c}	0.92^{a}
1	0.84^{c}	0.81^{d}	1.01^{a}	0.99^{b}
2	0.98^{c}	0.96^{d}	1.27^{b}	1.61^{a}
3	0.94^{d}	1.00^{c}	1.31^{b}	2.51^{a}
4	1.26^{d}	1.32^{c}	2.13^{b}	3.42^{a}
7	1.31^{d}	1.79^{c}	2.27^{b}	3.70^{a}
8	1.54^{d}	2.38^{c}	2.76^{b}	4.07^{a}
9	1.78^{d}	3.22^{c}	3.49^{b}	4.27^{a}
11	2.81^{d}	4.06^{c}	4.77^{b}	4.96^{a}
14	3.08^{d}	4.59^{c}	5.03^{b}	5.12^{a}

[a, b, c, d.] Different superscript letters indicate differences in treatments with a significance of $p < 0.05$.

Table S7.3. Photosynthetic efficiency of *Elliptochloris* sp. as a function of carbon source in CO_2 bubble cultures.

Time (d)	Photoautot. CO_2	Glycerin Veg.	Glycerin UCO	Glucose
0	0.68^{a}	0.68^{a}	0.68^{a}	0.68^{a}
2	0.64^{a}	0.63^{a}	0.59^{b}	0.41^{c}
4	0.60^{a}	0.51^{b}	0.44^{c}	0.50^{b}
7	0.65^{a}	0.53^{b}	0.37^{c}	0.53^{b}
9	0.66^{a}	0.58^{b}	0.45^{c}	0.56^{b}
11	0.66^{a}	0.58^{b}	0.44^{c}	0.55^{b}
14	0.65^{a}	0.56^{b}	0.47^{c}	0.59^{b}
16	0.65^{a}	0.59^{c}	0.54^{d}	0.63^{b}

[a, b, c, d.] Different superscript letters indicate differences in treatments with a significance of $p < 0.05$.

Table S7.4. Photosynthetic efficiency of *Elliptochloris* sp. as a function of carbon source in air bubble cultures.

Time (d)	Photoautot. air	Glycerin Veg.	Glycerin UCO	Glucose
0	0.68^{a}	0.68^{a}	0.68^{a}	0.68^{a}
2	0.59^{b}	0.60^{a}	0.60^{a}	0.41^{c}
4	0.59^{b}	0.57^{b}	0.53^{c}	0.61^{a}
7	0.59^{a}	0.53^{b}	0.53^{b}	0.53^{b}
9	0.58^{a}	0.50^{b}	0.51^{b}	0.56^{a}
11	0.57^{a}	0.51^{b}	0.55^{a}	0.54^{b}
14	0.58^{a}	0.53^{b}	0.55^{a}	0.53^{b}
16	0.52^{a}	0.52^{a}	0.53^{a}	0.51^{a}

[a, b, c, d.] Different superscript letters indicate differences in treatments with a significance of $p < 0.05$.

Statistical analysis Figure 7.7

Table S7.5. Intracellular lipid content of *Elliptochloris* sp. as a function of carbon source in CO_2 bubbled cultures.

Time (d)	Photoautot. CO_2	Glycerin Veg.	Glycerin UCO	Glucose
0	27.26^{a}	27.26^{a}	27.26^{a}	27.26^{a}
2	18.32^{c}	21.55^{b}	17.63^{d}	25.86^{a}
4	25.44^{c}	27.00^{b}	22.94^{d}	28.46^{a}
7	28.82^{a}	23.12^{d}	25.45^{b}	24.06^{c}
8	24.20^{a}	18.50^{c}	20.24^{b}	16.90^{d}
9	21.63^{b}	22.10^{a}	19.20^{d}	20.60^{c}
11	24.37^{c}	25.10^{a}	17.75^{d}	25.50^{b}
14	24.52^{c}	26.28^{a}	23.11^{d}	25.00^{b}

[a, b, c, d.] Different superscript letters indicate differences in treatments with a significance of $p < 0.05$.

Table S7.6. Intracellular lipid content of *Elliptochloris* sp. as a function of carbon source in air bubbled cultures.

Time (d)	Photoautot. air	Glycerin Veg.	Glycerin UCO	Glucose
0	27.26^{a}	27.26^{a}	27.26^{a}	27.26^{a}
2	18.36^{d}	19.24^{c}	21.24^{b}	22.89^{a}
4	16.33^{d}	21.29^{c}	25.00^{a}	24.34^{b}
7	16.86^{d}	23.33^{c}	30.00^{a}	25.79^{b}
8	18.67^{d}	22.53^{c}	28.00^{a}	25.35^{b}
9	20.23^{d}	21.96^{b}	23.07^{a}	21.18^{c}
11	21.70^{a}	21.65^{b}	18.61^{d}	19.59^{c}

[a, b, c, d.] Different superscript letters indicate differences in treatments with a significance of $p < 0.05$.

Table S7.7. Intracellular fatty acid content of *Elliptochloris* sp. as a function of carbon source in CO_2 bubbled cultures.

Time (d)	Photoautot. CO_2	Glycerin Veg.	Glycerin UCO	Glucose
0	8.22^{a}	8.22^{a}	8.22^{a}	8.22^{a}
2	8.78^{c}	7.42^{b}	7.23^{b}	9.50^{a}
4	8.28^{d}	7.03^{a}	6.60^{c}	7.93^{b}
7	8.57^{d}	5.98^{a}	4.91^{b}	6.33^{c}
8	7.24^{d}	5.41^{a}	4.71^{b}	5.04^{c}
9	6.51^{c}	5.76^{b}	4.90^{a}	5.98^{d}
11	6.14^{b}	6.14^{c}	4.98^{a}	6.30^{d}

[a, b, c, d.] Different superscript letters indicate differences in treatments with a significance of $p < 0.05$.

Table S7.8. Intracellular fatty acid content of *Elliptochloris* sp. as a function of carbon source in air bubbled cultures.

Time (d)	Photoautot. air	Glycerin Veg.	Glycerin UCO	Glucose
0	8.22^{a}	8.22^{a}	8.22^{a}	8.22^{a}
2	6.00^{b}	7.30^{c}	7.28^{d}	7.65^{a}
4	6.59^{a}	9.28^{c}	7.36^{d}	7.84^{b}
7	6.80^{a}	9.37^{c}	7.77^{d}	7.64^{b}
8	7.08^{a}	8.31^{b}	8.16^{d}	7.35^{c}
9	7.36^{a}	7.86^{c}	8.40^{d}	7.05^{b}
11	7.49^{c}	7.41^{b}	8.63^{d}	7.06^{a}

$^{a, b, c, d.}$ Different superscript letters indicate differences in treatments with a significance of $p < 0.05$.

Statistical analysis Figure 7.8

Table S7.9. Temporal evolution of the saturated fatty acid content (SAFA) of *Elliptochloris* sp. as a function of carbon source in CO_2 bubbled cultures.

Time (d)	Photoautot. CO_2	Glycerin Veg.	Glycerin UCO	Glucose
0	4.41^{a}	1.85^{b}	1.85^{b}	1.85^{b}
2	3.90^{a}	2.16^{c}	2.19^{c}	2.76^{b}
4	4.25^{a}	2.30^{b}	2.23^{c}	2.19^{d}
7	4.41^{a}	1.55^{b}	1.56^{b}	1.48^{c}
8	3.56^{a}	1.58^{b}	1.33^{d}	1.35^{c}
9	3.39^{a}	1.51^{c}	1.21^{d}	1.57^{b}
11	3.17^{a}	1.65^{b}	1.36^{d}	1.57^{c}

$^{a, b, c, d.}$ Different superscript letters indicate differences in treatments with a significance of $p < 0.05$.

Table S7.10. Temporal evolution of the saturated fatty acid content (SAFA) of *Elliptochloris* sp. as a function of carbon source in air bubbled cultures.

Time (d)	Photoautot. air	Glycerin Veg.	Glycerin UCO	Glucose
0	5.73^{a}	5.08^{a}	5.08^{a}	5.08^{a}
2	5.39^{d}	4.98^{c}	3.84^{a}	6.88^{b}
4	4.93^{c}	4.29^{a}	4.06^{b}	5.38^{a}
7	5.77^{d}	4.07^{a}	2.97^{b}	4.00^{c}
8	4.64^{d}	3.33^{b}	3.06^{a}	3.28^{c}
9	4.28^{a}	3.80^{d}	3.42^{b}	3.86^{c}
11	4.25^{b}	4.08^{c}	3.16^{a}	4.21^{d}

$^{a, b, c, d.}$ Different superscript letters indicate differences in treatments with a significance of $p < 0.05$.

Table S7.11. Time dependent evolution of the unsaturated fatty acid (UFA) content of *Elliptochloris* sp. as a function of carbon source in CO_2 bubbled cultures.

Time (d)	Photoautot. CO_2	Glycerin Veg.	Glycerin UCO	Glucose
0	1.85^{a}	1.85^{b}	1.85^{b}	1.85^{b}
2	1.54^{b}	1.76^{c}	2.33^{d}	2.17^{a}
4	1.62^{b}	2.19^{c}	1.95^{d}	2.15^{a}
7	1.75^{a}	2.51^{b}	2.12^{d}	1.97^{c}
8	1.68^{a}	2.14^{b}	2.23^{d}	2.08^{c}
9	1.83^{a}	1.56^{a}	1.78^{a}	1.65^{a}
11	1.81^{a}	1.78^{c}	2.04^{d}	1.68^{b}

[a, b, c, d.] Different superscript letters indicate differences in treatments with a significance of $p < 0.05$.

Table S7.12. Time dependent evolution of the unsaturated fatty acid (UFA) content of *Elliptochloris* sp. as a function of carbon source in air bubbled cultures.

Time (d)	Photoautot. air	Glycerin Veg.	Glycerin UCO	Glucose
0	5.73^{a}	5.73^{a}	5.73^{a}	5.73
2	3.96^{d}	4.79^{b}	4.31^{c}	5.12
4	4.09^{d}	5.84^{a}	4.44	4.99
7	4.36^{d}	6.02^{a}	4.73	4.94
8	3.95^{d}	5.29^{b}	4.88	5.56
9	4.56^{a}	3.96^{d}	4.00	4.50
11	4.45^{d}	4.60^{b}	5.31	4.50

[a, b, c, d.] Different superscript letters indicate differences in treatments with a significance of $p < 0.05$.

8

CHAPTER

General discussion.

Table of contents

1. Introduction

Extremophilic microalgae are photosynthetic microorganisms with extraordinary genetic and metabolic plasticity which, perhaps surprisingly, have not yet been scientifically explored or industrially exploited. A few notable exceptions, such as *Spirulina* (alkalophilic microalga) and *Dunaliella* (saline microalga), demonstrated the biotechnological value of extremotolerant and extremophilic microalgae, as these species are used in the specialized food and natural pigment industries (Abreu et al., 2023; Mobin and Alam, 2017). It is only in the last two decades that the scientific community has begun, initially hesitantly and more recently with greater intensity, to turn its attention back to these microorganisms, a natural resource of great potential for the food, cosmetics, and health industries (Malavasi et al., 2020; Varshney et al., 2015), as previously discussed in detail in the Introduction of this Thesis document (**chapter 1**).

In this context, the Iberian Pyrite Belt in southwestern Spain—particularly in the northern region of the province of Huelva—represents one of the most unique hyperacidic extreme environments for microbial life worldwide. Acid mine drainage and the upper course of the well-known Tinto river serve as habitats for a wide range of photosynthetic microorganisms. Among the photosynthetic microorganisms found in the Tinto river and its surrounding areas, our research group isolated several species, two of which are the focus of this doctoral Thesis: *Coccomyxa onubensis* and –in a minor content– *Elliptochloris* sp.

This Thesis investigated the acclimation capacities of *C. onubensis* to stress conditions analogous to those of its native habitat, and from that understanding, to assess the biotechnological potential of the microalga. Accordingly, the aims of the Thesis are to: (i) partially understand how the photosynthetic machinery adjusts to the referred physicochemical stress (**chapter 2**); (ii) harness this acclimation capacity under controlled conditions to develop semi-continuous production processes for the microalga (**chapter 3**); (iii) examine the response of the lipid metabolism to inorganic nitrogen limitation –a chemical feature of its natural environment–, with the aim of identifying the microalga's potential for accumulating industrially valuable fatty acids under controlled cultivation conditions (**chapter 4**); (iv) partially elucidate the antioxidant response of the microalga to physicochemical stress, identifying key molecules involved and analyzing their accumulation (**chapter 5**); and finally, (v) evaluate the anti-inflammatory potential of the antioxidant molecular pool produced by the microalga, in human cell lines (**chapter 6**).

2. Exploring the biotechnological potential of a highly acidic-habitat microalga: *C. onubensis*

2.1. Photosynthesis in a highly acidic environment

There is a notable lack of studies on the photosynthetic activity of microalgae inhabiting highly acidic environments (Souza-Egipsy et al., 2011). Such knowledge would be highly valuable for, on one hand, understanding how photosynthetic activity develops under the stress conditions of such habitats (e.g., high concentrations of dissolved iron, high irradiance, and limited availability of inorganic nitrogen, among other factors), and on the other hand, applying this information to the design of production processes aimed at obtaining biomass and biotechnologically valuable molecules.

In **chapter 2**, we evaluated the photosynthetic response of *C. onubensis* cultures to exposure to the aforementioned stress factors. The experiments analyzed the evolution of intracellular chlorophyll content, photosynthetic performance, and growth over time under sublethal concentrations of Fe (III), salt, high irradiance, and limited levels of inorganic nitrogen (nitrate). *C. onubensis* responded to Fe (III) and high irradiance stress by reducing its intracellular chlorophyll content, while maintaining key photosynthetic parameters at typical levels of metabolically active cells. This suggests a reduction in antenna size as a strategy to optimize light utilization in photosynthesis, ultimately resulting in even higher biomass productivity compared to control cultures.

In contrast, short-term exposure (48–72 hours) to inorganic nitrogen limitation or increased salinity affected in a greater degree to the photosynthetic machinery of the microalga. The results obtained suggest an inactivation of reaction centers and a reduction of the electron transport flow leading, therefore, to increased levels of non-photochemical quenching as a protective mechanism. Nonetheless, the photosynthetic efficiency values obtained were close to those generally obtained for viable algal cells. This points to the ability of *C. onubensis* to adjust the photosynthetic machinery to maintain the efficiency of light conversion into chemical energy, even under nutritional stress (e.g., nitrogen limitation) or under oxidative stress caused by salinity which affect the turnover of PSII subunits and the synthesis of D1 protein. Similar results were obtained in studies for non-extremophilic microalgae species, although exposed to lower levels of stress.

The novelty presented in our study, compared to other microalgae species, was the improved photosynthetic performance of *C. onubensis* upon exposure to increasing Fe (III) levels. That is, the results indicated that microalgal viability increased when Fe (III) was added to *C. onubensis* cultures. PCA results (Figure 2.7) showed that the analyzed parameters were positively correlated with the performance of Fe (III)-supplemented cultures and accurately reflected the improved photosynthetic status of cultures under Fe (III) stress. Similarly, the lower values recorded for V_J and N suggested a reduction in pressure on the photosynthetic electron transport chain, which is consistent with a more efficient use of absorbed light in photosynthesis (Strasser et al., 2000). Additionally, the decrease in φ_{Do}, along with the reduction in DI_0/RC following the

addition of Fe (III) to *C. onubensis* cells, indicated a downregulation of non-photochemical quenching (NPQ) mechanisms (Singh et al., 2022).

Accordingly, our results support the conclusion that the addition of Fe (III) enhances electron transport chain activity in *C. onubensis*, thereby increasing photosynthetic efficiency while it resulted toxic to other non-extremophilic microalgae species leading to damages in photosynthetic machinery (Meriot et al., 2024). Thus, Fe (III)-enriched cultures of *C. onubensis* have an enhanced potential for the biochemical photoconversion of solar energy and exhibit improved microalgal viability (Swoczyna et al., 2019). This led to higher biomass productivity and improved photosynthetic performance in Fe (III)-treated cultures compared to non-extremophilic species (Meriot et al., 2024), which may reflect an exceptional natural capacity of acidophilic microalgae to perform photosynthesis under acidic conditions and solved metals that would be lethal to non-extremophiles.

2.2. Adjusting growth factors for biomass and valuable molecules production

As mentioned above, studying the photosynthetic performance of the microalga generates scientific information which is useful to design production processes of biomass and biotechnologically valuable molecules. Additionally, for large scale cultivation, optimization of key growth influencing factors is crucial to ensure light and nutrient availability and, therefore, the viability of the microalgal culture. Thus, in **chapter 3**, we elucidated the effect of different factors –3 levels of temperature, light irradiance and Fe (III)– on the growth of *C. onubensis*, by performing a factorial design (3^3) aiming at defining growth conditions for efficient biomass production under repeated-batch cultivation.

The effect of different factors in *C. onubensis* growth was analyzed by selecting temperature levels of 25, 30 and 35 °C, light irradiance levels of 150, 300 and 600 μmol photon·m^{-2}·s^{-1} and Fe (III) levels of 0, 0.25 and 2 mM of Fe (III). Temperature and light irradiance were the factors that exerted the greatest influence on the biomass concentration of the microalga. Therefore, when analyzing the synergistic effect of the three factors on the microalgal growth, the mathematical model predicted that the optimal condition for maximum biomass production were no addition of Fe (III) to *C. onubensis* cultures and moderate levels of temperature and light irradiance (28.9 °C and 486 μmol photon·m^{-2}·s^{-1}). The optimal average irradiance inside the culture (I_{av}) was estimated, through equation (3.4) described by Molina Grima et al. 1997, as, approximately, 700 μmol photon·m^{-2}·s^{-1}. Taking into account these optimal growth conditions, several cycles of repeated batch-cultivation in air-fluidized bags were performed in *C. onubensis* cultures grown without extra addition of Fe (III), at moderate temperatures and at the optimal light irradiance estimated (700 μmol photon·m^{-2}·s^{-1}) for efficient biomass concentration.

The massive production of acidophilic microalgae (not exploited yet) has been reported to be hypothetically constrained by limited productivity, primarily due to the extreme pH conditions of the medium. These conditions force microalgal metabolism to expend energy in maintaining the proton gradient across the cell wall, thereby

reducing the energy available for growth by approximately 10 % (Gross, 2000; Messerli et al., 2005). Nevertheless, the results of productivity obtained in this study with *C. onubensis* grown under repeated-batch mode suggest that microalgae from highly acidic environments could be produced as efficiently as other non-extremophilic photosynthetic microorganisms (Moheimani, 2013; Abomohra et al., 2014). In this sense, the photosynthetic capacity of *C. onubensis* to acclimate to the harsh conditions of the acidic environment **(chapter 2)** has been proven crucial to address efficient biomass production processes **(chapter 3)**.

Moreover, extreme conditions are unsuitable for most microorganisms, allowing only the proliferation of extremophilic species that can withstand such harsh environments. Indeed, although acidophilic microalgae can coexist with prokaryotic microorganisms associated with their growth, the proliferation of exogenous biological contaminants is rare in long-term acidic cultures, as shown for a large culture of *C. onubensis* in a previous study by our team (Fuentes et al., 2020). Based on this, the main advantage of producing acidic environment microalgae, such as *C. onubensis*, is that the acidic pH of the culture medium inhibits the growth of non-acidotolerant, competing microorganisms. The productivity data obtained for *C. onubensis* during the final cycles of repeated-batch cultivation (0.17 $g \cdot L^{-1} \cdot d^{-1}$) indicated that air-fluidized bag cultivation is a suitable system for its production.

The findings of **chapter 3** underscore the importance of controlling the dynamics of target molecules accumulation, including phenolic compounds, chlorophyll and carotenoids, during *C. onubensis* growth, which would be of relevance for planning mass production processes of this acidic habitat microalga. In this sense, several production strategies could be considered when cultivating *C. onubensis* under repeated-batch cultivation mode in air-fluidized bags depending on the growth stage and, therefore, light availability, as summarized in Figure 3.7.

The maximum level of light availability, i.e. at the beginning of the first cycles, should induce increased content of reactive oxygen species (ROS) in the microalga, therefore, generating oxidative stress. The direct consequence of that fact is the increase in antioxidant compounds (lutein and phenolic compounds, among other main metabolites) as a defense mechanism to neutralize these species, therefore reducing the oxidative pressure caused by the excess light, though the growth was proven limited to low rates by this scenario. Nonetheless, under reduced light pressure, i.e. during the second cycle of repeated-batch cultivation, the enhanced growth could be attributed to efficient functioning of the antioxidant system and the photoacclimation mechanism of the microalga, including shifted accumulation of photosynthetic pigments. Once the cultures acclimated to the imposed conditions, the reduced stress resulted into lutein and phenolic content to fall to its constitutive values. The increase in cell density makes the culture experience lower light availability, which results in decreased chlorophyll antenna size. This evidence a physiological acclimation of the microalga to the reduced light availability in high-cell density cultures, to maximize light absorption.

From an ecological perspective, one of the findings of this chapter –specifically the decrease in chlorophyll content in cultures with higher cell density– may help explain

the acclimation strategy of *Coccomyxa* in mining lakes. This strategy would involve counteracting the reduced light availability at depths of 8–10 meters below the lake surface, thereby enabling the microalga to bloom as long as other nutrients are sufficient. This interpretation is consistent with the findings of Sánchez-España et al. (2020). Thus, the discussed acclimation strategy could explain not only how to drive a controlled biomass production process of a highly acidic habitat-microalga but also could contribute to the understanding of microbial nutrition principles in mining lakes.

2.3. Fatty acid profile modulation for different applications

According to the aforementioned reference (Sánchez-España et al., 2020), the abundance of *Coccomyxa onubensis* in the deep waters of the redoxcline zone leads to a characteristic deep chlorophyll maximum. Consequently, *C. onubensis* could represent the most abundant source of organic carbon in the chemocline, thereby fulfilling the nutrient requirements of sulfide-producing bacteria in these deep waters. Notably, the inorganic nitrogen concentration at depths of 8–10 m in the acidic pit lakes of the Iberian Pyrite Belt (Huelva) is below 5 $mg \cdot L^{-1}$, which is significantly lower than the inorganic nitrogen saturation level for *C. onubensis* (above 5 mM) observed in artificial culture media. This low nitrogen availability was simulated in **chapter 4** through laboratory experiments of *C. onubensis* cultivation under limiting nitrogen conditions, aiming to mimic the deep waters scenario of acidic pit lakes, including the biomass density to light irradiance ratio.

The specific nitrogen concentration that limits cell growth varies depending on the species and culture conditions. In this study, nitrate concentrations below 1 mM were completely consumed within approximately two days, resulting in growth arrest (Figure 4.1) at biomass levels averaging around 0.2–0.3 g $(dw) \cdot L^{-1}$. Nevertheless, although nitrogen-limited cultures became nitrogen-depleted within 2–3 days (Figure 4.1), they remain photosynthetically viable for days, allowing sustained reduction of $NADP^+$ to NADPH. This maintains the anabolic reducing power required for fatty acid biosynthesis induced by nitrogen depletion (Figure 4.4). TEM observations (Figure 4.3) suggested that carbon and energy reserves of *C. onubensis* shifted toward triacylglycerol or starch accumulation depending on the degree of nitrogen limitation, as discussed in detail in **chapter 4**. Greater starch accumulation was addressed under moderate nitrogen limitation (0.3 mM), whereas increased vesicular activity under severe nitrogen depletion suggested carbon storage as fatty acids, molecules with a higher specific energy content (Wan and Zhang, 2012). This fact suggests, as described for microalgae, activation of an energy-saving mechanism when nitrogen depletion negatively impacts main energy production pathways, namely photosynthesis and mitochondrial oxidative phosphorylation (Markou et al., 2017).

From a biotechnological perspective, the results demonstrate that modulation of the degree of nitrogen limitation enables two distinct cultivation strategies for production of fatty acids. Specifically, under nitrogen-deprived conditions, the increase in saturated fatty acids (C16:0 and C18:0), and more notably the substantial rise in the monounsaturated fatty acid C18:1, renders a biomass composition which is more

suitable for biodiesel production. It is noteworthy that the C18:1 content reached 5.28 % dry weight under nitrogen limitation, which is significantly higher compared to several *Chlorella* strains with the highest reported fatty acid productivity, where C18:1 content ranged from 0.14 to 2.59 % dry weight (Hempel et al., 2012). These conditions appear to particularly enhance the *de novo* synthesis of fatty acids in *C. onubensis* (Figure 4.4b). Additionally, the reduced content of polyunsaturated fatty acids (PUFAs), particularly C18:3 (α-linolenic acid, ALA), further improves the lipid profile for applications such as biodiesel production. On the other hand, cultivation under moderate nitrogen availability (i.e., 5 mM nitrate) seemed efficient to address accumulation of polyunsaturated fatty acids as ALA (α-linolenic acid), roughly 3.6 % of dry weight. As noted in the Introduction section, ALA plays a significant role in regulating oxidative stress and enhancing mitochondrial function, which is the primary site of its biological activity (Lopez-Maldonado et al., 2021). In addition, the reduced content of SAFAs and MUFAs contributes to making the biomass composition more suitable for use as a food supplement rich in unsaturated fatty acids. Therefore, these cultivation strategies may guide the potential applications of *C. onubensis* biomass.

The novelty of our analysis of fatty acid biosynthesis in *C. onubensis* under nitrogen-limiting conditions lies in the unexpected production of docosadienoic acid (DDA, C22:2). This diene is extremely rare in microalgae, with its presence previously reported only in *Scenedesmus obliquus* at relatively low concentrations, around 3 % of total fatty acids measured as fatty acid methyl esters (FAMEs) (Ruiz-Marin et al., 2019). The biosynthetic pathway for C22:2 in microalgae has not yet been described. The physiological role of C22:2 remains unclear. However, substantial scientific evidence indicates that cis-13,16-docosadienoic acid (C22:2) acts as a potent inhibitor of topoisomerases and interferes with DNA polymerase activity in *in vitro* studies (Yonezawa et al., 2006). Inhibition of topoisomerases and polymerases typically leads to the arrest of DNA replication and the activation of cellular stress responses, which often culminates in cell death. Throughout this process, the integrity of the cell membrane becomes progressively compromised, resulting in the release of intracellular metabolites into the surrounding medium, including partially degraded enzymes, free fatty acids, nucleic acid fragments, phenolic compounds, and other cellular constituents.

The latter biochemical scenario becomes particularly relevant within the microbial ecology of acidic environments, especially regarding the activity of sulfate-reducing bacteria (SRB) in the acidic lagoon waters of pyrite mining areas. As elegantly described by Diez-Ercilla et al. (2014), sulfide precipitation in the chemocline of acidic pit lakes (PITs) appears to be associated with the activity of sulfate-reducing bacteria (SRB), which likely depends on the availability of organic carbon compounds originating from the photic zone. As described above in **chapter 4**, previous studies have identified *Coccomyxa* as the dominant photosynthetic eukaryotic species in the deep photic zone, in acidic pit lakes of the Iberian Pyrite Belt in southwestern Spain (Sánchez-España et al., 2020). According to the aforementioned reference, the abundance of *C. onubensis* in the deep waters of the redoxcline zone provides the most abundant source of organic carbon in the chemocline, thereby fulfilling the nutrient requirements of sulfide-

producing bacteria in these deep waters. The low nitrogen availability found at depths of 8–10 m in the acidic pit lakes of the Iberian Pyrite Belt (Huelva), simulated in the present study through laboratory experiments of *C. onubensis* cultivation under nitrogen-limited conditions (**chapter 4**), induced increased intracellular fatty acid and starch content. That is, the cells becoming enriched in reducing power molecules that could serve as electron donors for the biosulfidogenesis activity of sulfate-reducing bacteria.

Based on the discussion above, it should be reasonable to hypothesize that nitrogen limitation experienced by *C. onubensis* in the deeper layers (8–10 m) of the chemocline in the acidic lagoons of the Iberian Pyrite Belt (Huelva, Spain) can trigger a cascade of biochemical events in the microalga. These processes may be directed towards the accumulation of reducing power, primarily in the form of fatty acids and polysaccharides, ultimately contributing to programmed cell death and the subsequent release of molecular components. This release would supply essential nutrients to anaerobic prokaryotes inhabiting the mesocline, thereby sustaining sulfur-based reductive metabolic processes such as sulfidogenesis.

2.4. Design of biotechnological processes for producing antioxidant-enriched biomass and increasing its anti-inflammatory potential

As already described in the Introduction section and in several chapters of this Thesis, the harsh conditions of *C. onubensis* habitat, i.e. pH between 0.8 and 3 and ferric iron concentrations as high as 30 $g \cdot L^{-1}$ (Fernández-Remolar et al., 2004), this microalga species should be candidate to accumulate metabolites that maintain homeostasis by minimizing the impact of stress through their actions against oxidative chemical species. In **chapter 5**, growth and antioxidant response of *C. onubensis* to Fe-mediated stress was analyzed, attempting to find a suitable balance between stress and growth to trigger accumulation of antioxidant molecules while preventing culture productivity from decaying. Under certain cultivation conditions, *C. onubensis* stands out for accumulating antioxidant molecules such as linoleic and linolenic acid and lutein (Bermejo et al., 2018), among others, which have been reported to display anti-inflammatory and antimicrobial activities (Navarro et al., 2017). Accordingly, we also studied the anti-inflammatory capacity of *C. onubensis* stressed cells by analyzing the response of THP-1 Mac cells to the molecule content of *C. onubensis* extracts (**chapter 6**).

Fe plays a key role in the cellular biochemistry of microalgae due to its redox properties and the involvement in fundamental processes such as photosynthesis, respiration, nitrogen fixation, and DNA synthesis (Estevez et al., 2001; Hardie et al., 1983). Our results obtained with Fe (III)-supplemented cultures of *C. onubensis* are in good agreement with this fact showing that Fe (III), added to the cultures in a certain concentration range, in a much larger level than cultures of non-extremophilic microalgae, stimulates the growth of the microalga (Figure 5.2 and 5.3). The range of Fe (III) concentrations used in this study is toxic to non-extremophilic microalgae (Meriot et al., 2024) but still below toxic levels to *C. onubensis*, since the highest

concentration of Fe (III) added to the cultures resulted in the highest biomass productivity of the microorganism, as also demonstrated in **chapter 2** with the enhanced photosynthetic performance obtained under such conditions.

The results obtained in **chapter 5** showed that the presence of Fe (III) in *C. onubensis* cultures triggers biochemical responses which are typically expressed as a defense mechanism against ROS; particularly, the increased activity of the enzyme superoxide dismutase (SOD) (Figure 5.4a) evidenced Fe (III)-mediated increased oxidative stress. At higher concentrations of Fe (III), the expression of genes encoding the activity of antioxidant enzymes is induced, including ascorbate peroxidase, superoxide dismutase, dehydroascorbate reductase and catalase (Pikula et al., 2019; Pinto et al., 2003). Nevertheless, SOD enzyme has a constitutive presence according to scientific information (Al-Rashed et al., 2016) and is involved in the cellular antioxidant response, being responsible for catalyzing the transformation of $O_2^{\bullet-}$ into H_2O_2 (see reaction 5.2).

Interestingly, it should be noted here that while the levels of Fe (III) added to the culture medium favor growth (Figure 5.2), perhaps surprisingly the levels of antioxidant molecules seem to decrease –perhaps surprisingly–, in the case of phenolic and terpenoids compounds (**chapter 5** and **chapter 6**). Such unexpected scenario is discussed later within this Discussion section. The growth stimulated by Fe (III), the retracted synthesis of thylakoid membranes (Figure 6.4) and the lower intracellular concentration of chlorophyll and protein (Figure 5.3 and 5.4) in cultures with Fe (III) are compatible with an increase in the PSII efficiency (Figure 5.3c and **chapter 2**). This allows to postulate that the decreased microalgae's antenna size would have a regulatory function aimed at maximizing the use of light in grown cultures, as inferred from JIP parameters through the increase in ET values and decrease in ABS (Table 5.1).

The anti-inflammatory effects proven on THP-1 Mac cells by extracts of *C. onubensis* obtained from cultures exposed to Fe (III) showed a 50 % reduction in TNFα secretion. This finding suggested that acidophilic microalgae might be excellent natural sources of anti-inflammatory compounds, partly because of their ability to adapt to oxidative stress through the accumulation of anti-inflammatory molecules. The anti-inflammatory capacity of microalgal extracts could be improved by modulating oxidative stress during biomass production. Conversely, the results obtained apparently demonstrated the lower antioxidant capacity for cell extracts from Fe (III)-supplemented cultures (Figure 5.5a). The apparently lower antioxidant capacity should correspond to cultures under weaker oxidative stress. Coherently, the increase in the SOD activity (Figure 5.4a) as the Fe (III) concentration increases might be a sign of a more active antioxidant response of the microalga, though a more extensive analysis of other antioxidant enzymes (ascorbate peroxidase, glutathione reductase, catalase, etc.) is required to define the antioxidant response more accurately.

This scenario is coherent with a greater involvement of polyphenols, besides other antioxidants, in ROS neutralizing reactions (Figure 5.5b), which would explain their apparent decreased content in presence of Fe (III). In relation with the latter, the OH groups in the phenol structure, which must react with ROS to exhibit ROS-scavenging

activity, are also required to react with DPPH, free radical used for testing antioxidant capabilities. Gulcin and Alwasel (2023) studied the interaction between the DPPH radical and the (poly)phenolic group in usnic acid, which has two -OH units. They inferred that the withdrawal of H atoms from the (poly)phenolic -OH groups by a reactive radical species is a thermodynamically favorable chemical transformation, which can occur under high oxidative pressure. The latter is also coherent with the lower antioxidant capacity obtained in Fe (III)-added cultures of microalgal extracts and with the proposed structural changes in (poly)phenols due to eventual reactions with ROS. Therefore, part of the (poly)phenolic content in the microalgal extracts, especially in extracts from Fe (III)-added cultures, would not be acting in the chemical reduction of DPPH, thus resulting in an apparently lower antioxidant capacity, as obtained for extracts with high Fe (III) levels.

As (poly)phenolic compounds are determined spectrophotometrically based on the reaction of their hydroxyl groups with the Folin-Ciocolteu reagent (Pérez et al., 2023), and considering that a fraction of the hydroxyl groups could have reacted with ROS, fewer hydroxyl groups in (poly)phenolic compounds of microalgal extracts from Fe (III)-added cultures might be available for that colorimetric reaction, which might result in lower levels of (poly)phenols detection. Additionally, Havaux (2014) reported that ROS, especially singlet oxygen, produced in chloroplasts under stress, can oxidize β–carotene, leading to the production of various oxidized derivatives, such as β–cyclocitral or β–ionone, containing α,β-unsaturated carbonyl groups. Similarly, after reacting with ROS, (poly)phenolic compounds and xanthophylls may lose their hydroxyl groups to form α,β-unsaturated carbonyl groups (Hunyadi, 2019; Rajashekar, 2023). These structural changes can cause the actual contents of (poly)phenolic compounds and carotenoids to be underestimated (Figure 5.5 and 6.7). The polarity of carotenoids would change after reacting with ROS, thus their retention times in the HPLC separation process may change, making their identification on the chromatogram chart challenging. In this sense, conversely to what many times is accepted, an apparent lower antioxidant capacity might be compatible with the decrease of the chemically active antioxidant form of antioxidant molecules which can eventually be not detected through their specific standard determination methods.

Nonetheless, even modified structures of (poly)phenols and carotenoids (terpenoids) can decrease the inflammatory response measured in terms of LPS-induced secretion of TNFα by THP-1 macrophages (Araújo et al., 2020; Gallego et al., 2022), explaining the higher anti-inflammatory activity of extracts from Fe (III)-added *C. onubensis* cultures. Linnewiel-Hermoni et al. (2014) reported that carotenoid-oxidized derivatives, but not the intact carotenoid structures, can mediate the inhibition of NF-κB. Moreover, derivatives that contain α,β-unsaturated carbonyl groups interact even with higher affinity with the active site of NF-κB following the Michael addition reaction (Linnewiel-Hermoni et al., 2014). This concept provides insights into new approaches to studying the anti-inflammatory potential capacity of natural compounds, which also explains our findings of lower antioxidant capacity and higher anti-

inflammatory activity in extracts from microalgal cell cultures exposed to high levels of Fe (III)-induced oxidative stress.

In contrast to the pattern obtained with carotenes, xanthophylls, and (poly)phenols, the measurement procedure of flavonoids might not be affected by their previous reaction with ROS, as a direct correlation was found between the flavonoid content and anti-inflammatory activity (Figure 6.8d). This occurred probably because the determination of flavonoids is mediated by the oxidation of (poly)phenolic ring-hydroxyl groups to the carbonyl groups, which are also involved in the formation of Al (III)-flavonoid chelates, detected by spectrophotometry (Shraim et al., 2021). The transformation of hydroxyl groups into carbonyl groups in flavonoids by reacting with ROS does not hinder their detection. This fact would explain why a significant increase in flavonoid content was recorded under moderate levels of Fe (III)-induced oxidative stress in *C. onubensis* cultures.

Consequently, we hypothesized that structural changes in target antioxidant molecules after reacting with ROS might explain the observed reduction in antioxidant capacity and increase in anti-inflammatory activity. This hypothesis was supported by the results presented in Figure 6.7 and 6.8 and schematically represented in Figure 6.10, the data obtained allowed us to suggest the existence of a direct relationship between these structurally oxidized compounds and the increase in anti-inflammatory activity.

3. Biotechnological potential of other extremophilic microalgae

In addition to *Coccomyxa*, in **chapter 7** we have explored specific characteristics of the cultivation of two other extremophilic microalgae, *Chroococcidiopsis* sp. (cyanobacterium from endolithic, hyper-arid environment, Atacama) and *Elliptochloris* sp. (microalga from hyper-acidic habitat, Tinto River). The aim was to obtain initial key information of their production, as a first step toward the analysis of their biotechnological potential. On the one hand, in this thesis chapter we tested the efficacy of ultrasound pulses in cell disaggregation of *Chroococcidiopsis* sp. aggregates as a possible strategy to improve the productivity and operation of the cultures by favoring nutrient and light availability, and culture homogeneity. On the other hand, we tested mixotrophic growth as an alternative to the challenges of photoautotrophic cultivation in light availability in the autochthonous acidotolerant microalga *Elliptochloris* sp.

3.1. Chroococcidiopsis sp.

The cyanobacterium *Chroococcidiopsis* sp. was isolated from the endolithic habitat of gypsum rocks of the hyper-arid Atacama Desert (north Chile) (Wierzchos et al., 2015). This desert is one of the most challenging polyextreme environments on Earth due to its hyper-aridity, extreme solar irradiance, both ultraviolet radiation (UVR) and photosynthetic active radiation (PAR), high day/night temperature fluctuations and in some cases high salinity (Wierzchos et al., 2018). The high solar radiation in the Atacama Desert makes photosynthesis challenging due to the photo-oxidative damage suffered by the species growing in that habitat (Solovchenko and Merzlyak, 2008). To overcome these conditions, *Chroococcidiopsis* sp. produces a layer of exopolysaccharides (EPS) that surround the cells allowing them to retain some water and create a more humid endolithic environment to live (S. Singh et al., 2019), thereby promoting photosynthesis. This EPS layer favors the formation of cellular aggregates (Figure 7.1) (Das et al., 2018), allowing the cyanobacteria to dissipate part of the light received, eventually reducing the oxidative damage (Flemming and Wingender, 2010).

However, despite the above-referred advantage of the aggregates, the cell morphological configuration in aggregates can limit their growth due to the lowered availability of light and nutrients reaching the central cells of the aggregates compared to the peripheral ones (Conradi et al., 2019). One of the hypotheses of this work is that avoiding aggregation could improve the productivity of the cyanobacterium, eventually increasing the production and even extraction yields of valuable molecules. The strategies and intensity used to keep cells disaggregated, while avoiding cell disruption, should guarantee cell viability, which would potentially address improved nutrient availability of the whole culture. Consequently, cell growth would be enhanced, a first step towards modelling production on a photobioreactor. Based on this concept, we studied in culture flasks the efficacy of low-frequency ultrasound (LFU) in cell disaggregation as a treatment to eventually improve the productivity of the extremotolerant cyanobacterium *Chroococcidiopsis* sp.

To verify whether the proposed hypothesis is valid, we performed a test to analyze whether the application of ultrasound pulses had any effect on the aggregation state of *Chroococcidiopsis* sp. culture samples in a liquid medium. This was achieved by subjecting culture samples to LFU pulses of different duration and following the aggregation state of treated samples. The results indicated a direct relationship between the duration of the applied ultrasound pulses and the increase in the optical density value of ultrasound-treated samples. We attribute this relationship to the disaggregation caused by the ultrasound treatment in the cell aggregates, which was evidenced by the optical microscopic photographs (Figure 7.3b).

Based on the obtained results, a second test was performed to study the effect of ultrasound on the growth and viability of *Chroococcidiopsis* sp. subjected to different durations of ultrasound pulse. The data obtained supported the positive impact of modulated ultrasound pulses on the growth of *Chroococcidiopsis* sp. cultures. The improved growth of *Chroococcidiopsis* sp. cultures was a consequence of greater light and nutrient accessibility after disaggregation. Nonetheless, the natural aggregation of *Chroococcidiopsis* sp. can favor the economy of the harvesting process since larger particle size eases sedimentation or flocculation techniques, saving energy costs compared to centrifugation (Fasaei et al., 2018). However, additional energy costs may be required to keep cultures of large size aggregates in liquid medium homogeneously mixed (Montero-Lobato et al., 2020). Meanwhile, since light and nutrients may be less accessible to the inner cells of the aggregates, the cyanobacterium should expectedly reach lower biomass productivity. In this sense, specific cultivation strategies could be discussed for the eventual production of *Chroococcidiopsis* sp. evaluating conditions that can lead to acceptable biomass productivity and savings in process costs.

3.2. Elliptochloris sp.

Additionally, other strategies could be considered for efficient biomass production of acidophilic microalgae and their valuable molecules. This has been tested with another highly acidic-habitat microalga, *Elliptochloris* sp., isolated by our team at University of Huelva. During photoautotrophic growth, microalgal biomass and lipid production might be limited by the reduction in light availability. As an alternative to photoautotrophic growth, most of microalgal species can use organic carbon sources (OCS) and perform mixotrophic or heterotrophic growth. Although, the most commonly used OCS during mixotrophic growth at laboratory scale are glucose and acetate (Paranjape et al., 2016), these carbon sources are not suitable for industrial-scale production (Li et al., 2007). Glycerol, a by-product of biodiesel production, can be obtained at a lower price (Vivek et al., 2017). Thus, the large-scale production of microalgae based on glycerol can reduce production costs while increasing the added value of glycerol through its conversion into oil as a raw material for advanced biofuel (da Silva et al., 2009). In **chapter 7** the production of the highly acidic-habitat microalga *Elliptochloris* sp. was studied in photoautotrophic and mixotrophic conditions on crude technical glycerin or glucose bubbled with either only air or air containing 2.5 % (v/v) CO_2.

Elliptochloris is a genus of *Chlorophyta* similar to *Chlorella* and is closely related to the genus *Coccomyxa* (Darienko et al., 2016). This genus was first described by Tschermak-Woess (1988) based on the species *E. bilobata*. Species belonging to this genus are widely distributed throughout the world. They are found in terrestrial habitats in free-living form or as a photobiont with lichens (Darienko et al., 2016). Our experience with *Elliptochloris* sp. cultures allowed us to state that this strain is able to grow at around neutral pH, thus it behaves as an acidotolerant strain. The advantage of growing *Elliptochloris* sp. at acidic pH relies on the challenging growth of aerobic opportunist heterotrophs which is limited under the extreme pH conditions in which *Elliptochloris* sp. thrives.

The results obtained in Figure 7.6 evidenced that *Elliptochloris* sp. could assimilate an OCS. This was inferred by comparing the growth patterns of mixotrophic cultures supplemented with an OCS and bubbled with air with those patterns of cultures supplied only with air. The growth patterns obtained when supplementing the cultures with an OCS can be improved greatly by supplementing the cultures with CO_2. However, the maximum growth rate was recorded in cultures grown under photoautotrophic conditions. This finding showed that adding an OCS to cultures growing under conditions of standard light intensity and CO_2 concentration could partly slow down the growth of *Elliptochloris* sp. This could be probably due to temporary metabolic imbalances when assimilating the extra carbon source, resulting in the partial inhibition of growth as described by Paranjape et al. (2016). This might occur due to the combination of biochemical events which compete for the same metabolic aim (biomass production), including slow uptake rates and/or assimilation of the OCS and, low photosynthetic activity (Markou et al., 2021).

Nonetheless, in cultures supplemented with an OCS, part of the light energy fixed through photosynthesis in the form of NAD(P)H may exceed that required for the assimilation of nutrients (Figure 7.6); under such conditions, this excess chemical energy (NAD(P)H) might be partly oxidized by reactive oxygen species (ROS) formed in the chloroplast (Hasanuzzaman et al., 2020). One of the metabolic capacities of microalgae to dissipate excess reducing power, i.e., chemical energy from the photosynthetic fixation of light energy, is to divert excess NAD(P)H to the synthesis of triacylglycerides (TAG); using this strategy, they can store carbon and energy in the chemical form of fatty acids (Schüler et al., 2017). Additionally, part of the acetyl-CoA derived from the oxidative degradation of the OCS can be diverted to the production of fatty acids using excess NAD(P)H (Poddar et al., 2020). Based on this fact, the excess energy from light and organic carbon provided to the cultures in mixotrophic cultures could lead to the overproduction of NADPH. Excess production of NADPH, as presented in Figure 7.7d could be stored in the form of fatty acids to maintain the balance between NADPH and $NADP^+$ levels in the cells. Conversely, mixotrophic cultures bubbled with CO_2-enriched air had lower photosynthetic efficiency (Figure 7.6c), which might decrease the production of NADPH. Therefore, the decrease in the intracellular fatty acid content in mixotrophic cultures bubbled with CO_2-enriched air (Figure 7.7c)

could be justified by the lower production of NADPH through photosynthetic process, as needs of reducing power decrease if OCS are available by the cells.

The ratio of the saturated to unsaturated fatty acid content varies as a function of the carbon source supplied to the cultures. Therefore, we suggest two cultivation strategies for the effective production of *Elliptochloris* sp. First, mixotrophy in CO_2-enriched air allows higher biomass productivity, but metabolic imbalances can decrease the content of fatty acids and increase the relative abundance of saturated fatty acids. Second, mixotrophy in air alone can increase the content of both saturated and unsaturated fatty acids but biomass productivity decreases. These strategies can further determine the application of *Elliptochloris* sp. for biofuels or production of food supplements.

Overall, the results presented in this chapter demonstrate the significant potential of extremophilic photosynthetic microorganisms for growth, which have traditionally been regarded as less efficient for biomass production compared to non-extremophilic species. Intensive research into their physiology, biochemistry, genomics, proteomics, and process engineering is expected to reveal their considerable biotechnological potential.

Conclusions

1. In contrast to other microalgae species, the highly acidic-habitat microalga *C. onubensis* responds to Fe (III) stress by reducing its antenna size and enhancing the electron transport rate. This strategy optimized the photosynthetic use of light, resulting in increased biomass productivity. Similarly, *C. onubensis* adapts to high irradiance through a photoacclimation mechanism that decreases electron pressure within the photosynthetic electron transport chain (ETC), resulting in increased biomass productivity. This response involves a reduction in the photon flux reaching the ETC and an enhancement of non-photochemical quenching (NPQ) activity, serving as a protective mechanism to dissipate excess excitation energy.

2. *C. onubensis* exhibited biomass productivity comparable to that of non-extremophilic microalgae under repeated-batch cultivation in air-fluidized systems. These results challenge the assumption that acidic conditions limit microalgal growth and position *C. onubensis* as a robust candidate for open-system cultivation with low contamination risk. The accumulation of antioxidant compounds (lutein, polyphenols, and flavonoids) in *C. onubensis* is tightly regulated by light availability during repeated-batch cultivation, reflecting photoacclimation of the microalga. Thus, different cultivation strategies could be adapted: maximizing antioxidant accumulation at the expense of biomass, or achieving higher biomass yields with reduced metabolite content. This physiological and biochemical plasticity enhances the versatility of *C. onubensis* as a production platform for environmentally sustainable biotechnological applications.

3. Nitrogen deprivation markedly enhanced carbohydrates and lipids accumulation in *C. onubensis*. Modulating nitrogen levels in the cultures could serve as an effective strategy to obtain fatty acid-enriched biomass, eventually useful as raw material for either biofuel production or as a food supplement. These findings also suggest a potential ecological role for *C. onubensis* as a source of electron donors supporting bacterial growth in its natural habitat, such as acidic pit lakes. Under nitrogen limitation, *C. onubensis* increases its C18:1 content to levels significantly higher than those observed in several *Chlorella* strains. Moreover, nitrogen-limiting cultures exhibited an unexpected production of docosadienoic acid (DDA, C22:2), which is extremely rare in microalgae. C22:2 has been reported to inhibit DNA polymerase and topoisomerase, suggesting a possible role in controlling microbial populations in its natural habitat.

4. Fe (III) causes oxidative stress in *C. onubensis*. As a defense mechanism, the microalga expresses an increase in the intracellular levels of the enzyme SOD and flavonoids, while the content of other phenolic and terpenoid molecules suffers from an apparent decrease. In addition, modulating Fe (III) concentrations in *C. onubensis* promotes the biosynthesis of essential polyunsaturated fatty acids (PUFAs), particularly linoleic and linolenic acids. This effect could be a consequence of an impaired balance between the involvement of PUFAs in reactive oxygen species (ROS) neutralization and the moderate generation of ROS.

5. *C. onubensis* extracts exhibit *in vitro* anti-inflammatory activity, measured as TNFα inhibition in THP-1 Mac cells. Fatty acids, (poly)phenolic compounds and carotenoids are included among the bioactive compounds that can be exerting anti-inflammatory activity. The addition of Fe (III) to *C. onubensis* cultures led to enhanced anti-inflammatory activity of the extracts, with values exceeding those reported for other microalgae species cells.

6. Fe (III)-induced oxidative stress in *C. onubensis* might lead to the formation of derivative antioxidants, which are eventually effective as anti-inflammatory agents. This could explain the inverse correlations observed between antioxidant and anti-inflammatory capacities of *C. onubensis* extracts. The apparently lower antioxidant capacity may be due to those referred derivative antioxidants, which might not be properly detected or lack the ability to reduce DPPH in conventional antioxidant assays. This concept should be considered for developing experimental approaches to investigate the anti-inflammatory potential of natural compounds.

7. In this Thesis, two additional extremophilic photosynthetic microorganisms were analyzed for specific biotechnological features: a microalga from an extremely acidic habitat and a cyanobacterium from the world's driest desert. The microalga, *Elliptochloris* sp., demonstrated the capacity to grow mixotrophically achieving productivity of biomass and fatty acid comparable to photoautotrophic growth, likely via acetyl-CoA. The results suggest that acidophilic microalgae could recycle glycerol, a major byproduct of biodiesel production. Additionally, low-frequency ultrasound efficiently disrupted cell aggregates of the naturally aggregating extremophile *Chroococcidiopsis*, maintaining culture viability and improving nutrient access. These findings highlight the potential of extremophilic photosynthetic microorganisms for sustainable biotechnological applications and optimization of cultivation processes.

Conclusiones

1. A diferencia de otras especies de microalgas, *C. onubensis*, una microalga de hábitat altamente ácido, responde al estrés por Fe (III) reduciendo el tamaño de la antena y aumentando la tasa de transporte electrónico. Esta estrategia optimizaría el uso fotosintético de la luz, lo que resultó en una mayor productividad de biomasa. De igual manera, *C. onubensis* se adapta a la alta irradiancia mediante un mecanismo de fotoaclimatación que disminuye la presión electrónica dentro de la cadena de transporte de electrones (ETC) fotosintética, lo que resulta en una mayor productividad de biomasa. Esta respuesta implica una reducción del flujo de fotones que llega a la ETC y un aumento de la actividad de extinción no fotoquímica (NPQ), que actúa como mecanismo protector para disipar el exceso de energía de excitación.

2. *C. onubensis* exhibió una productividad de biomasa comparable a la de microalgas no extremófilas bajo cultivo en baño repetido en sistemas de aire-fluidizados. Estos resultados desafían la suposición de que las condiciones ácidas limitan el crecimiento de las microalgas y posicionan a *C. onubensis* como un candidato robusto para el cultivo en sistemas abiertos con bajo riesgo de contaminación. La acumulación de compuestos antioxidantes (luteína, polifenoles y flavonoides) en *C. onubensis* está estrechamente regulada por la disponibilidad de luz durante el cultivo en baño repetido, lo que refleja la fotoaclimatación de la microalga. Por lo tanto, se podrían adaptar diferentes estrategias de cultivo: maximizando la acumulación de antioxidantes a expensas de la biomasa, o logrando mayores rendimientos de biomasa con un contenido reducido de metabolitos. Esta plasticidad fisiológica y bioquímica mejora la versatilidad de *C. onubensis* como plataforma de producción para aplicaciones biotecnológicas ambientalmente sostenibles.

3. La limitación de nitrógeno mejoró notablemente la acumulación de carbohidratos y lípidos en *C. onubensis*. La modulación de los niveles de nitrógeno en los cultivos podría servir como una estrategia eficaz para obtener biomasa enriquecida con ácidos grasos, eventualmente útil como materia prima para la producción de biocombustibles o como suplemento alimenticio. Estos hallazgos también sugieren un posible papel ecológico para *C. onubensis* como fuente donadora de electrones para sostener el crecimiento bacteriano en su hábitat natural, como en las lagunas ácidas. Bajo limitación de nitrógeno, *C. onubensis* aumenta su contenido de C18:1 a niveles significativamente más altos que los observados en varias cepas de *Chlorella*. Además, los cultivos con limitación de nitrógeno exhibieron una producción inesperada de ácido docosadienoico (DDA, C22:2), que es extremadamente raro en microalgas. Se ha reportado que C22:2 inhibe la ADN polimerasa y la topoisomerasa, lo que sugiere un posible papel en el control de las poblaciones microbianas en su hábitat natural.

4. El Fe (III) causa estrés oxidativo en *C. onubensis*. Como mecanismo de defensa, la microalga presenta un aumento en los niveles intracelulares de la enzima SOD y flavonoides, mientras que el contenido de otras moléculas fenólicas y terpenoides disminuye. Además, la modulación de las concentraciones de Fe (III) en *C. onubensis* promueve la biosíntesis de ácidos grasos poliinsaturados (PUFAs) esenciales, en particular los ácidos linoleico y linolénico. Este efecto podría deberse a un balance entre la participación de los PUFAs en la neutralización de especies reactivas de oxígeno (ROS) y la generación moderada de ROS.

5. Los extractos de *C. onubensis* exhiben actividad antiinflamatoria *in vitro*, medida como inhibición del TNFα en células THP-1 Mac. Los ácidos grasos, compuestos (poli)fenólicos y carotenoides se incluyen entre los compuestos bioactivos que pueden ejercer actividad antiinflamatoria. La adición de Fe (III) a los cultivos de *C. onubensis* condujo a una mayor actividad antiinflamatoria de los extractos, con valores superiores a los reportados para células de otras especies de microalgas.

6. El estrés oxidativo inducido por Fe (III) en *C. onubensis* podría conducir a la formación de antioxidantes derivados, que eventualmente resultan eficaces como agentes antiinflamatorios. Esto podría explicar las correlaciones inversas observadas entre las capacidades antioxidantes y antiinflamatorias de los extractos de *C. onubensis*. La aparente menor capacidad antioxidante podría deberse a estos antioxidantes derivados, que podrían no detectarse correctamente o carecer de la capacidad de reducir el DPPH en los ensayos antioxidantes convencionales. Este concepto debería considerarse para el desarrollo de enfoques experimentales que investiguen el potencial antiinflamatorio de los compuestos naturales.

7. En esta tesis, se analizaron dos microorganismos fotosintéticos extremófilos adicionales para determinar sus características biotecnológicas específicas: una microalga de un hábitat extremadamente ácido y una cianobacteria del desierto más árido del mundo. La microalga, *Elliptochloris* sp., demostró la capacidad de crecer mixotróficamente, logrando una productividad de biomasa y ácidos grasos comparable al crecimiento fotoautotrófico, probablemente a través de acetil-CoA. Los resultados sugieren que las microalgas acidófilas podrían reciclar el glicerol, un subproducto importante de la producción de biodiésel. Además, ultrasonidos de baja frecuencia interrumpió eficientemente los agregados celulares de *Chroococcidiopsis*, un extremófilo de agregación natural, manteniendo la viabilidad del cultivo y mejorando el acceso a los nutrientes. Estos hallazgos resaltan el potencial de los microorganismos fotosintéticos extremófilos para aplicaciones biotecnológicas sostenibles y la optimización de los procesos de cultivo.

References

Abdul Latif, N.-I. S., Ong, M. Y., Nomanbhay, S. (2019). Hydrothermal liquefaction of Malaysia's algal biomass for high-quality bio-oil production. *Engineering in Life Sciences*, *19*(4), 246–269.

Abiusi, F., Trompetter, E., Pollio, A., Wijffels, R. H., Janssen, M. (2022). Acid Tolerant and Acidophilic Microalgae: An Underexplored World of Biotechnological Opportunities. *Frontiers in Microbiology*, *13*.

Abomohra, A. E.-F., El-Sheekh, M., Hanelt, D. (2014). Pilot cultivation of the chlorophyte microalga *Scenedesmus obliquus* as a promising feedstock for biofuel. *Biomass and Bioenergy*, *64*, 237–244.

Alishah Aratboni, H., Rafiei, N., Garcia-Granados, R., Alemzadeh, A., Morones-Ramírez, J. R. (2019). Biomass and lipid induction strategies in microalgae for biofuel production and other applications. *Microbial Cell Factories*, *18*(1), 178.

Allahverdiyeva, Y., Mustila, H., Ermakova, M., Bersanini, L., Richaud, P., Ajlani, G., Battchikova, N., Cournac, L., Aro, E.-M. (2013). Flavodiiron proteins Flv1 and Flv3 enable cyanobacterial growth and photosynthesis under fluctuating light. *Proceedings of the National Academy of Sciences*, *110*(10), 4111–4116.

Allakhverdiev, S. I., Nishiyama, Y., Miyairi, S., Yamamoto, H., Inagaki, N., Kanesaki, Y., Murata, N. (2002). Salt Stress Inhibits the Repair of Photodamaged Photosystem II by Suppressing the Transcription and Translation of psbAGenes in *Synechocystis*. *Plant Physiology*, *130*(3), 1443–1453.

Allen, J. W., DiRusso, C. C., Black, P. N. (2015). Triacylglycerol synthesis during nitrogen stress involves the prokaryotic lipid synthesis pathway and acyl chain remodeling in the microalgae *Coccomyxa subellipsoidea*. *Algal Research*, *10*, 110–120.

Al-Rashed, S. A., Ibrahim, M. M., El-Gaaly, G. A., Al-Shehri, S., Mostafa, A. (2016). Evaluation of radical scavenging system in two microalgae in response to interactive stresses of UV-B radiation and nitrogen starvation. *Saudi Journal of Biological Sciences*, *23*(6), 706–712.

Amils, R., Fernández-Remolar, D., Team, T. I. (2014). Río Tinto: A Geochemical and Mineralogical Terrestrial Analogue of Mars. *Life*, *4*(3), 511–534.

Aparicio, S., Robles, Á., Ferrer, J., Seco, A., Borrás Falomir, L. (2022). Assessing and modeling nitrite inhibition in microalgae-bacteria consortia for wastewater treatment by means of photo-respirometric and chlorophyll fluorescence techniques. *Science of The Total Environment*, *808*, 152128.

Araújo, N., Viegas, C. S. B., Zubía, E., Magalhães, J., Ramos, A., Carvalho, M. M., Cruz, H., Sousa, J. P., Blanco, F. J., Vermeer, C., Simes, D. C. (2020). Amentadione from the Alga *Cystoseira usneoides* as a Novel Osteoarthritis Protective Agent in an Ex Vivo Co-Culture OA Model. *Marine Drugs*, *18*(12).

Ávila-Román, J., García-Gil, S., Rodríguez-Luna, A., Motilva, V., Talero, E. (2021). Anti-Inflammatory and Anticancer Effects of Microalgal Carotenoids. *Marine Drugs*, *19*(10).

Ávila-Román, J., Gómez-Villegas, P., de Carvalho, C. C. C. R., Vigara, J., Motilva, V., León, R., Talero, E. (2023). Up-Regulation of the Nrf2/HO-1 Antioxidant Pathway in Macrophages by an Extract from a New Halophilic Archaea Isolated in Odiel Saltworks. *Antioxidants*, *12*(5).

Barone, M. E., Parkes, R., Herbert, H., McDonnell, A., Conlon, T., Aranyos, A., Fierli, D., Fleming, G. T. A., Touzet, N. (2021). Comparative Response of Marine Microalgae to H_2O_2-Induced Oxidative Stress. *Applied Biochemistry and Biotechnology*, *193*(12), 4052–4067.

Bates, P., Browse, J. (2012). The Significance of Different Diacylgycerol Synthesis Pathways on Plant Oil Composition and Bioengineering. *Frontiers in Plant Science*, *3*, 147.

Bermejo, E., Ruiz-Domínguez, M. C., Cuaresma, M., Vaquero, I., Ramos-Merchante, A., Vega, J. M., Vílchez, C., Garbayo, I. (2018). Production of lutein, and polyunsaturated fatty acids by the acidophilic eukaryotic microalga *Coccomyxa onubensis* under abiotic stress by salt or ultraviolet light. *Journal of Bioscience and Bioengineering*, *125*(6), 669–675.

Bhol, N. K., Bhanjadeo, M. M., Singh, A. K., Dash, U. C., Ojha, R. R., Majhi, S., Duttaroy, A. K., Jena, A. B. (2024). The interplay between cytokines, inflammation, and antioxidants: mechanistic insights and therapeutic potentials of various antioxidants and anti-cytokine compounds. *Biomedicine & Pharmacotherapy*, *178*, 117177.

Blackhall, V., Orioli, G. A., Colavita, M. G. (2020). Special issue in honour of Prof. Reto J. Strasser - JIP-test parameters to study apple peel photosystem II behavior under high solar radiation stress during fruit development. *Photosynthetica*, *58*(2), 314–322.

Blasio, M., Balzano, S. (2021). Fatty Acids Derivatives From Eukaryotic Microalgae, Pathways and Potential Applications. *Frontiers in Microbiology*, *Volume 12-2021*.

Bottaro, M., Abramov, S., Amils, R., Martinez-Bonilla, A., ThomasArrigo, L., Straub, D., Mansor, M., Kleindienst, S., Kappler, A. (2025). Coupling of Fe and N cycles by nitrate-reducing Fe (II)-oxidizing microorganisms in the tidal sediments of an extreme acidic river (Río Tinto, Spain). *Applied Geochemistry*, *190*, 106488.

Boyd, E. S., Thomas, K. M., Dai, Y., Boyd, J. M., Outten, F. W. (2014). Interplay between Oxygen and Fe–S Cluster Biogenesis: Insights from the Suf Pathway. *Biochemistry*, *53*(37), 5834–5847.

Brand-Williams, W., Cuvelier, M. E., Berset, C. (1995). Use of a free radical method to evaluate antioxidant activity. *LWT - Food Science and Technology*, *28*(1), 25–30.

Briat, J.-F., Dubos, C., Gaymard, F. (2015). Iron nutrition, biomass production, and plant product quality. *Trends in Plant Science*, *20*(1), 33–40.

Burg, D. A., Kleiman, R. (1991). Preparation of meadowfoam dimer acids and dimer esters, and their use as lubricants. *Journal of the American Oil Chemists Society*, *68*(8), 600–603.

Cahoon, E. B., Marillia, E.-F., Stecca, K. L., Hall, S. E., Taylor, D. C., Kinney, A. J. (2000). Production of Fatty Acid Components of Meadowfoam Oil in Somatic Soybean Embryos. *Plant Physiology*, *124*(1), 243–252.

Calella, P., Cerullo, G., Di Dio, M., Liguori, F., Di Onofrio, V., Gallè, F., Liguori, G. (2022). Antioxidant, anti-inflammatory and immunomodulatory effects of spirulina in exercise and sport: A systematic review. *Frontiers in Nutrition*, *Volume 9-2022*.

Canganella, F., Wiegel, J. (2011). Extremophiles: from abyssal to terrestrial ecosystems and possibly beyond. *Naturwissenschaften*, *98*(4), 253–279.

Casero, M. C., Ascaso, C., Quesada, A., Mazur-Marzec, H., Wierzchos, J. (2020). Response of endolithic *Chroococcidiopsis* strains from the polyextreme Atacama Desert to light radiation. *BioRxiv*.

Castillo, T., Ramos, D., García-Beltrán, T., Brito-Bazan, M., Galindo, E. (2021). Mixotrophic cultivation of microalgae: An alternative to produce high-value metabolites. *Biochemical Engineering Journal*, *176*, 108183.

Chacón-Lee, T. L., González-Mariño, G. E. (2010). Microalgae for “Healthy” Foods—Possibilities and Challenges. *Comprehensive Reviews in Food Science and Food Safety*, *9*(6), 655–675.

Chen, X., He, Y., Liu, L., Zhu, X., Sen, B., Wang, G. (2022). Nitrogen Starvation Enhances the Production of Saturated and Unsaturated Fatty Acids in *Aurantiochytrium* sp. PKU#SW8 by Regulating Key Biosynthetic Genes. *Marine Drugs*, *20*(10).

Chen, Y., Qiu, X., Yang, J. (2021). Comparing the In Vitro Antitumor, Antioxidant and Anti-Inflammatory Activities between Two New Very Long Chain Polyunsaturated Fatty Acids, Docosadienoic Acid (DDA) and Docosatrienoic Acid (DTA), and Docosahexaenoic Acid (DHA). *Nutrition and Cancer*, *73*(9), 1697–1707.

Chen, Y., Sun, L., Liu, Z., Martin, G., Sun, Z. (2017). Integration of Waste Valorization for Sustainable Production of Chemicals and Materials via Algal Cultivation. *Topics in Current Chemistry*, *375*(6), 89.

Chisti, Y. (2007). Biodiesel from microalgae. *Biotechnology Advances*, *25*(3), 294–306.

Chojnacka, K., Noworyta, A. (2004). Evaluation of Spirulina sp. growth in photoautotrophic, heterotrophic and mixotrophic cultures. *Enzyme and Microbial Technology*, *34*(5), 461–465.

Chunzhuk, E. A., Grigorenko, A. V, Kiseleva, S. V, Chernova, N. I., Ryndin, K. G., Kumar, V., Vlaskin, M. S. (2023). The Influence of Elevated CO_2 Concentrations on the Growth of Various Microalgae Strains. *Plants*, *12*(13).

Conradi Fabian, Rui-Qian, Z., Sabrina, O., Nils, S., Annegret, W., W, M. C. (2019). Factors Controlling Floc Formation and Structure in the Cyanobacterium *Synechocystis* sp. Strain PCC 6803. *Journal of Bacteriology*, *201*(19), 10.1128/jb.00344-19.

Cuaresma, M., Buffing, M., Janssen, M., Vílchez, C., Wijffels, R. (2012). Performance of *Chlorella sorokiniana* under simulated extreme winter conditions. *Journal of Applied Phycology*, *24*, 693–699.

Cuaresma, M., Casal, C., Forján, E., Vílchez, C. (2011). Productivity and selective accumulation of carotenoids of the novel extremophile microalga *Chlamydomonas acidophila* grown with different carbon sources in batch systems. *Journal of Industrial Microbiology & Biotechnology*, *38*(1), 167–177.

Curcuraci, E., Manuguerra, S., Messina, C. M., Arena, R., Renda, G., Ioannou, T., Amato, V., Hellio, C., Barba, F. J., Santulli, A. (2022). Culture Conditions Affect Antioxidant Production, Metabolism and Related Biomarkers of the Microalgae *Phaeodactylum tricornutum*. *Antioxidants*, *11*(2).

da Silva, G. P., Mack, M., Contiero, J. (2009). Glycerol: A promising and abundant carbon source for industrial microbiology. *Biotechnology Advances*, *27*(1), 30–39.

Dąbrowski, P., Baczewska, A. H., Pawluśkiewicz, B., Paunov, M., Alexantrov, V., Goltsev, V., Kalaji, M. H. (2016). Prompt chlorophyll a fluorescence as a rapid tool for diagnostic changes in PSII structure inhibited by salt stress in *Perennial ryegrass*. *Journal of Photochemistry and Photobiology B: Biology*, *157*, 22–31.

Darienko, T., Gustavs, L., Pröschold, T. (2016). Species concept and nomenclatural changes within the genera *Elliptochloris* and *Pseudochlorella* (*Trebouxiophyceae*) based on an integrative approach. *Journal of Phycology*, *52*(6), 1125–1145.

Das, K., Roychoudhury, A. (2014). Reactive oxygen species (ROS) and response of antioxidants as ROS-scavengers during environmental stress in plants. *Frontiers in Environmental Science*, *2*.

Das, P., Abdulquadir, M., Chaudhary, A., Thaher, M., Khan, S., Alghazal, G., Aljabri, H. (2018). Outdoor Continuous Cultivation of Self-Settling Marine Cyanobacterium *Chroococcidiopsis* sp. *Industrial Biotechnology*, *14*, 45–53.

Depraetere, O., Deschoenmaeker, F., Badri, H., Monsieurs, P., Foubert, I., Leys, N., Wattiez, R., Muylaert, K. (2015). Trade-Off between Growth and Carbohydrate Accumulation in Nutrient-Limited

Arthrospira sp. PCC 8005 Studied by Integrating Transcriptomic and Proteomic Approaches. *Plos one*, *10*(7), e0132461-.

Diez-Ercilla, M., Sánchez-España, J., Yusta, I., Wendt-Potthoff, K., Koschorreck, M. (2014). Formation of biogenic sulphides in the water column of an acidic pit lake: biogeochemical controls and effects on trace metal dynamics. *Biogeochemistry*, *121*(3), 519–536.

D'Imporzano, G., Silvia, S., Davide, V., Barbara, S., Fabrizio, A. (2017). Microalgae Mixotrophic Growth: Opportunity for Stream Depuration and Carbon Recovery. In B. N. Tripathi & D. Kumar (Eds.), *Prospects and Challenges in Algal Biotechnology* (pp. 141–177). Springer Singapore.

Dineshkumar, R., Subramanian, G., Dash, S. K., Sen, R. (2016). Development of an optimal light-feeding strategy coupled with semi-continuous reactor operation for simultaneous improvement of microalgal photosynthetic efficiency, lutein production and CO_2 sequestration. *Biochemical Engineering Journal*, *113*, 47–56.

DuBois, Michel., Gilles, K. A., Hamilton, J. K., Rebers, P. A., Smith, Fred. (1956). Colorimetric Method for Determination of Sugars and Related Substances. *Analytical Chemistry*, *28*(3), 350–356.

Dumorné, K., Camacho Córdova, D., Astorga-Eló, M., Renganathan, P. (2017). Extremozymes: A Potential Source for Industrial Applications. *Journal of Microbiology and Biotechnology*, *27*, 649–659.

Eid, R., Arab, N. T. T., Greenwood, M. T. (2017). Iron mediated toxicity and programmed cell death: A review and a re-examination of existing paradigms. *Biochimica et Biophysica Acta (BBA) - Molecular Cell Research*, *1864*(2), 399–430.

Ejaz, U., Khan, S. M., Khalid, N., Ahmad, Z., Jehangir, S., Fatima Rizvi, Z., Lho, L. H., Han, H., Raposo, A. (2023). Detoxifying the heavy metals: a multipronged study of tolerance strategies against heavy metals toxicity in plants. *Frontiers in Plant Science*, *Volume 14-2023*.

Eliáš, M., Neustupa, J., Škaloud, P. (2008). *Elliptochloris bilobata* var. *corticola* var. nov. (*Trebouxiophyceae*, *Chlorophyta*), a novel subaerial coccal green alga. *Biologia*, *63*(6), 791–798.

Estevez, M. S., Malanga, G., Puntarulo, S. (2001). Iron-dependent oxidative stress in *Chlorella vulgaris*. *Plant Science*, *161*(1), 9–17.

Falcioni, R., Antunes, W. C., Demattê, J. A. M., Nanni, M. R. (2023). Biophysical, Biochemical, and Photochemical Analyses Using Reflectance Hyperspectroscopy and Chlorophyll a Fluorescence Kinetics in Variegated Leaves. *Biology*, *12*(5).

Fasaei, F., Bitter, J. H., Slegers, P. M., van Boxtel, A. J. B. (2018). Techno-economic evaluation of microalgae harvesting and dewatering systems. *Algal Research*, *31*, 347–362.

Faseela, P., Sinisha, A. K., Brestic, M., Puthur, J. T. (2020). Special issue in honour of Prof. Reto J. Strasser - Chlorophyll a fluorescence parameters as indicators of a particular abiotic stress in rice. *Photosynthetica*, *58*(2), 293–300.

Felsenstein, J. (1985). Confidence Limits on Phylogenies: An Approach Using the Bootstrap. *Evolution*, *39*(4), 783–791.

Fenton, H. J. H. (1894). LXXIII.—Oxidation of tartaric acid in presence of iron. *J. Chem. Soc., Trans.*, *65*(0), 899–910.

Fernández-Remolar, D. C., Rodriguez, N., Gómez, F., Amils, R. (2003). Geological record of an acidic environment driven by iron hydrochemistry: The Tinto River system. *Journal of Geophysical Research: Planets*, *108*(E7).

Fernández-Remolar, D., Gómez-Elvira, J., Gómez, F., Sebastian, E., Martíin, J., Manfredi, J. A., Torres, J., González Kesler, C., Amils, R. (2004). The Tinto River, an extreme acidic environment under control of iron, as an analog of the Terra Meridiani hematite site of Mars. *Planetary and Space Science*, *52*(1), 239–248.

Ferrat, L., Pergent-Martini, C., Roméo, M. (2003). Assessment of the use of biomarkers in aquatic plants for the evaluation of environmental quality: application to seagrasses. *Aquatic Toxicology*, *65*(2), 187–204.

Fini, A., Cecilia, B., Martina, D. F., Francesco, F., Tattini, M. (2011). Stress-induced flavonoid biosynthesis and the antioxidant machinery of plants. *Plant Signaling & Behavior*, *6*(5), 709–711.

Flemming, H.-C., Wingender, J. (2010). The biofilm matrix. *Nature Reviews Microbiology*, *8*(9), 623–633.

Forján, E., Navarro, F., Cuaresma, M., Vaquero, I., Ruíz-Domínguez, M. C., Gojkovic, Ž., Vázquez, M., Márquez, M., Mogedas, B., Bermejo, E., Girlich, S., Domínguez, M. J., Vílchez, C., Vega, J. M., Garbayo, I. (2015). Microalgae: Fast-Growth Sustainable Green Factories. *Critical Reviews in Environmental Science and Technology*, *45*(16), 1705–1755.

Foyer, C. H., Hanke, G. (2022). ROS production and signalling in chloroplasts: cornerstones and evolving concepts. *The Plant Journal*, *111*(3), 642–661.

Friedland, N., Negi, S., Vinogradova-Shah, T., Wu, G., Ma, L., Flynn, S., Kumssa, T., Lee, C.-H., Sayre, R. T. (2019). Fine-tuning the photosynthetic light harvesting apparatus for improved photosynthetic efficiency and biomass yield. *Scientific Reports*, *9*(1), 13028.

Fuentes, J. L., Huss, V. A. R., Montero, Z., Torronteras, R., Cuaresma, M., Garbayo, I., Vílchez, C. (2016). Phylogenetic characterization and morphological and physiological aspects of a novel acidotolerant and halotolerant microalga *Coccomyxa onubensis* sp. nov. (*Chlorophyta*, *Trebouxiophyceae*). *Journal of Applied Phycology*, *28*(6), 3269–3279.

Fuentes, J.-L., Montero, Z., Cuaresma, M., Ruiz-Domínguez, M.-C., Mogedas, B., Nores, I. G., del Valle, M., Vílchez, C. (2020). Outdoor Large-Scale Cultivation of the Acidophilic Microalga *Coccomyxa onubensis* in a Vertical Close Photobioreactor for Lutein Production. *Processes*, *8*(3).

Gallego, R., Valdés, A., Suárez-Montenegro, Z. J., Sánchez-Martínez, J. D., Cifuentes, A., Ibáñez, E., Herrero, M. (2022). Anti-inflammatory and neuroprotective evaluation of diverse microalgae extracts enriched in carotenoids. *Algal Research*, *67*, 102830.

Gan, T., Yin, G., Zhao, N., Tan, X., Wang, Y. (2023). A Sensitive Response Index Selection for Rapid Assessment of Heavy Metals Toxicity to the Photosynthesis of *Chlorella pyrenoidosa* Based on Rapid Chlorophyll Fluorescence Induction Kinetics. *Toxics*, *11*(5).

Gao, D., Ran, C., Zhang, Y., Wang, X., Lu, S., Geng, Y., Guo, L., Shao, X. (2022). Effect of different concentrations of foliar iron fertilizer on chlorophyll fluorescence characteristics of iron-deficient rice seedlings under saline sodic conditions. *Plant Physiology and Biochemistry*, *185*, 112–122.

Garbayo, I., Cuaresma, M., Vílchez, C., Vega, J. M. (2008). Effect of abiotic stress on the production of lutein and β-carotene by *Chlamydomonas acidophila*. *Process Biochemistry*, *43*(10), 1158–1161.

Garbayo, I., Torronteras, R., Forján, E., Cuaresma, M., Bejarano, C., Mogedas, B., Ruiz-Dominguez, M. C., Márquez, M., Vaquero, I., Jl, F., Fuentes, R., González-delValle, M. A., Vílchez, C. (2012). Identification and physiological aspects of a novel carotenoid-enriched, metal-resistant microalga isolated from an acidic river in Huelva (Spain). *Journal of Phycology*, *48*, 607–614.

Georgé, S., Brat, P., Alter, P., Amiot, M. J. (2005). Rapid Determination of Polyphenols and Vitamin C in Plant-Derived Products. *Journal of Agricultural and Food Chemistry*, *53*(5), 1370–1373.

Giacomelli, L., Rudella, A., van Wijk, K. J. (2006). High Light Response of the Thylakoid Proteome in *Arabidopsis* Wild Type and the Ascorbate-Deficient Mutant vtc2-2. A Comparative Proteomics Study. *Plant Physiology*, *141*(2), 685–701.

Gimmler, H., Kugel, H., Leibfritz, D., Mayer, A. (1988). Cytoplasmic pH of *Dunaliella parva* and *Dunaliella acidophila* as monitored by in vivo 31P-NMR spectroscopy and the DMO method. *Physiologia Plantarum*, *74*(3), 521–530.

Goiris, K., Muylaert, K., Voorspoels, S., Noten, B., De Paepe, D., E Baart, G. J., De Cooman, L. (2014). Detection of flavonoids in microalgae from different evolutionary lineages. *Journal of Phycology*, *50*(3), 483–492.

Gómez, F., Aguilera, A., Amils, R. (2007). Soluble ferric iron as an effective protective agent against UV radiation: Implications for early life. *Icarus*, *191*(1), 352–359.

Gómez-Chávez, F., Correa, D., Navarrete-Meneses, P., Cancino-Diaz, J. C., Cancino-Diaz, M. E., Rodríguez-Martínez, S. (2021). NF-κB and Its Regulators During Pregnancy. *Frontiers in Immunology*, *12*.

Gonçalves, A. L., Pires, J. C. M., Simões, M. (2017). A review on the use of microalgal consortia for wastewater treatment. *Algal Research*, *24*, 403–415.

González-López, C., Acien, G., Fernandez-Sevilla, J. M., Fernández, J., Cerón-García, M. C., Molina-Grima, E. (2009). Utilization of the cyanobacteria *Anabaena* sp. ATCC 33047 in CO_2 removal processes. *Bioresource Technology*, *100*, 5904–5910.

Granado-Lorencio, F., Herrero-Barbudo, C., Acién-Fernández, G., Molina-Grima, E., Fernández-Sevilla, J. M., Pérez-Sacristán, B., Blanco-Navarro, I. (2009). In vitro bioaccesibility of lutein and zeaxanthin from the microalgae *Scenedesmus almeriensis*. *Food Chemistry*, *114*(2), 747–752.

Griffiths, M. J., van Hille, R. P., Harrison, S. T. L. (2012). Lipid productivity, settling potential and fatty acid profile of 11 microalgal species grown under nitrogen replete and limited conditions. *Journal of Applied Phycology*, *24*(5), 989–1001.

Gross, W. (2000). Ecophysiology of algae living in highly acidic environments. *Hydrobiologia*, *433*(1), 31–37. https://doi.org/10.1023/A:1004054317446

Guedes, A. C., Meireles, L. A., Amaro, H. M., Malcata, F. X. (2010). Changes in Lipid Class and Fatty Acid Composition of Cultures of *Pavlova lutheri*, in Response to Light Intensity. *Journal of the American Oil Chemists' Society*, *87*(7), 791–801.

Guerin, M., Huntley, M. E., Olaizola, M. (2003). *Haematococcus* astaxanthin: applications for human health and nutrition. *Trends in Biotechnology*, *21*(5), 210–216.

Gulcin, İ., Alwasel, S. H. (2023). DPPH Radical Scavenging Assay. *Processes*, *11*(8).

Gustavs, L., Görs, M., Karsten, U. (2011). Polyol patterns in biofilm-forming aeroterrestrial green algae (*Trebouxiophyceae*, *Chlorophyta*). *Journal of Phycology*, *47*(3), 533–537.

Halliwell, B. (2006). Reactive Species and Antioxidants. Redox Biology Is a Fundamental Theme of Aerobic Life. *Plant Physiology*, *141*, 312–322.

Hantzis, L. J., Kroh, G. E., Jahn, C. E., Cantrell, M., Peers, G., Pilon, M., Ravet, K. (2018). A Program for Iron Economy during Deficiency Targets Specific Fe Proteins. *Plant Physiology*, *176*(1), 596–610.

Hardie, L. P., Balkwill, D. L., Stevens, S. E. (1983). Effects of Iron Starvation on the Physiology of the Cyanobacterium *Agmenellum quadruplicatum*. *Applied and Environmental Microbiology*, *45*(3), 999–1006.

Hasanuzzaman, M., Bhuyan, M. H. M. B., Parvin, K., Bhuiyan, T. F., Anee, T. I., Nahar, K., Hossen, Md. S., Zulfiqar, F., Alam, Md. M., Fujita, M. (2020). Regulation of ROS Metabolism in Plants under Environmental Stress: A Review of Recent Experimental Evidence. *International Journal of Molecular Sciences*, *21*(22).

Havaux, M. (2014). Carotenoid oxidation products as stress signals in plants. *The Plant Journal*, *79*(4), 597–606.

Hellebust, J. A., Ahmad, I. (1989). Regulation of Nitrogen Assimilation in Green Microalgae. *Biological Oceanography*, *6*(3–4), 241–255.

Hempel, N., Petrick, I., Behrendt, F. (2012). Biomass productivity and productivity of fatty acids and amino acids of microalgae strains as key characteristics of suitability for biodiesel production. *Journal of Applied Phycology*, *24*(6), 1407–1418.

Henchion, M., Hayes, M., Mullen, A. M., Fenelon, M., Tiwari, B. (2017). Future Protein Supply and Demand: Strategies and Factors Influencing a Sustainable Equilibrium. *Foods*, *6*(7).

Hillis, D. M., Dixon, M. T. (1991). Ribosomal DNA: Molecular Evolution and Phylogenetic Inference. *The Quarterly Review of Biology*, *66*(4), 411–453.

Holzinger, A., Pichrtová, M. (2016). Abiotic Stress Tolerance of Charophyte Green Algae: New Challenges for Omics Techniques. *Frontiers in Plant Science*, *Volume 7-2016*.

Huang, G., Chen, F., Wei, D., Zhang, X., Chen, G. (2010). Biodiesel production by microalgal biotechnology. *Applied Energy*, *87*(1), 38–46.

Hunyadi, A. (2019). The mechanism(s) of action of antioxidants: From scavenging reactive oxygen/nitrogen species to redox signaling and the generation of bioactive secondary metabolites. *Medicinal Research Reviews*, *39*(6), 2505–2533.

Hutner, S. H., Provasoli, L., Schatz, A., Haskins, C. P. (1950). Some Approaches to the Study of the Role of Metals in the Metabolism of Microorganisms. *Proceedings of the American Philosophical Society*, *94*(2), 152–170.

Ji, X., Cheng, J., Gong, D., Zhao, X., Qi, Y., Su, Y., Ma, W. (2018). The effect of NaCl stress on photosynthetic efficiency and lipid production in freshwater microalga—*Scenedesmus obliquus* XJ002. *Science of The Total Environment*, *633*, 593–599.

Jiang, X., Zhang, J., Zhao, J., Gao, Z., Zhang, C., Chen, M. (2017). Regulation of lipid accumulation in *Schizochytrium* sp. ATCC 20888 in response to different nitrogen sources. *European Journal of Lipid Science and Technology*, *119*(10), 1700025.

Johnson, D. B., Kanao, T., Hedrich, S. (2012). Redox Transformations of Iron at Extremely Low pH: Fundamental and Applied Aspects. *Frontiers in Microbiology*, *3*.

Joyce, E. M., King, P. M., Mason, T. J. (2014). The effect of ultrasound on the growth and viability of microalgae cells. *Journal of Applied Phycology*, *26*(4), 1741–1748.

Joyce, E. M., Xiaoge, W., Mason, T. J. (2010). Effect of ultrasonic frequency and power on algae suspensions. *Journal of Environmental Science and Health, Part A*, *45*(7), 863–866.

Jukes, T. H., Cantor, C. R. (1969). Evolution of Protein Molecules. *Mammalian Protein Metabolism*, 21–132.

Kalaji, H. M., Jajoo, A., Oukarroum, A., Brestic, M., Zivcak, M., Samborska, I. A., Cetner, M. D., Łukasik, I., Goltsev, V., Ladle, R. J. (2016). Chlorophyll a fluorescence as a tool to monitor physiological status of plants under abiotic stress conditions. *Acta Physiologiae Plantarum*, *38*(4), 102.

Kolber, Z., Zehr, J., Falkowski, P. (1988). Effects of Growth Irradiance and Nitrogen Limitation on Photosynthetic Energy Conversion in Photosystem II. *Plant Physiology*, *88*, 923–929.

Korhonen, J., Honkasalo, A., Seppälä, J. (2018). Circular Economy: The Concept and its Limitations. *Ecological Economics*, *143*, 37–46.

Krzemińska, I., Szymańska, M., Ciempiel, W., Piasecka, A. (2023). Auxin supplementation under nitrogen limitation enhanced oleic acid and MUFA content in *Eustigmatos calaminaris* biomass with potential for biodiesel production. *Scientific Reports*, *13*(1), 594.

Kühl, M., Glud, R., Borum, J. (2001). Photosynthetic performance of surface-associated algae below sea ice as measured with a pulse-amplitude-modulated (PAM) fluorometer and O_2 microsensors. *Marine ecology-progress series*, *223*, 1–14.

Kumar, D., Singh, H., Bhatt, U., Soni, V. (2022). Analyzing the Effects of Urban Photopollution on Photosynthetic Efficiency of Certain Trees through Chlorophyll Fluorescence OJIP Transient. *Stresses*, *2*(4), 437–449.

Kumar, D., Singh, H., Raj, S., Soni, V. (2020). Chlorophyll a fluorescence kinetics of mung bean (*Vigna radiata* L.) grown under artificial continuous light. *Biochemistry and Biophysics Reports*, *24*, 100813.

Laizet, Y., Pontier, D., Mache, R., Kuntz, M. (2004). Subfamily Organization and Phylogenetic Origin of Genes Encoding Plastid Lipid-Associated Proteins of the Fibrillin Type. *Journal of Genome Science and Technology*, *3*, 19–28.

Laloi, C., Przybyla, D., Apel, K. (2006). A genetic approach towards elucidation of the biological activity of different reactive oxygen in *Arabidopsis thaliana*. *Journal of Experimental Botany*, *57*, 1719–1724.

Lambrev, P. H., Miloslavina, Y., Jahns, P., Holzwarth, A. R. (2012). On the relationship between non-photochemical quenching and photoprotection of Photosystem II. *Biochimica et Biophysica Acta (BBA) - Bioenergetics*, *1817*(5), 760–769.

Lamers, P. P., Janssen, M., De Vos, R. C. H., Bino, R. J., Wijffels, R. H. (2008). Exploring and exploiting carotenoid accumulation in *Dunaliella salina* for cell-factory applications. *Trends in Biotechnology*, *26*(11), 631–638.

Lee, T. J., K., N., Matsumara, M. (2001). Ultrasonic Irradiation for Blue-Green Algae Bloom Control. *Environmental Technology*, *22*(4), 383–390.

Li, X., Xu, H., Wu, Q. (2007). Large-scale biodiesel production from microalga *Chlorella protothecoides* through heterotrophic cultivation in bioreactors. *Biotechnology and Bioengineering*, *98*(4), 764–771.

Li-Beisson, Y., Shorrosh, B., Beisson, F., Andersson, M., Arondel, V., Bates, P., Baud, S., Bird, D., DeBono, A., Durrett, T., Franke, R., Graham, I., Katayama, K., Kelly, A., Larson, T., Markham, J., Miquel, M., Molina, I., Nishida, I., Ohlrogge, J. (2013). Acyl-Lipid Metabolism. *The Arabidopsis Book*, *11*.

Linnewiel-Hermoni, K., Motro, Y., Miller, Y., Levy, J., Sharoni, Y. (2014). Carotenoid derivatives inhibit nuclear factor kappa B activity in bone and cancer cells by targeting key thiol groups. *Free Radical Biology and Medicine*, *75*, 105–120.

Liu, M., Li, X. Q., Weber, C., Lee, C. Y., Brown, J., Liu, R. H. (2002). Antioxidant and Antiproliferative Activities of Raspberries. *Journal of Agricultural and Food Chemistry*, *50*(10), 2926–2930.

Lobell, D., Burke, M., Tebaldi, C., Mastrandrea, M., Falcon, W., Naylor, R. (2008). Prioritizing Climate Change Adaptation Needs for Food Security in 2030. *Science (New York, N.Y.)*, *319*, 607–610.

López-Archilla, A. I., Marin, I., Amils, R. (2001). Microbial Community Composition and Ecology of an Acidic Aquatic Environment: The Tinto River, Spain. *Microbial Ecology*, *41*(1), 20–35.

Lopez-Maldonado, A., Pastoriza, S., Rufián-Henares, J. Á. (2021). Assessing the antioxidant and metabolic effect of an alpha-lipoic acid and acetyl-L-carnitine nutraceutical. *Current Research in Food Science*, *4*, 336–344.

Lourenço, S. C., Moldão-Martins, M., Alves, V. D. (2019). Antioxidants of Natural Plant Origins: From Sources to Food Industry Applications. *Molecules*, *24*.

Lowry, O. H., Rosebrough, N. J., Farr, A., Randall, R. J. (1951). Protein measurement with the folin Phenol Reagent. *J. Biol. Chemistry*, *193*, 256–275.

Lysenko, E. A., Klaus, A. A., Kartashov, A. V, Kusnetsov, V. V. (2020). Specificity of Cd, Cu, and Fe effects on barley growth, metal contents in leaves and chloroplasts, and activities of photosystem I and photosystem II. *Plant Physiology and Biochemistry*, *147*, 191–204.

Mandal, M., Sarkar, M., Khan, A., Biswas, M., Masi, A., Rakwal, R., Agrawal, G. K., Srivastava, A., Sarkar, A. (2022). Reactive Oxygen Species (ROS) and Reactive Nitrogen Species (RNS) in plants–maintenance of structural individuality and functional blend. *Advances in Redox Research*, *5*, 100039.

Marillia, E. F., Giblin, E. M., Covello, P. S., Taylor, D. C. (2002). Expression of meadowfoam Des5 and FAE1 genes in yeast and in transgenic soybean somatic embryos, and their roles in fatty acid modification. *Plant Physiology and Biochemistry*, *40*(10), 821–828.

Markou, G., Dao, L. H. T., Muylaert, K., Beardall, J. (2017). Influence of different degrees of N limitation on photosystem II performance and heterogeneity of *Chlorella vulgaris*. *Algal Research*, *26*, 84–92.

Markou, G., Depraetere, O., Muylaert, K. (2016). Effect of ammonia on the photosynthetic activity of *Arthrospira* and *Chlorella*: A study on chlorophyll fluorescence and electron transport. *Algal Research*, *16*, 449–457.

Markou, G., Diamantis, A., Korozi, E., Tsagou, V., Kefalogianni, I., Chatzipavlidis, I. (2021). Effects of Monochromatic Illumination with LEDs Lights on the Growth and Photosynthetic Performance of *Auxenochlorella protothecoides* in Photo- and Mixotrophic Conditions. *Plants*, *10*(4).

Martin, G. J. O., Hill, D. R. A., Olmstead, I. L. D., Bergamin, A., Shears, M. J., Dias, D. A., Kentish, S. E., Scales, P. J., Botté, C. Y., Callahan, D. L. (2014). Lipid Profile Remodeling in Response to Nitrogen Deprivation in the Microalgae *Chlorella* sp. (*Trebouxiophyceae*) and *Nannochloropsis* sp. (*Eustigmatophyceae*). *Plos one*, *9*(8), e103389-.

Martínez, F., Orús, M. I. (1991). Interactions between Glucose and Inorganic Carbon Metabolism in *Chlorella vulgaris* Strain UAM 101 1. *Plant Physiology*, *95*(4), 1150–1155.

Martínez, M. E., Camacho, F., Jiménez, J. M., Espínola, J. B. (1997). Influence of light intensity on the kinetic and yield parameters of *Chlorella pyrenoidosa* mixotrophic growth. *Process Biochemistry*, *32*(2), 93–98.

Matorin, D. N., Todorenko, D. A., Seifullina, N. Kh., Zayadan, B. K., Rubin, A. B. (2013). Effect of silver nanoparticles on the parameters of chlorophyll fluorescence and P700 reaction in the green alga *Chlamydomonas reinhardtii*. *Microbiology*, *82*(6), 809–814.

Maxwell, K., Johnson, G. N. (2000). Chlorophyll fluorescence—a practical guide. *Journal of Experimental Botany*, *51*(345), 659–668.

Mccord, J., Fridovich, I. (1969). The Utility of Superoxide Dismutase in Studying Free Radical Reactions. *Journal of Biological Chemistry*, *244*, 6056–6063.

Meriot, V., Roussel, A., Brunet, N., Chomerat, N., Bilien, G., Le Dean, L., Berteaux-Lecellier, V., Coulombier, N., Lebouvier, N., Jauffrais, T. (2024). *Heterocapsa* cf. *bohaiensis* (dinoflagellate): identification and response to nickel and iron stress revealed through chlorophyll a fluorescence. *Photosynthetica*, *62*(1), 27–39.

Messerli, M. A., Amaral-Zettler, L. A., Zettler, E., Jung, S.-K., Smith, P. J. S., Sogin, M. L. (2005). Life at acidic pH imposes an increased energetic cost for a eukaryotic acidophile. *Journal of Experimental Biology*, *208*(13), 2569–2579.

Miller, M. A., Zachary, J. F. (2017). Chapter 1 - Mechanisms and Morphology of Cellular Injury, Adaptation, and Death11For a glossary of abbreviations and terms used in this chapter see E-Glossary 1-1. In J. F. Zachary (Ed.), *Pathologic Basis of Veterinary Disease (Sixth Edition)* (pp. 2-43.e19). Mosby.

Moheimani, N. R. (2013). Long-term outdoor growth and lipid productivity of *Tetraselmis suecica*, *Dunaliella tertiolecta* and *Chlorella* sp (*Chlorophyta*) in bag photobioreactors. *Journal of Applied Phycology*, *25*(1), 167–176.

Molina Grima, E., García Camacho, F., Sánchez Pérez, J. A., Acién Fernández, F. G., Fernández Sevilla, J. M. (1997). Evaluation of photosynthetic efficiency in microalgal cultures using averaged irradiance. *Enzyme and Microbial Technology*, *21*(5), 375–381.

Montero-Lobato, Z., Fuentes, J. L., Garbayo, I., Ascaso, C., Wierzchos, J., Vega, J. M., Vílchez, C. (2020). Identification, biochemical composition and phycobiliproteins production of *Chroococcidiopsis* sp. from arid environment. *Process Biochemistry*, *97*, 112–120.

Montero-Lobato, Z., Vázquez, M., Navarro, F., Cordero, J., Bermejo, E., Garbayo, I., Vílchez, C., Cuaresma, M. (2018). Chemically-Induced Production of Anti-Inflammatory Molecules in Microalgae. *Marine Drugs*, *16*, 478.

Nagi, G. K., Corcoran, A. A., Mandal, S. (2023). Application of fluorescent transients to indicate nutrient deficiencies in a microalga *Nannochloropsis oceanica*. *Algal Research*, *69*, 102947.

Natrah, F. M. I., Yusoff, F. M., Shariff, M., Abas, F., Mariana, N. S. (2007). Screening of Malaysian indigenous microalgae for antioxidant properties and nutritional value. *Journal of Applied Phycology*, *19*(6), 711–718.

Navarro, F., Forján, E., Vázquez, M., Montero, Z., Bermejo, E., Castaño, M. Á., Toimil, A., Chagüaceda, E., García-Sevillano, M. Á., Sánchez, M., Domínguez, M. J., Pásaro, R., Garbayo, I., Vílchez, C., Vega, J. M. (2016). Microalgae as a safe food source for animals: nutritional characteristics of the acidophilic microalga *Coccomyxa onubensis*. *Food & Nutrition Research*, *60*(0).

Navarro, F., Forján, E., Vázquez, M., Toimil, A., Montero, Z., Ruiz-Domínguez, M. del C., Garbayo, I., Castaño, M. Á., Vílchez, C., Vega, J. M. (2017). Antimicrobial activity of the acidophilic eukaryotic microalga *Coccomyxa onubensis*. *Phycological Research*, *65*(1), 38–43.

Nielsen, S. L., Hansen, B. W. (2019). Evaluation of the robustness of optical density as a tool for estimation of biomass in microalgal cultivation: The effects of growth conditions and physiological state. *Aquaculture Research*, *50*(9), 2698–2706.

Nikkanen, L., Solymosi, D., Jokel, M., Allahverdiyeva, Y. (2021). Regulatory electron transport pathways of photosynthesis in cyanobacteria and microalgae: Recent advances and biotechnological prospects. *Physiologia Plantarum*, *173*.

Nishikawa, K., Onodera, A., Tominaga, N. (2006). Phytochelatins do not correlate with the level of Cd accumulation in *Chlamydomonas* spp. *Chemosphere*, *63*(9), 1553–1559.

Okamoto, O. K., Asano, C. S., Aidar, E., Colepicolo, P. (1996). Effects of Cadmium on growth and superoxide dismutase activity of the marine microalga *Tetraselmis gracilis* (*Prasinophyceae*). *Journal of Phycology*, *32*(1), 74–79.

Ort, D., Melis, A. (2010). Optimizing Antenna Size to Maximize Photosynthetic Efficiency. *Plant Physiology*, *155*, 79–85.

Ott, L. W., Resing, K. A., Sizemore, A. W., Heyen, J. W., Cocklin, R. R., Pedrick, N. M., Woods, H. C., Chen, J. Y., Goebl, M. G., Witzmann, F. A., Harrington, M. A. (2007). Tumor Necrosis Factor-α- and Interleukin-1-Induced Cellular Responses: Coupling Proteomic and Genomic Information. *Journal of Proteome Research*, *6*(6), 2176–2185.

Paliwal, C., Mitra, M., Bhayani, K., Bharadwaj, S. V. V., Ghosh, T., Dubey, S., Mishra, S. (2017). Abiotic stresses as tools for metabolites in microalgae. *Bioresource Technology*, *244*, 1216–1226.

Paranjape, K., Leite, G. B., Hallenbeck, P. C. (2016). Strain variation in microalgal lipid production during mixotrophic growth with glycerol. *Bioresource Technology*, *204*, 80–88.

Payne, D. T., Webre, W. A., Matsushita, Y., Zhu, N., Futera, Z., Labuta, J., Jevasuwan, W., Fukata, N., Fossey, J. S., D'Souza, F., Ariga, K., Schmitt, W., Hill, J. P. (2019). Multimodal switching of a redox-active macrocycle. *Nature Communications*, *10*(1), 1007.

Pérez, M., Dominguez-López, I., Lamuela-Raventós, R. M. (2023). The Chemistry Behind the Folin–Ciocalteu Method for the Estimation of (Poly)phenol Content in Food: Total Phenolic Intake in a Mediterranean Dietary Pattern. *Journal of Agricultural and Food Chemistry*, *71*(46), 17543–17553.

Pérez-Gálvez, A., Viera, I., Roca, M. (2020). Carotenoids and Chlorophylls as Antioxidants. *Antioxidants*, *9*, 505.

Perez-Garcia, O., Bashan, Y. (2015). Microalgal Heterotrophic and Mixotrophic Culturing for Bio-refining: From Metabolic Routes to Techno-economics. In A. Prokop, R. K. Bajpai, M. E. Zappi (Eds.), *Algal Biorefineries: Volume 2: Products and Refinery Design* (pp. 61–131). Springer International Publishing.

Phull, S. S., Newman, A. P., Lorimer, J. P., Pollet, B., Mason, T. J. (1997). The development and evaluation of ultrasound in the biocidal treatment of water. *Ultrasonics Sonochemistry*, *4*(2), 157–164.

Pikula, K. S., Zakharenko, A. M., Aruoja, V., Golokhvast, K. S., Tsatsakis, A. M. (2019). Oxidative stress and its biomarkers in microalgal ecotoxicology. *Current Opinion in Toxicology*, *13*, 8–15.

Pinto, E., Sigaud-kutner, T. C. S., Leitão, M. A. S., Okamoto, O. K., Morse, D., Colepicolo, P. (2003). Heavy metal–induced oxidative stress in algae. *Journal of Phycology*, *39*(6), 1008–1018.

Poddar, N., Elahee Doomun, S. N., Callahan, D. L., Kowalski, G. M., Martin, G. J. O. (2020). The assimilation of glycerol into lipid acyl chains and associated carbon backbones of *Nannochloropsis*

salina varies under nitrogen replete and deplete conditions. *Biotechnology and Bioengineering*, *117*(11), 3299–3309.

Pollard, M. R., Stumpf, P. K. (1980). Biosynthesis of C20 and C22 Fatty Acids by Developing Seeds of *Limnanthes alba*: chain elongation and Δ5 desaturation. *Plant Physiology*, *66*(4), 649–655.

Raddadi, N., Cherif, A., Daffonchio, D., Neifar, M., Fava, F. (2015). Biotechnological applications of extremophiles, extremozymes and extremolytes. *Applied Microbiology and Biotechnology*, *99*(19), 7907–7913.

Rajasekhar, P., Fan, L., Nguyen, T., Roddick, F. A. (2012). A review of the use of sonication to control cyanobacterial blooms. *Water Research*, *46*(14), 4319–4329.

Rajashekar, C. (2023). Dual Role of Plant Phenolic Compounds as Antioxidants and Prooxidants. *American Journal of Plant Sciences*, *14*, 15–28.

Rana, M. S., Prajapati, S. K. (2021). Resolving the dilemma of iron bioavailability to microalgae for commercial sustenance. *Algal Research*, *59*, 102458.

Ren, L., Hu, X., Zhao, X., Chen, S., Wu, Y., Li, D., Yu, Y., Geng, L., Ji, X., Huang, H. (2017). Transcriptomic Analysis of the Regulation of Lipid Fraction Migration and Fatty Acid Biosynthesis in *Schizochytrium* sp. *Scientific Reports*, *7*(1), 3562

Richmond, A. (2003). Biological Principles of Mass Cultivation. In *Handbook of Microalgal Culture* (pp. 125–177).

Rismani-Yazdi, H., Haznedaroglu, B. Z., Hsin, C., Peccia, J. (2012). Transcriptomic analysis of the oleaginous microalga *Neochloris oleoabundans* reveals metabolic insights into triacylglyceride accumulation. *Biotechnology for Biofuels*, *5*(1), 74.

Robles, M., Torronteras, R., Ostojic, C., Oria, C., Cuaresma, M., Garbayo, I., Navarro, F., Vílchez, C. (2023). Fe (III)-Mediated Antioxidant Response of the Acidotolerant Microalga *Coccomyxa onubensis*. *Antioxidants*, *12*(3).

Robles, M., Viegas, C. S. B., Torronteras, R., Garbayo, I., Vega, J. M., Simes, D. C., Vílchez, C. (2025). An extremely acidic environment microalga from Tinto River as a novel source of anti-inflammatory activity. *Plant Physiology and Biochemistry*, *223*, 109815.

Rodrigues, H. G., Vinolo, M. A. R., Magdalon, J., Fujiwara, H., Cavalcanti, D. M. H., Farsky, S. H. P., Calder, P. C., Hatanaka, E., Curi, R. (2010). Dietary Free Oleic and Linoleic Acid Enhances Neutrophil Function and Modulates the Inflammatory Response in Rats. *Lipids*, *45*(9), 809–819.

Rodziewicz, P., Swarcewicz, B., Chmielewska, K., Wojakowska, A., Stobiecki, M. (2014). Influence of abiotic stresses on plant proteome and metabolome changes. *Acta Physiologiae Plantarum*, *36*(1), 1–19.

Ruiz-Domínguez, M. C., Robles, M., Martín, L., Beltrán, Á., Gava, R., Cuaresma, M., Navarro, F., Vílchez, C. (2023). Ultrasound-Based Recovery of Anti-Inflammatory and Antimicrobial Extracts of the Acidophilic Microalga *Coccomyxa onubensis*. *Marine Drugs*, *21*(9).

Ruiz-Marin, A., Canedo-Lopez, Y., Narvaez-Garcia, A., Zavala-Loría, J. del C., Dzul-López, L. A., Sámano-Celorio, M. L., Crespo-Álvarez, J., García-Villena, E., Agudo-Toyos, P. (2019). Harvesting Scenedesmus obliquus via Flocculation of Moringa oleifera Seed Extract from Urban Wastewater: Proposal for the Integrated Use of Oil and Flocculant. *Energies*, *12*(20).

Saini, R. K., Prasad, P., Sreedhar, R. V., Akhilender Naidu, K., Shang, X., Keum, Y.-S. (2021). Omega−3 Polyunsaturated Fatty Acids (PUFAs): Emerging Plant and Microbial Sources, Oxidative Stability, Bioavailability, and Health Benefits—A Review. *Antioxidants*, *10*(10).

Saito, A., Shinjo, S., Ito, D., Doi, Y., Sato, A., Wakabayashi, Y., Honda, J., Arai, Y., Maeda, T., Ohyama, T., Higuchi, K. (2021). Enhancement of Photosynthetic Iron-Use Efficiency Is an Important Trait of *Hordeum vulgare* for Adaptation of Photosystems to Iron Deficiency. *Plants*, *10*(2).

Saitou, N., Nei, M. (1987). The neighbor-joining method: a new method for reconstructing phylogenetic trees. *Molecular Biology and Evolution*, *4*(4), 406–425.

Sánchez-España, J., Falagán, C., Ayala, D., Wendt-Potthoff, K. (2020). Adaptation of *Coccomyxa* sp. to Extremely Low Light Conditions Causes Deep Chlorophyll and Oxygen Maxima in Acidic Pit Lakes. *Microorganisms*, *8*(8).

Santin, A., Russo, M. T., Ferrante, M. I., Balzano, S., Orefice, I., Sardo, A. (2021). Highly Valuable Polyunsaturated Fatty Acids from Microalgae: Strategies to Improve Their Yields and Their Potential Exploitation in Aquaculture. *Molecules*, *26*(24).

Sanz-Luque, E., Chamizo-Ampudia, A., Llamas, A., Galvan, A., Fernandez, E. (2015). Understanding nitrate assimilation and its regulation in microalgae. *Frontiers in Plant Science*, *Volume 6-2015*.

Schagerl, M., Siedler, R., Konopáčová, E., Ali, S. S. (2022). Estimating Biomass and Vitality of Microalgae for Monitoring Cultures: A Roadmap for Reliable Measurements. *Cells*, *11*(15).

Schenk, P. M., Thomas-Hall, S. R., Stephens, E., Marx, U. C., Mussgnug, J. H., Posten, C., Kruse, O., Hankamer, B. (2008). Second Generation Biofuels: High-Efficiency Microalgae for Biodiesel Production. *BioEnergy Research*, *1*(1), 20–43.

Schreiber, U. (2004). Pulse-Amplitude-Modulation (PAM) Fluorometry and Saturation Pulse Method: An Overview. In G. C. Papageorgiou & Govindjee (Eds.), *Chlorophyll a Fluorescence: A Signature of Photosynthesis* (pp. 279–319). Springer Netherlands.

Schüler, L. M., Santos, T., Pereira, H., Duarte, P., Katkam, N. G., Florindo, C., Schulze, P. S. C., Barreira, L., Varela, J. C. S. (2020). Improved production of lutein and β-carotene by thermal and light intensity upshifts in the marine microalga *Tetraselmis* sp. CTP4. *Algal Research*, *45*, 101732.

Schüler, L. M., Schulze, P. S. C., Pereira, H., Barreira, L., León, R., Varela, J. (2017). Trends and strategies to enhance triacylglycerols and high-value compounds in microalgae. *Algal Research*, *25*, 263–273.

Schuurmans, R. M., van Alphen, P., Schuurmans, J. M., Matthijs, H. C. P., Hellingwerf, K. J. (2015). Comparison of the Photosynthetic Yield of Cyanobacteria and Green Algae: Different Methods Give Different Answers. *Plos one*, *10*(9), e0139061-.

Serhan, C. N., Chiang, N., Van Dyke, T. E. (2008). Resolving inflammation: dual anti-inflammatory and pro-resolution lipid mediators. *Nature Reviews Immunology*, *8*(5), 349–361.

Shraim, A. M., Ahmed, T. A., Rahman, M. M., Hijji, Y. M. (2021). Determination of total flavonoid content by aluminum chloride assay: A critical evaluation. *LWT*, *150*, 111932.

Shuler ML, Kargi F. (2005). *Bioprocess Engineering: Basic Concepts* (2nd edition). Pearson Education.

Silverman, M. P., Lundgren, D. G. (1959). Studies on the chemoautotrophic iron bacterium *Ferrobacillus ferrooxidans*: I. An improved medium and a harvesting procedure for securing high cell yields. *Journal of Bacteriology*, *78*(3), 326–331.

Singh, H., Kumar, D., Soni, V. (2022). Performance of chlorophyll a fluorescence parameters in *Lemna minor* under heavy metal stress induced by various concentration of copper. *Scientific Reports*, *12*(1), 10620.

Singh, J., Dhar, D. W. (2019). Overview of Carbon Capture Technology: Microalgal Biorefinery Concept and State-of-the-Art. *Frontiers in Marine Science*, *Volume 6-2019*.

Singh, S., Kant, C., Yadav, R. K., Reddy, Y. P., Abraham, G. (2019). Cyanobacterial Exopolysaccharides: Composition, Biosynthesis, and Biotechnological Applications. *Cyanobacteria: From Basic Science to Applications*, 347–358.

Singla, R. K., Dubey, A. K., Garg, A., Sharma, R. K., Fiorino, M., Ameen, S. M., Haddad, M. A., Al-Hiary, M. (2019). Natural Polyphenols: Chemical Classification, Definition of Classes, Subcategories, and Structures. *Journal of Aoac Imternational*, *102*(5), 1397–1400.

Smirnoff, N. (2000). Ascorbic acid: metabolism and functions of a multi-facetted molecule. *Current Opinion in Plant Biology*, *3*(3), 229–235.

Solovchenko, A. E., Merzlyak, M. N. (2008). Screening of visible and UV radiation as a photoprotective mechanism in plants. *Russian Journal of Plant Physiology*, *55*(6), 719–737.

Souza-Egipsy, V., Altamirano, M., Amils, R., Aguilera, A. (2011). Photosynthetic performance of phototrophic biofilms in extreme acidic environments. *Environmental Microbiology*, *13*(8), 2351–2358.

Spolaore, P., Joannis-Cassan, C., Duran, E., Isambert, A. (2006). Commercial applications of microalgae. *Journal of Bioscience and Bioengineering*, *101*(2), 87–96.

Srilatha, N., Madireddi, S., Yadav, R., Subramanyam, R. (2019). Non-photochemical quenching-dependent acclimation and thylakoid organization of *Chlamydomonas reinhardtii* to high light stress. *Photosynthesis Research*, *139*.

Strasser, R., Srivastava, A., Tsimilli-Michael, M. (2000). The fluorescence transient as a tool to characterize and screen photosynthetic samples. *Probing Photosynthesis: Mechanism, Regulation and Adaptation*.

Südfeld, C., Hubáček, M., Figueiredo, D., Naduthodi, M. I. S., van der Oost, J., Wijffels, R. H., Barbosa, M. J., D'Adamo, S. (2021). High-throughput insertional mutagenesis reveals novel targets for enhancing lipid accumulation in *Nannochloropsis oceanica*. *Metabolic Engineering*, *66*, 239–258.

Swanson, D., Block, R., Mousa, S. A. (2012). Omega-3 Fatty Acids EPA and DHA: Health Benefits Throughout Life. *Advances in Nutrition*, *3*(1), 1–7.

Swoczyna, T., LATA, B., Stasiak, A., Stefaniak, J., Latocha, P. (2019). JIP-test in assessing sensitivity to nitrogen deficiency in two cultivars of *Actinidia arguta* (Siebold et Zucc.) Planch. ex Miq. *Photosynthetica*, *57*.

Tamura, K., Stecher, G., Kumar, S. (2021). MEGA11: Molecular Evolutionary Genetics Analysis Version 11. *Molecular Biology and Evolution*, *38*(7), 3022–3027.

Tarafdar, A., Sowmya, G., Yogeshwari, K., Rattu, G., Negi, T., Awasthi, M. K., Hoang, A., Sindhu, R., Sirohi, R. (2023). Environmental pollution mitigation through utilization of carbon dioxide by microalgae. *Environmental Pollution*, *328*, 121623.

Tonstad, S., Clifton, P. (2017). 20 - Vegetarian Diets and the Risk of Type 2 Diabetes. In F. Mariotti (Ed.), *Vegetarian and Plant-Based Diets in Health and Disease Prevention* (pp. 355–367). Academic Press.

Tschermak-Woess, E. (1988). *The algal partner* (M. Galun, Ed.; Vol. 1). Handbook of Lichenology.

Tzachor, A., Rozen, O., Khatib, S., Jensen, S., Avni, D. (2021). Photosynthetically Controlled *Spirulina*, but Not Solar *Spirulina*, Inhibits TNF-α Secretion: Potential Implications for COVID-19-Related Cytokine Storm Therapy. *Marine Biotechnology*, *23*(1), 149–155.

Vaquero, I., Mogedas, B., Ruiz-Domínguez, M. C., Vega, J. M., Vílchez, C. (2014). Light-mediated lutein enrichment of an acid environment microalga. *Algal Research*, *6*, 70–77.

Vaquero, I., Ruiz-Domínguez, M. C., Mogedas, B., Vílchez, C., Vega, J. M. (2016). Production of Lutein-enriched Biomass by Growing *Coccomyxa* sp. (strain *onubensis*; *Chlorophyta*) under Spring Outdoor Conditions of Southwest Spain. *Journal of advances in biotechnology*, *6*(1), 828–834.

Vaquero, I., Vázquez, M., Ruiz-Dominguez, M. C., Vílchez, C. (2013). Enhanced production of a lutein-rich acidic environment microalga. *Journal of Applied Microbiology*, *116*.

Varshney, P., Mikulic, P., Vonshak, A., Beardall, J., Wangikar, P. P. (2015). Extremophilic micro-algae and their potential contribution in biotechnology. *Bioresource Technology*, *184*, 363–372.

Vítek, P., Jehlička, J., Ascaso, C., Mašek, V., Gómez-Silva, B., Olivares, H., Wierzchos, J. (2014). Distribution of scytonemin in endolithic microbial communities from halite crusts in the hyperarid zone of the Atacama Desert, Chile. *FEMS Microbiology Ecology*, *90*(2), 351–366.

Vitova, M., Bisova, K., Kawano, S., Zachleder, V. (2015). Accumulation of energy reserves in algae: From cell cycles to biotechnological applications. *Biotechnology Advances*, *33*(6, Part 2), 1204–1218.

Vivek, N., Sindhu, R., Madhavan, A., Anju, A. J., Castro, E., Faraco, V., Pandey, A., Binod, P. (2017). Retracted: Recent advances in the production of value added chemicals and lipids utilizing biodiesel industry generated crude glycerol as a substrate – Metabolic aspects, challenges and possibilities: An overview. *Bioresource Technology*, *239*, 507–517.

Wan, L., Zhang, H. (2012). Cadmium toxicity effects on cytoskeleton, vesicular trafficking and cell wall construction. *Plant Signaling and Behavior*, *7*.

Wierzchos, J., Casero, M. C., Artieda, O., Ascaso, C. (2018). Endolithic microbial habitats as refuges for life in polyextreme environment of the Atacama Desert. *Current Opinion in Microbiology*, *43*, 124–131.

Wierzchos, J., DiRuggiero, J., Vítek, P., Artieda, O., Souza-Egipsy, V., Skaloud, P., Tisza, M., Davila, A., Vílchez, C., Garbayo, I., Ascaso, C. (2015). Adaptation strategies of endolithic chlorophototrophs to survive the hyperarid and extreme solar radiation environment of the Atacama Desert. *Frontiers in Microbiology*, *6*.

Wijffels, R., Barbosa, M. J. (2010). An Outlook on Microalgal Biofuels. *Science (New York, N.Y.)*, *329*, 796–799.

Wu, X., Joyce, E. M., Mason, T. J. (2011). The effects of ultrasound on cyanobacteria. *Harmful Algae*, *10*(6), 738–743.

Yonezawa, Y., Hada, T., Uryu, K., Iijima, H., Yoshida, H., Mizushina, Y. (2006). Inhibitory action of C22-fatty acids on DNA polymerases and DNA topoisomerases. *International Journal of Molecular Medicine*.

Yoshihara, D., Fujiwara, N., Suzuki, K. (2010). Antioxidants: Benefits and risks for long-term health. *Maturitas*, *67*(2), 103–107.

Zandalinas, S. I., Fritschi, F. B., Mittler, R. (2021). Global Warming, Climate Change, and Environmental Pollution: Recipe for a Multifactorial Stress Combination Disaster. *Trends in Plant Science*, *26*(6), 588–599.

Zanella, L., Vianello, F. (2020). Microalgae of the genus *Nannochloropsis*: Chemical composition and functional implications for human nutrition. In *Journal of Functional Foods* (Vol. 68).

Zijffers, J.-W. F., Schippers, K. J., Zheng, K., Janssen, M., Tramper, J., Wijffels, R. H. (2010). Maximum Photosynthetic Yield of Green Microalgae in Photobioreactors. *Marine Biotechnology*, *12*(6), 708–718.

List of publications derived from the Thesis

Published

Robles, M.; Garbayo, I.; Wierzchos, J.; Vílchez, C.; Cuaresma, M. Effect of low-frequency ultrasound on disaggregation, growth and viability of an extremotolerant cyanobacterium. *Journal of Applied Phycology* **2022**, *34*, 2895–2904. https://doi.org/10.1007/s10811-022-02831-x

Robles, M.; Torronteras, R.; Ostojic, C.; Oria, C.; Cuaresma, M.; Garbayo, I.; Navarro, F.; Vílchez, C. Fe (III)-Mediated Antioxidant Response of the Acidotolerant Microalga *Coccomyxa onubensis*. *Antioxidants* **2023**, *12*, 610. https://doi.org/10.3390/antiox12030610

Robles, M., Ostojic, C., Ruiz-Domínguez, M.C.; Cuaresma, M.; Gonzalo, C.; Obregón, V.; Fuentes, JL.; Bartolomé, A.; Vílchez, C. Mixotrophic growth of a highly acidic habitat microalga for production of valuable fatty acids *Journal of Applied Phycology* **2024**, *36*, 2489–2502. https://doi.org/10.1007/s10811-024-03255-5

Robles, M.; Viegas, CSB.; Torronteras, R.; Garbayo, I.; Vega, JM.; Simes, D.C.; Vílchez, C. An extremely acidic environment microalga from Tinto River as a novel source of anti-inflammatory activity. *Plant physiology and biochemistry: PPB* **2025**, *223*, 109815. https://doi.org/10.1016/j.plaphy.2025.109815

Submitted

Robles, M.; Ruiz-Domínguez M.C.; Garbayo, I.; Vílchez, C. Photosynthesis of a highly acidic-habitat microalga under abiotic stress. *Physiologia Plantarum* **2025**.

Robles, M.; Martín-Gordillo, L.; de la Luz, N; Cuaresma, M.; Vílchez, C; Ruiz-Domínguez M.C. Biomass Production and Green Extraction of Phenolic Compounds of the Highly Acidic Environment Microalga *Coccomyxa onubensis*. *Journal of Applied Phycology* **2025**.